

# bradscholars

## Suitability of cellulose ester derivatives in hot melt extrusion. Thermal, rheological and thermodynamic approaches used in the characterization of cellulose ester derivatives for their suitability in pharmaceutical hot melt extrusion

Item Type	Thesis
Authors	Karandikar, Hrushikesh M.
Rights	<p><a href="http://creativecommons.org/licenses/by-nc-nd/3.0/">&lt;a rel="license" href="http://creativecommons.org/licenses/by-nc-nd/3.0/"&gt;&lt;img alt="Creative Commons License" style="border-width:0" src="http://i.creativecommons.org/l/by-nc-nd/3.0/88x31.png" /&gt;&lt;/a&gt;&lt;br /&gt;</a>The University of Bradford theses are licenced under a <a href="http://creativecommons.org/licenses/by-nc-nd/3.0/">&lt;a rel="license" href="http://creativecommons.org/licenses/by-nc-nd/3.0/"&gt;Creative Commons Licence&lt;/a&gt;.</a></p>
Download date	2025-07-03 20:53:48
Link to Item	<a href="http://hdl.handle.net/10454/14862">http://hdl.handle.net/10454/14862</a>



## **University of Bradford eThesis**

This thesis is hosted in [Bradford Scholars](#) – The University of Bradford Open Access repository. Visit the repository for full metadata or to contact the repository team



© University of Bradford. This work is licenced for reuse under a [Creative Commons Licence](#).

**SUITABILITY OF CELLULOSE ESTER DERIVATIVES  
IN HOT MELT EXTRUSION**

**THERMAL, RHEOLOGICAL AND THERMODYNAMIC APPROACHES  
USED IN THE CHARACTERIZATION OF CELLULOSE ESTER  
DERIVATIVES FOR THEIR SUITABILITY IN PHARMACEUTICAL HOT  
MELT EXTRUSION**

**Hrushikesh Mahesh KARANDIKAR**

**Submitted for the degree of  
Doctor of Philosophy**

**School of Life Sciences  
University of Bradford**

**2015**

## Abstract

**Hrushikesh Mahesh Karandikar**

### **Suitability of cellulose ester derivatives in hot melt extrusion**

(Thermal, rheological and thermodynamic approaches used in the characterization of cellulose ester derivatives for their suitability in pharmaceutical hot melt extrusion)

**Key words:** *HME, HPMCAS, HPMCP, Plasticisers, Thermal Degradation-Kinetics and Mechanism, Polymer-Plasticiser Interactions, Thermodynamics of Miscibility, Low-High Shear Rate Rheology, Impurity Quantitation, Chlorpropamide*

Applications of Hot Melt Extrusion (HME) in pharmaceuticals have become increasingly popular over the years but nonetheless a few obstacles still remain before wide scale implementation. In many instances these improvements are related to both processing and product performance. It is observed that HME process optimisation is majorly focused on the active pharmaceutical ingredient's (API) properties. Characterising polymeric properties for their suitability in HME should be equally studied since the impact of excipients on both product and process performance is just as vital. In this work, two well-established cellulose ester derivatives: Hydroxy Propyl Methyl Cellulose Acetate Succinate (HPMCAS) and Hydroxy Propyl Methyl Cellulose Phthalate (HPMCP) are studied for their HME suitability. Their thermal, thermodynamic, rheological, thermo-chemical and degradation kinetic properties were evaluated with model plasticisers and APIs. It was found the thermal properties of HPMCP are severely compromised whereas HPMCAS is more stable in the processing zone of 150 to 200 °C. Thermodynamic properties revealed that both polymers share an important

solubility parameter range (20-30 MPa<sup>1/2</sup>) where the majority of plasticisers and BCS class II APIs lie. Thus, greater miscibility/solubility can be expected. Further, the processability of these two polymers investigated by rheometric measurements showed HPMCAS possesses better flow properties than HPMCP because HPMCP forms a weak network of chain interactions at a molecular level. However, adding plasticisers such as PEG and TEC the flow properties of HPMCP can be tailored. The study also showed that plasticisers have a major influence on thermo-chemical and kinetic properties of polymers. For instance, PEG reduced polymer degradation with reversal in kinetic parameters whereas blends of CA produced detrimental effects and increased polymer degradation with reduction in onset degradation temperatures. Further, both polymers are observed to be chemically reactive with the APIs containing free -OH, -SO<sub>2</sub>N- and -NH<sub>2</sub> groups. Finally, these properties prove that suitability of HPMCP is highly debated for HME and demands great care in use while that of HPMCAS is relatively better than HPMCP in many instances.

**DEDICATED TO SCIENCE AND MY  
BELOVED FAMILY MEMBERS**

## ACKNOWLEDGEMENT

On the verge of completion of my PhD, I now look back fondly towards all the hardship that has been a learning experience for me and have made me stronger and clear in thoughts. I would like to take an opportunity to humbly acknowledge and appreciate the efforts of all the people who have contributed in my research.

I take the foremost opportunity to express my heartfelt reverence to my respected supervisors *Prof. Anant Paradkar, Dr. Tim Gough and Dr. Adrian Kelly*, who always boosted my morale with their valuable guidance, creative suggestions, helpful discussion, unfailing advice, keen interest in research, dedicated efforts and enduring support on all occasions. I consider myself privileged to have worked under their guidance, as they always shared their vast experience generously and patiently in spite of their busy schedule. I sincerely appreciate the interactive help received from all of them by the way of advice, suggestions and spirit. I specially thank *Prof. Anant Paradkar* for giving me the liberty of decision making throughout the work.

My sincere thanks and remembrance to *Prof. Phil Coates*, University of Bradford, for providing the necessary infrastructure and facilities required for carrying out my research work in interdisciplinary research centre (IRC) polymer engineering sciences and in centre for chemical and structural analysis respectively. It gives me immense pleasure to express my sincere gratitude towards **Mr. John Wyborn, Mr. Keith Norris and Mr. Andrew Healey** for their guidance in laboratory practical work. It gives me immense pleasure to express my gratitude to my friends **Rohan, Aniket, Niten, Sudhir, Sachin Amit and Ratnadeep** for their unconditional support.

This acknowledgement will not be complete until I express my feelings for my family, especially **My Father, Mother, my wife Madhura, Grandfather, Grandmother, brother Parikshit and my best friends** who blessed me with their good wishes and enthusiasm to see this work complete. I am gratified for their eternal love, innocent forbearance, trust and support which always has a positive influence on my performance and is a driving force towards my success.

# TABLE OF CONTENTS

<b>Abstract</b>	<b>i</b>
<b>Acknowledgements</b>	<b>ii</b>
<b>Table of contents</b>	<b>iii</b>
<b>List of figures</b>	<b>iv</b>
<b>List of tables</b>	<b>v</b>
<b>Glossary</b>	<b>vi</b>
<b>CHAPTER 1. INTRODUCTION</b>	<b>1</b>
<b>1.1 Research objectives</b>	<b>4</b>
<b>1.2 Thesis outline</b>	<b>5</b>
<b>CHAPTER 2. BACKGROUND</b>	<b>7</b>
<b>2.1 Pharmaceutical Excipients</b>	<b>7</b>
<b>2.2 Hot Melt Extrusion</b>	<b>12</b>
2.2.1 Principle, equipment and process of HME	13
2.2.2 Extrusion process	17
2.2.3 Important variables of melt extrusion process	18
<b>2.3 Polymers and plasticisers used in HME</b>	<b>20</b>
2.3.1 Overview of cellulose ester derivatives: HPMCAS and HPMCP	24
2.3.2 HME with HPMCAS and HPMCP: Potential challenges	32
<b>2.4 Excipient characterisation approaches</b>	<b>34</b>
2.4.1 Thermal and thermo-chemical properties of the polymers	35
2.4.2 Thermodynamic properties of pure and blends of polymers	43
2.4.3 Polymer melt rheology	48
2.4.4 Thermo-mechanical degradation kinetics of polymers	53
<b>2.5 Summary</b>	<b>58</b>
<b>CHAPTER 3. MATERIALS AND METHODS</b>	<b>60</b>
<b>3.1 Materials</b>	<b>60</b>
3.1.1 APIs	61
3.1.2 Polymers and plasticisers	61
3.1.3 Chemicals	61

3.1.4	Instruments and software	62
<b>3.2</b>	<b>Methods</b>	<b>63</b>
3.2.1	Characterisation of polymers, plasticisers and APIs properties	63
3.2.2	Extrusion of pure and blends of polymers	72
3.2.3	Characterisation of extrudates	75
3.2.4	Degradation products of polymer and drug-polymer incompatibilities	79
<b>CHAPTER 4.</b>	<b>RESULTS AND DISCUSSION</b>	<b>83</b>
<b>4.1</b>	<b>Material properties of polymers, plasticisers and APIs</b>	<b>83</b>
4.1.1	Thermal properties of materials	83
4.1.2	Thermodynamic properties of pure and polymeric blends	86
4.1.3	Polymer melt rheology	121
4.1.4	Thermo-chemical stability of pure polymers	152
4.1.5	Summary	161
<b>4.2</b>	<b>Hot melt extrusion and processing attributes</b>	<b>164</b>
4.2.1	Influence of pure and blend polymeric properties on processability	164
4.2.2	Polymer melt flow behaviour inside extruder	167
4.2.3	Summary	169
<b>4.3</b>	<b>Characterisation of polymer melt extrudates</b>	<b>171</b>
4.3.1	Thermodynamic approaches	171
4.3.2	Polymer melt rheology	177
4.3.3	Thermo-chemical stability of melt extrudates	181
4.3.4	Summary	208
<b>4.4</b>	<b>Polymer degradation mechanism and kinetic modelling</b>	<b>211</b>
4.4.1	Degradation mechanism (publication I)	211
4.4.2	Isothermal degradation kinetics and implications of plasticisers	214
4.4.3	Summary	235
<b>CHAPTER 5.</b>	<b>CONCLUSIONS</b>	<b>237</b>
<b>CHAPTER 6.</b>	<b>FUTURE PERSPECTIVES</b>	<b>241</b>
<b>REFERENCES</b>		<b>243</b>
<b>APPENDIX I</b>	<b>THERMAL AND RHEOLOGICAL DATA</b>	<b>259</b>
<b>APPENDIX II</b>	<b>PUBLICATION &amp; CONFERENCES</b>	<b>261</b>

## List of Figures

Figure 2.1 : The need for modified and novel excipients.	9
Figure 2.2: Schematic representation of melt extruder and its process.	13
Figure 2.3: (a) Screw rotations (b) angles of kneading elements.	15
Figure 2.4: Important monitoring parameters of melt extrusion processes.	19
Figure 2.5 Commercial synthesis of HPMCAS and HPMCP (Shin-Etsu, 2009).	25
Figure 2.6: Pharmaceutical applications of cellulose esters (Science.gov, 2015).	29
Figure 2.7: Excipient characterisation techniques utilised in the current work.	35
Figure 2.8: Structure of a polymer (Omidian H, 2006).	38
Figure 2.9: Typical thermal degradation mechanism and pathway.	39
Figure 2.10: Onset and oxidative degradation temperatures in TGA.	41
Figure 2.11: Schematic diagrams of rheometers (Kelly, 1997).	52
Figure 2.12: HME product and performance stability.	59
Figure 3.1: Schematic representation and photograph of DSC.	64
Figure 3.2: Schematic representation and photograph of TGA.	65
Figure 3.3: Rotational rheometer.	67
Figure 3.4: Capillary rheometer.	72
Figure 3.5: PharmaLab Extruder.	73
Figure 3.6: Screw configuration used during extrusion.	73
Figure 3.7: DVS instrument and parameters.	76
Figure 4.1: TGA thermograms of (a) polymers and plasticisers (b) APIs.	84
Figure 4.2: DSC thermograms of (a) polymers and (b) crystalline components.	88
Figure 4.3: Fox equation for (a) polymer-plasticisers (b) polymer-API blends.	89
Figure 4.4: Fragility parameter-graphs of $\ln(Q)$ against $1/T_g$ .	91
Figure 4.5: DSC thermograms of PEG-HPMCAS showing MPD.	105
Figure 4.6: Plots determining interaction parameter near melting point.	106
Figure 4.7: Gibbs free energy near melting point of the plasticisers.	107
Figure 4.8: Mechanism of phase separation by mathematical approach.	109
Figure 4.9: (a) First order linear and (b) non-linear relationship between interaction parameter and $1/T$ .	113
Figure 4.10: Plots of Gibbs free energy as a function of volume fractions of plasticisers at different temperatures.	116
Figure 4.11: Theoretical solid state solubility-miscibility phase diagram.	118

Figure 4.12: Representative phase diagrams of (a) CA-HPMCP (b) PEG-HPMCP.	121
Figure 4.13: Representative graphs for strain amplitude test.	123
Figure 4.14: Representative graphs for frequency sweep test.	124
Figure 4.15: Frequency sweep test (a) HPMCAS (B) HPMCP.	126
Figure 4.16: Complex viscosity results and Arrhenius relationship for HPMCP.	130
Figure 4.17: TTS curves for HPMCP and HPMCAS.	132
Figure 4.18: Pressure drop for HPMCAS and HPMCP polymers.	135
Figure 4.19: Temperature dependent shear viscosity of virgin polymers.	136
Figure 4.20: Amplitude sweep of blends of HPMCP.	139
Figure 4.21: Effects of plasticisers on polymer melt viscosity.	140
Figure 4.22: Shift of cross over points towards higher frequency.	141
Figure 4.23: Amplitude sweep tests for drug-polymer complex.	142
Figure 4.24: Complex viscosity values for IBU-HPMCAS compositions.	144
Figure 4.25: Storage and loss moduli of IBU-HPMCAS samples.	144
Figure 4.26: Pressure versus time graphs (a) comparison at 140 °C for polymer-plasticisers and (b) IBU-HPMCAS compositions.	146
Figure 4.27: Graphs showing linear dependence of viscosity.	148
Figure 4.28: Applications of Cox-Merz rule.	151
Figure 4.29: FTIR spectra of polymers upon isothermal heating.	154
Figure 4.30: HPLC method development and validation, a QbD like approach.	157
Figure 4.31: Resolution solution of AA, SA, and PA in a gradient method.	157
Figure 4.32: A representative chart showing statistics utilised during validation (a) LOD-LOQ (b) robustness parameter.	160
Figure 4.33: Percentage torque versus extrusion temperatures for samples	166
Figure 4.34: Activation energy plots of (a) pure and (b) polymer blends.	167
Figure 4.35: Thermodynamic phase diagrams of (a) polymer-plasticiser and (b) IBU-polymer mixtures.	172
Figure 4.36: DSC thermograms of melt extrudates of (a) PEG-HPMCP (b) CA-HPMCP during stability studies.	173
Figure 4.37: A representative figures of (a) XRD of melt extrudates of PEG-HPMCP upon stability (b) effect of moisture on 10% PEG mixtures	174
Figure 4.38: DSC thermograms of blends of Ibuprofen post extrusion.	177
Figure 4.39: Complex viscosity comparison between of pre and post processed materials of (a) HPMCAS and (b) HPMCP.	179
Figure 4.40: Decay rates of polymeric samples.	181

Figure 4.41: HPLC chromatogram of HPMCP polymer extrudates.	183
Figure 4.42: Sublimation product of HPMCP.	184
Figure 4.43: Infra Red spectroscopy of Cryst-A.	185
Figure 4.44: <sup>1</sup> H-NMR spectra of (a) PA and (b) Cryst-A.	186
Figure 4.45: <sup>13</sup> C-NMR of PA and Cryst-A.	187
Figure 4.46: GC-MS of Cryst-A and the fragmentation pathway of Cryst-A.	188
Figure 4.47: Schematic representation of formation of environmental related impurity below onset degradation temperature of HPMCP.	189
Figure 4.48: Quantification of degradation products of HPMCP.	191
Figure 4.49: (a) Thermal properties of CPM (b) components miscibility by DSC.	196
Figure 4.50: Chromatograms of CPM-HPMCP (a) TGA (b) Melt extrudates.	198
Figure 4.51: Chromatograms of TGA exposed CPM-HPMCAS.	199
Figure 4.52: Chemical structure of Chlorpropamide and Ibuprofen	200
Figure 4.53: GC spectra of extrudates of CPM.	203
Figure 4.54: Unknown impurities (a) of CPM-HPMCP (b) CPM-HPMCAS	204
Figure 4.55: Degradation mechanisms of chlorpropamide.	205
Figure 4.56: Schematic representation of degradation of HPMCP.	212
Figure 4.57: Linear to curvilinear graphs of polymers.	217
Figure 4.58: Curvilinear to linear weight loss changes with addition of PEG.	219
Figure 4.59: TGA and DTGA of polymer blends.	220
Figure 4.60: Decomposition ratios of polymeric samples.	221
Figure 4.61: (a) Graph of $\alpha$ versus T (b) Kinetic expressions of polymeric samples over range of temperatures and concentrations.	222
Figure 4.62: A graph of $\log k_1$ over the range of temperature.	225
Figure 4.63: $E_a$ and A dependence for the polymer plasticiser blends.	227
Figure 4.64: Reduced complex viscosity against time for polymeric samples (a) HPMCP (b) with blends of PEG.	232
Figure 4.65: (a) Rheology data for determination of degradation kinetics of HPMCP and (b) comparison of $k_a$ values over temperatures.	233
Figure 4.66: Arrhenius plots for determination of $E_a$ based on rheology data.	235
Figure 6.1: Phase diagrams of CPM mixtures with HPMCAS and HPMCP	259
Figure 6.2: Cox Merz applications for the blends of CA-HPMCP.	259
Figure 6.3: Percentage torque versus extrusion temperatures for TEC-HPMCP and TEC-HPMCAS	260
Figure 6.4: Schematic representation of degradation mechanism of HPMCAS	260

## List of Tables

Table 2.1: Applications of modified and novel excipients in dosage forms.	11
Table 2.2: Single screw and twin screw extrusion characteristics.	14
Table 2.3: Degree of substitutions of polymers (Shin-Etsu, 2009).	26
Table 3.1: List of instruments and software used for analysis.	62
Table 3.2: Steady shear rate test stages.	70
Table 3.3: Screw elements and configuration.	74
Table 3.4: Temperature profile.	74
Table 3.5: Dilutions for Accuracy (% Recovery).	79
Table 4.1: TGA processed values of decompositions.	86
Table 4.2: MDSC results for HPMCAS and HPMCP polymers	87
Table 4.3: Group contributions to HPMCAS by Van Krevelen method.	98
Table 4.4: Solubility parameter of different materials.	99
Table 4.5: Values of $\chi$ based on the solubility parameters.	100
Table 4.6: Interaction parameter values near melting points.	106
Table 4.7: Constants A and B determined using equation 4.12.	114
Table 4.8: Comparison of derived constants A and B obtained by the two approaches of investigating of $\chi$ .	115
Table 4.9: Energy of activation for polymer-melt viscosities.	131
Table 4.10: Shift factor calculations for HPMCP and HPMCAS.	133
Table 4.11: Power law index and consistency index for virgin polymers.	137
Table 4.12: Calculated power law index for plasticised polymer.	149
Table 4.13: Linearity, LOD and LOQ for AA, SA and PA.	158
Table 4.14: Extrusion parameters and processability of pure polymers.	165
Table 4.15: Flow activation energy of polymers during extrusion.	169
Table 4.16: Degradation products of polymers upon extrusion.	192
Table 4.17: HPLC analysis CPM-HPMCP samples.	200
Table 4.18: HPLC analysis CPM-HPMCAS samples.	201
Table 4.19: Isothermal weight loss of materials.	218
Table 4.20: Calculated kinetic parameters for HPMCAS samples.	223
Table 4.21: Calculated kinetic parameters for HPMCP samples.	224
Table 4.22: Investigation of kinetic parameters by MacCallum method.	229
Table 4.23: Degradation Kinetic parameters determined by Daly et al.	235

## Abbreviations

AA	:	Acetic Acid
API	:	Active Pharmaceutical Ingredient
AR	:	Analytical grade
ASD	:	Amorphous Solid Dispersion
<sup>13</sup> C-NMR	:	Carbon Nuclear Magnetic Resonance
DSC	:	Differential Scanning Calorimetry
DVS	:	Dynamic Vapour Sorption
EMA	:	European Medicine Agency
FECD	:	Free energy composition diagram
FDA	:	Food Drug Administration
FTIR	:	Fourier Transform Infra Red
GC	:	Gas Chromatography
HPLC	:	High performance Liquid Chromatography
HME	:	Hot Melt Extrusion
HPMCAS	:	Hydroxyl Propyl Methyl Cellulose Acetate Succinate
HPMCP	:	Hydroxy Propyl Methyl Cellulose Phthalate
ICH	:	International Conference on Harmonization
LOD	:	Limit of Detection
LOQ	:	Limit of Quantitation
MS	:	Mass spectroscopy
NF	:	National Formulary
<sup>1</sup> H-NMR	:	Proton Nuclear Magnetic Resonance
PA	:	Phthalic Acid
PAH	:	Phthalic Anhydride
PDA	:	Photo Diode Array
RBF	:	Round Bottom Flask
rpm	:	Revolutions Per Minute
Rt	:	Retention Time
SA	:	Succinic Acid
SD	:	Solid Dispersion
TGA	:	Thermogravimetric Analysis
UV	:	Ultra-Violet Spectroscopy
USP	:	United States Pharmacopeia
WHO	:	World Health Organization
XRD	:	X -Ray Diffraction

## Chapter 1. Introduction

Active Pharmaceutical Ingredients (APIs) are seldom administered as a single entity, more often being part of a formulation with one or more other specialised pharmaceutical agents known as excipients. Excipients are included in the dosage forms to aid in stabilising and processing of different dosage forms (Swarbrick and Boylan, 1990 , Crowley *et al.*, 2002). Excipients are generally treated as inert compounds however; they can participate or initiate physicochemical reactions that can lead to physicochemical incompatibilities. Broadly these interactions are either associated with degradation of the materials or physical stability of the dosage form which compromises its purpose. Thus, detailed characterisation of excipients demands greater attention.

Physicochemical properties of pharmaceutical solid materials significantly depend upon the inherent properties of materials, interactions between two or more components, environmental factors such as humidity, temperature and on manufacturing conditions (Liu *et al.*, 2002 , Yadav *et al.*, 2009 , Heljo *et al.*, 2013). These properties, in many instances, produce various challenges in conventional manufacturing techniques related to compaction, dissolution, flow properties, stability and packaging (Kaerger *et al.*, 2004 , Andrews, 2007 , Qiu *et al.*, 2009). Therefore, over the last two decades, researchers have been attracted towards emerging manufacturing technologies such as melt granulation processes (Yang *et al.*, 2007 , Kidokoro *et al.*, 2002), Hot Melt Extrusion (HME) and injection moulding because of their advantages over conventional manufacturing technologies.

HME is one of the most widely investigated techniques for a variety of pharmaceutical solid dosage forms including solid dispersions (Six *et al.*, 2003a), implants (Rothen-Weinhold *et al.*, 2000), ophthalmic inserts and oral dosage

forms (Follonier *et al.*, 1995). The melt extrusion process is defined as the process of continuously shaping a fluidic polymer or formulation through the orifice of a suitable die and subsequently solidifying it into a product. HME has many benefits such as process continuity and it can alleviate the problem of residual solvents in the final product. It can also reduce the required number of excipients owing to wide functionality of novel as well as modified excipients employed.

Literature reviews suggest that HME-based formulations involve the extrusion of various model APIs with a limited number of conventional excipients such as cellulose derivatives, polyethylene glycols, polyethylene oxide, poly(vinyl pyrrolidone), Eudragit® and certain newly designed polymers such as Soluplus®. This limited number can be attributed to the excipients' 'extrudability' and the requirement of FDA approval. Moreover, it was also observed that in the majority of these cases, cellulose derivatives have been most extensively studied based on their wide range of availability and well known properties in conventional dosage forms. Different grades of cellulose derivatives: Hydroxy Propyl Methyl Cellulose (HPMC) and Cellulose Acetate Phthalate (CAP) have been used in melt extruded systems while recently two of its derivatives namely: Hydroxy Propyl Methyl Cellulose Acetate Succinate (HPMCAS) and Hydroxy Propyl Methyl Cellulose Phthalate (HPMCP) have attracted most research.

HPMCAS and HPMCP are two of most the well-established chemically modified polymers having been available in the market for the last three decades. Their applications include coating (Thoma and Bechtold, 1999) and targeted drug delivery systems (Siepmann *et al.*, 2008) are well known to the pharmaceutical industry. Recently, these two polymers have been investigated for their applications in HME products and various groups have reported their

applications as crystallisation inhibitors, improvement in dissolution of poorly water-soluble drugs and for targeted drug delivery systems (Li and Mei, 2006 , Sarode *et al.*, 2014 , Ghosh *et al.*, 2011 , Mahmah *et al.*, 2014). However, despite their popularity and unique advantages, their utility for HME has so far been limited owing to certain critical physicochemical polymeric properties as well as demanding processing conditions of HME.

HME, being a thermal process can be incompatible with thermolabile APIs/polymers. Both these polymers are known for releasing their acidic contents at elevated processing conditions (Zedong Dong and Choi, 2008). Thus, chemical stability at HME temperatures is a major concern for their applicability. Furthermore, a critical overview of HME based systems containing these two polymers suggests an inadequacy of known polymeric properties related to their suitability and processibility in HME. For instance, thermal properties such as thermal stability at different processing temperature, polymer degradation products, reactivity, degradation mechanisms and thermal degradation kinetics have not been studied in detail. Additionally, the flow behaviour of these molten polymers is sparsely known and very few reports can be found in the literatures which relate melt properties of polymers with processing attributes of HME (Ghosh *et al.*, 2011). This suggests a lack of detailed preformulatory melt rheology studies. Additionally it can be observed that thermo-chemical stability of excipients, excipient impurities and their in-process degradation has not yet received due consideration for HME as compared to API characterisation. It is important to note that in-process changes in physico-chemical properties within the excipients can be a potential reason for the failure of a formulation (Aljaberi *et al.*, 2009 , Baldrick, 2000 , Bharate *et al.*, 2010). Hence, although characterisation of API is indeed important, the material properties of the excipients must also be understood in order to investigate process suitability and to ensure safety of the final dosage

form. This thesis aims to investigate the suitability of HPMCAS and HPMCP in HME technology via a full investigation of thermo-chemical stability, thermodynamic and melt rheological properties.

## 1.1 Research objectives

The main goal of this research is to characterise and quantify the physicochemical properties of HPMCAS and HPMCP to establish their suitability in HME. A literature review suggests that these polymers may be processed for several dosage forms in a solution state while the melt behaviour of HPMCAS and HPMCP polymers remains largely unexplored. Potential challenges are related to the thermal, thermodynamic and melt rheological properties with or without use of plasticisers and/or APIs. Specific objectives of this research are:

### A. Thermo-chemical properties of polymers and other processing aids

- To address the effect of temperature on chemical features of materials
- To investigate degradation products of polymers and their chemical interactions during and post extrusion studies with added compounds.
- To study the influences of processing parameters on polymer chemical stability.

### B. Thermodynamic properties of pure polymers and polymeric blends

- To study "glass forming ability" of different crystalline entities
- To investigate miscibility-solubility studies of solid state components and construct phase diagrams based on thermodynamic data.
- To predict maximum safe loadings of plasticiser and/or API (s) to incorporate in the polymer matrix to prevent problems of recrystallisation

### C. Melt rheology of polymers

- To investigate polymer melt rheology particularly the effects of plasticisers on visco-elasticity at preformulatory stages.
- To investigate effect of polymer melt viscosity on processibility and to quantify the influence of processing parameters on melt rheology inside the extruder.

#### D. Polymer degradation mechanism and kinetics

- To elucidate polymer degradation mechanisms using a systematic approach.
- To design thermal and degradation rheology based kinetic modelling to predict polymeric properties at different processing temperatures.
- To assess the implications of plasticisers both on degradation mechanisms and kinetics of pure polymers and their relevance to HME.

### **1.2 Thesis outline**

Chapter 2 provides a background to the work; the literature being divided into four sections:

1. The role and applications of pharmaceutical excipients, including the need for modified and new polymers for this emerging technology.
2. HME is discussed including operating principles, relevant equipment the extrusion process and critical processing variables of HME.
3. A comprehensive overview of cellulose ester derivatives with detailed descriptions on commercial synthesis, material properties, applications and the present limitations of HPMCAS and HPMCP in HME is discussed.
4. The techniques involved in characterisation of excipients including:
  - i. Thermal and thermo-chemical properties
  - ii. Thermodynamic properties (polymer miscibility-solubility studies).
  - iii. Polymer-melt rheology (role of melt rheology and measurement techniques).

- iv. Thermo-mechanical degradation kinetics of polymers (thermal and rheology based kinetic modelling).

Chapter 3 provides details of the materials and methods used in the current work while Chapter 4 contains the results and discussion of polymeric properties, divided into four sub sections:

1. Material properties of pure and blends of polymers (plasticisers and APIs). This chapter focuses on four major properties: thermal, thermodynamic (fragility parameter, miscibility solubility studies and construction of phase diagrams), melt rheological and thermo-chemical stability of polymeric samples at preformulatory stages.
2. HME of polymeric samples and processing attributes. In this section, the influence of polymeric properties on processibility and simultaneously the influence of processing parameters on material properties, especially polymer melt flow behaviour inside the extruder is discussed.
3. Characterisation of melt extrudates. This section correlates properties of polymer melt extrudates with that of fundamental properties of polymeric samples and processing attributes of HME. Further, it majorly targets at thermo-chemical properties of melt extrudates for chemical interactions.
4. Polymer degradation mechanism and kinetic modelling. In this chapter, degradation mechanisms of polymers are suggested. A time dependent thermal and rheological stability of polymeric samples is modelled for degradation kinetic studies. Additionally, influences of plasticisers on both polymer degradation mechanism and kinetics are highlighted.

Chapter 5 provides an overall summary of the work and conclusions of the work presented in this thesis. Chapter 6 provides information about future work followed by list of references cited for the current work and appendix sections.

## Chapter 2. Background

This chapter includes an introduction to pharmaceutical excipients and applications of excipients in product development and processing. It provides details about Hot Melt Extrusion (HME) including critical processing attributes, excipients or polymers and plasticisers used in HME and their implications on product and process quality attributes. In this work, special attention has been given to two cellulose ester derivatives, HPMCAS and HPMCP.

### 2.1 Pharmaceutical Excipients

An excipient can be found in every therapeutic product and is normally added to the formulation to increase the bulk of the active preparations. Excipients are traditionally considered as stable materials which act simply as a vehicle to release the Active Pharmaceutical Ingredient (API) from the formulation. APIs are not generally administered directly into the body and are often modified into the formulation with the aid of excipients. The mass of excipients utilised in the formulation is normally greater than that of active ingredients. Therefore, an excipient is one of the major contributing parameters of formulation development.

The major role of excipients in drug formulations is to protect and support it. Moreover, it helps in the manufacturing and development of dosage forms by improving the processibility of the API. Looking at these functionalities, the United States Pharmacopeia National Formulary (USP-NF) defined excipients as, *"substances other than the active drug or finished dosage form, that have been appropriately evaluated for safety and are included in drug delivery systems 1) to aid in the processing of the drug delivery system during its manufacture; 2) to protect, support, or enhance stability, bioavailability or patient acceptability; 3) to assist in product purification; or 4) to enhance any*

*other attribute of the overall safety, effectiveness or delivery of the drug during storage or use"* (Pharmacopeia, USP29-NF24). Thus, it can be understood that excipients are not only added to increase the bulk of the formulation but are intentionally added to the formulation to increase the quality of the dosage form (Pifferi and Restani, 2003).

Excipients have been classified in a number of ways however; broadly their choice of selection can be classified into two major categories:

- a) Product performance: In solid orals, they are mainly used as binders, fillers, lubricants, disintegrating agents, preservatives and plasticisers. Whereas in liquid dosage forms they are widely used as solvents, co-solvents, anti-microbial, emulsifying agents, colouring agents, pH modifiers and rheological modifiers (Crowley *et al.*, 2002 , Ghebremeskel *et al.*, 2006 , Kemsley, 2014)
- b) Processing attributes: Aqueous, non-aqueous or organic solvent solubility, particle size-shape-distribution properties, flow properties, polymer molecular weight, degree of substitution, swelling properties, thermal properties (melting point, glass transition, recrystallisation and degradation temperature), solution or melt rheology and downstream properties (Kemsley, 2014 , Marshall Steinberg, 2001 , Nachaegari *et al.*, 2004).

Over the years, excipients have evolved from natural to synthetic origins in order to fulfil the different functionalities both in terms of product performance and processibility in different manufacturing technologies (Pifferi and Restani, 2003 , Ali, 2010) (see Figure 2.1). Therefore, the demand for tailor-made excipients (modified, new or novel excipients) has increased significantly with emerging novel pharmaceutical technologies. Modified or new excipients are generally derived from modifications of previous excipients or synthesis of completely new excipient by combinations of two or more structurally independent moieties. However, it is important to note that one of the primary

requirements of pharmaceutical excipients is their inertness in the formulation whilst having an acceptable safety profile. Therefore, while synthesising new excipients, their purity should be strictly monitored.

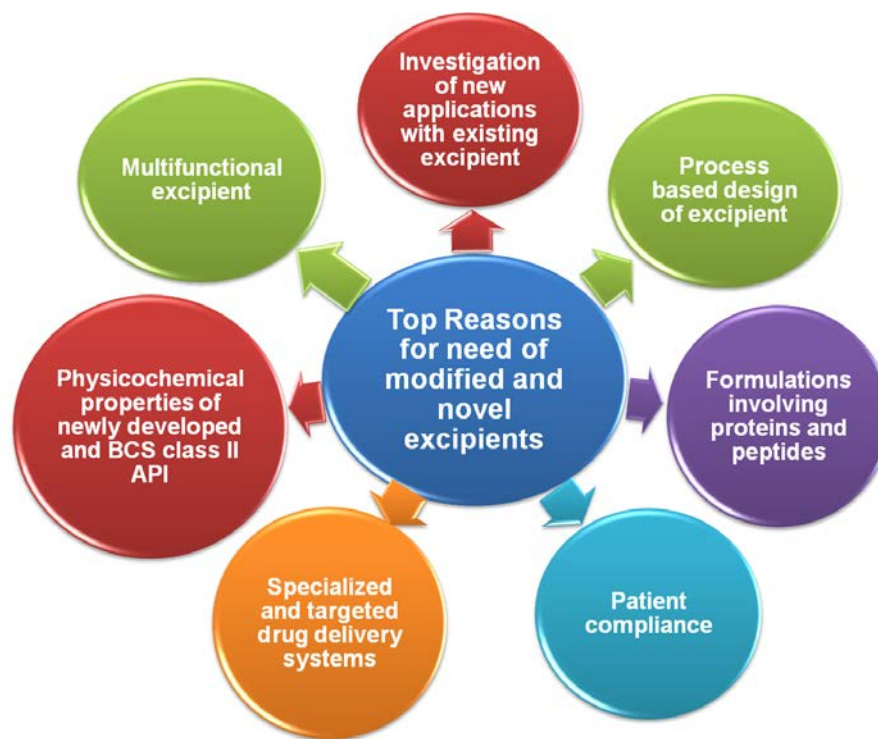


**Figure 2.1 : The need for modified and novel excipients.**

A mandatory requirement of regulatory authorities is that pharmaceutical companies must thoroughly (and expensively) investigate the toxicity profile of an API. It could be argued, the investigation of the same for excipients has been less stringent (Nachhaegari et al., 2004 , Pifferi and Restani, 2003 , Kemsley, 2014). In order to formulate a robust formulation, screening of individual components within the formulation is required. Therefore, modified or newly synthesised polymers should be screened as thoroughly as the active ingredients. Considering these facts, the International Pharmaceutical Excipients Council (IPEC) has announced guidelines for excipients which clearly state that "it is important to perform risk-benefit assessments on proposed new excipients in drug products and to establish permissible and safe limits for these substances" (IPEC, 2013).

An excipient can be categorised into three categories: (a) conventional excipients (or well-established or food grade excipients), (b) structurally modified excipients (essentially new but derivatives of conventional excipients) and (c) novel excipients (Pifferi and Restani, 2003). Literature reports suggest that the excipients from categories (b) and (c) are the most prevalent dosage forms, especially in the field of solid orals (Pifferi and Restani, 2003) (Table 2.1). Note that the list provided in the table 2.1 is not an exhaustive list but just a reference to give an idea about most popular excipients from categories (b) and (c) used recently for pharmaceutical applications. A more exhaustive list can be found elsewhere in the literature (Patel, 2011 , Moreton, 2010). In the case of modified excipients, a well-established conventional polymer is generally modified in order to achieve the desired physicochemical characteristics. A highly pure polymer (here onwards an excipient is replaced with a term, polymer) with minimal related impurities can be utilised with different APIs to increase the stability of the dosage form. Typical examples of modified excipients include HPMC, HPMCAS and HPMCP from Shin-Etsu and Kollidon® VA 64 from BASF which have been widely used as binding agents, film forming agents, in coatings and in targeted drug delivery systems.

Novel excipients offer opportunities where a well established drug can be reformulated and dispensed with better functionality whilst maintaining the quality of the formulation. However, investigation of novel excipients requires sizable investments of time and money; and excipient manufacturers are investing in new excipients though few have been successful in deriving novel polymers. For instance, recently, BASF has marketed a novel excipient called Soluplus® (polyvinyl caprolactam-polyvinyl acetate-polyethylene glycol graft co-polymer) which is targeted particularly at the melt extrusion process (Djuris et al., 2013 , Ali, 2010). Similar to Soluplus®, BASF also designed Kollicoat® Smartseal 30 D (co-polymer comprising of methyl methacrylate and

diethylaminoethyl methacrylate) exclusively for solid orals for taste masking and moisture protection. In summary it can be seen that pharmaceutical excipients have an important role in formulation development and during formulation, selection of excipients, their material properties must be considered along with an API to produce rational dosage form.

**Table 2.1: Applications of modified and novel excipients in dosage forms.**

<b>No.</b>	<b>Name of excipient and <u>manufacturer</u></b>	<b>Benefits</b>	<b>Applications</b>
1.	Pharmacoat® and Metolose® ( <u>Shin-Etsu Inc</u> )	Binder for granulation	Fluidized bed granulation and high shear mixer granulation, sustained release dosage form, taste masking, solid dispersion
2.	Flowlac® 100 ( <u>MEGGLE Group Wasserburg BG Excipients &amp; Technology</u> )	Direct compression technique. Very good flow property since the grains are spherical in nature	Tablets of low doses, effervescence tablets and filling of capsules
3.	Kollicoat® sr 30 d ( <u>BASF</u> )	Matrix retarding agent, film former, stabiliser	Direct compression, pH-independent sustained-release
4.	Silicified microcrystalline	Direct compression, wet and dry granulation	Multifunctional excipient
5.	Plasdone s-630 ( <u>Ashland Inc</u> )	Direct compressible excipient. Higher compressibility, soluble in water, viscosity modifier	Drug granulation, wet granulation
6.	Emdex® ( <u>JRS PHARMA LP, USA</u> )	Binder, highly water soluble	Chewable tablets, taste masking
7.	Vivastar® ( <u>JRS PHARMA LP, USA</u> )	Super disintegrant	Tablet formulations
8.	AQOAT® and HPMCP® ( <u>Shin-Etsu</u> )	Coating agents	Enteric dosage forms, solid dispersions,

9.	Prosolv smcc® ( <u>JRS PHARMA LP, USA</u> )	Enhanced lubrication and blending property. High compactibility	Oral dispersible tablets. Extra-granular filler
10.	Ludiflash® ( <u>BASF</u> )	Filler, binder and disintegrant	Oral disintegrating formulations
<ol style="list-style-type: none"> <li>1. (Kokubo, 2008 , Ghosh <i>et al.</i>, 2011 , Pasztor <i>et al.</i>, 2011 , Mako <i>et al.</i>, 2009)</li> <li>2. (Kaialy <i>et al.</i>, 2012 , Harjunen <i>et al.</i>, 2002)</li> <li>3. (Shao <i>et al.</i>, 2002 , Elkordy <i>et al.</i>, 2013)</li> <li>4. (Aljaberi <i>et al.</i>, 2009 , Luukkonen <i>et al.</i>, 2001 , Tobyn <i>et al.</i>, 1998 , Edge <i>et al.</i>, 1999)</li> <li>5. (Bejugam <i>et al.</i>, 2009 , Casana <i>et al.</i>, 2010)</li> <li>6. (Olmo and Ghaly, 1999)</li> <li>7. (Remya <i>et al.</i>, 2010 , Wu <i>et al.</i>, 2011a)</li> <li>8. (Kokubo, 2008 , Siepmann <i>et al.</i>, 2006b , Tanno <i>et al.</i>, 2004)</li> <li>9. (Gowda <i>et al.</i>, 2014 , Jin and Tataavarti, 2010 , Staniforth, 2003)</li> <li>10. (Roblegg <i>et al.</i>, 2011 , Valducci <i>et al.</i>, 2010)</li> </ol>			

## 2.2 Hot Melt Extrusion

The Hot Melt Extrusion (HME) process is one of the emerging manufacturing processes in pharmaceutical technology and has a number of advantages (listed below) over standard processing techniques.

The extrusion process was applied for the first time in pharmaceuticals in 1969 by Rippie and Johnson (Rippie and Johnson, 1969) who investigated ram extruded Cellulose Acetate Phthalate (CAP) pellets to study the effect on dissolution rates of drugs based upon pellet geometry. Since then HME has been investigated for the production of pellets, (Follonier *et al.*, 1995 , Follonier, 1994), sustained release tablets (James and Feng, 2003), floating tablets, transdermal drug delivery systems (Prodduturi *et al.*, 2005), solid dispersions (Six *et al.*, 2003a), implants (Rothen-Weinhold *et al.*, 2000) and is proving its applicability over conventional manufacturing processes of dosage forms. A key advantage of HME is its continuous and solvent free production capability hence it is receiving great attention from industry.

### 2.2.1 Principle, equipment and process of HME

HME converts a mixture of powders (or other solid products) into a defined product shape through an intermediate melt phase (Crawford, 1998). HME involves pumping of the raw materials under elevated temperatures allowing for distributive and dispersive mixing, before forcing the molten product through a die to form a uniform shape.

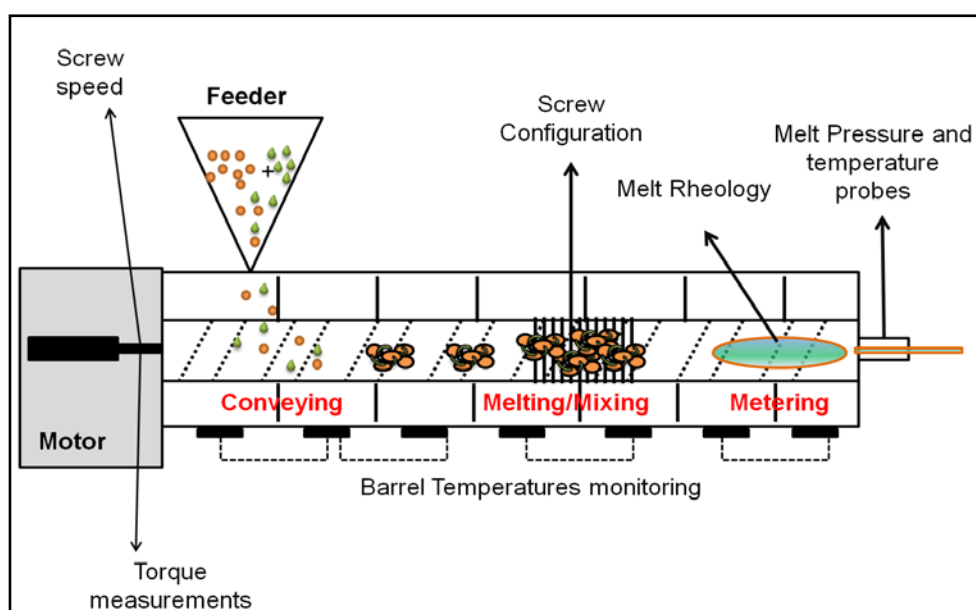


**Figure 2.2: Schematic representation of melt extruder and its process.**

Literature studies suggest HME can be broadly divided into two categories: ram extrusion (vertical extrusion) and screw extrusion. Screw extrusion is widely investigated in various pharmaceutical as well as in the plastic industries. Ram extrusion is a positive displacement technique where a piston pressurises the material placed in a heated barrel, where it softens or melts before passing through the die, transforming to the required shape (Kurtz et al., 2006). Screw extrusion consists of rotating screws inside a heated barrel which generate shear and energy causing the material to melt before being delivered to the die for final shaping (Crowley et al., 2007b). Both extruder designs have advantages and disadvantages which can be found in other articles (Nakamichi K. et al., 2002 , Bruno Paillard et al., 2011 , Isaac Ghebre-

Sellassie and Martin, 2003 , Hampson and Manley, 1976) but screw extrusion is a more common choice since it can provide higher shear stresses, better mixing ability, more uniform temperatures and continuous processing.

**Table 2.2: Single screw and twin screw extrusion characteristics.**

<b>Single screw extrusion</b>	<b>Twin screw extrusion</b>
Simple profile extrusion	Complex type of extrusion
Fair mixing of the materials	Very good mixing
Less efficient and expensive process	Efficient and more expensive process
Do not possess self wiping	Self-wiping capacity
Longer residence of time	Shorter residence of time
Not applicable	Co-rotation and counter rotation
Fixed screw design	Reconfigurable screws

The extrusion process is divided into several parts such as feeding section, hopper, barrels, mixing screws, heating zones and die for shaping the molten extrudate (Figure 2.2). Shear is controlled by varying the screw speed or using different screw configurations. Typically, extrusion offers two configurations: single screw and twin screw. Single screw extrusion is the most basic form of extrusion using pre-prepared compounds for extrusion. Twin-screw extruders provide more uniform mixing for simultaneous addition of two or more different components and can provide increased shear to the material. As it provides controllable mixing, it can offer addition of reactive agents (liquid or gaseous) inside the extruder to carry out branching and polymerisation reactions (Raquez et al., 2008). Twin-screw extruders have inherent design and operating characteristics to provide a number of process variables in terms of screw configurations or design and can provide a number of functions in a single instrument. Comparative advantages and disadvantages of single and twin screw extruder systems are shown in Table 2.2.

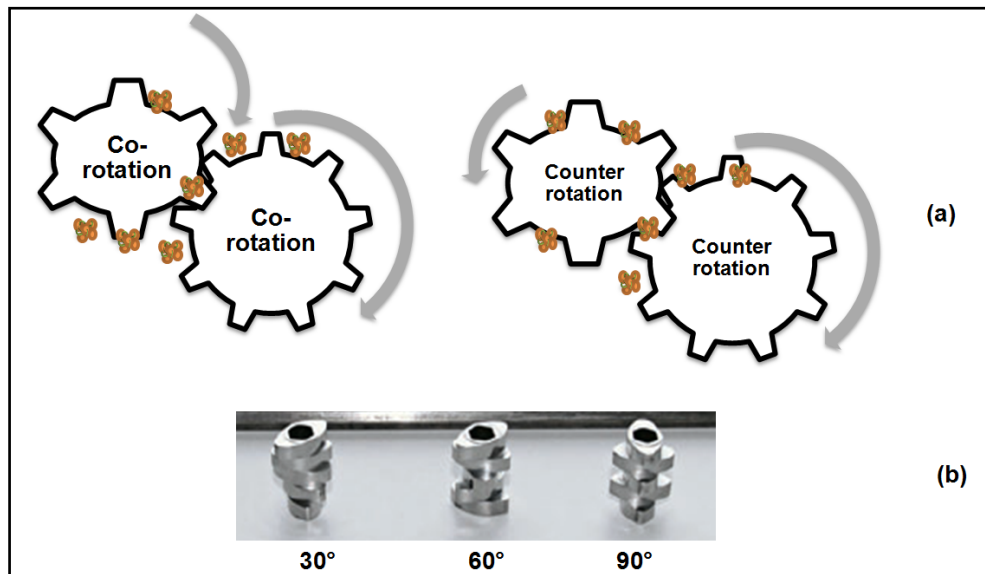


**Figure 2.3: (a) Screw rotations (b) angles of kneading elements.**

Twin screw extrusion offers two kinds of screw rotations which are classified into co-rotating and counter rotating (Figure 2.3). Co-rotating screws are widely used since they can be run at higher screw speeds than counter-rotating screws. Speeds can reach up to 1000 rpm and thus high outputs can be gained. Moreover since the rotations are in the same directions, screw abrasion is reduced compared to counter rotating screws (Isaac Ghebre-Sellassie and Martin, 2003). However, the co-rotating design offers lower shear which can be limiting (Isaac Ghebre-Sellassie and Martin, 2003). This contrasts with the conveying characteristics and layout of counter rotating screws. During processing, whenever the material falls between the gaps of counter rotating screws, energy is dissipated and high localised shear forces are experienced. These shear forces generate high torque within the extruder barrel, thus high shear, which can lead to wear and tear of the extruder parts and potential material degradation hence counter rotating screws are generally run at lower screw speeds. This configuration can also provide significant air entrapment in materials therefore counter rotating screws, although providing uniform material temperature and residence time of the extrudates are not widely

preferred configurations for HME, especially in pharmaceutical developments (Isaac Ghebre-Sellassie and Martin, 2003). There are hardly any reports which cite use of counter rotating screws in the development of HME based pharmaceutical formulations.

Further, kneading elements also play an important role in the HME, especially in terms of mixing and melting of the materials. Uniform mixing of the materials is one of the critical parameters of HME and mixing abilities of the materials can be modified by changing the configuration of kneading elements. Generally, kneading elements are arranged at three angles, 30°, 60° and 90° (Figure 2.3) for plasticising, mixing, dispersing and distributing purposes (Isaac Ghebre-Sellassie and Martin, 2003). Moreover, these angles play an important role in the direction of the mixing such as forward, backward and neutral mixing. Angle 30° offer both forward and backward mixing movements whereas 60° aids in forward movement and 90° neither show forward nor backward movement of the materials. The precise nature of the forward backward mixing mechanism of screws is not discussed in the current work since it is not the focus of the thesis. More detailed descriptions can however be found in the text book, "Pharmaceutical Extrusion Technology " (Isaac Ghebre-Sellassie and Martin, 2003) .

The configuration of screw elements not only exerts pressures and movement of materials but also affects two important mixing mechanisms: dispersive and distributive mixing (Sakai and Thommes, 2014 , Isaac Ghebre-Sellassie and Martin, 2003 , Gogos et al., 2012 , Alemaskin et al., 2004). Dispersive mixing is defined as the process where solid agglomerates and particles are broken down whereas distributive mixing ensures the homogenous distribution of components within the mixture. During dispersive mixing, materials get trapped between the screw elements. This exerts

pressure on materials (shears) to undergo melting and materials begin to elongate in the direction of applied shear. Whereas distributive mixings do not make changes in the morphology of a polymeric system, thus negligible shear stresses are involved. Angle of screw flights also affects these mixing mechanisms where larger angles (90°) provide intense mixing while smaller angles (30°) display distributive mixing.

### **2.2.2 Extrusion process**

The screw of a conventional twin screw extruder has two zones (feeding and extrusion zone) related to the geometry of screw barrel. Inside the extruder, the screws are aligned with the motor, which facilitates rotation of the screws, imparting shear into the system.

- (a) Feeding zone: The first section beneath the hopper is called the feeding zone and transfers the material (generally a mixture of powder and/or granules) into the barrel of the extruder. Material is fed through the hopper at a constant rate where it falls on the screw(s).

The extrusion zone can be sub-classified into the conveying zone, molten mass transfer zone (metering and distribution zone) and die zone.

(b) Extrusion zone

- *Conveying and mixing elements*: The solid material from the hopper is conveyed to the mixing zone where it experiences additional shear and generates heat in addition to the temperature imposed, melting or softening of the material (Breitenbach, 2002).
- *Molten mass transfer*: Molten material is then transferred to the metering zone, where the melt flow is stabilised before it comes out of the die. The molten mass transfers here via a helical path (Rina Chokshi, 2004 , Crowley *et al.*, 2007b). The melt experiences different pressures during

flow and a homogeneous form of molten mass reaches the metering zone. During extrusion, pulsating flow can occur, a result of lack of feed consistency or improper mixing of the materials. The metering zone functions to dampen the pulsating flow (Breitenbach, 2002).

- *Die*: the molten mass from the metering zone is extruded through the die and can be further subjected to downstream processes such as milling, pelletizing or cutting to convert it into final dosage form.

### **2.2.3 Important variables of melt extrusion process**

Processing variables have a significant impact on the quality of any formulation and a precise understanding of these variables is key for a successful formulation. It also applies to HME however; it requires extra care, particularly in terms of melt flow properties, component miscibility and thermo-mechanical degradations, compared with conventional techniques. Additionally, the design and process of extrusion is relatively complex which further requires close monitoring and understanding of the process variables. For instance, variables such as type of feeders, feed rates, screw speeds, screw design, set temperatures (see Figure 2.4) have direct links with materials properties such as component miscibility, melt flow, melt stability and most importantly shear-temperature induced degradation of materials. Therefore, some important processing variables influencing HME processibility are discussed briefly.

The first step of the melt extrusion process is introduction of materials (feeding) to the extrusion barrel. Empirically, the process of the material falling onto the screws and being transported through the extruder should be continuous and smooth since variability in feed rate causes unstable flow and subsequently causes improper output from the die. Feeding is dependent on raw material properties, hopper design and extruder type. Material properties such as particle size, density, particle shape and particulate interactions significantly affect the feeding process

especially in the case of single screw extruders since the conveying mechanism depends on the 'frictional relationship between the raw materials and extruder surface' (Isaac Ghebre-Sellassie and Martin, 2003). In contrast, the feeding process to twin screw extrusion (TSE) is less affected by the material properties since the conveying mechanism differs from the single screw extruders (SSE). Often, TSE comes with an independent metering device and this facility with TSE gives an additional advantage over SSE since pharmaceutical materials with a wide range of powder flow properties can be introduced via these metering devices.

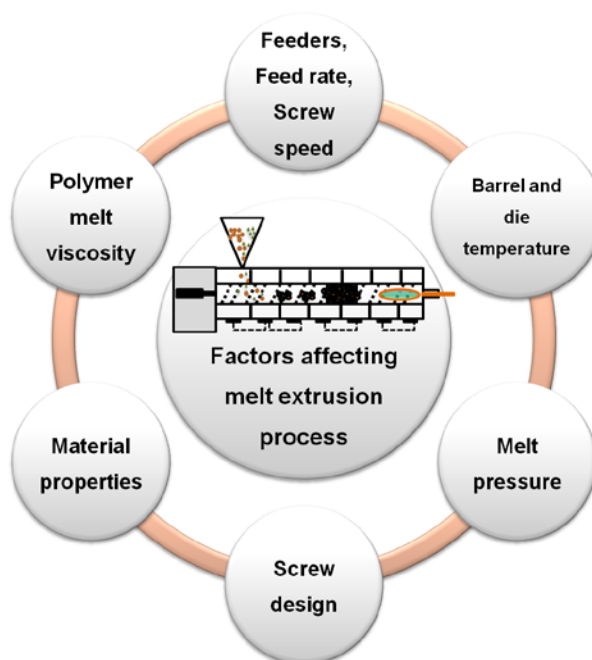


**Figure 2.4: Important monitoring parameters of melt extrusion processes.**

Other important parameters are feed rate and screw speeds which determine the level of material fill inside the extruder ensuring smooth and continuous flow. With a given constant screw speed and feed rate, the molten mass is transferred at a constant speed. These factors significantly affect motor load and melt pressure, in other words these two parameters influence the shear stresses within the extruder. The set barrel temperature is dependent on the glass transition temperature ( $T_g$ ) or melting point ( $T_m$ ) of the excipients/polymers and drugs. The

optimum barrel temperatures maintain smooth flow of molten mass transfer inside the extruder. Melting efficiency of polymers varies with polymeric properties; however, they can be manipulated with the arrangement of screws and with a series of set temperatures inside the extruder. Electrical heating zones and shear between the rotating screws generate thermal energy inside the extruder and within the materials. Moreover, different configurations of screws impart a variety of shear on the material that can melt the material quickly and facilitate smooth melt flow with an increase in melting efficiency.

Extrusion processing conditions are also dependent upon the chemical stability of the materials. Inherent polymer properties such as molecular weight,  $T_g$ ,  $T_m$  and degradation temperature are rate-limiting properties for quality based HME products. Thus, an understanding of material properties is one of the prerequisite factors of melt extrusion. Generally low melt temperature polymers are considered to be best for the extrusion process since processing temperatures of extrusion can be significantly reduced and degradation of the drug or any deterioration can be prevented. However, in the case of high  $T_g$  polymers, plasticizers and other additives are often included in the formulation (James and Feng, 2003).

### **2.3 Polymers and plasticisers used in HME**

HME dosage forms are composite mixtures of an API and different functional polymers or excipients where selections of these polymers are made via a desired set of functionalities. Generally low melting polymers are considered to be best for the extrusion process since processing temperatures can be lowered and degradation of the materials can be prevented. However, in the case of high melting polymers and to avoid material degradation, additives (plasticisers) are generally added to the formulation. A plasticiser increases molecular mobility, decreases glass transition temperature or melting point of the mixture and thus, extrusion temperatures can be lowered. Additionally these plasticisers are also

known to modify release kinetics of drug, melt viscosity of the polymer and they can be utilised in formulations as an antioxidant or as a solubility enhancer.

A variety of excipients have been utilised in pharmaceutical melt extruded systems and most commonly utilised excipients in the majority of melt extruded systems are summarised in the current work. Certain well-established pharmaceutical polymers such as hydroxypropyl methylcellulose (HPMC), polyethylene glycol (PEG), polyvinylpyrrolidone or povidone (PVP), polyethylene oxide (PEO) and methyl 2-methoxyprop-2-enoate (Eudragit®) etc have been investigated as carriers/excipients for emerging HME technology. Based on the physico-chemical properties, certain water-soluble polymers (e.g. polyethylene glycols, urea) or hydrophobic carriers (Eudragit®) have been investigated for their effect on the preparations of granules or pellets or solid dispersions (Sinha et al., 2010). Similarly, target specific polymers such as hydroxypropyl methylcellulose phthalate (HPMCP), hydroxypropyl methylcellulose acetate succinate (HPMCAS) have been extruded for enteric drug delivery and sustained release dosage forms. Moreover, other polymers such as, polyvinyl alcohol (PVA), polyvinylpyrrolidone-polyvinylacetate copolymer (PVP-PVA), crosspovidone (PVP-CL), hydroxypropyl cellulose (HPC) have been investigated for stabilising the API in the extruded matrix (Six et al., 2003b), sustained and immediate dosage forms (Leuner and Dressman, 2000). Similar to these excipients, a variety of FDA approved plasticisers such as citrates (triethyl citrate, citric acid, acetyl triethyl citrate), phthalate esters (diethyl phthalates, dibutyl phthalate), fatty acid esters and glycol derivatives (propylene glycol, polyethylene glycols) have been investigated for HME.

In the past, different natural or semi synthetic polymers were utilised in HME based formulations. However to meet different functionalities, process based excipients have been explored in the recent years for various emerging

manufacturing technologies. For instance, BASF Inc developed a novel polymer called Soluplus® and next generation AFFINISOL™- HPMC from DOW which is marketed to be better polymers available for pharmaceutical HME processing. Soluplus® has been utilised in various melt extruded solid dispersion based on its solubilising properties, ability to form solid dispersions and extrudability properties (Ali, 2010 , Djuris et al., 2013 , Maniruzzaman et al., 2013 , Tian et al., 2013). Chemically it is a polyvinyl caprolactum-polyvinyl acetate-polyethylene glycol graft polymer which possesses amphiphilic characteristics for increase in solubility of poorly-water soluble drug and at the same time because of its low glass transition temperature and better flow properties, it is considered to be ideal for HME.

Despite the applicability of Soluplus®, it is interesting to note that it is the only new polymer (AFFINISOL™ is not investigated extensively till to date for HME applications) in the market which is claimed to be ideal for pharmaceutical HME. However, majority of HME based formulations commercially available and studied in the literature are manufactured by modified excipients (Maniruzzaman et al., 2012). The choice of modified polymers is attributed to following the reasons. According to latest guidelines of IPEC, new chemical excipients are treated as a new API where the regulatory bodies demand safety aspects of newly developed excipients. The evaluation of a new excipient requires considerable amounts of money and excipient discovery-development is a relatively time consuming process. Moreover, new excipients should meet the pharmacopeial requirement (IPEC, 2013). In contrast, modified excipient strategies have been the most successful in the pharmaceutical industry over the years. Modified excipients are manufactured by derivatising certain groups of the existing polymers keeping the backbone constant. Thus, although modified polymers possess different structure and physicochemical properties, development of modified excipients is considered to be economical and tailoring the properties of these excipients is relatively simple.

One of the best examples of modified excipients is cellulose derivatives. The applications of cellulose derivatives in conventional as well as in novel or emerging technologies are well known both academically and commercially. Cellulose is a natural, straight chain semi-crystalline polymer. It is insoluble in water, though it is hydrophilic in nature. Cellulose is available in the market in different grades based on the mechanical and desired pharmaceutical properties such as size, shape, degree of crystallinity etc. Chemically, cellulose offers various hydroxyl sites which can be further derivatised into respective esters and ether moieties. For example, modified cellulose derivatives such Hydroxypropyl Methylcellulose (HPMC), Cellulose Acetate Phthalate (CAP), Methyl Cellulose (MC), Hydroxypropyl Cellulose (HPC), Hydroxypropyl Methylcellulose Phthalate (HPMCP), Hydroxypropyl Methylcellulose Acetate Succinate (HPMCAS) and Hydroxypropyl Cellulose (HPC) have been investigated widely in a variety of manufacturing techniques.

It is interesting to note that out of several modified cellulose ester derivatives, HPMCAS and HPMCP attracts most interest by researchers in melt processes. Both polymers have been studied for improvement of water solubility of poorly water soluble APIs, enteric drug delivery, stabilising the API in the extruded matrix (Six et al., 2003b), sustained and immediate dosage forms (Leuner and Dressman, 2000). However despite of their usefulness, these two polymers are criticised for their thermolabile properties. Thus, polymeric properties of HPMCAS and HPMCP suitable for HME applications are largely still unclear. Since the current research work is focused on investigating suitability of these polymers in the melt extrusion system; a detailed review of literature discussing polymeric properties including their applications and limitations is presented in the section 2.3.1.

### **2.3.1 Overview of cellulose ester derivatives: HPMCAS and HPMCP**

#### *2.3.1.1 Commercial synthesis of polymers*

HPMCAS and HPMCP polymers are ester derivatives of hydroxy methylcellulose (HPMC) or Hypromellose, while HPMC is an ether derivative of pure cellulose. Schematic representations of the synthesis of both polymers can be found in the brochures of Shin-Etsu manufactured HPMCAS and HPMCP (Shin-Etsu, 2009) and are represented in Figure 2.5.

As shown, the synthesis of HPMCAS and HPMCP uses a chemical derivatisation process (Figure 2.5). The manufacturing process involves a series of chemical reactions. Production of HPMCAS and HPMCP involves three major steps: Etherification of cellulose pulp, reactions with acids and precipitation-purification of the pure polymers. Firstly, cellulose pulp collected from natural sources is washed several times with water to remove any unwanted material and this pulp then undergoes an etherification reaction where free hydroxyl groups present on  $\beta$ -glucose sub-units of the cellulose back bone are converted into ether derivatives to form a pure mass of HPMC. This HPMC is further derivatised in to its ester forms while in the case of HPMCAS, acetyl groups are esterified on either of the hydroxyl group of HPMC while succinoyl groups being esterified on the other hydroxyl group by reacting the mixtures of HPMC with respective acid anhydrides. The reaction continues until the entire anhydride reacts with HPMC reactive mixtures with the final polymer being precipitated and purified with water and then typically packaged in the powdered form.

Similarly, HPMCP possesses ether linkages and hydroxypropoxy units in the long chain of polymer. However in this case, the hydroxyl groups of the HPMC backbone are esterified with phthalic acid derivatives and further procedures of the precipitation-purifications are the same for HPMCP. The detailed synthetic

procedures for HPMCAS and HPMCP can be found in the Shin-Etsu patent US 4226981 A (Onda et al., 1980).

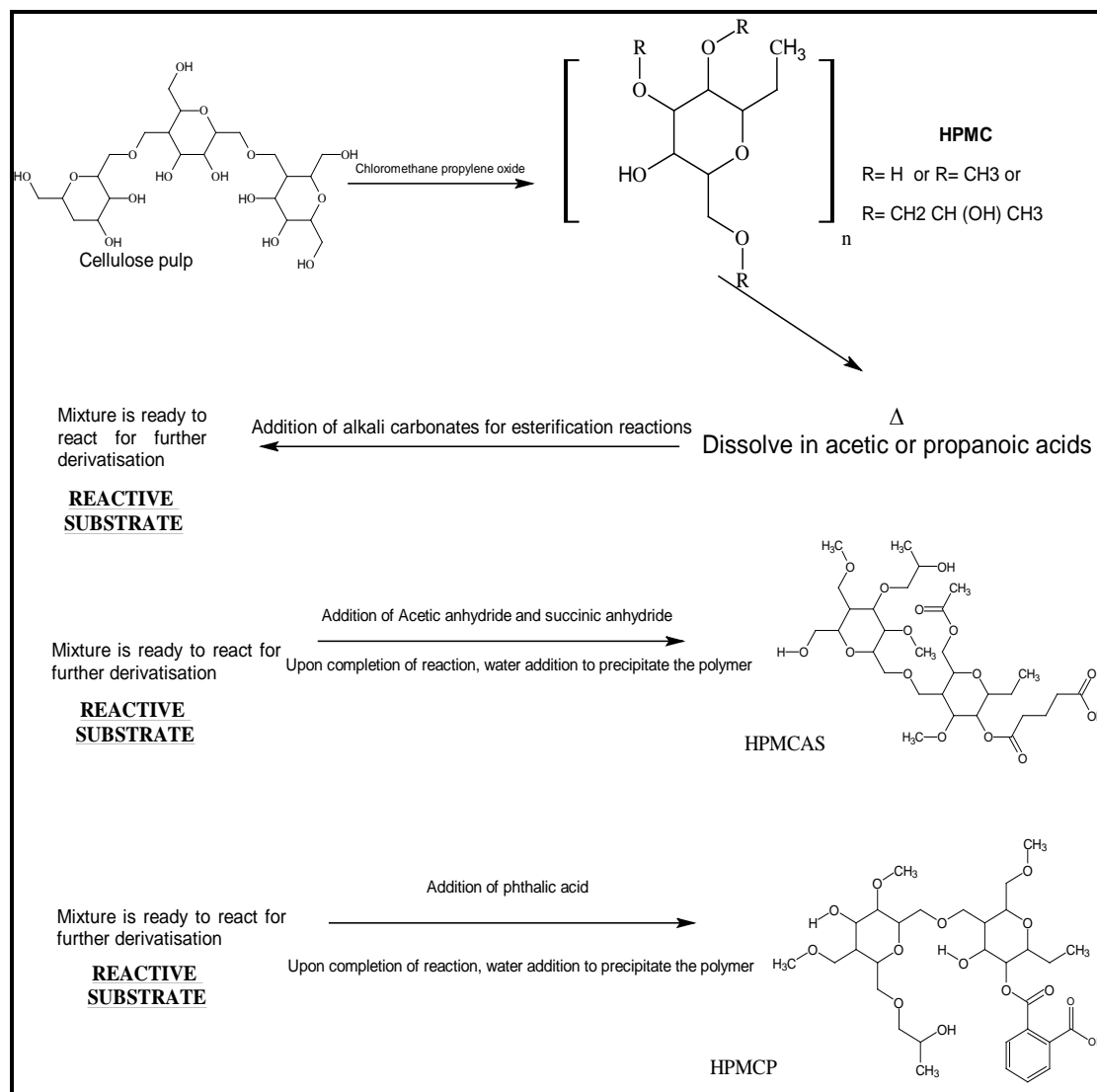


Figure 2.5 Commercial synthesis of HPMCAS and HPMCP (Shin-Etsu, 2009).

### 2.3.1.2 Material properties of polymers

In the current section, the important material properties of both HPMCAS and HPMCP are discussed as reported in the literature. Shin-Etsu manufactured HPMCAS and HPMCP are available in different grades (Table 2.3) with the material properties being dependent on the degree of substitutions of the chemical substituent.

**Table 2.3: Degree of substitutions of polymers (Shin-Etsu, 2009).**

<b>Grade</b>	<b>Methoxyl (Wt %)</b>	<b>Hydroxy propoxyl (Wt %)</b>	<b>Acetyl (Wt %)</b>	<b>Succinoyl (Wt %)</b>	<b>Phthalyl (Wt %)</b>	<b>pH dependent water solubility</b>
HPMCAS-L	22.3	7.1	7.6	15.36	-	≥5.5
HPMCAS-M	23.2	7.6	9.06	11.26	-	≥6.0
HPMCAS-H	23.8	7.8	11.8	6.03	-	≥6.8
HPMCP-HP50	22.3	7.1	-	-	22.5	>5
HPMCP-HP55	19.3	6.2	-	-	33.3	>5.5
HPMCP-HP55S	19.1	6.2	-	-	33.0	>5

Commercially, HPMCAS is available in 3 different grades which are classified based on the acidic substitutions of acetyl to succinoyl ratio, whereas different degrees of substitutions of phthalyl groups provide 3 different grades of HPMCP polymers. HPMCAS is divided into 3 grades such as L, M and H grades where the acetic substitutions increases and succinic acid substitutions decreases from L to H grades, whereas in the case of HPMCP, the percentage of phthalyl substitutions increases from HP50 to HP55 grade (Table 2.3). Moreover, these grades also vary based on the particle size of the polymer. HPMCP is often supplied in a granular grade and the flow properties of the HPMCP polymers are deemed suitable for melt extrusion. HPMCAS grades are further divided into granular grade (G) and fine grade (F) for supply to specific applications.

Shin-Etsu claim the granular grades of HPMCAS are specifically meant for pharmaceutical coating solutions since fine grades requires a long time to dissolve in the solvents and are also reported to form 'lumps' in organic solvents (Shin-Etsu, 2009). Selection of the granular or fine grades of HPMCAS for HME is an important criterion in preformulation since both grades have individual advantages and disadvantages. Granular HPMCAS produces better flow properties however,

since the particle size of the granular grade is significantly higher, attainment of uniform mixing with most of the APIs can be a challenge for granular grades (Shin-Etsu, 2009). On the other hand, although the fine grade allows for uniform mixing with the added API, its poor flow properties and high surface area can produce bridging effects at the neck of the extruder barrel (Shin-Etsu, 2009).

Organic and pH dependent solubility of HPMCAS and HPMCP polymers are considered as two of the major advantages for their uses in pharmaceuticals. HPMCAS-LG or HPMCAS-LF dissolve in water at pH  $\geq 5.5$  and subsequent grades MF and HF dissolve at pH  $\geq 6$  and  $\geq 6.8$  respectively. On the other hand, HPMCP polymer dissolves at pH  $\geq 6.0$  and  $6.8$ . Moreover, HPMCAS is insoluble in ethanol, hexane and chloroform but it is soluble in acetone or methanol. HPMCP on the other hand shares a similar solubility profile but; it offers solubility in a wider range of organic solvents compared to HPMCAS. Additionally, although both polymers are hydrophobic in nature, interestingly they show some moisture uptake when exposed to different relative humidity environments (unbound water). It has been claimed that HPMCAS-LF uptakes moisture up to 5-8% whereas the other two grades shows lesser uptake. On the other hand HPMCP polymer uptakes moisture in the range of 2-10% which is higher than HPMCAS at 90% relative humidity.

Mechanical properties of both polymers are also widely discussed in the literature. HPMCAS and HPMCP have been used in solvent evaporation techniques because of their ability to form a film with better mechanical properties compared to other polymers. Recently, molecular solid dispersions of Posaconazole-HPMCAS have been prepared by a solvent evaporation technique giving excellent mechanical properties of SD suitable for further downstream processes such as milling (Fang et al., 2011). The tensile strength of the HPMCAS films falls between 35-45 MPa from L to H grade with a modulus of more than 1500 MPa and elongation values 10-20% (AquaSolve-AS). Recently, mechanical

properties of virgin and processed HPMCAS (by HME and spray drying) were compared against commonly used excipients such as microcrystalline cellulose (MCC) and lactose monohydrate (Iyer et al., 2013). It was observed that HPMCAS required a low compression force (CP) and exhibited a higher tensile strength than corresponding excipients at its 'as-is' conditions during tableting process. Interestingly when HPMCAS was processed by spray drying and HME, compression force was increased compared with 'as-is' values and the values were in order of 'as-is' (55%) < spray drying (68%) < HME (89%). However, the relative tensile strengths of the polymer decreased in the same order and these results were attributed to elastic and brittle properties of the polymer.

#### *2.3.1.3 Applications of HPMCAS and HPMCP in HME*

Applications of HPMCAS and HPMCP in both conventional and emerging pharmaceutical manufacturing techniques producing variety of dosage forms are extensive and a broader picture showing these capabilities are presented in Figure 2.6. This justifies the reasons behind their popularity as a choice of excipient in pharmaceuticals in conventional dosage forms. This is majorly attributed to the peculiar characteristic properties of these polymers. These two polymers also offer a few more characteristic properties which are discussed briefly below especially for HME technique.

One of the major applications of HME is in formulations of amorphous solid dispersions where a crystalline drug is embedded in a semi-crystalline or an amorphous polymer. Use of an amorphous polymer is generally selected in HME since it avoids complex recrystallisation of the polymer itself, allows for a larger processing window above the glass transition temperature and helps a "crystalline API" to remain in an amorphous form by solubilising in the polymer matrix upon melt processing. HPMCAS and HPMCP are amorphous and high glass transition temperature polymers - HPMCAS having T<sub>g</sub> in the range of 115 to 120 °C (grade

dependent) and HPMCP having Tg between 135 to 145 °C. These polymers are used in amorphous solid dispersions (ASD) since they allow the maintenance of high Tg of the processed samples thus forming stable glasses of the amorphous solid dispersions or solutions. Moreover, these polymers offer H-bonding and act as recrystallisation inhibitors which aids in stability of the ASD (Tanno et al., 2004 , Al-Obaidi and Buckton, 2009 , Fukui et al., 2001 , Ghosh et al., 2011). Some of the examples stating above properties are explained below.

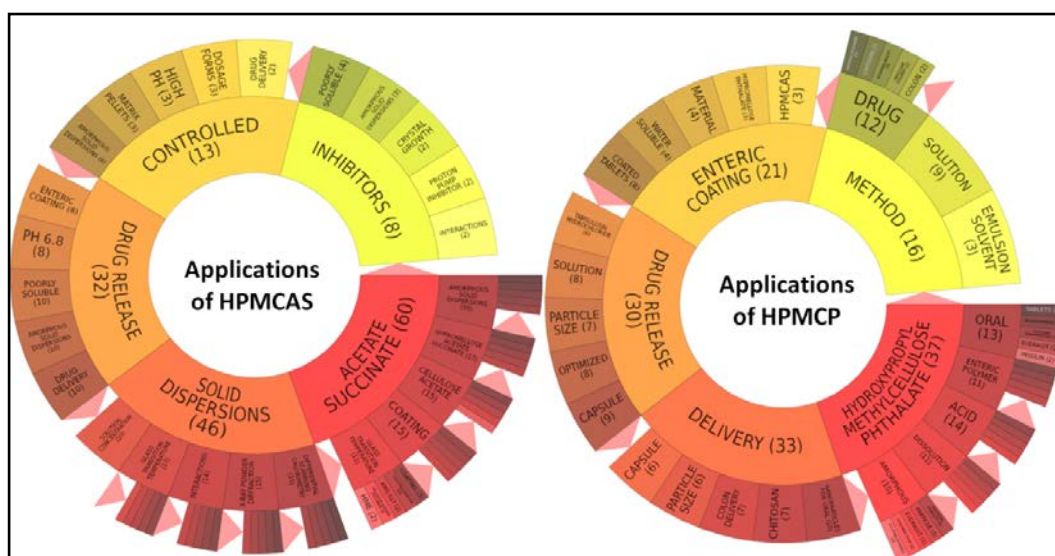


**Figure 2.6: Pharmaceutical applications of cellulose esters (Science.gov, 2015).**

Unlike HPMC ( $T_g > 160^\circ\text{C}$ ), the  $T_g$  of HPMCAS ( $T_g = 115$  to  $120^\circ\text{C}$ ) and HPMCP ( $T_g = 135$  to  $145^\circ\text{C}$ ) is significantly lower and therefore these polymers were investigated for their utility for HME. For the first time in 1996, Nakamichi investigated the application of HPMCP, with the light sensitive and thermolabile poorly water-soluble drug nifedipine, in the manufacture of solid dispersions by HME (Nakamichi K. et al., 1996). The method was purely non-solvent and represented a comparatively new technique compared to spray drying and co-fusion techniques. The results of the experiments showed that HPMCP aided twin-screw extrusion of nifedipine at a lower temperature without any degradation. The drug dissolution properties were also improved with the application of this polymer. Later these authors also investigated the crystallinity and dissolution rate of the

materials produced based on the configuration of twin-screw elements (Nakamichi K. et al., 2002). The study utilised different configurations of screws to understand transformation of the crystalline nifedipine to amorphous nifedipine and its impact on the dissolution properties of the drug. The authors further showed that samples adhering to the different kneading elements produced different dissolution profiles as well as changes in crystallinity of the drug. For example, samples collected from 60° kneading elements showed a supersaturation in dissolution studies compared with samples collected from the site without any kneading paddle element where no supersaturation was observed. Further, the authors also reported the use of water addition in the same process to prepare SD of nifedipine, since addition of a small % of water helped them to reduce the softening temperature to 100°C.

In another study, a solid dispersion of HPMCAS with the thermolabile drug ROA (manufactured by Hoffman-La Roche, Inc) was tested for HME. The polymer and drugs were mixed in the ratio of 1:2 ROA/HPMCAS and the solid dispersion was extruded at 160 °C without any plasticisers. The resulting SD was found to be effective in increasing drug dissolution properties (Hughey et al., 2010).

Ghosh et al., 2011 extruded HPMC based polymers namely, HPMC (3cps grade), HPMCP and HPMCAS with a poorly water soluble API. The solid dispersion prepared by HME was studied for ease of manufacture, physical stability, recrystallization potential and phase separation. The polymers were selected based on their low glass transition temperatures and the melting point of the API and were loaded with 20% and 50% of the drug. Propylene glycol was included as a plasticiser from 2.5% to 4.5%. It was observed that with a 50% drug loading less plasticiser was required compared to the 20% loadings showing the drug's plasticising activity in the formulation (Parameter used for plasticisation activity: % Torque values). The ASD made with HPMCAS polymer did not show any phase separations or recrystallisation of drug when stored at accelerated

stability conditions. Moreover, dissolution studies demonstrated that the SD made up of HPMCP showed a significant increase in the release of drug compared to the HPMCAS.

Hot melt extruded controlled release mini-matrices were investigated with enteric polymers, methacrylate (Eudragit®) and cellulosic polymers (HPMCAS and HPMCP) (Apichatwatana, 2011). The authors utilised triethyl citrate (TEC) as a plasticiser during the production of the mini matrices. However, it was noted that amongst methacrylate and cellulosic polymers, HPMCAS had lower molecular weight (18000g/mol) and therefore lower processing temperatures requiring less plasticisers. The low molecular weight of the polymer also resulted in less die swelling compared to methacrylate polymers. The drugs used with these polymers in particular, showed significant changes in the dissolution properties with respect to the pH of the solutions. The release patterns of drugs were entirely dependent upon the pH threshold of the polymer matrices (Apichatwatana, 2011).

Sarode et al., investigated the influence of HPMCAS-LF on the dissolution, crystallisation inhibition and supersaturation of BCS class II drugs in biphasic dissolution media (Sarode et al., 2013b). Amorphous solid dispersions were prepared by hot melt mixing and the solid dispersions were compared against a number of different polymers including HPMCAS-LF. It was reported that amorphous dispersions prepared with HPMCAS increased the dissolution rate and maintained the supersaturated phase over a longer time compared with dispersions with Eudragit while also acting as a crystallisation inhibitor for felodipine. However, when the same drug was used with HPMC, the dissolution did not achieve supersaturation levels and thus the recrystallisation step was completely hindered. Similar results were observed in the case of solid dispersions of itraconazole prepared with these polymers. Thus, Sarode et al summarised that HPMCAS is a better choice of excipient to improve dissolution profile of the drug

compared with other polymers. However, according to the author, recrystallisation inhibitor activity of HPMCAS is relatively poor compared with Eudragit post extrusion studies and thus the author raised concerns over physical stability of HPMCAS based solid dispersions.

### **2.3.2 HME with HPMCAS and HPMCP: Potential challenges**

Few studies have been carried out with HPMCAS and HPMCP for their use in HME, perhaps owing to some major limitations of these materials especially related to their temperature dependent physico-chemical stability, lack of polymer melt flow data and their processibility.

HPMCAS and HPMCP, being high T<sub>g</sub> polymers, are normally processed in HME at a temperature greater than 150 °C. However, being ester derivatives, they are prone to hydrolysis when subjected to heat and shear producing respective acids. Unless processing aids are added or the drug itself acts as a plasticiser, processing of these polymers below this temperature is difficult and with the introduction of high shear, the polymer melt often produces maximum torque within the extruder which in turn may damage processing equipment (Ghosh et al., 2011). Therefore, addition of plasticisers is suggested with the extrusion of HPMCAS and HPMCP. However, this addition produces ternary systems which additionally may cause physical destabilisation of amorphous dispersions. These events were reported by Ghosh et al., 2011.

Further, additions of plasticisers, their thermodynamically maximum safe loading concentrations and implications of plasticisation on downstream processibility are also important points to consider for use in HME. For example, solute migration or evaporation of plasticisers during processing causes destabilisation of the system while plasticiser induced flexibility potentially affects downstream processes such as milling, pelletising or tableting which require higher

energy inputs. Rheological studies can help to understand the effect of plasticisers on viscosity of these polymers. The melt rheology of HPMCAS and HPMCP has only been sparsely studied in the literature. Moreover to the author's knowledge, implications of plasticisers on melt viscosity, stability and behaviour (shear thinning, thickening, viscoelastic) of both HPMCAS and HPMCP are hardly discussed. There are only a couple of reports which discuss melt properties of these polymers-and its relevance in HME (Nakamichi K. et al., 2002 , Sarode et al., 2014 , Lu; et al., 2014).

Chemical instability of these polymers is also one of the major limitations in their extrusion since high processing temperatures required for their processing can produce the unwanted release of their acidic substitutions causing chemical incompatibility with added drugs. A review of the literature has revealed that these free acids can react with APIs, forming complex impurities of the drug. One of the possible reactions of these free acids with the drug is esterification. A drug candidate having a free hydroxyl group (-OH) in its structure tends to undergo esterification within the acidic environment. Authors, Zedong Dong and Choi (2008) proved that succinic acid released from HPMCAS undergo similar esterification with added drug producing incompatible reactions with the API. Moreover, since these polymers are reactive towards the free hydroxyl groups of other chemical entities, many additives like lactose and mannitol, which are otherwise inert, can become incompatible with HPMCAS and HPMCP. Consequently, polymer-additive interactions present an additional hurdle to formulation efforts creating new problems of excipient-exci-pient interactions.

Overall, there is a distinct lack of information about material properties of these two polymers precisely related to thermal, thermodynamic, melt rheological and thermo-chemical properties which all together are responsible for their processibility in HME and development of product performance.

## 2.4 Excipient characterisation approaches

A detailed literature review of a variety of polymers including HPMCAS and HPMCP for their use in HME provided an important point that pharmaceutical excipients could no longer be treated as inert materials. They have their own physicochemical properties that can influence both the manufacturing process and properties of API in the formulation. Thus, collecting information about their material properties can only be a relevant approach while investigating their functionalities for different dosage forms in emerging manufacturing technologies. As a consequence, systematic approaches should be utilised while characterising material properties of polymers.

Suitability of polymeric properties in the emerging technology of HME can be characterised by four approaches and are broadly divided into:

1. Thermal and thermo-chemical properties of the polymers
2. Thermodynamic properties of polymer and polymer-plasticiser interactions
3. Polymer melt rheology
4. Thermo-mechanical degradation kinetics of the polymer and the role of plasticisers

A schematic representation of these approaches along with their sub topics is shown in the Figure 2.7 and detailed descriptions of each approach along with certain important aspects of material properties as well as characterisation methods have been elaborated in this section.

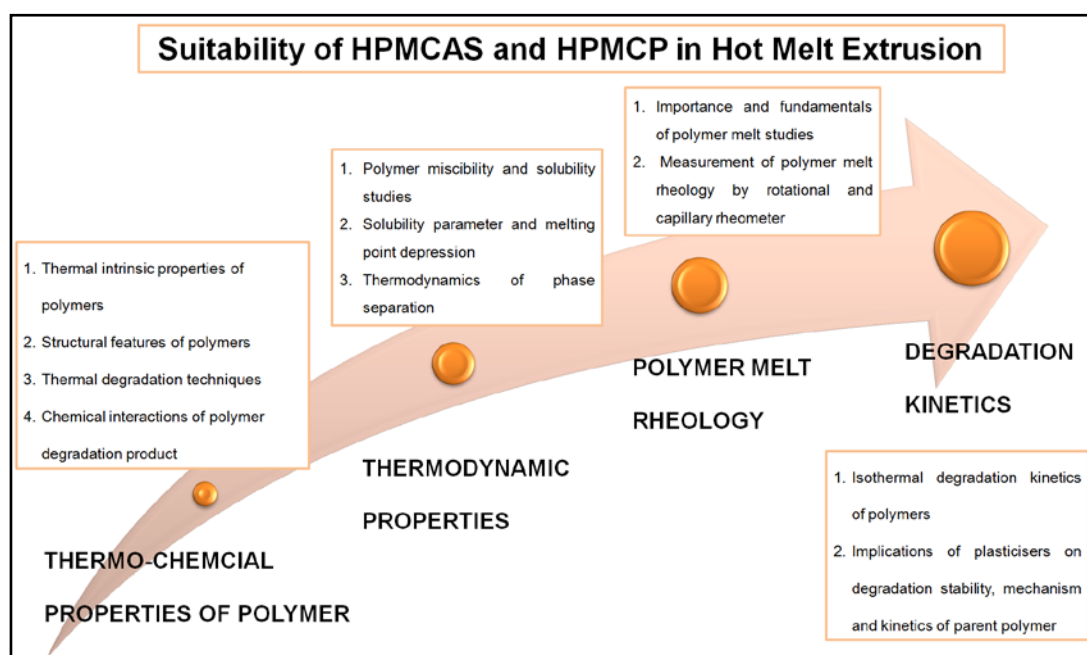


**Figure 2.7: Excipient characterisation techniques utilised in the current work.**

## **2.4.1 Thermal and thermo-chemical properties of the polymers**

### *2.4.1.1 Thermal intrinsic properties of polymers*

Materials can be broadly classified into two forms: amorphous and crystalline. A crystalline structure possesses a specific periodic arrangement of atoms held together by intermolecular forces while in amorphous materials these atoms are placed irregularly and their positions are considered to be relative to the material in the liquid state. Amorphous and crystalline materials can be distinguished by their intrinsic thermal properties, crystalline materials showing a sharp melting point ( $T_m$ ) while amorphous materials soften beyond the critical temperature known as the glass transition temperature ( $T_g$ ).  $T_g$  is considered to be one of the important intrinsic properties of the amorphous material since the properties above and below this temperature change significantly. Moreover, molecular mobility of the polymeric chains significantly varies with  $T_g$ , where below  $T_g$  the polymer remains in the solid glassy phase with decreased molecular mobility (kinetically arrested phase) and above  $T_g$ ,

the polymer starts behaving like a rubber with increased molecular mobility (Sun *et al.*, 2014 , Qian and Yu, 2009 , Potuzak *et al.*, 2013).

Differential Scanning Calorimetry (DSC) is often used to determine  $T_g$  and  $T_m$  values. In this technique the sample material and a suitable reference are programmed to a controlled temperature profile and the change of the heat flow rate to the sample material compared to reference material is measured.

$T_g$  is very important in HME based formulations since it is directly related to the miscibility of the components, viscosity of the polymer matrix, selection of thermal processing temperatures and physical stability of the melt extruded systems. For miscible systems, normally a single value of  $T_g$  can be observed while, for immiscible or partially miscible systems, more than one value of  $T_g$  is observed (Aubin and Prud'homme, 1988 , Ao and Jiang, 2006). This value is the representation of both physical and chemical stability of the drug-polymer matrix and thus is considered to be one of the benchmarks of formulation stability (Pimbert *et al.*, 2005 , Pajula *et al.*, 2010 , Patterson *et al.*, 2007 , Tian *et al.*, 2013). Processing temperatures are also dependent on the  $T_g$  of the system since both softening or melting events as well as polymer viscosity are related to it. For instance, melt viscosity of the polymer near its  $T_g$  produces maximum values up to  $10^{12}$  Pa.s (Hancock *et al.*, 1999 , Baird and Taylor, 2012). This creates significant hurdles during HME since processing under these circumstances demands enormous energy to create material flow resulting in generation of extreme pressures within the extruder barrel. In general, HME processing temperatures are generally held at 30 to 100 °C greater than the  $T_g$  of the samples.

Investigations of thermal properties of blends are also important for HME since  $T_g$  varies with addition of components.  $T_g$  can also correlate with

plasticisation efficiency when a plasticising agent (perhaps an API) is added to the formulation. Researchers often co-relate efficiency and extent of plasticisation based on  $T_g$  values of polymeric blends. Generally, values of  $T_g$  reduce with increase in plasticiser concentration and a plot of  $T_g$  of polymeric blend against concentration of plasticisers yields a relationship which determines the plasticisation efficiency. Such a relationship can also be obtained theoretically by use of the Fox equation (equation 2.1) or the Gordon-Taylor equation (equation 2.2) (Marsac *et al.*, 2010 , Schneider, 1988) which simply relate glass transitions of two pure compounds against their percentage weights along with density of the systems.

$$\frac{1}{T_g \text{ mixture}} = \frac{W_1}{T_{g1}} + \frac{W_2}{T_{g2}} \quad \text{Equation 2.1}$$

$$T_g \text{ mixture} = \frac{W_1 T_{g1} + K W_2 T_{g2}}{W_1 + K W_2} \quad \left[ \text{Where } K = \frac{\text{Density } 1 * T_{g1}}{\text{Density } 2 * T_{g2}} \right] \quad \text{Equation 2.2}$$

During DSC studies, many compounds exhibit temperature dependent crystallisation-recrystallisation behaviour. For example, during heating and with constant increase in temperature, if the material shows an exothermic peak in DSC this indicates crystallisation phenomenon. This event occurs always at a lower temperature than the melting endotherm of the pure compound. During cooling from the melt a crystalline exothermic peak indicative of recrystallisation may occur. Understanding of these thermal transitions are important in excipient characterisation since these transitions directly relate to the physical stability or solid state miscibility of two or more components.

#### 2.4.1.2 Structural features of polymer

Solid state materials exhibit physico-chemical changes when exposed to heat or temperature. These effects can be beneficial in terms of flow behaviour until high temperatures produce detrimental effects on the structural features of

the polymers. Structurally, polymers are made of multiple repeating units of simple molecules. These multiple units are linked covalently by either linear and/or branched networks during polymerisation (Figure 2.8).

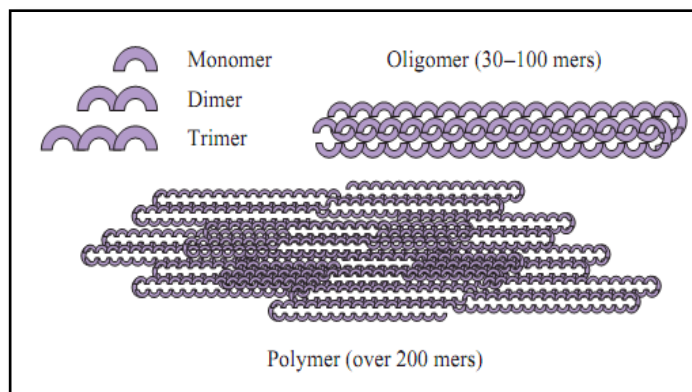


**Figure 2.8: Structure of a polymer (Omidian H, 2006).**

Thermal degradation of the polymer is the process of molecular deterioration as a result of overheating. At high temperatures (more precisely at thermal degradation temperatures), monomers of polymer begin to separate from each other with the breakdown of their covalent bonds. In other words, under thermal effects and near/above degradation temperatures, heat energy exceeds the bond dissociation energies of the materials causing covalent bonds in the materials to break. Though the covalent bond is generally considered to be the strongest among all possible bonds, the strength of covalent linkages is entirely dependent upon the covalent bonds between different chemical groups of materials. Usually, the weaker bond (usually esters, ethers) present on the polymer backbone breaks first and bond breakage between the polymer molecule results directly in loss of polymeric molecular weight. Many organic and semi-synthetic polymeric materials show melting points below 200-250 °C and these materials also show rapid degradation beyond these temperatures (Bruck, 1965) since the majority of these polymers possess weaker covalent linkages such as hydroxyl, ester, anhydrides and azo functional groups on their side chains which makes them relatively thermolabile (Kricheldorf *et al.*, 2004).

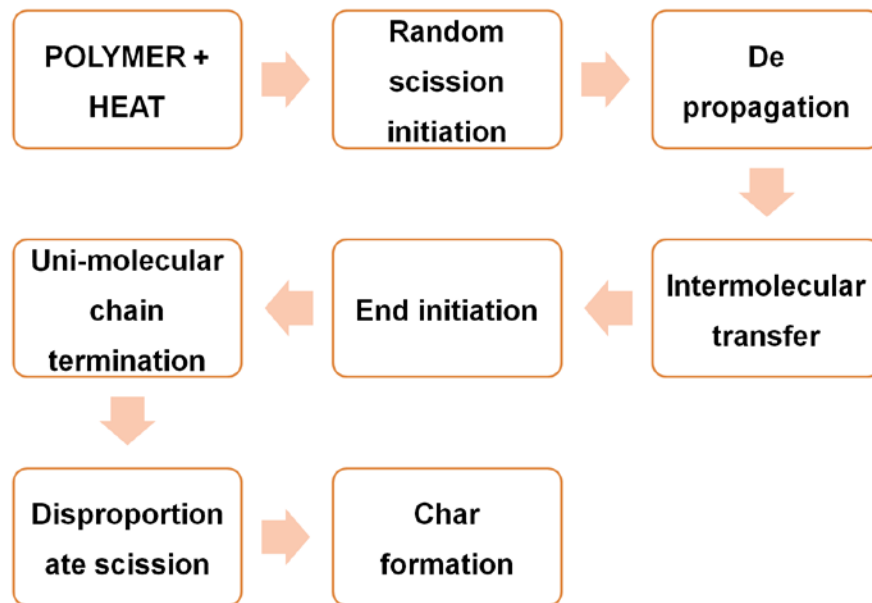


**Figure 2.9: Typical thermal degradation mechanism and pathway.**

Sequential chain fragmentation and depolymerisation of the polymer is generally the basis of thermal degradation. Thermal degradation is speculated to follow four pathways: side group elimination, chain scission, depolymerisation and cross linking of the polymeric chains (Beyler and Hirschler, 2002). Elimination of side groups not only removes the side chains of the polymeric backbone but can also further react to form a variety of small molecular weight aromatic compounds which vaporise during thermal treatment. This step leaves behind the polymeric backbone where random chain scission causes free radicals to form which further divides the long polymeric chains into variable oligomers. This is then followed by depolymerisation reactions where various oligomers degrade to monomers to form a char at the completion of the thermal degradation process (Bruck, 1965). A typical representation of degradation mechanism and thermal degradation pathway is depicted in Figure 2.9.

Thus, in summary it can be understood that thermal degradation of the polymer involves cascade reactions and controlling this type of degradation requires knowledge of the underlying complex diverse degradation mechanisms of the polymer, its degradation pathway, impact of filler(s) on the degradation of

the polymer, interactions with the plasticisers, processed impurities and diffusion of volatile contents of the polymers which often occur (Gupta and Viswanath, 1996 , Bruck, 1965 , Dahiya et al., 2008 , Daly et al., 2005 , Guru et al., 2012 , Jan Pospíšil, 1999 , Li et al., 1999 , Krongauz, 2010). Therefore, the study of thermo-chemical stability of the polymers is as important as investigating solid state miscibility since understanding of degradation ultimately influences a polymer's usability, processibility and storage conditions.

#### *2.4.1.3 Thermal degradation analysis*

Over the years thermal analytical techniques have been used to identify the processing temperatures especially techniques which run on the basis of high temperatures and shear. Of interest, thermogravimetric analysis (TGA) and DSC have been widely used for qualitative and quantitative estimation of thermal properties including thermal degradation of the polymer. Thermal degradation temperature is also one of the important intrinsic properties of the polymer which is often evaluated by TGA whereas volatile compounds of polymeric degradants are often investigated by certain hyphenated analytical techniques such as TGA-MS (mass spectroscopy) and TGA-FTIR tools.

TGA measures the mass change in a sample as a function of temperature or time and is widely used to determine the stability and decomposition of the materials. The measurements are generally carried out in air (in presence of oxygen) or in an inert environment. Investigations of polymers by TGA provide valuable information about material degradation temperature and volatile weight loss of the samples when exposed to time and temperature. The TGA thermogram provides two numerical values such as degradation temperature or oxidative temperature and residual mass or char. Figure 2.10 shows a typical TGA thermogram. Representation of oxidative temperature is generally carried out by two methods either explaining the onset temperature (T<sub>1</sub>) or calculating

derivative-weight loss curvature point ( $T_2$ ). Investigation of  $T_2$  is more often used in TGA since it describes the characteristic temperature profile of the material which helps to identify the impurities or physical mixtures of blends. Investigation of  $T_1$  and  $T_2$  allows a formulator to design a processing window for HME based on the material's  $T_g$  and degradation temperature.

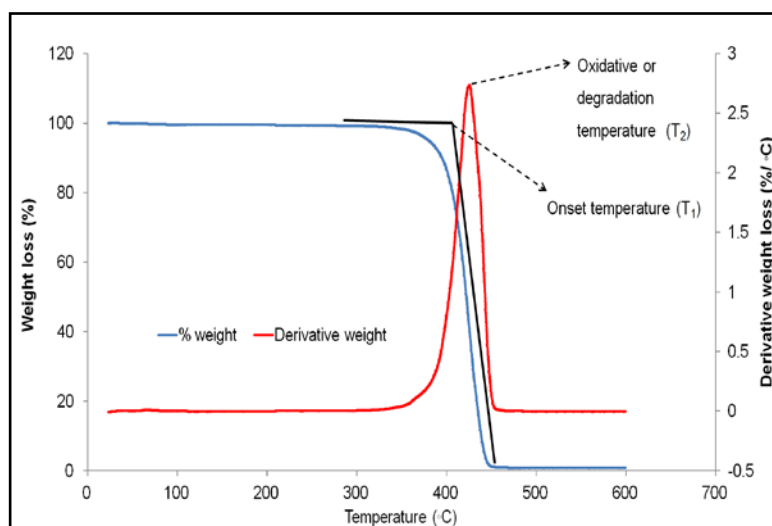


**Figure 2.10: Onset and oxidative degradation temperatures in TGA.**

TGA studies of polymers not only provide the degradation temperature range but also provide information about polymer degradation patterns. For example, from the above figure, it can be concluded that the material degrades in a single step and complete degradation occurs within the range of 350 to 450 °C. Literature reports suggest that comparison between the polymer weight losses at its respective degradation steps can be related to the degree of side chain substitutions and thus a preliminary degradation mechanism of material can be constructed based on these data. However, TGA cannot be utilised thoroughly to investigate degradation mechanisms of polymer and it has to be integrated with other analytical tools to deduce the thermal degradation products of polymers. TGA-MS and TGA-FTIR have been utilised recently in number of polymer degradation studies to analyse the volatile contents from the polymer when subjected to TGA studies.

#### *2.4.1.4 Chemical interactions*

From the literature it is clear that excipients obtained by any source potentially contain impurities in the polymeric samples which may cause incompatibility when processed with different active compounds. Incompatibility reactions generally occur due to interactions between two or more different components. In simple terms this generally occurs due to drug-polymer interactions and these interactions are broadly classified as physical and chemical interactions.

Physical or process based mixing of two components produces interactions at their molecular levels. In the case of physical interactions, if the interactions are supportive, physical stability can be maintained however, if non-cooperative it can result in destabilisation or phase transformations of the system. In comparison to physical interactions, chemical interactions of drug-polymer complexes are more dangerous since these interactions often involve degradation of drugs and production of unknown impurities which can produce toxic effects upon administration. Chemical incompatibility occurs only when two or more reactive compounds interact to form new compounds during formulation. However, according to FDA regulations, any unknown or known compound(s) formed either due to degradation of an active and an excipient or due to reaction between a drug-polymer complex during formulation or at pharmaceutical stability studies is (are) equally considered as chemical incompatibility. Further, these studies should be extensive for thermolabile polymers because the reaction between degradation products of polymers and that of added APIs cannot be underestimated. Many researchers have paid attention to the degradation products of APIs during HME however, equal attention should be given to extract and enlist different degradation products of polymers. Therefore, investigations of possible chemical interactions demands

greater attention while formulating any medicinal product especially in cases where temperature-shear induced degradations are likely.

Chemical interactions between two or more components are investigated by a number of advanced analytical techniques involving the use of Fourier Transform Infrared Spectroscopy (FTIR), High Performance Liquid Chromatography (HPLC), Gas Chromatography (GC) and Mass Spectroscopy (MS). Structural elucidation of any unknown degradation products is performed with the help of hyphenated techniques such as GC-MS, TGA-FTIR and TGA-MS techniques.

#### **2.4.2 Thermodynamic properties of pure and blends of polymers**

Recrystallisation or phase separation of an API and migration of plasticiser during and post extrusion are commonly reported in HME formulations. This issue relates to physical interactions between the components of mixtures which ultimately decide the physical stability of the melt based system. Physical stability of a melt based system is dependent on the fragility of the system and solid state miscibility-solubility studies. Elucidation of physical stability can be provided with the help of thermodynamic concepts. These studies play an important role in both pre- and post-formulation studies and provide information on the fundamentals of solid state miscibility, temperature dependent stable-unstable compositions and relative processing temperatures of HME.

##### *2.4.2.1 Polymer miscibility and solubility studies*

Solid-solid compatibility of two substances is generally referred to as the ability to form a homogeneous blend at the molecular level. This is also one of the primary requirements of amorphous solid dispersions. Solid state miscibility and solubility concepts have been developed on the basis of thermodynamic events which explain interactions between two or more phases. It has been

seen that drug-polymer interactions play a significant role in the physical stability of dispersions. For instance, Kothari, Huang, Lynn Taylor and Gavin Andrews groups relate this physical stability of dispersion to various interactions including hydrogen bonding (H-bonding) and Van der Waals interactions (Kothari *et al.*, 2015 , Huang *et al.*, 2008) whereas physical instability is often related to the miscibility of two components by these researchers.

Solid-state interactions include four main interactions: H-bonding, ionic, Van der Waals, and dipole interaction which influence the miscibility and solubility of the components. Thus, effects of miscibility and solubility of two or more components on the physical stability of the formulation cannot be foreseen especially when plasticisers are being used in the melt extrusion process.

Generally every component has some solubility in another component and thermodynamically these events can be defined by the terminologies of change in the entropy and enthalpy of the system, where the energy of interactions between different components determines the miscibility and immiscibility. This relationship is generally expressed by the Gibbs equation which states:

$$\Delta G_{mix} = \Delta H_{mix} - T \Delta S_{mix} \quad \text{Equation 2.3}$$

Where,  $\Delta G_{mix}$ ,  $\Delta H_{mix}$ , and  $\Delta S_{mix}$  are the Gibb's free energy, the change in enthalpy and entropy of mixing at temperature T, respectively. The achievement of a single phase system is one of the prime requirements of amorphous solid dispersions (ASD) and thermodynamically, relates to negative values of  $\Delta G_{mix}$ . In other words, immiscibility or phase separation of the system is favoured when the values of Gibbs free energy are positive. During melting, the entropy of the system increases and this gain in entropy contributes negativity to  $\Delta G_{mix}$  and thus one can generally observe miscibility or solubility of two or more compounds at elevated temperatures. However, post extrusion, only certain concentrations remain in the amorphous state while others may show

recrystallisation or phase separation of a crystalline compound from the polymeric system. These difficulties are often observed when the concentration of the crystalline component crosses the miscibility limit of the polymer.

The miscibility limit is concentration and temperature dependent. However, it has been seen that other factors such as kinetic energy barriers, polymer melt viscosity and humidity surrounding the polymeric system (Higgins *et al.*, 2010b) may also contribute. The solubility of a crystalline component in the polymer is equally important. If the crystalline loading (API or plasticiser concentration in a polymer) is within the solubility range of the polymer then the compositions of API-polymers or plasticiser-polymer show thermodynamically stable amorphous formulations despite of several kinetic fluctuations.

Polymer miscibility studies are generally determined by several methods which normally use measurements of glass transition temperature (DSC, Dynamic Mechanical Analysis (DMA), dielectric methods and thermo-optical analysis), microscopy studies (optical, electron and hot stage microscopy) and scattering methods (neutron, light and X-ray scattering techniques). Solid state miscibility and solubility studies can also be performed by use of theoretical approaches such as solubility parameter and interaction parameter approaches which are often correlated with practical methods in which the melting point depression approach has been used most frequently (Higgins *et al.*, 2010a , Baird and Taylor, 2012 , Djuris *et al.*, 2013 , Flory, 1942 , Liu *et al.*, 2002).

- *Solubility parameter approach*

The solubility of a given compound in a given polymer is entirely dependent on the chemical structures of both compounds -cohesive properties and subsequently, solubility of the materials can be predicted based on the similarity of the solubility parameters (Tian *et al.*, 2013 , Sakellariou *et al.*, 1986). Utilising the concept of 'like dissolves like' various scientists have utilised

the approach in which the solubility parameter ( $\delta$ ) is defined as " the ratio of square root of cohesive energy density ( $E_{\text{coh}}$ ) to the molar volume ( $V$ ) of the given substance at room temperature" [i.e.  $\delta = \sqrt{\frac{E_{\text{coh}}}{V}}$ ] (Barton, 1991 , Pearce, 1977 , Hoftyzer, 1976). Cohesive energy density is the total energy required to divide and remove the neighbouring molecules of the materials (Askadskii *et al.*, 1977 , Cowie, 1968).  $\delta$  of a given compound can be predicted by investigating the energy of evaporation of compounds though this can be applied only to compounds that are stable above their boiling points. Generally, high molecular weight materials such as polymers do not exhibit stability above their boiling points and thus a group contribution technique must be utilised to investigate  $\delta$  of these compounds (Barton, 1991).

Polymer miscibility studies of HPMCAS and HPMCP with different crystalline entities such as felodipine, indomethacin (IND), itraconazole (ITZ), and griseofulvin (GSF) have been performed using a solubility parameter approach (Sarode, 2010 , Sarode *et al.*, 2013a , Repka *et al.*, 2013 , Tian *et al.*, 2013). Initially, authors investigated solubility parameter approach for API-polymer miscibility studies and based on smaller differences ( $< 7 \text{ MPa}^{1/2}$ ) between the  $\delta$  values of individual API and polymer, a better miscibility between these two materials was predicted. However, despite of these observations, phase separation and recrystallisation of drugs have been reported by authors. This suggests that investigation of  $\delta$  is not a fully quantitative technique for investigation of the miscibility of solid state components though it can be useful at initial developmental stages.

- *Melting point depression approach miscibility and solubility studies:*

The MPD approach has been used in ASD technology to understand the thermodynamics of drug-polymer miscibility and solubility and to predict

miscibility phase diagrams. The MPD technique uses shifts in the melting points of the crystalline entity when mixed with other component(s). The melting point can be defined as the temperature at which a solid turns into the liquid state. Thermodynamically the same phenomenon can be stated as the temperature at which the chemical potential of the same substance in two different physical states remains constant (Flory, 1953). Thus the chemical potential of a crystalline compound in solid state is equal to the chemical potential of its molten mass.

A chemical potential (or activity) is a form of potential energy that can be defined as the change in free energy as a function of composition (Kittel, 2004 , Job and Herrmann, 2006 , Ruffler *et al.*, 2009). Chemical potential plays an important role in explaining the depression of melting points of two or more components in a mixture. For example, if 2 components are present in a mixture and during heating; if the chemical potential of a mixture falls below the chemical potential of the individual components then the mixture will produce a depression in the melting point. In other words, during the process of melting, particles having higher chemical potential (or higher activity) would diffuse to lower chemical potential until equilibrium is achieved and when the sum of the chemical potential of the two components reaches zero miscibility is favoured which causes a depression in the melting point.

MPD can be simply investigated by means of the DSC technique where different concentrations of crystalline and amorphous entities are mixed physically or by a solvent evaporation technique and shifts in melting points can be measured. Depression of melting points is an indication of the miscibility of two components and thus this method can be utilised for understanding the thermodynamics of solid state miscibility and solubility. Data obtained from MPD studies is usually utilised in the Gibbs free energy and Flory-Huggins interaction

parameter determination. This data can aid in construction of a temperature-concentration dependent phase diagram as described in section 4.1.2.3.

### **2.4.3 Polymer melt rheology**

HME involves several important stages of processing operations which can be categorised as: solid state transportation, melting, mixing and homogenising, melt transport and finally melt shaping. Further, it is also understood that this process requires application of temperature and pressure in order to force material from its solid state to molten. Thus, it is evident that in order to process the materials via HME, one needs to understand the melting properties and complex melt flow behaviour of different thermoplastic polymers or materials. However, the majority of the polymers show resistance to flow with the applied mechanical stress and their behaviour is dependent upon the structure, molecular weight and arrangement of the polymeric chains. In other words, polymers exhibit resistance to deformation: compression or stretching (tensile strength) or bending. The "science of deformation and flow is known as rheology" (Mezger, 2006) and it is the relationship between stress-strain rates. Moreover, methods to determine the rheological properties are known as rheometry.

Materials exhibit flow properties with applied pressure (stress) and velocity (shear rate) and depending on their flow properties, they are broadly categorized into Newtonian and non-Newtonian materials. Material deformation and flow properties are complex phenomena. Flow behaviour can be differentiated into three categories, ideal elastic flow, ideal viscous flow, and viscoelastic flow. However, very few materials follow ideal flow properties and most of the materials exhibit viscoelastic properties (Mezger, 2006). To generalise these phenomenon elastic materials (e.g. metals and ceramics) show linear stress verses strain correlation up to the failure point. Particularly,

elastic materials follow stretching behaviour (time dependent phenomenon) and elastic materials return to their original state when the stress is removed while the ideal viscous flow is irreversible (e.g. water). Viscoelastic materials such as polymers are neither a purely elastic material nor a pure liquid. However, they possess the both properties to store energy (elastic behaviour) and to dissipate energy (viscous behaviour).

Literature reports suggest that shear stress-strain behaviour of viscoelastic materials is a time dependent process and these materials exhibit non-Newtonian behaviour i.e. viscosity of polymer melts is not always constant meaning that the relationship between shear stress and deformation rate can be non-linear. For instance, when viscoelastic materials are exposed to low shear stresses over short periods of time the material behaves like an elastic solid by storing the energy which can be further utilised to return to its normal state upon stress removal. On the other hand, when the same material is exposed to constant increase in shear stress over a longer period of time it starts to behave as a viscous- liquid (Mezger, 2006). Further, polymer melts are non-Newtonian fluids and they show shear thinning behaviour; meaning melt viscosity decreases as a function of increase in shear rate. This characteristic phenomenon of viscoelastic materials is considered to be important since this ultimately facilitates variety of melt processing techniques including HME.

Rheological measurements can be performed for a number of applications however in the current research work; these are majorly focused for two things: material characterisation and its processability. For instance, polymer melt viscosity is directly related to molecular weight of the polymer especially viscosity measured at zero shear rate ( $\eta_0 = k M_w^{3.4}$ ). Thus, different grades of the same polymer having difference in their molecular weights (Ratio of maximum to minimum molecular weight) can be expected to behave differently

in the extrusion process (Cogswell, 1997 , Lyons *et al.*, 2008 , Palade *et al.*, 2001 , Vlachopoulos and Strutt, 2003). Further typical elastic and viscous behaviour of polymers observed at lower shear rates of rotational rheometer can easily be compared with the other polymeric materials. Thus, melt rheology can be utilised as a tool for material characterisation. In the case of processability, with careful rheological measurements, one can select ratios of polymeric mixtures including plasticisers, stabiliser or APIs for optimum extrudability. Further rheological investigations can be utilised for trouble shooting purposes such as unstable melt flow, overload of torque or generation of high pressures inside the extruder and "shark skin effects" which are discussed below.

Overload of torque inside the extruder is one of the most common processing problems occurring due to improper temperature control and leads to unstable melt flow in the extruder. This affects motor load of the extruder and the high torque generated within the extruder barrel may damage the mixing screw elements. Another important parameter of troubleshooting is roughness on the surface of the melt extruded product. Roughness or "shark skin" effects on the melt extrudates can be observed by two mechanisms such as less shear thinning property of the material and "stick-slip phenomenon" (Mezger, 2006). Less shear thinning phenomenon is generally observed due to improper selection of temperature and shear configuration while stick-slip is generally observed at the exit of the extruder die (Vlachopoulos and Strutt, 2003). These two problems can be solved with the aid of plasticisers. However, poor blending of polymer-additives or polymer-drug combinations or polymer blend incompatibility or miscibility often results in extrudate products with poor final product properties. In summary it can be understood that polymer melt properties, melt flow, melt processability and physical properties of end products of melt extrudates can be precisely quantified by means of rheological

investigations and therefore, investigations of polymer melt rheology is considered as one of the primary requisites of HME studies.

#### *2.4.3.1 Measurement of melt rheology*

Rheological measurements can determine melt viscosity, elastic-viscous moduli, yield stresses, elongation viscosities, shear and extensional stresses, and are material and temperature specific as well as varying with the size of macromolecules. Measurements of polymer melts by rheometry normally involve two types of rheometer where one runs on the principle of low shear rate (rotational rheometer) while other runs on the principle of high shear rate (capillary rheometer) (Figure 2.11).

A dynamic rotational rheometric test involves forced harmonic oscillation where both stress and strain are monitored with the time. These tests are performed to examine the viscoelastic regime of the polymer by investigating linear responses of dynamic viscosity and elasticity with increasing strain rate. In rotational methods, the test sample experiences a continuous shear between the rotating shaft and a stationary surface. Rotational rheometry generally measures polymer melt rheology between the shear rates  $0.001$  to  $100 \text{ s}^{-1}$ . On the other hand, capillary rheometers can measure shear rates from  $10$  to  $10^6 \text{ s}^{-1}$  and are effective in the investigation of polymeric properties under high shear rates. Capillary rheometry is a pressure driven technique, which mimics flow through an extruder die or injection-moulding nozzle by pushing the polymer melt through a capillary having defined bore diameter. This generates a pressure gradient across the instrument and across the entry of die (shear stress), which varies with the volume flow rate (shear rate).

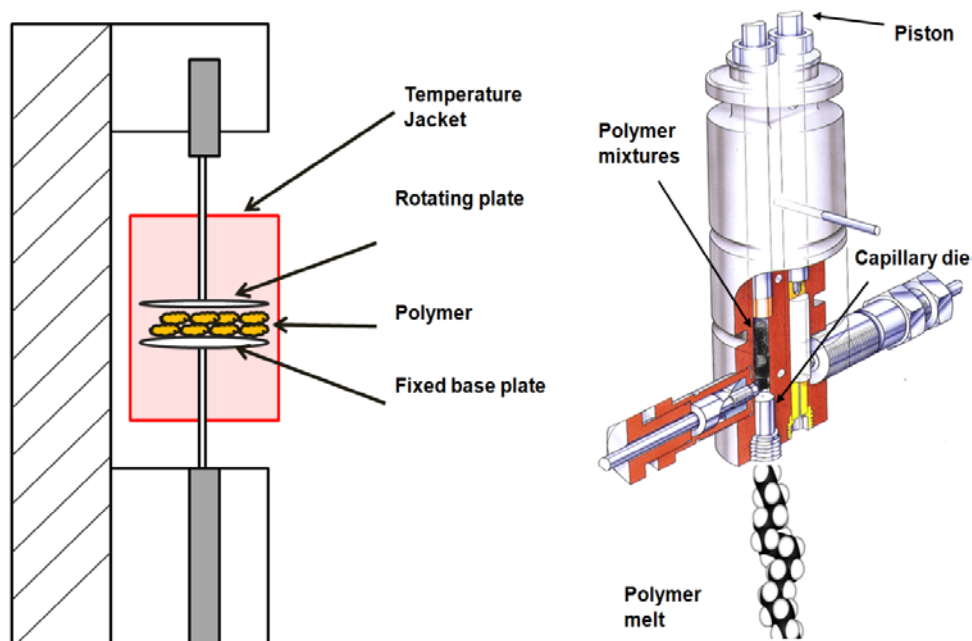


**Figure 2.11: Schematic diagrams of rheometers (Kelly, 1997).**

The rotational rheometer instrument is composed of a two-plate system, the bottom stationary plate and an upper movable plate. An upper plate revolves around its axis of rotation to a fixed angle and the sample sandwiched between the two plates experiences shear and undergoes deformation. The instrument measures strain (deflection angle) within the sample by applying stress (torque) followed by calculations of the different rheological moduli and viscosity measurements. Generally, two types of upper movable plates, the flat parallel plate or the cone shaped, are utilised. Empirically, the cone ensures a constant shear rate over the entire plate surface and therefore it is usually preferred to conduct rotational tests. However, polymers under these investigations takes a long time to reach equilibrium between the internal and the external stress which limit its use for such viscoelastic materials such as, polymers (Mezger, 2006). On the other hand, the parallel plate offers great flexibility in gap size between the lower plate and upper plate, which is useful for viscoelastic materials. Certain terminologies such as storage modulus ( $G'$ ), loss

modulus ( $G''$ ) and complex viscosity associated with rotational rheometry experiments are referred from "The rheology handbook" (Mezger, 2006).

Advanced capillary rheometers possess twin bores technology with temperature control where the temperatures sensors present inside the barrel ensure isothermal conditions throughout the barrel by measuring top, middle and die end temperatures (Majidi *et al.*, 2011 , Paradkar *et al.*, 2009). The pressure transducers are generally mounted immediately above the dies. The rheometers along with the integrated software calculate and convert applied pressures and velocities of pistons into necessary rheological parameters like shear stress, shear rate etc.

#### **2.4.4 Thermo-mechanical degradation kinetics of polymers**

It is often said that polymer degradation studies and the mechanism of degradation plays an important role in HME studies. However the word degradation should be more specifically explored since the degradation of material is also a time dependent process (Gopferich, 1996). It is indeed true that the degradation temperature of a material provides an indication of the maximum processing temperatures for any kind of polymeric material. However; investigation of stability of the polymer below its degradation temperature for an appreciable length of time should also be investigated. For example, consider a polymer which has to be process in HME at elevated temperature. The first basic requirement demands its thermal stability over long periods of time followed by its melt stability over the period of extrusion time. It is important to note that both stability profiles are correlated with respect to time since thermo-mechanical stability of material is time dependent. Therefore, from the literature reports it can be seen that various researchers prefer residence times < 15 min for pharmaceutical extrusions (Singhal *et al.*, 2011 , Jani, 2015).

Thermo-mechanical stability of polymeric materials is generally investigated by different degradation kinetic approaches. A polymer degradation kinetic study speculates material properties under given conditions of time and temperature and can also provide valuable information about a polymer's thermal or mechanical life. Thermal degradation kinetics can be used to investigate the extent of degradation as a function of time and temperature while rheology based degradation kinetic studies provide similar data with respect to change in polymer melt viscosity. From the literature, it is clear with regard to molecular weights of the polymer, temperature and melt viscosity are strongly interdependent and based on these parameters the kinetics of degradation can be deduced.

#### 2.4.4.1 Thermal degradation kinetics

Thermal degradation kinetics of the polymer with or without additives is one of the most popular investigations in polymer degradation kinetic studies. The kinetics of thermal degradation is reported to comprise complex since material degradation involves a series of complicated reactions running simultaneously. As discussed earlier, if the extent of degradation for the given time at given temperature is known, the weight loss observed with TGA studies can be co-related to degradation kinetics of the polymer.

Degradation kinetics of a polymer are often calculated by different mathematical models involving the degree of degradation ( $\alpha$ ), order of reaction ( $n$ ), activation energy ( $E_a$ ), degradation rate constant ( $k$ ) and pre-exponential factor ( $A$ ). Different models have been developed by Klaric and coworkers; MacCallum and Schoff; MacCallum; Judd and Norris; Chatterjee; Rozyckie et al; Anderson and Freeman; etc (Chatterjee and Conrad, 1968 , B. Janković *et al.*, 2008 , Klaric, 1993 , MacCallum, 1989 , MacCallum and Schoff, 1971 , Judd and Norris, 1973 , Rozycki, 1987 , Maciejewski, 1987) using TGA as the

experimental method. In the current work the equations of conventional degradation kinetics have been used and the results of these kinetic equations are compared with the mathematic model of MacCallum.

Thermal degradation kinetics of polymer can be evaluated by applying equations of material degradation. According to this method,

$$\frac{d\alpha}{dt} = k(T)f(\alpha) \quad \text{Equation 2.4}$$

Where  $\alpha$  is the degree of degradation,  $k(T)$  is the temperature dependent reaction rate constant, and  $f(\alpha)$  is the mathematical function that is completely dependent on reaction type. As the reaction rate of the system (equation 2.4) is completely dependent on the temperature, the Arrhenius equation was taken into consideration and according to Arrhenius,

$$k = A e^{-E_a/RT} \quad \text{Equation 2.5}$$

Where  $A$  is the pre-exponential factor,  $E_a$  is the activation energy (KJ/mol) and  $R$  ( $\text{J}\cdot\text{mol}^{-1}\cdot\text{K}^{-1}$ ) is the gas constant. Generally,  $\alpha$  is the normalised weight loss and can be calculated from the simple equation,

$$\alpha = \frac{[w(t)-w(i)]}{[w(i)-w(f)]} \quad \text{Equation 2.6}$$

$w(t)$ ,  $w(i)$  and  $w(f)$  are weight of the polymer at time,  $t$ ; initial polymer weight and final weight of polymer. During isothermal measurements ( $T_{\text{iso}}$ ), perhaps the simplest way to analyse the TGA data is by fitting the equation 2.4 and calculate order of reaction, rate constant, and subsequently calculating the energy activation values. However, many authors have mathematically modified  $f(\alpha)$  to  $(1-\alpha)^n$  where  $n$  is the order of reactions. Combining the equation 2.4 and 2.5, gives:

$$\frac{d\alpha}{dt} = A e^{-\frac{E_a}{RT}} \cdot (1-\alpha)^n \quad \text{Equation 2.7}$$

By taking logarithmic forms of both sides,

$$\log \frac{d\alpha}{dt} = \log A - \frac{E_a}{RT_{iso}} + n \log (1 - \alpha) \quad \text{Equation 2.8}$$

Repeating tests at different isothermal temperatures allows us to plot  $\log \frac{d\alpha}{dt}$  against  $\log (1 - \alpha)$  to yield a slope of a straight-line proportional to the value of  $n$  and the intersection yields the reaction rate constant  $k$ . Furthermore, to calculate  $E_a$  and the constant  $A$ , a plot of  $\log k$  against  $1/T$  yields a straight line with slope proportional to  $E_a$  and an intercept of  $A$ .

#### 2.4.4.2 Degradation rheology

One of the major drawbacks of cellulose ester derivatives and perhaps the majority of the pharmaceutical materials is their thermolability and potential for degradation during high temperature processing. From the literature, it was evident that HPMCAS and HPMCP show thermal sensitivity approximately beyond  $\sim 180$  °C, where chances of both alterations of physical and chemical properties can be expected.

Since polymer melt viscosity and molecular weight are interrelated, mechanical degradation of the polymers can be utilised to determine the degradation rate of the polymer based on its melt rheology (Ahmed and Ramaswamy, 2005 , Harrison and Melik, 2006). Literature reviews suggest a number of techniques to estimate degradation kinetics by melt rheology (Harrison and Melik, 2006 , Daly *et al.*, 2005) using time sweeps, frequency sweeps and reduced complex viscosity measurements over the range of processing temperatures and shear rates. However, the most common methods utilised in the literature involve the use of Williams, Landel and Ferry (WLF) - Eyring equation and the Daly *et al.*, approach discussed below.

The temperature dependent viscosity and theory of rate process can be determined by the combined equations of Williams, Landel and Ferry (WLF)

and Eyring equation approaches (Mezger, 2006). These equations are represented as follows. According to WLF:

$$\text{Log } \frac{\eta_{T_1}}{\eta_T} = \frac{C_1 (T_1 - T)}{C_2 + (T_1 - T)} \quad \text{Equation 2.9}$$

Where  $\eta_T$  and  $\eta_{T_1}$  are viscosities at standard temperature, T and reference temperature  $T_1$  while  $C_1$  and  $C_2$  are two constants.

The viscosity ( $\eta_{T_1}$ ) obtained by such method can be further utilised in the Arrhenius-Eyring equations as,

$$\eta_{T_1} = A e^{-E_a/RT} \quad \text{Equation 2.10}$$

Combining these two equations (equation 2.9 and 2.10), the activation energy of the polymer melts at different temperatures can be determined by:

$$E_a = R * \frac{\text{Log } \eta_{T_1}}{1/T} = \frac{2.303 * C_1 C_2 R T^2}{(C_2 + T_1 - T)^2} \quad \text{Equation 2.11}$$

In another study, the degradation kinetics of the polymer based on melt rheology was investigated by Daly et al where the authors assumed that degradation of the polymer is a result of chain scission and that the rate of degradation is directly proportional to the concentration of the polymeric chain links (Daly *et al.*, 2005). According to Daly et al.,

$$\frac{d(\alpha)}{dt} = k_{\text{thermal rate}} * \alpha \quad \text{Equation 2.12}$$

where  $\alpha$  is the number of polymeric chain links per unit volume, and  $k_{\text{thermal rate}}$  is the degradation rate constant. Since the degree of polymerisation and molecular weight of the polymer are closely related to values of  $\alpha$ , their correlation was expressed as,

$$\text{log } \alpha = \text{log} \left[ N \left( 1 - \frac{1}{\text{Degree of polymerisation}} \right) \right] = \text{log } N - \frac{Mw_{\text{monomer}}}{Mw_{\text{polymer}}} \quad \text{Equation 2.13}$$

Where N is the number of monomer units. Thus when equation 2.12 and 2.13 are combined,

$$\frac{Mw_{monomer}}{Mw_{initial\ weight\ of\ polymer}} - \frac{Mw_{monomer}}{Mw_{polymer}} = k_{thermal\ rate} * t \quad \text{Equation 2.14}$$

since,  $\eta_0 = k M_w^{3.4}$  Equation 2.15

Combining equation 2.14 and 2.15 provides an equation 2.16 to yield degradation rate constant of a polymer based on melt rheology.

$$\frac{1}{\eta^{3.4}} = \frac{1}{\eta_0^{3.4}} + k_a * t \quad \text{Equation 2.16}$$

Where  $\eta$  is the viscosity at time  $t$ ,  $\eta_0$  is the viscosity at  $t=0$  and  $k_a$  is apparent thermal degradation rate constant.

## 2.5 Summary

After detailed investigation of literature reports about HPMCAS and HPMCP for HME, it was noticed that despite the wide variety of polymer applications, researchers have expressed mixed reviews about their properties. To date the suitability of these polymers for HME is largely unclear due to limited information about their properties. Mainly, these polymers have been discussed for their thermolability however even this information is very sparse and does not give rational ideas. Investigating the material properties of polymeric samples for their suitability in HME should be performed in a systematic way, which to the author's best knowledge has not been performed for HPMCAS and HPMCP. Further, it is thought that through quantification of their thermal, thermodynamic and rheological properties; and constructing their relationship with thermo-chemical-mechanical stabilities, polymer degradation, degradation kinetics and chemical incompatibility studies is one of the better rational approaches for HME process design (Figure 2.12).

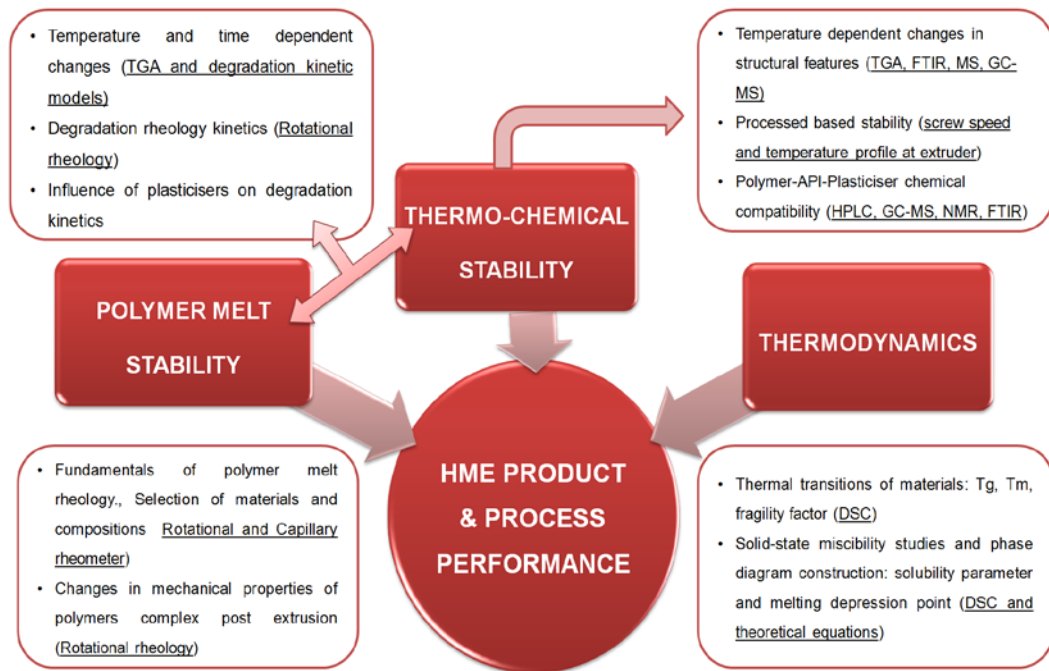


**Figure 2.12: HME product and performance stability.**

## **Chapter 3. Materials and Methods**

In this chapter, the materials and method used for investigating the polymeric properties of pure and blends of polymers (both plasticisers and APIs) are discussed in detail. The chapter is divided into two major sections: materials and methods. In the first section, all utilised materials are discussed while the method section is further divided into subsections on, (a) characterisation; of pure materials (b) hot melt extrusion, (c) characterisation of melt extrudates and (d) chemical reactions of drug-polymer complexes.

Initially, the different grades of polymers along with different plasticisers were screened to understand their polymeric properties and suitable processing conditions for HME. Based on these investigations, single grades of each polymer were selected along with suitable plasticisers and extrusion studies were carried out at specific conditions. Finally, post extrudate analysis of polymeric samples was investigated for thermo-chemical and mechanical properties, compatibility and potential degradation. Characterisations of the polymer melt properties along with properties of API and plasticisers were performed by systematic approaches where different analytical tools such as thermal studies (TGA, DSC), spectroscopic studies (FTIR, NMR) and chromatographic techniques (HPLC, GC-MS) were used.

### **3.1 Materials**

The different grades of polymers, plasticisers and APIs used along with the chemicals, instruments and software used during investigations are described in the current section.

### **3.1.1 APIs**

In the current research work two APIs: chlorpropamide (purity 99.80%) and Ibuprofen (purity 99.75%) were purchased from Sigma Aldrich and Taj Pharmaceuticals respectively. The structural and chemical properties of these APIs along with their key physical properties are discussed in results and discussion separately. Chlorpropamide is a sulfonyl urea derivative. It has anti-diuretic activity because of which it has been investigated for anti-hypertensive therapy. Ibuprofen is a well established API known for several decades due to its non steroidal anti-inflammatory activity.

### **3.1.2 Polymers and plasticisers**

Different grades of polymers such as HPMCAS-L (Lot number: 1023032), HPMCAS-M (Lot number: 0063162), HPMCAS-H (Lot number: 10113027), HPMCP-HP50 (Lot number: 1052107) and HPMCP-HP55 (Lot number: 1031015) were received as gift samples from Shin-Etsu Chemical Co. Three plasticisers; polyethylene glycol-2000 [PEG] (Lot number 81221), triethyl citrate [TEC] (Lot number: 251275) and citric acid (anhydrous) [CA] (lot number: 12245) were purchased from Sigma Aldrich.

### **3.1.3 Chemicals**

HPLC analysis of different samples was performed by utilisation of standard samples of acetic acid [AA] (HPLC grade 99.98%), succinic acid [SA] (HPLC grade, 99.87%), phthalic acid [PA] (HPLC grade, 98.98%), phthalic anhydride [PAH] (analytical grade, 98.87%), chlorpropamide related impurity-A (USP grade, 99.99%) and chlorpropamide related impurity-B (USP grade, 99.87%). These were purchased from Sigma Aldrich. In order to prepare suitable mobile phases and diluents and blank solutions of the respective samples; HPLC grades of methanol, acetonitrile and o-phosphoric acid were

utilised and buffers such as sodium dihydrogen phosphate monohydrate (99.78%), potassium dihydrogen phosphate monohydrate (98.87%) and potassium dihydrogen phosphate dehydrate (98.65%) were purchased from Fisher Scientific.

### **3.1.4 Instruments and software**

Instruments utilised during characterisation are listed in Table 3.1.

**Table 3.1: List of instruments and software used for analysis.**

<b>Name of the instrument</b>	<b>Specifications</b>	<b>Software</b>	<b>Manufactured by</b>
Twin screw extruder	Pharmalab 16 mm	-	Thermo Scientific, UK
Thermogravimetric analysis	Q500	Universal Analysis	TA Instruments (UK)
Differential scanning calorimetry	Q2000	Universal Analysis	TA Instruments (UK)
Powder X-ray diffraction (PXRD)	D8 powder diffractometer	Commander	Bruker (USA)
High performance liquid chromatography	e-2695 separation module	Empower 3	Waters (USA)
Rotational rheometer	Physica MCR 501	Rheoplus	Anton Paar (Graz, Austria)
Capillary rheometer	RH10 capillary rheometer	Flowmaster	Malvern (UK)
Gas chromatography-Mass Spectroscopy	Model: 7890A and 5975C	ChemStation	Agilent (USA)
Mass Spectrometer	Micromass Quattro	MassLynx	Waters (USA)
Nuclear Magnetic Resonance spectroscopy (NMR)	Model: 400 Ultrashield	Top Spin NMR	Bruker (USA)
FTIR	NA	Digilab FTS	Digilab FTIR spectrophotometer

## 3.2 Methods

### 3.2.1 Characterisation of polymers, plasticisers and APIs properties

Preformulatory thermo-mechanical properties of raw materials and blends of polymers (polymer-plasticiser mixtures) were investigated prior to HME. In the thermal methods, two techniques: thermogravimetric analysis (TGA) and differential scanning calorimetry (DSC) were used to investigate thermal transitions of cellulose polymers as well as for plasticisers and an API. Rheological investigations were carried out to understand the critical factors affecting melt flow properties of the raw materials and blends of polymers.

#### 3.2.1.1 *Differential Scanning Calorimetry (DSC)*

All DSC experiments were performed on a Q-2000 DSC (TA Instruments). In the current research work, DSC (Figure 3.1) was primarily used to investigate glass transition temperature ( $T_g$ ) and melting points ( $T_m$ ) of all samples, to investigate the fragility index of the plasticisers and thirdly, to investigate the thermodynamics of phase separation using the melting point depression method. Initially,  $T_g$  and  $T_m$  of the pure compounds: polymers, plasticisers and API were investigated. A ramp method was utilised and all measurements were performed in duplicate. Approximately, 2.0 ( $\pm$  0.5) mg of sample was weighed, sealed in an aluminum pan and heated from 20 to 200 °C at a heating rate of 10 °C/minute. Thermal transitions were analysed using Universal Analysis 2000 v.4.3A software.

To confirm the observed glass transition values of ramp DSC, modulated DSC (MDSC) tests were performed. Samples of the polymers weighing around 3 $\pm$ 2 mg were sealed in an aluminum pan with a pin-holed lid allowing evaporation of moisture. A modulated cycle was carried out for all samples. Pure polymers were equilibrated at 0 °C for 8 minutes and then heated to 200

°C under modulation conditions of  $\pm 1$  °C for every 60 sec with a heating rate of 2 °C/min (Ghosh *et al.*, 2011) whereas pure APIs and plasticisers were treated similarly except for their equilibration temperature which was set up for -70 °C.

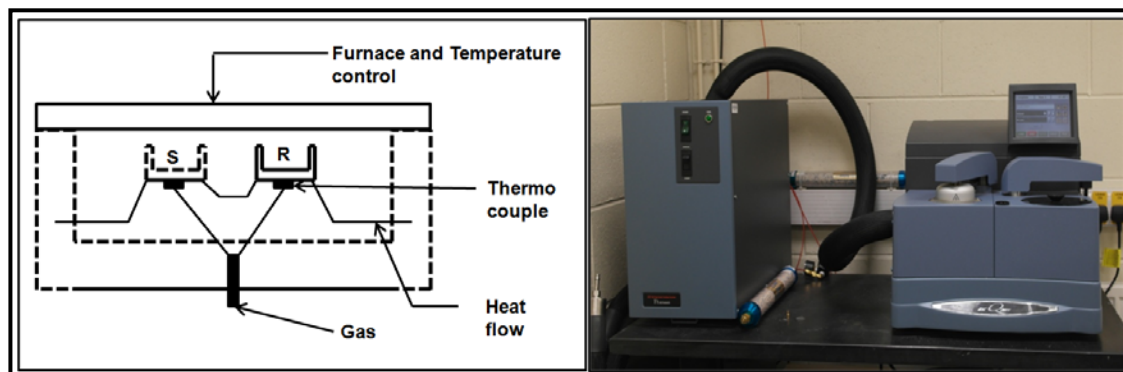


**Figure 3.1: Schematic representation and photograph of DSC.**

The fragility parameter of crystalline and semi-crystalline plasticisers was determined by using a heat-cool-heat (HCH) cycle. Independent samples of crystalline and semi-crystalline plasticisers, CA and PEG-2000 were initially equilibrated at 20 °C prior to heating to 'stability temperature above melting point' (here it is  $T_m + 10$  °C) at a heating rate of 2 °C/min (first heating cycle). At the end of the first heating cycle, the molten mass of the sample was held isothermally for one minute prior to being cooled at the same heating rate to -80 °C and held isothermally for one further minute (first cooling cycle). A second heating cycle was then applied to the restricting temperature (here it is  $T_m - 10$  °C) at the same heating rate and the glass transition temperature of the samples was noted. A similar procedure was carried out where fresh samples were investigated for HCH cycle at heating rates of 5, 8, 10, 12, 15 and 20°C/min and the fragility parameter calculated based on the change in the glass transition temperature of the samples with respect to heating rates. The details of the equations are described in the section 4.3.3.4.

The thermodynamics of phase separation were studied based on the depression in melting temperature of the crystalline components. A

homogeneous mixture of semi-crystalline PEG with HPMCP was prepared by a solvent evaporation technique. Both compounds were dissolved in acetone and the solvent mixture was evaporated by pouring into a wide mouth petri plate. Petri plates were kept in a vacuum oven for 24 hours at 70 °C to remove residual solvents. Samples ranging from 10-95 % w/w PEG in HPMCP were prepared and homogeneous mixtures were analysed by DSC for their melting endotherm. The same method was utilised to prepare blends of CA and PEG with HPMCAS and HPMCP.

### 3.2.1.2 Thermogravimetric analysis (TGA)

TGA analysis of different samples of pure and blends of polymers was performed on TGA-Q500 (TA instruments, Figure 3.2). The detailed procedure of the TGA investigations is explained below.

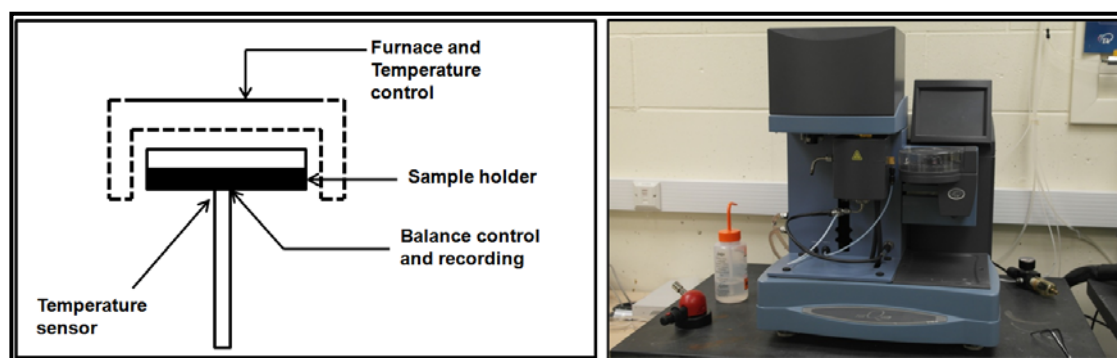


**Figure 3.2: Schematic representation and photograph of TGA.**

Prior to every independent investigation, the empty pans of TGA were first tared in an inert nitrogen environment. Thermal investigations of polymeric samples were performed by two methods, non-isothermal (ramp technique) and isothermal technique. In the first method, polymeric samples: grades of HPMCAS and HPMCP and plasticisers: TEC, PEG and Citric acid (CA) weighing approximately 5-8 mg were heated from 30 to 600°C at a heating rate of 10 °C/min under a nitrogen gas atmosphere at a gas flow rate of 20mL/min. A similar procedure was used to investigate blends of PEG with HPMCAS and

HPMCP (10, 15 and 20% w/w) and blends of CA with HPMCAS and HPMCP (10, 15 and 20% w/w) for their thermal degradation pattern. In all cases, measurements were performed in duplicate and TGA thermograms were analyzed by Universal Analysis 2000 v.4.3A software.

For isothermal investigations; raw polymers (HPMCAS-LG and HPMCP-HP55), plasticisers (PEG-2000 and CA), blends of PEG with HPMCAS and HPMCP (10, 15 and 20% w/w) and blends of CA with HPMCAS and HPMCP (10, 15 and 20% w/w) were used. In this method, each sample was initially equilibrated to 20 °C followed by heating to 150 °C at 10 °C/minute, held isothermally for 30 minutes and cooled to 20 °C at the same rate. A similar procedure was used in studies over different isothermal temperature ranges for raw and blends of HPMCP (150-200 °C with increments of 10 °C) and HPMCAS (190-260 °C with increments of 10 °C). Isothermal investigations of samples were used primarily for two studies: changes in the structural features of the polymer upon heat exposure and polymer degradation kinetics. The former study was conducted by FTIR and the latter using mathematical equations for degradation kinetics.

### *3.2.1.3 Infrared spectroscopy of thermally exposed samples of polymers*

FTIR of isothermally exposed samples of HPMCAS and HPMCP was performed using a potassium bromide (KBr) disc method. Before every experiment, the KBr (IR grade) was oven dried and individual samples of HPMCAS and HPMCP heated at different temperatures mixed with KBr. Discs of independent samples were analysed on a Digilab FTS 2000 spectrophotometer. For each run, a total of 16 scans were performed and samples were investigated in the wave number range of 600-4000  $\text{cm}^{-1}$ .

### 3.2.1.4 Polymer melt rheology: rotational rheology

All rotational rheological testing was carried out using a Physica MCR 501 rheometer (Anton Paar, Austria, Figure 3.3) with a parallel plate geometry (diameter 25mm). For each test, polymeric samples were weighed in the range of  $1.5 \pm 0.2$  g. Three sets of oscillatory tests: a strain amplitude test, frequency sweep test and time sweep tests were carried out. Detailed descriptions of each test are discussed below.

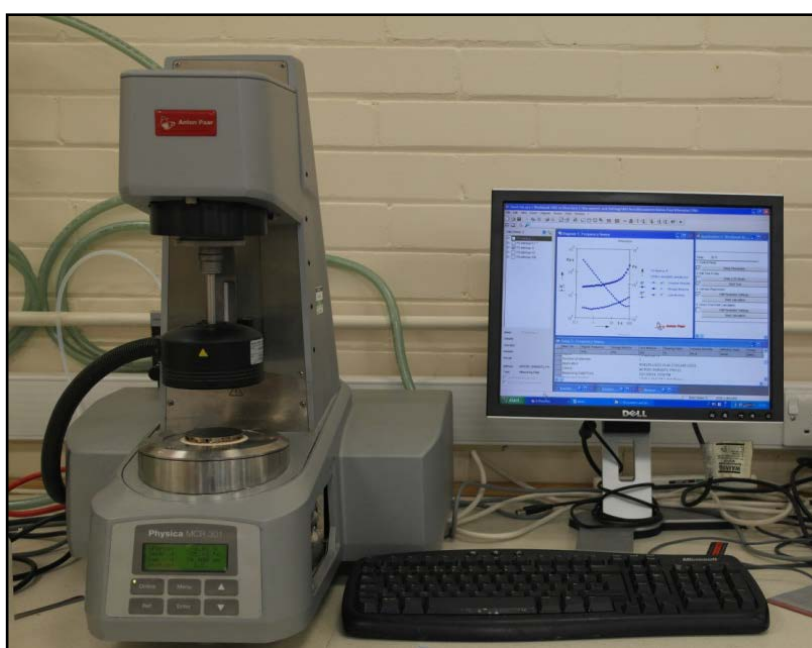


**Figure 3.3: Rotational rheometer.**

Samples containing physical mixtures of PEG, CA and TEC with HPMCP and PEG-HPMCAS were prepared in the ratio of 10, 15 and 20% w/w (plasticiser to polymer ratio) by blending them in a pestle and mortar for 20-30 minutes until an apparently homogenous mixture was formed (homogenous mixture was confirmed by HPLC studies for content uniformity). Before investigations, samples of raw polymers were dried in an oven for 2 hours at 100 °C. During these investigations a common procedure was followed for all samples. Individual polymer raw materials as well as physical mixtures of polymeric samples were added to the bottom plate after setting up the desired

temperature for each individual test. The distance between the two parallel plates was reduced to 5mm in order to equilibrate sample uniformly with the heating temperature surroundings. When the subjected sample was melted, the distance between the two parallel plates was reduced to the set experimental distance of 1mm, the molten mass coming from the sides of parallel plates was trimmed and further experiments were performed on the molten mass of the samples.

- *Strain amplitude frequency*

In this test, the amplitude of strain was varied and frequency was kept constant. The angular frequency was set to  $1.0 \text{ s}^{-1}$  and the strain amplitude range was set between 0.01 - 100%. Both raw and plasticised polymers were investigated at temperatures between 150-200 °C and 130-150 °C respectively. The storage modulus  $G'$  and the loss modulus  $G''$  were plotted against the deformation. The linear viscoelastic regions (LVER) was calculated from the straight line of  $G'$  and  $G''$  until it deviates and taken into consideration for frequency sweep tests.

- *Frequency sweep (FS)*

In this test, frequency was varied while the amplitude kept constant. The FS test plays an important role in determining the viscoelastic properties of material as a function of shear rate. The polymers and blends of plasticised polymers were tested in FS tests at 150-200 °C and 130-150 °C respectively. The angular frequency range tested was  $0.1-100 \text{ s}^{-1}$ . Plots of complex viscosity against angular frequency were obtained. Different samples produced different strain values or LVER values in amplitude sweep test. However to maintain uniformity during FS test, all tests were conducted at 0.1% strain values.

- *Time sweep*

The degradation of samples as a function of time was measured using time sweep tests at very low shear rates. This test was performed to study the viscosity of polymers over periods at a specific temperature, at fixed strain (0.1%) and at fixed frequency (10 Hz). The test was performed over a period of one hour for each sample. The degradation kinetics based on the melt rheology data was conducted by exposing raw and blends of HPMCAS between 190-260 °C while for raw HPMCP and its blends this range was reduced to between 150-200 °C.

### 3.2.1.5 *Polymer melt rheology: capillary rheology*

- *Steady shear rate test:*

A constant shear rate test was employed. The polymers were dried in an oven at 100°C for 24 hours before rheological investigation. The rheometer (Rosand RH10 capillary rheometer, Malvern Instruments Ltd, Figure 3.4), mounted with 30,000 psi (Long die) and 10,000 psi (short die) pressure transducers, was set at the test temperature and allowed to stabilise. Temperatures were controlled to within  $\pm 0.5$  °C of the set values and monitored by platinum resistance thermometers fitted in the three (top, middle and bottom) zones of the barrel. The polymer was fed into both barrels and manually compressed before the test was started. The polymers were subjected to a pre-compression pressure of 0.5 MPa, and a total pre-heating time of 540 seconds. The experiment was run in a 5-stage discrete speed program (Table 3.2) and the material passed through 2 dies having dimensions of 1.0 mm diameter with 16.0 mm (long die) and 0.25mm (zero length die, short die) of length. Please note that the shear rate values mentioned in the table 3.2 are provided by software upon fixing the 5-stage discrete speed program.

**Table 3.2: Steady shear rate test stages.**

Stage number	Piston speed (mm/min)	Wall shear rate (/s)
1	1.66	50.00
2	4.39	131.82
3	11.74	205.00
4	31.34	940.55
5	83.34	2499.60

Values of shear rate and shear viscosity were calculated based on the theory explained by Paradkar and co-workers (Paradkar *et al.*, 2009). In capillary rheometry, a sample is melted before being extruded by a piston through a capillary die. Pressure drop through the die is measured at a known flow rate, defined by piston velocity. The rheometer consists of a temperature-controlled barrel into which the piston is inserted. A capillary die (diameter 0.5 – 3.0mm) is inserted at the end of the barrel and a pressure transducer is mounted directly above the die to record pressure drop. Usually the capillary rheometers measure shear rates up to  $10^6 \text{ s}^{-1}$  and the power law describes shear flow as,

$$\eta = K^* \dot{\gamma}^{(n-1)} \quad \text{Equation 3.1}$$

Where  $\eta$  represents shear viscosity (Pa s),  $\dot{\gamma}$  represents shear rate ( $\text{s}^{-1}$ ), K indicates consistency index and 'n' denotes power law index. Wall shear stress ( $\tau_w$ ) (Pa) and apparent shear rate ( $\dot{\gamma}_{app}$ ) ( $\text{s}^{-1}$ ) can be calculated from equation 3.2 & (3.3)

$$\tau_w = \Delta P / 4L \quad \text{Equation 3.2}$$

$$\dot{\gamma}_{app} = 4Q / \pi R^3 \quad \text{Equation 3.3}$$

Where  $\Delta P$ ,  $L$ ,  $D$   $R$  and  $Q$  are pressure drop, die length, die diameter and volume flow rate, respectively.

Shear viscosity is the ratio of equation (3.2) to equation (3.3). These terminologies are related to Newtonian fluids. However, most polymeric melts follow non-Newtonian behaviour. Therefore some corrections were suggested and these are termed true shear rates  $\dot{\gamma}_{\text{true}}$  calculated as indicated in the equation (3.4),

$$\dot{\gamma}_{\text{true}} = \frac{\{3n+1\}}{4n} * \dot{\gamma}_{\text{app}} \quad \text{Equation 3.4}$$

Where  $n$  is the power law index.

Practically, the pressure transducers are present above the capillary die for measurement of pressure. Empirically, these pressure transducers do not measure the melt pressure generated at the entrance of the die. Thus, the pressure drop along the capillary remains hidden. Therefore, the pressure along the walls of capillary barrel and the pressure drop ( $\Delta P$ ) at the entry of capillary die need to be corrected and the corrections were suggested by Bagely (Bagley, 1957). He suggested that the pressure drop ( $\Delta P$ ) in the capillary tube could be calculated from a pressure difference between a long capillary die and an orifice die pressure ( $P_o$ ). Thus, true shear stress ( $\tau_w$ ) can be calculated as,

$$\tau_w = \frac{\{P_L - P_o\}}{2L} * R \quad \text{Equation 3.5}$$

Where  $P_L$  is the pressure drop through die. Moreover, the material under capillary pressure, not only involves shear flow but also extensional flow. Extension (stretching) of a polymeric melt involves loss of energy that is rarely considered in converging flow but has significant impact on melt rheology. Cogswell (1978) derived an expression for determination of extensional stress and extensional strain for flat entry dies as

$$\eta_E = \frac{9}{32} \frac{(n+1)^2}{\eta} \frac{P_0}{\gamma} \quad \text{and} \quad \sigma_E = \frac{3}{8} \frac{(n+1)}{P_0} \quad \text{Equation 3.6}$$

where  $\eta_E$  is extensional viscosity (Pa.s) and  $\sigma_E$  is extensional stress (Pa)



**Figure 3.4: Capillary rheometer.**

### **3.2.2 Extrusion of pure and blends of polymers**

Hot melt extrusion of raw and blends of HPMCAS and HPMCP was performed using a Thermo Scientific pharma-lab co-rotating twin screw extruder (Figure 3.5) with screw length to diameter ratio of 40:1. The extrusion temperature profile utilised for different samples of raw, plasticised polymers and drug-polymer-plasticiser mixtures are explained in the Table 3.4. The polymer was fed into the extruder at the rate of 0.10 kg/h using a gravimetric twin-screw feeder (Brabender, Germany). The extruded strands of polymeric mixtures were air cooled, pelletised and stored.



**Figure 3.5: PharmaLab Extruder.**

### *3.2.2.1 Screw configuration and screw speeds*

One of the main factors affecting the quality of the pharmaceutical extruded products is residence time. Residence time of the extrusion is majorly dependent upon two parameters: screw configuration and screw speeds. In the current work, the screw configuration (see Figure 3.6 and Table 3.3) was kept constant whereas two screw speeds, 80 and 100 rpm, were employed at the maximum barrel temperatures of extruder as shown in Table 3.4. The screw configuration for extrusion is explained below.



**Figure 3.6: Screw configuration used during extrusion.**

**Table 3.3: Screw elements and configuration.**

Cumulative Length	Element
28	Forward facing
2.25	30°
1.25	60°
1	90°
6	Forward facing
1.5	Discharge
40	Total

### 3.2.2.2 Temperature profiles and zones

Material properties and degradation studies of HPMCAS and HPMCP with and without additives as well as APIs were investigated over different temperature ranges. These temperatures were selected based on the rotational and capillary rheology data. The Pharmalab extruder has nine temperature zones and based on the screw configuration, maximum barrel temperatures were maintained from zone 7 since this zone was related to an intense mixing zone and melting zone for extruded materials. The typical temperature profiles used for different samples in the investigation are represented in table 3.4.

**Table 3.4: Temperature profile.**

Temperature profile	Zones								
	2	3	4	5	6	7	8	9	Die
V-T1	50	70	90	110	140	150	150	150	150
V-T2	50	80	100	130	150	160	160	160	160
V-T3	50	80	110	140	160	170	170	170	170
V-T4	50	90	120	150	170	180	180	180	180

V-T5	50	90	130	160	180	190	190	190	190
V-T6	50	90	140	170	190	200	200	200	200
P-T1	25	40	60	90	110	130	130	130	130
P-T2	25	40	60	90	120	140	140	140	140
P-T3	25	40	60	100	130	150	150	150	150
CHL-AS-T1	25	40	60	90	110	130	130	130	130
CHL-AS-T2	25	40	60	90	120	140	140	140	140
CHL-AS-T3	25	40	60	100	130	150	150	150	150
CHL-HP-T1	25	40	60	90	110	130	130	130	130
CHL-HP-T2	25	40	60	90	120	140	140	140	140
CHL-HP-T3	25	40	60	100	130	150	150	150	150
CHL-HP-PEG-T1	25	40	60	90	110	120	120	120	120
CHL-HP-PEG-T2	25	40	60	90	120	130	130	130	130
V: Virgin, P: Plasticised, CHL: Chlorpropamide, AS: HPMCAS, HP: HPMCP									

### **3.2.3 Characterisation of extrudates**

#### *3.2.3.1 Physical characterisation*

- *DSC*

Extruded samples of plasticised polymers as well as extrudates of chlorpropamide and ibuprofen were investigated for melting endotherms and were also compared for thermodynamic phase diagram studies. A ramp cycle was performed. Samples were heated between -40°C and 200°C at a rate of 10 °C/min and the glass transition temperature as well as melting endotherm of crystalline components was mapped.

- *Long term stability*

Extruded materials of HPMCAS and HPMCP with semi/crystalline plasticisers (citric acid and PEG) and API (ibuprofen) were stored for stability

studies in an open tray system at ambient temperatures for 6, 18 and 24 months. These samples were then further investigated for DSC studies to validate the predicted thermodynamics of phase separation.

- *Dynamic vapour sorption (DVS)*

Samples were analysed using DVS intrinsic, Surface Measurement Systems, UK (Figure 3.7). In DVS the sample was kept in the balance. The controlled gas is perfused over the sample [relative humidity (RH) in this case]. The mass is plotted with respect to time as function of RH. The sample holder was cleaned using methanol. The balance was tared and allowed to stabilize initially to 0% RH. Around 20 mg of sample was weighed and the sample was re-equilibrated to humidity condition: 0% RH and then the final weights were noted. Humidity was maintained using water vapour and nitrogen gas mixture. The software used for analysing the samples was Version 5.1.0.8, standard DVS. The samples were run using the following parameters (Figure 3.7).

	Parameter	Conditions
	Constant temperature	25 °C
	Starting RH	0%
	End RH	90%
	Cycle	Full cycle , 0-90%
	Sample Mass used	10.23
	Humidity interval	10%
	Mass/ Time interval	dm/dt
<p><b>Figure 3.7: DVS instrument and parameters.</b></p>		

- *X-ray diffraction*

XRD patterns of all samples were recorded using a Bruker D8 diffractometer with wavelength 0.154 nm, from a copper source, a voltage of 40kV and filament emission of 40 mA. Powder XRD of all samples was gained over the angle from 2 to 30° (2θ) with a scanning speed of 0.02°/min step width.

### 3.2.3.2 *Rheological characterisation*

FS Tests were performed for melt extrudates as discussed above.

### 3.2.3.3 *Chemical characterisation by HPLC*

Chemical characterisation and impurity analysis of polymer extrudates and drugs were performed using a Waters e-2695 separation module. The HPLC unit was integrated with a degasser and photodiode array detector-2998. Polymer extrudates of HPMCAS and HPMCP with and without plasticisers were analysed at a wavelength of 215nm using a flow rate of 1 ml/min while for chlorpropamide samples the samples were analysed at 210 nm. A Waters Spherisorb ODS2 Column, 3 μm, and 4.6 x 60 mm column was used to investigate different samples. The peaks and area under the curves were analysed with Empower 3 software. The column and samples were stored at 27 °C during injection. A gradient pattern was followed whereby the mobile phase of 0.05 M potassium dihydrogen phosphate (pH=3) (solvent A) and methanol (solvent B), was run for 25 minutes. For the first 5 minutes, 100% of solvent A was used, which mixed further with solvent B to the ratio to 60:40 (solvent A: solvent B) linearly over 15 minutes and the sequence was reversed at the end of 25 minutes. Potassium dihydrogen phosphate (pH=3) was used as a diluent and was used as a blank injection in the HPLC. A standard resolution solution consisting of known concentrations of acetic acid (200 μg/mL), succinic acid

(200 µg/mL) and phthalic acid (50 µg/mL) were prepared in diluent and injected into the systems and % assay were calculated against these known concentrations. The developed method was validated as per the ICH guidelines and samples were prepared as follows

a. Preparation of HME samples (test solution)

300 mg of extruded polymer was poured into a 100 ml volumetric flask, and allowed to dissolve in 100 ml methanol to extract the free acids from the extrudates. From this stock, 5 ml of solution was pipetted out into a 10 ml volumetric flask, further diluted with diluents and then filtered through 0.45 µm syringe filters prior to injection into the HPLC system.

b. Preparation of extruded sample spiked with impurities

300 mg of extruded polymer was poured into a 100 ml volumetric flask and allowed to dissolve in 100 ml methanol to extract the free acids from the extrudates. 5 ml of this solution was then pipetted out into a 10 ml volumetric flask. To this, 2.0 ml of each acetic acid (AA) and succinic acid (SA) (1000 µg/ml) and 0.4 ml of phthalic acid (PA) (1000 µg/ml) was spiked into 10 ml a volumetric flask and the volume were made up with the diluent.

c. Linearity, limit of detections and limit of quantitation:

Five different concentrations of AA, SA (100, 120 140, 160, 180 µg/ml) and PA (20, 32, 40 48 and 60 µg/ml) were prepared. The responses were measured in terms of peak areas and plotted against concentration.

d. Accuracy (% Recovery):

300 mg and 100 mg of HPMCAS and HPMCP extruded polymer respectively were poured into a 100ml volumetric flask, followed by addition of 100ml methanol to dissolve the polymer and to extract the free acids from the extrudates. From this solution, 5 ml of solution was added in a 10 ml volumetric flask. Spiked solutions were prepared by adding an appropriate amount of acid

solutions to the extruded sample solutions as mentioned in the Table 3.5 and the volume made with the diluent. Diluent blank and standard solutions were prepared as per the analytical method. Each of the sample preparations was injected in triplicate and then average area count taken for calculations.

**Table 3.5: Dilutions for Accuracy (% Recovery).**

Sample Name	AA (1000 µg/ml)	SA (1000 µg/ml)	PA (1000 µg/ml)	Make up volume (ml)	Spiked solution AAxSAxPA (µg/ml)
Recovery Sol 1	0.5	0.5	0.1	10	50x50x10
Recovery Sol 2	1.0	1.0	0.2	10	100x100x20
Recovery Sol 3	1.5	1.5	0.3	10	150x150x30
Recovery Sol 4	2.0	2.0	0.4	10	200x200x40

e. Robustness:

A set of solutions including diluent blank, standard solutions of AA, SA and PA and two test solutions were injected into HPLC system. The robustness parameter was investigated by changing column lot (same manufacturer though different serial number), changing in mobile phase composition ( $\pm 0.1$  of absolute pH) and changing the flow rate ( $\pm 0.1$  ml/minute of absolute) of the original method.

**3.2.4 Degradation products of polymer and drug-polymer incompatibilities**

*3.2.4.1 Characterisation of unknown degradant of HPMCP*

- *Extraction of polymer degradant*

An unknown chemical degradant of HPMCP was initially obtained at the mouth of the crucible by heating the polymer placed in the crucible covered with aluminium foil. However, since the amount obtained was limited, to investigate

its structure elucidation, the vapour condensed degradant was obtained in a condensation assembly. Approximately 4-5 g of HPMCP was placed in a RBF and this was then attached to the condensation assembly having water circulation. The polymeric sample was exposed to the maximum temperatures of V-T1 to V-T6 for an hour and cooled to room temperatures. The RBF was removed from the condensation assembly and crystalline compound deposited on the body of the condensation unit was recovered and stored in a glass vial under a nitrogen environment. Similar procedures with different temperature profiles of V-T2 to V-T6 were utilised for independent samples of HPMCP and the vapour condensed crystals were obtained.

- *NMR analysis*

Vapour condensed crystals of HPMCP and pure crystals of phthalic acid were analysed by  $^1\text{H}$  NMR (128 scans) and  $^{13}\text{C}$  NMR (1024 scans) studies by dissolving samples in acetone- $d_6$  and using a Bruker 400 MHz NMR spectrometer.

- *MS analysis*

A mass fragmentation study of degradants was performed using Micromass Quattro Ultima-triple quadruple mass spectrometer (Waters Ltd, USA). To analyse the sample, the system was kept at 25 °C where the instrument was set up for atmospheric solid admittance probe mode and the fragmentation pattern of the degradant was performed in a positive mode of chemical ionisation.

- *GC-MS analysis*

Gas chromatography coupled with mass spectroscopy of the unknown crystals obtained from HPMCP were analysed by Agilent's GC-MS instrument. The column used in the analysis of degradant was HP-5-MS, 25 m x 0.25 mm, 0.25  $\mu\text{m}$  film thickness. Throughout the analysis, a helium gas was utilised as a

carrier. Samples of the crystals were dissolved in methanol prior to injection. The parameters of the GC were set in such a way that injections were set in a split mode while the temperature of the injector was set at 300 °C. The injected and separated sample was further analysed *in-situ* for its mass fragmentation pattern by setting up the GC interface-mass ion chamber at 280 °C, samples being analysed by MSD Chem-station software.

#### 3.2.4.2 *Characterisation of melt extrudates of Chlorpropamide*

Assay and related impurity analysis of extrudates of chlorpropamide (CPM) with HPMCAS and HPMCP and their chemical incompatibility post-extrusion was analysed by the HPLC method. Extrudates containing chlorpropamide were analysed at the wavelength of 210 nm and flow rate of 0.8 ml/minute. The column temperature and sample compartment temperature were set to 40 and 15 °C respectively. A gradient pattern was followed where the mobile phase of 0.05M potassium dihydrogen phosphate (pH=3) (solvent A) and acetonitrile (solvent B) were run for 20 minutes. For the first 4 minutes, 100% of solvent A was used, which was then mixed further with solvent B in the ratio to 75:25 (solvent A: solvent B) linearly over the next 4 minutes. Following this first 8 minutes, the gradient was changed to 50:50 for a further 4 minutes and the sequence was reversed. Methanol was used as diluent. Chlorpropamide and its two USP related impurities: A and B was used in the analysis. Standard solutions of AA, SA (200 µg/ml), PA (10 µg/ml), phthalic anhydride (10 µg/ml), chlorpropamide (10 µg/ml), impurities A and B (10 and 50 µg/ml) were prepared in diluent and injected into the systems.

#### 3.2.4.3 *Characterisation of melt extrudates of Ibuprofen*

Extrudates containing Ibuprofen were analysed by HPLC technique for assay and chemical incompatibility study at the wavelength of 214 nm and flow

rate of 2 ml/minute. A mobile phase comprising water: acetonitrile (1340: 680), pH=2.5 was utilised in a isocratic mode using a column, Luna® 5 µm C18(2) 100 Å, LC Column 250 x 4.6. This method is published in United State Pharmacopeia (USP), USP Monographs: Ibuprofen (Pharmacopeia, USP29) and followed strictly. However, related impurities of polymer and other drug-polymer interactions were analysed as per the procedure given in 3.2.3.3.

The Utilising the above techniques, polymeric suitability was investigated and these results are discussed in the next chapter.

## **Chapter 4. Results and Discussion**

In the current chapter the thermal, thermodynamic, rheological and thermo-chemical properties of pure polymers and their blends are presented. The chapter is divided into 4 major subchapters which focus on these four fundamental properties. Firstly, the material properties of pure materials (polymers, plasticisers and API) are discussed prior to melt extrusion studies. Secondly, the processing attributes and troubleshooting observed during HME are presented. Thirdly, physicochemical, thermodynamic and rheological stabilisation properties of melt extrudates are discussed. Finally, based on the above investigations, a systematic approach is adopted for polymer degradation properties through construction of polymer degradation mechanisms and degradation kinetic modelling. The implications of plasticisers on degradation kinetics of parent polymers are also investigated.

### **4.1 Material properties of polymers, plasticisers and APIs**

This section specifically focuses on investigating processing temperatures of polymeric samples including  $T_g$ ,  $T_m$ , application of the Fox equations, fragility index as well as solid state miscibility of amorphous-crystalline (semi-crystalline) entities. Additionally, low and high shear rate polymer melt rheology is investigated. Further, changes in thermo-chemical properties of polymeric samples as a function of temperature are also discussed.

#### **4.1.1 Thermal properties of materials**

The thermal properties of the HPMCAS, HPMCP, three plasticisers (TEC, PEG and CA) and two APIs (Chlorpropamide and Ibuprofen) were studied with the help of TGA. The selection of model plasticisers was made based on their proven track record, their wide applicability in HME systems

while the model APIs were selected based on their chemical structural properties, poor water solubility and easy availability.

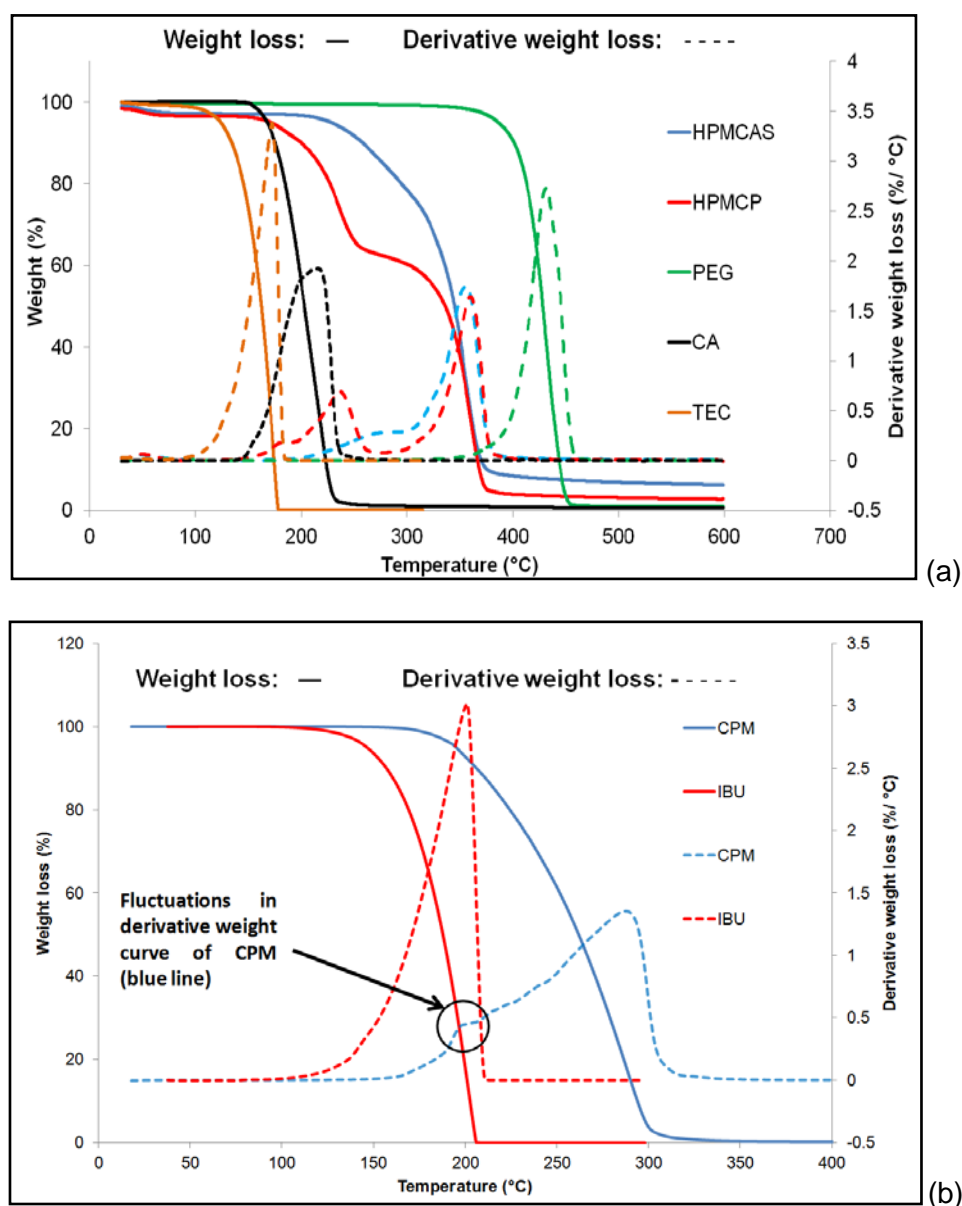


**Figure 4.1: TGA thermograms of (a) polymers and plasticisers (b) APIs.**

Initially, HPMCAS (LF, MF and HF) and HPMCP (HP50 and HP55) were investigated using TGA. TGA thermograms of the polymer exhibited a drop in the weight below 100 °C due to the evaporation of the residual moisture and moisture content was observed between 0.5 - 2.5% w/w for the different polymers (Table 4.1). the thermograms for all polymers produced similar qualitative degradation patterns. The values of polymeric weight loss for

respective polymeric grades at first degradation showed comparable results against the percent acidic substitutions of both polymers according to manufacturer specifications (see Table 2.3 background chapter). Moreover, the percent weight loss, degradation pattern and temperature of second degradation transition was comparable with degradation patterns of hydroxypropyl methylcellulose (HPMC) which was further confirmed in the literature and by our own tests (Li *et al.*, 1999 , Wang *et al.*, 2007). Representative thermograms of both polymers indicating patterns of degradation are given in Figure 4.1a and the degradation temperatures for each grade are presented in Table 4.1.

TGA thermograms of HPMCAS and HPMCP showed a distinct pattern in their degradation transitions. For instance, TGA thermogram of HPMCAS was observed to split into two decomposition steps while in the case of HPMCP two distinct decomposition steps were noted (Figure 4.1a). Derivative weight loss (DWL) curves were plotted for their confirmation and step degradation transitions were compared for number of maximum slopes. The DWL chart provided precise information and confirmation of dual transitions for all grades of HPMCAS polymers. This indicates that DWL plots can provide a useful preformulatory tool for pharmaceutical HME studies. Further, the onset degradation temperature ( $T_0$ ) for both polymers was observed to be in the range of approximately 190 - 200 °C while the first degradation transition step ( $T_1$ ) was observed between 230-250 °C for HPMCAS polymeric grades and 200-230 °C for HPMCP polymeric grades. Their corresponding DWL curvature point ( $T_2$ ) values were observed to be between 260 - 280 °C and 230- 260 °C respectively (Table 4.1). The values of  $T_0$  are generally indicative of the beginning of material weight loss hence the maximum processing temperatures for HPMCAS and HPMCP are noted to be around 200 °C and 180 °C respectively.

**Table 4.1: TGA processed values of decompositions.**

Name	Water loss (%)	First Transition (°C)			Second transition		
		T <sub>1</sub>	T <sub>2</sub>	Loss (%)	T <sub>1</sub>	T <sub>2</sub>	Loss (%)
HPMCAS-LF	0.81	249.49	283.04	16.38	348.25	368.58	75.05
HPMCAS-MF	0.67	248.58	274.	12.13	345.86	364.08	79.60
HPMCAS-HF	0.60	238.12	261.41	9.76	349.74	366.25	83.14
HPMCP-HP50	2.30	224.48	261.07	24.11	361.66	384.52	67.80
HPMCP-HP55	1.23	199.53	229.41	33.15	362.95	371.64	63.27
PEG-2000	-	404.02	426.56	99.25	-	-	-
Citric acid	-	179.12	210.12	99.22	-	-	-
TEC	-	120.12	173.23	99.34	-	-	-
Ibuprofen	-	170.93	200.11	100.00			
Chlorpropamide	-	232.05	287.70	100.00	-	-	-

Similar studies were conducted for plasticisers and APIs. The degradation of PEG started at approximately 350 °C and complete decomposition took place at 450 °C whereas the degradation of TEC and CA commenced at 110-120 °C and 165-170 °C and completed at 170-180 °C and 210-220 °C respectively. Moreover, these three plasticisers produced single step degradation curve. Chlorpropamide (CPM) and Ibuprofen (IBU) were also investigated for TGA studies. CPM produced T<sub>1</sub> and T<sub>2</sub> values at 232.05 and 287.70 °C respectively. DWL analysis of CPM showed a small peak prior to its maximum degradation slope. This may indicate that CPM is following a different degradation mechanism or undergoing chemical changes prior to, or at its onset of degradation.

## 4.1.2 Thermodynamic properties of pure and polymeric blends

### 4.1.2.1 Glass transition temperature ( $T_g$ ) and Fox equation

DSC thermograms of different grades of polymers with two solid state plasticisers (PEG and CA) and crystalline APIs were investigated. Initially, pure polymers were investigated. Different grades of polymers were heated from 20 °C to 200 °C followed by being cooled down to 0 °C and reheated to 200 °C at a rate of 10 °C/min. Since both HPMCAS and HPMCP are amorphous in nature, the materials exhibited only a  $T_g$ . The  $T_g$  values of all grades of HPMCAS were found to be in the range of 110-140°C (for LF, MF, HF grades) and for HPMCP (HP50, HP55)  $T_g$  was observed between 135-145°C. However, it was difficult to distinguish precise  $T_g$  curves for both polymers in conventional DSC and thus samples were subjected to modulated DSC (MDSC) studies. These MDSC results showed more distinguished glass transition temperature curves (Figure 4.2a) - the difference in the results from the two techniques are presented in Table 4.2.

**Table 4.2: MDSC results for HPMCAS and HPMCP polymers**

Polymer Name	DSC $T_g$ (°C)	MDSC $T_g$ (°C)
HPMCAS-LF	110.81	119.94
HPMCAS-MF	125.04	131.53
HPMCAS-HF	137.99	134.29
HPMCP-HP50	150.24	142.77
HPMCP-HP55	145.45	139.07

For solid state plasticisers, an identical heat cool heat technique was utilised. The melting endotherm of PEG-2000 was observed between 52-53 °C while CA melted between 155-156 °C. The  $T_g$  of both plasticisers was found to be in the range of -30 to -27°C and 17-20 °C respectively.

Investigation of  $T_g$  of triethyl citrate (TEC) proved practically difficult since its melting point was observed to be in the range of -53 to -55 °C and it was speculated that this value could be lower than -90 °C since a  $T_g$  event was not observed. Further, in-house instrument capability of DSC was limited to -90 °C which restricted studies below -90 °C. Ibuprofen melted in the range of 75-76 °C while chlorpropamide provided two melting endotherms at 124 and 128 °C attributed to a thermal polymorphic transformation (Figure 4.2b) from form III to form I (Drebushchak *et al.*, 2008). Further details of these chlorpropamide polymorphs are discussed in the section 4.3.

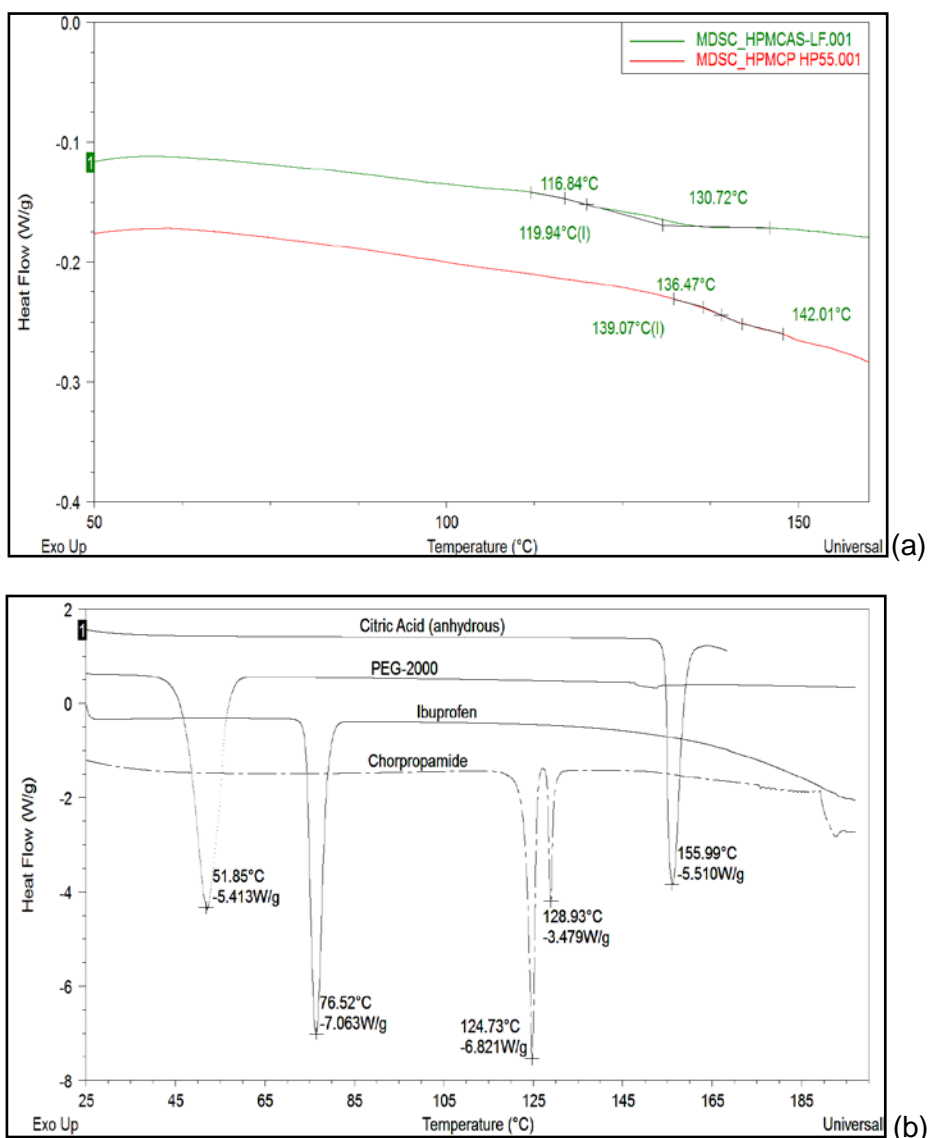
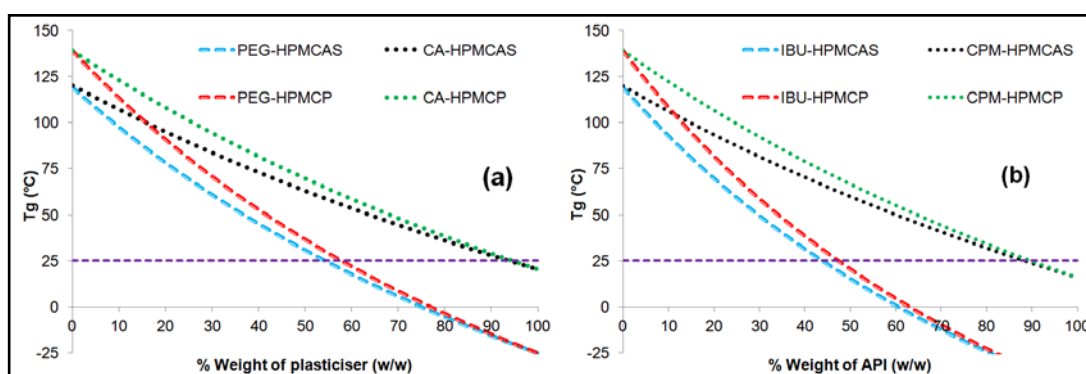


Figure 4.2: DSC thermograms of (a) polymers and (b) crystalline components.

Typically, the  $T_g$  of a parent compound is affected when a small amount of low molecular weight compounds, for instance additives or plasticisers, are added as the plasticisers increase the free volume of the polymers, resulting in a lowering of the  $T_g$  of the system (Wilson, 1996). Thus, based on the  $T_g$ , melting point and TGA values of all materials, it was thought that the pure polymers could be processed in the range 150-200°C and plasticisers will aid in the processing these polymers below 150 °C by lowering  $T_g$  of the mixture. Similarly in the case of mixtures of APIs, IBU was anticipated as a plasticiser for both polymers (De Brabander *et al.*, 2002 , Siepmann *et al.*, 2006a) while CPM's plasticising activity can be seen more prominently in the case of HPMCP than that of HPMCAS since both melting point as well as  $T_g$  of CPM is lower than HPMCP.



**Figure 4.3: Fox equation for (a) polymer-plasticisers (b) polymer-API blends.**

To investigate this phenomenon, theoretical approaches were considered and the glassy-liquid nature of the solid state mixtures was studied over a range of concentrations. Theoretically a reduction in the values of  $T_g$  for different ratios of mixtures can be calculated using equations of Fox and Gordon-Taylor (Baird and Taylor, 2012 , Lin and Huang, 2010). Generally these studies are carried out to investigate behaviour of polymeric mixtures at particular a temperature and concentration in order to predict

processing conditions of HME. In the current investigation, the Fox equation was utilised to estimate theoretical  $T_g$  of the blends of the polymers.

$$\frac{1}{T_{g \text{ mixture}}} = \frac{W_{\text{plasticiser}}}{T_{g \text{ plasticiser}}} + \frac{W_{\text{polymer}}}{T_{g \text{ polymer}}} \quad \text{Equation 4.1}$$

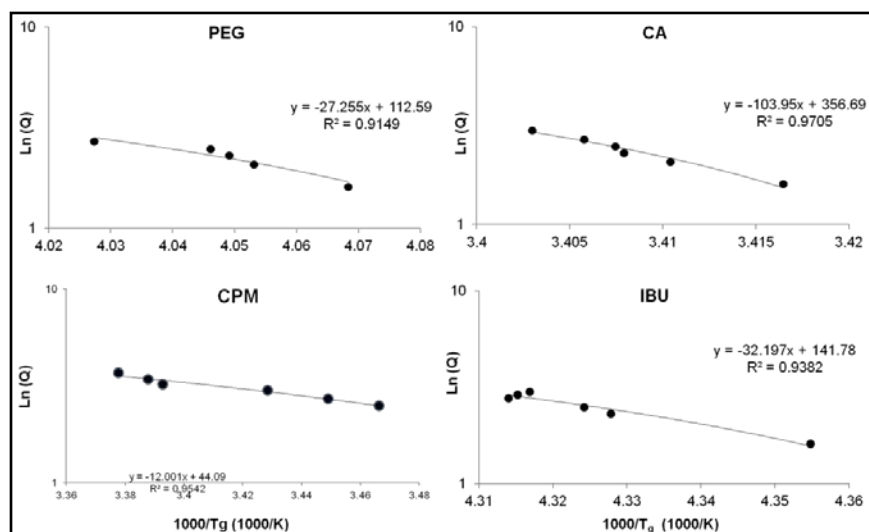
Theoretical  $T_g$  values of mixtures of plasticiser to polymeric as well as API to polymer ratios were calculated and are presented in the Figure 4.3. It was observed that at room temperature (25 °C), the mixtures of PEG with both polymers beyond 55-60% w/w concentration would behave in a liquid-like manner while similar behaviour of the plasticised CA would be produced only when the concentration reached 95% w/w. Ibuprofen would produce liquid structure with HPMCAS and HPMCP beyond 40 and 50% of IBU loadings respectively whereas 90% of CPM loadings would be required to achieve this type of behaviour. This behaviour is rather similar to CA mixtures. Further, variations in the values of  $T_g$  provided important insights about processing temperatures of HME. For example, 10% PEG added to HPMCP will produce a mixture  $T_g$  of approximately 120 °C, thus processing temperature should be > 120 °C however at the same loadings with HPMCAS, processing would be relatively easy at 120 °C since the  $T_g$  of the 10% PEG-HPMCAS would be 100 °C.

Apart from these speculations, the Fox equations can also be utilised in investigations of physical stability of melt extruded systems.

#### 4.1.2.2 Fragility parameter of solid state plasticisers and APIs

$T_g$  is considered one of the critical kinetic parameters of amorphous and crystalline materials because of its link to molecular and/or chain mobility, structural arrangements and physico-chemical destabilisation of the materials. It is frequently stated that when a liquid is cooled below its melting point, it crystallises. However, if the cooling rate is sufficiently high then the liquid

attains a state known as a "super-cooled liquid" which is considered to be non-equilibrium (i.e. amorphous materials) (Thomas Rades, 2013 , Gustavo V. Barbosa-Cánovas, 2008) to the crystalline state but it is important to note that "when a liquid is cooled through  $T_g$  region, it reaches a temperature at which the time required for structural rearrangement becomes too long to be experimentally observed" (Borde *et al.*, 2002). Hence, cooling of materials brings structural changes in materials and below  $T_g$  structural relaxation occurs.



SUMMARY OUTPUT		FRAGILITY INDEX FOR CITRIC ACID		ANOVA																																																								
<b>Regression Statistics</b> Multiple R: 0.965158751 R Square: 0.970537764 Adjusted R Square: 0.963172206 Standard Error: 0.093471327 Observations: 6				<table border="1"> <thead> <tr> <th></th> <th>df</th> <th>SS</th> <th>MS</th> <th>F</th> <th>Significance F</th> </tr> </thead> <tbody> <tr> <td>Regression</td> <td>1</td> <td>1.151233853</td> <td>1.151233853</td> <td>131.7670224</td> <td>0.00032876</td> </tr> <tr> <td>Residual</td> <td>4</td> <td>0.034947556</td> <td>0.008736899</td> <td></td> <td></td> </tr> <tr> <td>Total</td> <td>5</td> <td>1.18618141</td> <td></td> <td></td> <td></td> </tr> </tbody> </table> <p><b>Statistical significance of data drawn in MS Office Excel 2007</b></p> <table border="1"> <thead> <tr> <th></th> <th>Coefficients</th> <th>Standard Error</th> <th>t Stat</th> <th>P-value</th> <th>Lower 95%</th> <th>Upper 95%</th> <th>Lower 95.0%</th> <th>Upper 95.0%</th> </tr> </thead> <tbody> <tr> <td>Intercept</td> <td>356.6851393</td> <td>30.86702796</td> <td>11.55554</td> <td>0.00032</td> <td>270.9845306</td> <td>442.3857479</td> <td>270.9845306</td> <td>442.3857479</td> </tr> <tr> <td>X Variable 1</td> <td>-103.9525368</td> <td>9.055902248</td> <td>-11.479</td> <td>0.000329</td> <td>-129.0957523</td> <td>-78.80932132</td> <td>-129.0957523</td> <td>-78.80932132</td> </tr> </tbody> </table>							df	SS	MS	F	Significance F	Regression	1	1.151233853	1.151233853	131.7670224	0.00032876	Residual	4	0.034947556	0.008736899			Total	5	1.18618141					Coefficients	Standard Error	t Stat	P-value	Lower 95%	Upper 95%	Lower 95.0%	Upper 95.0%	Intercept	356.6851393	30.86702796	11.55554	0.00032	270.9845306	442.3857479	270.9845306	442.3857479	X Variable 1	-103.9525368	9.055902248	-11.479	0.000329	-129.0957523	-78.80932132	-129.0957523	-78.80932132
	df	SS	MS	F	Significance F																																																							
Regression	1	1.151233853	1.151233853	131.7670224	0.00032876																																																							
Residual	4	0.034947556	0.008736899																																																									
Total	5	1.18618141																																																										
	Coefficients	Standard Error	t Stat	P-value	Lower 95%	Upper 95%	Lower 95.0%	Upper 95.0%																																																				
Intercept	356.6851393	30.86702796	11.55554	0.00032	270.9845306	442.3857479	270.9845306	442.3857479																																																				
X Variable 1	-103.9525368	9.055902248	-11.479	0.000329	-129.0957523	-78.80932132	-129.0957523	-78.80932132																																																				
<b>RESIDUAL OUTPUT</b>																																																												
	Observation	Predicted Y	Residuals																																																									
	1	1.53468902	0.074748892																																																									
	2	2.164517252	-0.06507571																																																									
	3	2.424274724	-0.121689631																																																									
	4	2.472559704	0.012346946																																																									
	5	2.647482475	0.080567726																																																									
	6	2.936630497	0.059101777																																																									

Figure 4.4: Fragility parameter-graphs of  $\ln(Q)$  against  $1/T_g$ .

Literature reports suggest that structural relaxation of amorphous or crystalline materials is a function of cooling rates and cooling kinetics and hence, different glasses may be obtained. These different types of glasses are generally determined by a 'fragility parameter' which can be determined by the  $T_g$  of samples achieved as a function of cooling rates. In 1991, Angell defined the idea of fragility and differentiated glass-forming liquids into fragile and strong glasses (Angell, 1991). According to Angell, fragile glasses are unstable in nature whereas strong glasses are stable structures and these thermodynamic properties can be calculated by use of a fragility parameter.

HME is well known for production of amorphous solid dispersion (ASD) through a melt solidification process. However, the physical stability of ASD still remains one of the critical concerns of formulation strategies with several authors observing a correlation of this phenomenon with the formation of unstable glasses within ASD (Al-Obaidi and Buckton, 2009 , Janssens and Van den Mooter, 2009 , Lourdin *et al.*, 2002). Although the physical stability of an ASD is dependent upon a number of factors, including the  $T_g$  of a mixture, the material properties of any crystalline components related to their glass forming ability should also be studied. It was observed in the literature that components with fragile glass forming ability exhibit much greater increases in molecular mobility than that for strong glass formers above their  $T_g$  values. Therefore, it is important to understand fragility parameter phenomenon while extruding crystalline components for stable ASD.

Fragility is considered to be part of structural relaxation of a material when it is cooled down to its  $T_g$ . The fragility parameter (denoted here by  $m_1$ ) can be investigated from simple DSC experiments where measurements of  $T_g$  at the different cooling rates can be correlated with the material's activation energy ( $E_{a\text{-fragility}}$ ) near or at its  $T_g$  value (Borde *et al.*, 2002). In the current

investigations, the following equations were utilised to investigate the fragility parameter of the crystalline components:

$$m_1 = \frac{E_{a-fragility}}{2.303 * R * T_g} \quad \text{Equation 4.2}$$

$$\frac{d \ln(Q)}{d(1/T_g)} = \frac{E_{a-fragility}}{R} \quad \text{Equation 4.3}$$

where R is the ideal gas constant, and Q is the cooling rate of the DSC test.

The fragility parameters for PEG, CA, IBU and CPM were quantified using DSC at cooling rates of 2, 5, 8, 10, 12, 15 and 20 °C/min. Equation 4.3 was utilised and a plot of  $\ln(Q)$  against  $1/T_g$  was produced – the slope of the line being utilised to calculate  $E_{a-fragility}$  for the crystalline components (Figure 4.4). Further, the values of  $E_{a-fragility}$  were utilised in equation 4.2 in order to calculate the fragility parameter for each material.

Fragility parameters for PEG, CA, IBU and CPM were observed to be 47.73, 153.85, 60.47 and 17.70 respectively. Literature reviews suggests that values of  $m_1 < 70$  and  $m_1 > 100$  suggest strong and fragile or weak glass respectively (Borde *et al.*, 2002). Thus, based on the values, it was speculated that PEG would form a strong glass while CA would form a fragile glass. Similarly APIs such as IBU and CPM would produce strong glasses.

#### 4.1.2.3 Thermodynamics of solid state interactions

The physical stability of ASDs is one the key areas of formulation research due to concerns over phase separation or recrystallisation issues. This stability depends on several factors including the thermodynamic stability and maintenance of a homogeneous single phase system over a satisfactory time scale. Attainment of thermodynamically stable dispersions demands mixing of components at molecular level and component solubility at required concentrations and temperatures.

These physical destabilisations of ASD are also  $T_g$  and molecular mobility dependent (Ivanisevic, 2010 , Qian *et al.*, 2010 , Bhardwaj *et al.*, 2014). Thermodynamically, molecular mobility and  $T_g$  are very closely related. A kinetically stable-low molecular mobility phase can be found below values of  $T_g$ . Hence it can be seen that a low  $T_g$  formulation (e.g  $T_g$  of the ASD  $\leq 20$  °C), when placed at pharmaceutical stability temperatures (25-40 °C), would exhibit greater molecular mobility causing API to migrate from an amorphous to crystalline state. Therefore, ASD usually requires high  $T_g$  systems ( $\geq 70$ -80 °C) in order to maintain the physical stability of solid dispersions and high  $T_g$  polymers are generally recommended (e.g., HPMCAS and HPMCP).

Applications of HME in ASD manufacture has recently increased since molecular level mixings, solubilising of multiple components, amorphisation of crystalline component and embedding crystalline melts into a polymer barrier, allowing maintenance of an amorphous state, can be achieved in a single operation. However, despite these advantages only two HME produced ASDs - NORVIR<sup>®</sup> and KALETRA<sup>®</sup> - have made it to market (Parthasaradhi *et al.*, 2013 , Scholler-Gyure *et al.*, 2013 , Maniruzzaman *et al.*, 2012). To the author's knowledge this low success rate can be attributed to process induced physical destabilisation and poor understanding of the thermodynamic properties of these materials.

Physical destabilisation of ASDs manufactured by HME is dependent on HME process parameters and their relation to the thermodynamic properties of materials. During the extrusion process a homogeneous two component single phase amorphous system can be achieved and maintained at elevated temperature and pressure. Upon exit from the extruder die the extrudate experiences significant temperature drops. This forces dispersed systems to

re-equilibrate and can cause recrystallisation or phase separation of two components.

In addition, it is often seen that plasticisers are included in the extruded formulation (including the API). The majority of these plasticisers are crystalline, semi-crystalline or liquid in nature, and tend to recrystallise or evaporate during or following extrusion. Evaporation can lead to migrations of solute to phase separate while plasticiser induced molecular mobility can potentially destabilise the ASD. Thus, it is imperative to understand the compatibility and miscibility of components of melt extrusion systems including the effects of any plasticisers. Literature studies on HPMCAS and HPMCP polymers for ASDs and their unsuccessful adoption for HME (Sarode *et al.*, 2013a , Ghosh *et al.*, 2011) show the use of plasticisers but no attempt to correlate their role in the destabilisation of ASD post- extrusion , though there is some discussion on the solubility of the API in the polymer matrix. In the current work, emphasis was given on understanding the thermodynamics of polymer-plasticiser miscibility and its role in destabilisation of the polymer matrix to ensure the maximum safe solid state plasticiser's loadings for incorporation in HPMCAS and HPMCP formulations without producing recrystallisation or immediate phase separation post extrusion. Further, a model drug, IBU was utilised to perform similar studies. The thermodynamic properties of polymeric blends were investigated by use of the solubility and interaction parameters and a melting point depression approach.

- *Solubility and interaction parameter approach*

The importance of miscibility and solubility of solid state components have been stressed earlier where the theory of miscibility of two components is considered to be based on the mixing of two liquids to form a homogenous

blend while the theory of solubility is considered to be based on aqueous solution theory. Theoretically the solubility and miscibility of two components can be described by means of solubility parameter ( $\delta$ ), interaction parameter ( $\chi$ ) and from the literature it can be seen that various approaches have been utilised to calculate these.

#### Solubility parameter ( $\delta$ ) approach

The solubility parameter approach utilises assumptions and calculations of cohesive energy density ( $E_{coh}$ ) and molar volumes ( $V$ ) of individual fragments or molecules. Hildebrand and Hansen contributed significantly in this area. However it has been found that Hildebrand's assumptions and methods possess limitations; for instance, according to the Hildebrand approach,  $\delta$  depends solely on the dispersion forces between the two solutions (*i. e.*  $\delta = \sqrt{\frac{E_{coh}}{V}}$ ) whereas Hansen showed that the values of cohesive energy density ( $E_{coh}$ ) are not only dependent on the dispersion forces between the entities but also on the interactions between the two components: *i.e.* polar groups and hydrogen bonding capacity (Barton, 1991 , Hansen, 2002). Therefore, the equations of solubility parameters [ $\delta = \sqrt{\frac{E_{coh}}{V}}$ ] were modified to equation 4.4,

$$\delta = \sqrt{\delta_p^2 + \delta_h^2 + \delta_d^2} \quad \text{Equation 4.4}$$

where,  $\delta_p$ ,  $\delta_h$  and  $\delta_d$  are the polar forces, hydrogen bonding energy and dispersive forces of the components respectively. These individual parameters can be calculated as  $\delta_d = \frac{\sum F_{di}}{V}$ ,  $\delta_p = \frac{\sqrt{\sum F_{pi}^2}}{V}$  and  $\delta_h = \frac{\sqrt{\sum E_{hi}}}{V}$ .

Thermodynamically, the solubility or miscibility of components may be described based on the equation of Gibbs free energy *i.e.*  $\Delta G_{mix} = \Delta H_{mix} -$

$T\Delta S$ . According to this equation, miscibility is favoured only when the value of  $\Delta G_{mix} < 0$ . From the equation, it can be understood that the values of entropy ( $T\Delta S$ ) will be negative so in order to achieve  $\Delta G_{mix} < 0$ , values of enthalpy ( $\Delta H$ ) should be  $\leq T\Delta S$  values. In other words, miscibility of components is largely dependent on the values of  $\Delta H_{mix}$  (Barton, 1991, Pearce, 1977, Hoftyzer, 1976). Thus, the relationship of  $\Delta H_{mix}$  with component solubility and perhaps solubility parameter was further studied by Hildebrand. Hildebrand noted that  $\Delta H_{mix}$  is dependent on two parameters: volume fractions ( $\phi$ ) and  $\delta$  and proposed,

$$\Delta H_m = \phi_a * \phi_b * (\delta_a - \delta_b)^2 \quad \text{Equation 4.5}$$

From equation 4.5, it is clear that difference between the solubility parameters of components a and b will be responsible for positive and negative values of  $\Delta H_m$ . Thus  $\Delta G_{mix} < 0$  can only be obtained when  $\delta_a$  and  $\delta_b$  are either identical or  $\delta_b > \delta_a$ .

Considering these facts, the values of  $\delta$  for pure components were calculated. A group contribution technique was utilised and the van Krevelen-Hoftyzer contribution method (Barton, 1991) (widely known as van Krevelen method) was utilised while calculating solubility parameter. A representative chart of calculations of  $\delta$  for HPMCAS is shown in Table 4.3 and values of  $\delta$  for HPMCP, PEG, TEC, CA and IBU were calculated.

According to van Krevelen method, the values of  $\delta$  for HPMCAS and HPMCP were found to be 26.89 and 25.75  $\text{MPa}^{1/2}$  respectively whereas the solubility parameters for PEG and CA were found to be 22.78 and 30.88  $\text{MPa}^{1/2}$ . Moreover, the  $\delta$  difference between HPMCAS-PEG, HPMCAS-CA, HPMCP-PEG and HPMCP-CA were noted to be 4.11, 3.99, 2.97 and 5.13  $\text{MPa}^{1/2}$  respectively (Table 4.4). From the literature it was noted that small

molecules such as crystalline APIs in polymers favour miscibility only when the difference in their  $\delta$  values is less than  $7 \text{ MPa}^{1/2}$  and immiscibility is favoured when the difference increases beyond  $10 \text{ MPa}^{1/2}$  (Tian *et al.*, 2013 , Djuris *et al.*, 2013). Based on the  $\delta$  values calculated for individual polymer-plasticisers here, it was speculated that both polymers will be miscible with these two plasticisers. A similar approach was utilised for IBU-HPMCAS and IBU-HPMCP giving values of 7.93 and 6.83  $\text{MPa}^{1/2}$  respectively. These values are close to the miscibility boundary (close to 7) and thus these systems will exhibit only marginal miscibility. Similar approaches utilised for CPM-HPMCAS and CPM-HPMCP showed difference in their values as 6.28 and 5.14 respectively which suggested that CPM would produce good miscibility with both polymers compared with Ibuprofen.

**Table 4.3: Group contributions to HPMCAS by Van Krevelen method.**

Group	$F_{di}$	$F_{pi}$	$E_{hi}$	Repeating units	$\Sigma F_{di}$	$F_{pi}^2$	$\Sigma E_{hi}$
-CH <sub>3</sub> -	420	0	0	5	2100	0	0
-CH <sub>2</sub> -	270	0	0	10	2700	0	0
-CH-	80	0	0	1	80	0	0
Cyclohexane substituted	1620	0	0	2	3240	0	0
-OH	210	500	20000	3	630	2250000	60000
-O-	100	400	3000	4	400	2560000	12000
-COOH	530	420	10000	2	1060	705600	20000
-COO	390	490	7000	2	780	960400	14000
Total $\Sigma$				-	10990	6476000	106000
					$\delta_d = 21.98$	$\delta_{pi} = 5.08$	$\delta_h = 14.56$
$\delta = 26.85$ (see equation 4.4)							

**Table 4.4: Solubility parameter of different materials.**

Name	Group contribution based calculated $\delta$ (MPa <sup>1/2</sup> )		Values of Solubility Parameter mentioned in references
	Van Krevelen	Fedors	
HPMCAS	26.85	23.17	$\delta_{\text{Hildebrand}}=21.99-22.75$ (Babcock Walter C, 2008)
HPMCP	25.75	23.36	$\delta_{\text{Krevelen}}=26.4$ , $\delta_{\text{Hoy}}=22.4$ (Sakellariou <i>et al.</i> , 1986)
PEG-2000	22.78	20.41	PEG1000 $\delta_{\text{Krevelen}}=23.4$ , PEG4000 $\delta_{\text{Krevelen}}=22.5$
Citric acid	30.88	36.47	$\delta_{\text{Krevelen}}=28.69$ , $\delta_{\text{Hansen}}=31.76$ (Barra <i>et al.</i> , 1997)
Ibuprofen	18.92	20.43	$\delta_{\text{Hansen}}=20.90$ (Greenhalgh <i>et al.</i> , 1999),
Chlorpropamide (CPM)	20.61	22.25	No references found

#### Interaction parameter approach

Investigations of miscibility based on the solubility parameter provide valuable insights about thermodynamic properties of pure materials but it is important to consider that values of  $\delta$  relate mainly to non-polar or weak interactions between the components (Barton, 1991). However many polymeric solutions exhibit strong or polar interactions which can be described by the Flory-Huggins interaction parameter ( $\chi$ ) (Li *et al.*, 2014, Pajula *et al.*, 2010) which describe these interactions as a function of component miscibility and solubility.

Flory-Huggins (F-H) developed a lattice-based theory in which the polymeric solution (solvent + polymer) gains a structure similar to a crystal lattice where each single molecule of polymer and solvent occupies single lattice in the structure. Three interactions such as polymer-polymer, solvent-solvent and polymer-solvent interactions are assumed in the lattice based

model. To define difference in their energy of interactions, the interaction parameter  $\chi$  was introduced (Rubinstein and Colby, 2003) allowing the original Gibbs free energy equation to be modified to:

$$\Delta G_{mix} = RT(\chi_{a,b} * \phi_a * \phi_b) - RT(n * \log \phi_a + n * \log \phi_b) \quad \text{Equation 4.6}$$

Where,  $\Delta H_{Mix} = RT(\chi_{a,b} * \phi_a * \phi_b)$ ,  $T \Delta S_{mix} = RT(n * \log \phi_a + n * \log \phi_b)$ , n is number of moles and R is the real gas constant.

Furthermore, Hildebrand and Scot (Charles, 2007) developed a relationship between  $\chi$  and  $\delta$  to precisely determine miscibility values for two components at room temperature (25°C):

$$\chi = \frac{V_{site}}{RT} * (\delta_a - \delta_b)^2 \quad \text{Equation 4.7}$$

Where  $V_{site}$  is the volume per lattice site.

Using the assumptions of Flory-Huggins interaction parameter and Hildebrand-Scot approach (equation 4.6 and 4.7), interaction parameters of HPMCAS, HPMCP, PEG, CA and IBU were investigated. Initially, Hildebrand-Scot approach was investigated in the current research work whereas the F-H  $\chi$  approach is discussed in the melting point depression approach.

**Table 4.5: Values of  $\chi$  based on the solubility parameters.**

Name	HPMCAS				HPMCP			
	PEG	CA	IBU	CPM	PEG	CA	IBU	CPM
Interaction parameter ( $V_{site} = 100 \text{ cm}^3 / \text{mol}$ )	0.68	0.64	2.55	1.58	0.35	1.06	1.86	1.05
Interaction parameter ( $V_{site} = 500 \text{ cm}^3 / \text{mol}$ )	3.395	3.19	12.77	7.90	1.76	5.2	9.338	5.28

According to the Hildebrand and Scot equation, investigation of  $\chi$  requires values of  $V_{\text{site}}$  which is defined as a hypothetical volume of a lattice in which the interactions between polymer and a small molecule occurs. It was observed that various researchers have mixed views about the values of  $V_{\text{site}}$  while calculating  $\chi$  of individual mixtures. In the majority of the cases, the volume of lattice is considered either as  $100 \text{ cm}^3/\text{mol}$  (Miller-Chou and Koenig, 2003) or the molecular volume of the polymer chain or molar volume of the drug (Paudel et al., 2010). However to investigate effects of  $V_{\text{site}}$  on the predictions of polymer-plasticiser thermodynamic interactions, the values of  $\chi$  were calculated at two different values of  $V_{\text{site}}$  in the current studies. In the first case, values of  $V_{\text{site}}$  were considered to be  $100 \text{ cm}^3/\text{mol}$  whereas in the second case the molecular volume of a polymeric chain ( $\sim 500 \text{ cm}^3/\text{mol}$ ) was considered. The values of the interaction parameter so obtained by these methods are presented in Table 4.5.

It was noted that HPMCAS interacts similarly with both plasticisers while significant differences were noted in the case of HPMCP interactions with a marked difference being noted for HPMCP-plasticiser interactions. According to this interaction parameter approach, miscibility is favoured at lower  $\chi$  values. Hence, based on these assumptions, it was noted that HPMCP-PEG will produce better miscibility than CA. The Hildebrand and Scot approach utilised for the mixture of IBU-Polymers provided important understanding about thermodynamic properties of materials. For example,  $\chi$  values of Ibuprofen with both polymers are higher than that of PEG, CA and CPM mixtures with both polymers at  $25 \text{ }^\circ\text{C}$ . This indicated that enthalpic contribution would produce poor response in over all Gibbs free energy equation and majority of IBU-HPMCAS and IBU-HPMCP compositions would show positive values of  $\Delta G_{\text{mix}}$ . This supported the assumptions of Ibuprofen-polymer mixtures showing partial miscibility or complete immiscibility with

these two polymers and based on these values, it was speculated that Ibuprofen mixtures would produce profound miscibility gap in the phase diagrams (See section 4.1.2.4 for more details).

It is important to note that the interactions parameter values obtained by this method are strictly applied to interactions at room temperature and cannot be applied directly to the temperatures of interest especially at temperatures necessary for HME. In addition, it should be noted that two of the most important factors must be taken into account since the  $\delta$  approach does not consider the entropy term ( $T\Delta S$ ) while values of  $\chi$  calculated based on the 'regular solution model' do not consider any change in volume upon mixing (Barton, 1991 , Cherdrion, 1978 , Flory, 1953 , Hansen, 2002 , Rubinstein and Colby, 2003 , Rudolf *et al.*, 1995). Empirically, these factors significantly affect the thermodynamics of miscibility-solubility and thus prediction of miscibility based on  $\chi$  and  $\delta$  alone can be inaccurate. This further demands a strong theoretical approach to link miscibility both at ambient and non-ambient temperatures. Nonetheless lower values of interaction parameter suggest that the miscibility predicted by both  $\chi$  and  $\delta$  can be a useful tool for preformulatory studies.

- *Melting point depression (MPD)*

It has been seen that addition of small molecules (here API or plasticisers) in the polymer matrix (usually amorphous) has a significant impact on the melting point of a crystalline compound when present in a mixture. In many of such instances and over a range of different concentrations, these are related to melting point depressions (Tian *et al.*, 2013 , Nishi and Wang, 1975 , Paudel *et al.*, 2010). In the majority of cases, this phenomenon is attributed to the solubility of crystalline component in an amorphous polymer (Nishi and Wang, 1975). Literature reviews suggest that

the phenomenon of MPD is closely associated with drug-polymer miscibility and such a depression is an indicator of strong interactions between the two components.

In 1975, Nishi and Wang investigated polymer-polymer miscibility as a function of MPD by utilising Flory Huggin's ' $\chi$ ' terminology (Nishi and Wang, 1975). Since  $\chi$  is a representation of the solid-state interactions, these authors deduced an equation to calculate miscibility of the component based on the difference in melting points between two component mixtures and their pure constituents (see equation 4.8).

$$\frac{1}{T_m} - \frac{1}{T_{m0}} = -\frac{R}{\Delta H} \left[ \frac{\log \phi_2}{m_2} + \phi_1 * \left( \frac{1}{m_2} - \frac{1}{m_1} \right) + \chi_{12} * \phi_1^2 \right] \quad \text{Equation 4.8}$$

Where  $T_m$  and  $T_{m0}$  are the melting points of polymer blends and pure polymers respectively,  $m$  is the degree of polymerisation,  $\phi$  is the volume fraction of components and subscripts denote the two components.

A variety of researchers have applied equation 4.8 to investigations of solid state miscibility. Several limitations were observed resulting in modifications to the original equation. For instance a parameter has been introduced where the degree of polymerisation term utilised by Nishi and Wang was replaced by the ratio of molar volume of polymer to drug. This modified equation is suggested in various research articles and different authors such as Lynne Taylor (Baird and Taylor, 2012 , Rumondor *et al.*, 2009a , Rumondor *et al.*, 2009b , Rumondor *et al.*, 2009c , Rumondor and Taylor, 2009), Gavin Andrews, David Jones and co-workers (Donnelly *et al.*, 2015 , Tian *et al.*, 2013) have investigated equation 4.9 to estimate both solid-state miscibility and solubility.

$$\frac{1}{T_m} - \frac{1}{T_{m0}} = -\frac{R}{\Delta H} \left[ \log \phi_1 + \phi_2 * \left( 1 - \frac{1}{mv} \right) + \chi_{12} * \phi_2^2 \right] \quad \text{Equation 4.9}$$

Where,  $mv = [(\text{Mol wt}_2/\text{Density}_2)/(\text{Mol wt}_1/\text{Density}_1)]$

In the current investigation, subscript '1' for plasticiser (plasti) and '2' as a polymer (poly) has been used and thus equations are modified accordingly in equation 4.10. It has also been reported that values of  $\chi$  of different compositions near the melting point of the crystalline compound are often found to be negative since miscibility of the components is favoured at melting points (Paudel *et al.*, 2010 , Tian *et al.*, 2013). In other words, at these temperatures,  $\Delta G_{mix}$  is expected to be negative and one can estimate its values by equating the interaction parameter on two compounds in equation 4.11,

$$\frac{1}{T_m} - \frac{1}{T_{m0}} = -\frac{R}{\Delta H} [\log \phi_{plasti} + \phi_{poly} * \left(1 - \frac{1}{mv}\right) + \chi_{plasti-poly} * \phi_{poly}^2] \quad \text{Equation 4.10}$$

$$\Delta G_{mix} = RT[\phi_{plasti} * \log \phi_{plasti} + \frac{\phi_{poly}}{mv} * \log \phi_{poly} + \chi_{plasti-poly} * \phi_{plasti} * \phi_{poly}] \quad \text{Equation 4.11}$$

Thermodynamic interactions between the samples of polymer-plasticisers and polymer-API were analysed independently by the use of this MPD approach. Different concentrations of polymer-plasticiser mixtures were prepared from 10 to 95 % plasticiser in polymer and MPDs were screened against 100% pure crystalline components (here meaning CA or PEG alone). Mixtures of samples were prepared by two methods. In the first method, physical mixtures were prepared by a mortar-pestle technique prior to running DSC while in the second method similar concentrations were prepared by a solvent evaporation method having been dried in a vacuum oven for 24 hours prior to DSC investigations. One of the limitations of the first method is the delivery of a precise concentration of physical mixture into the DSC pan and hence the reliability of any observed depressions. Thus, in general the solvent evaporation method was utilised. Use of a solvent evaporation approach has been discussed in other articles for MPD based thermodynamic measurements (Lin and Huang, 2010).

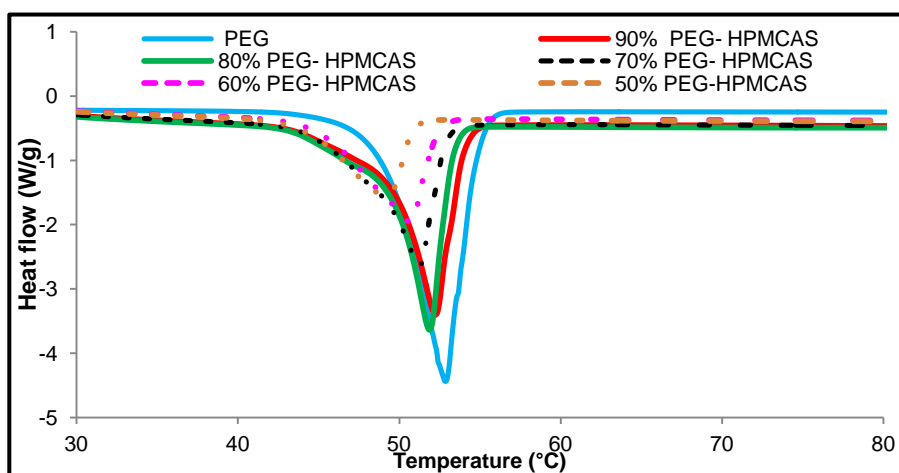


**Figure 4.5: DSC thermograms of PEG-HPMCAS showing MPD.**

Since solvent evaporation can increase the amorphisation of crystalline components and certain concentrations will not show a melting endotherm due to the lowering of the chemical potential of the plasticiser, the same technique was utilised over the range of concentrations and melting depressions of different concentrations of polymer plasticisers were investigated at heating rate of 5 °C/min. Figure 4.5 shows the DSC thermogram for pure PEG-2000 and its physical mixtures with HPMCAS at different concentrations. A clear evidence of melting depression can be observed in the figure indicating a significant degree of mixing and physical interactions near the melting point of PEG. Similar effects were observed with blends of HPMCP with citric acid and PEG. PEG blends with polymer showed substantial depressions over the blends of CA. Thus, it is speculated that interactions of PEG would be higher than that of CA with HPMCAS and HPMCP.

This melting depression data set was further utilised in the equation 4.10 and a graph of  $[-[1/T_m - 1/T_{m0}]/(R/\Delta H) - \log \phi_{\text{plasti}} - \phi_{\text{poly}} * (1 - 1/m)]$  against  $\phi_{\text{poly}}^2$  was used to determine  $\chi$  of polymer-plasticisers near their melting points. The graph yielded a linear relationship with its slope representing  $\chi$  as seen in Figure 4.6. In all cases, negative values of  $\chi$  were

obtained. However the values of  $\chi$  obtained with PEG were more strongly negative than the corresponding CA blends which supports the previous assumption that PEG is more miscible with both polymers when compared with CA (Table 4.6). Similarly in the case of blends of IBU-Polymers, the values of  $\chi$  were also negative, its interactions with both polymers being similar. This phenomenon is speculated to be due to closeness of their difference in solubility parameter - near a value of 7. CPM-HPMCP showed value of  $\chi$  close to that of CA-HPMCP thus, interactions of CPM-HPMCP was speculated to be similar to that of CA-HPMCP blends.

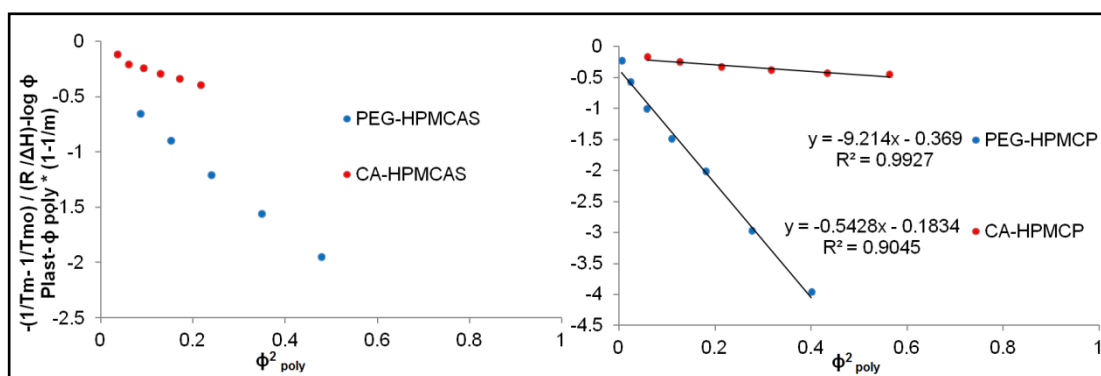


Figure 4.6: Plots determining interaction parameter near melting point.

Table 4.6: Interaction parameter values near melting points.

Name	Linear equation obtained practically	$r^2$	Interaction parameter near melting point
HPMCAS-PEG	$y = -5.9645x - 0.6000$	0.9762	-5.965
HPMCAS-CA	$y = -1.4044x - 0.1639$	0.9992	-1.4044
HPMCP-PEG	$y = -9.214x - 0.3690$	0.9927	-9.214
HPMCP-CA	$y = -0.5428x - 0.1834$	0.9045	-0.5428
HPMCAS-IBU	$y = -1.0146x - 0.1040$	0.8885	-1.014
HPMCP-IBU	$y = -1.2022x - 0.0767$	0.9609	-1.2022
HPMCP-CPM	$y = -0.6029x - 0.0507$	0.9453	-0.6029

To further investigate the impact of these interaction parameters on the Gibbs free energy of the polymeric systems, equation 4.11 was utilised. As indicated with melting depressions, all six systems showed negative values of Gibbs free energy that suggest miscibility is favoured near and above the melting temperatures of the crystalline entities irrespective of their solubility parameter differences (Figure 4.7). Moreover, the values of  $\Delta G_{mix}$  of HPMCP-PEG showed maximum negative values whereas IBU blends showed minimum  $\Delta G_{mix}$  values, correlating with their corresponding negative  $\chi$  values (Table 4.6). However, since pharmaceutically relevant stability temperatures lie in the range 2- 40 °C, attaining miscibility or solubility at the melting points of two components cannot be considered as forming stable ASDs at pharmaceutical stability temperatures. Thus, equation 4.11 can be applied to the composition near the melting point of the crystalline component and this equation does not describe miscibility below this melting temperature. Moreover, equation 4.11 does not explain sudden phase separation (decomposition phase) or kinetic based recrystallisation of certain compositions in post-extrusion studies.

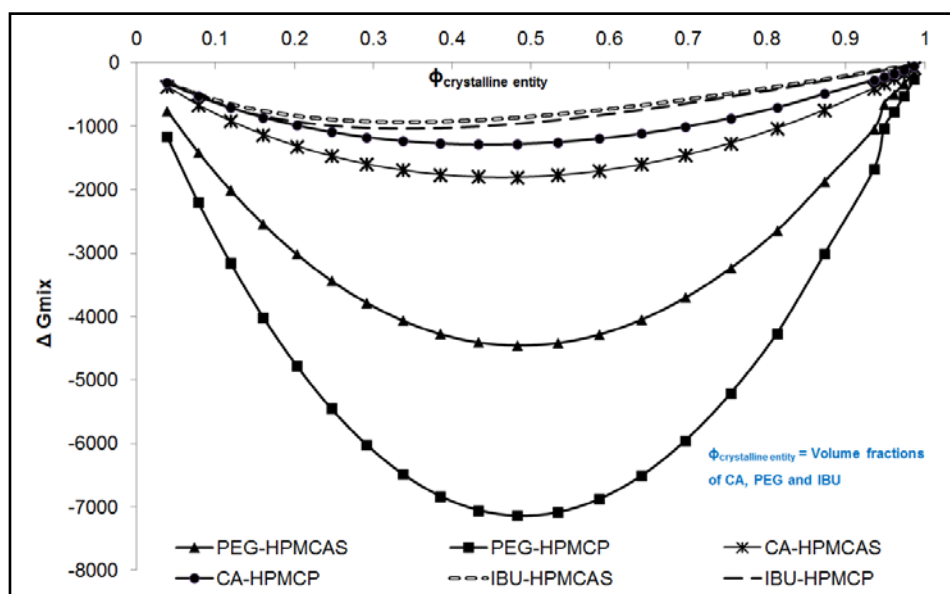


Figure 4.7: Gibbs free energy near melting point of the plasticisers.

#### *4.1.2.4 Mechanism of phase separation and construction of phase diagram*

It is important to understand that although components are showing complete miscibility or solubility near to or above melting point of a mixture, very few compositions would remain in the single phase homogeneous state when store at room temperatures. This suggest that physical stability of two or more components is completely temperature and composition dependent and several kinetic factors (or displacements or barriers) such as time, polymer melt viscosity, moisture altogether affecting the system will ultimately decide its decomposition in to two phases.

Normally during extrusion, and in majority of the cases, a homogeneous melt of a crystalline drug and an amorphous polymer is obtained (due to complete miscibility and increased solubility favours at high temperatures) since the process usually runs at higher temperature. However, as soon as the extrudate comes out the extruder die, it faces fluctuations in temperatures, viscosity modifications and moisture adsorptions which might force a homogeneous system to decompose into two phases. This suggests that a homogeneous single phase system produced by HME should survive to kinetic displacements and then only problems related to physical stability can be solved. Phase separation of two components can be anticipated at preformulatory stage by constructing thermodynamic phase diagrams where theoretical as well as empirical values of interaction parameters are taken into considerations. Further, in order to strengthen the understandings of phase separation, a mathematical approach should be utilised which in theoretically enable to utilise infinite concentrations to design a precise and accurate phase diagram.

Although HPMCAS and HPMCP have been used in a number of solid API dispersion systems, only few studies have investigated thermodynamic

approaches associated with recrystallisation of the API during stability studies. Furthermore, researchers who have used this approach have also utilised plasticisers with these polymers and polymer-plasticiser interactions or maximum safe loadings of plasticisers have not been investigated. Therefore, in the current work, thermodynamic phase diagrams of polymer-plasticiser and polymer-API were constructed using mathematical approaches.

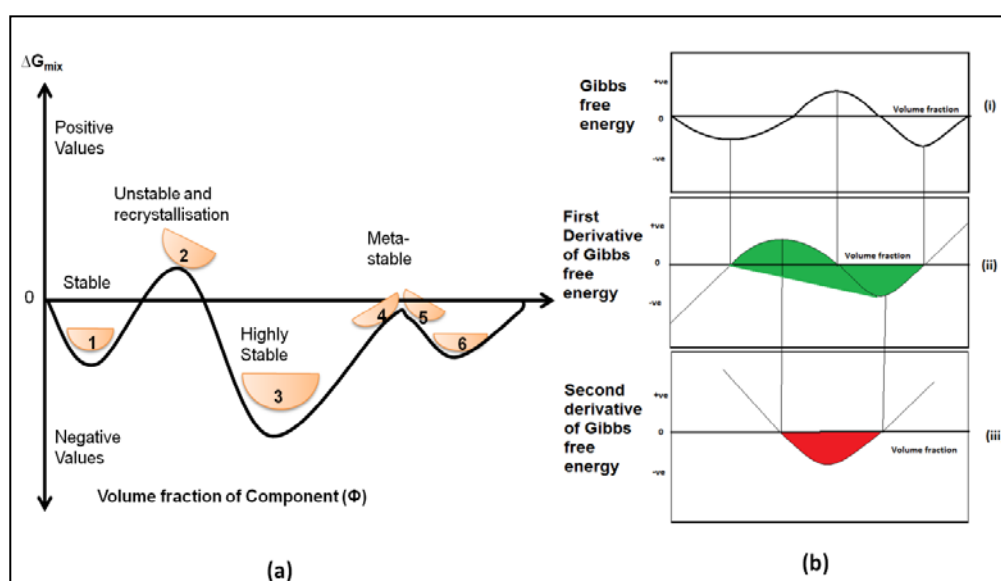


**Figure 4.8: Mechanism of phase separation by mathematical approach.**

### **Theory:**

In order to understand the mechanism of phase separation a hypothetical mixture are considered. These processed over the range of concentrations (0-100% w/w) in the melt extrusion process and Gibbs free energy curve of these systems is discussed below. The free energy composition diagram (FECD) shows three main states of stability: stable, unstable and metastable regions, as shown in Figure 4.8a. It can be seen that the composition at position 1 and 3 attains maximum negative values of  $\Delta G_{mix}$  whereas the composition at the position 2 attains maximum positive values of Gibbs free energy. According to the Gibbs free energy equation and

composition diagram, stable compositions are defined as those compositions whose  $\Delta G$  remains  $< 0$  while the compositions showing values of  $\Delta G \geq 0$  are considered as unstable since one of the component of mixture is either suddenly decomposed in to 2 phases or recrystallise over a period of time.

Recrystallisation from the amorphous state generally requires kinetic displacement (e.g. temperature, pressure, humidity and molecular mobility) which forces system to move from a lower  $\Delta G_{\text{mix}}$  value to higher i.e. from negative to positive value. From the figure, the composition at positions 1 and 3 are considered as highly stable compositions because even if the system re-equilibrates, the compositions in the same region will return to lower energy state and the amorphous state will not recrystallise. However, the composition between the position 1 and 2 or precisely on the line of 3, 4, and 5 will not produce the same effect as that of 1 and 3 upon kinetic displacements. For compositions on the line of 3, 4, 5 when subjected to kinetic displacements, composition at position 4 could survive kinetic displacements (since the second of derivative of Gibbs free energy is positive) and return back to lower values of Gibbs free energy whereas composition at 5 would not survive in these displacements (since the second of derivative of Gibbs free energy is negative) and eventually would recrystallise. Thus, the thermodynamic stability of the compositions on the line of 3, 4 and 5 can be ambiguous. This region is termed as the metastable region where the miscibility gap between components plays a dominant role.

Recrystallisation or phase separation of the mixture occurs due to miscibility gaps between the 2 or more components (Horst and Wolf, 1994 , Marsac *et al.*, 2007 , Salamone, 1996). Thus, if the mixture is showing a miscibility gap in the phase diagram then the Gibbs FECD can be observed as shown in Figure 4.8b (i). Earlier it was understood that the compositions

which show  $\Delta G_{\text{mix}}$  close to zero or increasing to zero from negatives are thermodynamically unstable since values of  $\Delta G_{\text{mix}}$  show apparent low energy states (Jan H. Los, 2002). Mathematically, the regions of unstable and metastable zones within the Gibbs free energy curves can be calculated from the first and second derivative of  $\Delta G_{\text{mix}}$  with respect to the volume fraction. These two derivatives produce unique regions within the FECD when the values of slopes reach to zero as shown in Figure 4.8b (ii, iii). The first derivative produces a 'binodal' region at the values of  $\frac{d\Delta G_{\text{mix}}}{d\phi} = 0$  (Figure 4.8b ii) while the second derivative produces a 'spinodal' decomposition region at the values of  $\frac{d^2\Delta G_{\text{mix}}}{d\phi^2} = 0$ . Investigations of binodal and spinodal decompositions play a significant role in understanding phase separation in solid state thermodynamics since the binodal line separates the region between unstable and miscible phases (Figure 4.8b ii) whereas the spinodal decomposition region separates unstable region into regions of metastable and unstable phase (Figure 4.8b iii). Of interest, the regions of spinodal decompositions are of much importance since this region shows metastable compositions where amorphous dispersions crystallise through a nucleation and growth mechanism.

In summary, the thermodynamic stability of the dispersions can be predicted by mathematical functions of Gibbs free energy as: homogeneous stable phase [ $\Delta G_{\text{mix}} < 0$  and  $\frac{d^2\Delta G_{\text{mix}}}{d\phi^2} > 0$  (position 1, 3 and 6)], metastable phase [ $\Delta G_{\text{mix}} < 0$  and  $\frac{d^2\Delta G_{\text{mix}}}{d\phi^2} < 0$  (position 4 and 5)] and unstable phase [ $\Delta G_{\text{mix}} > 0$  (position 2)].

### **Discussion:**

Investigations of FECD and mathematical calculations of first and second derivatives of the Gibbs free energy near the melting point (Figure 4.7) would provide binodal and spinodal lines of a particular polymer-plasticiser system. However, it is extremely important to note that values of  $\chi$  are highly temperature and concentration dependent; in other words, exhibit "non-trivial dependence on temperature, concentration and polymer chain length" (Rubinstein and Colby, 2003). Therefore, to develop and correlate the values of  $\Delta G$  with the focus of temperature dependency, a temperature dependent  $\chi$  is defined as:

$$\chi_{\text{plasti-poly}} = A + B/T \quad \text{Equation 4.12}$$

where A is the entropic contribution and B is enthalpic contribution of the system (Rubinstein and Colby, 2003).

The lattice based theory of Flory-Huggins assumes important considerations about non-trivial dependency of  $\chi$ . According to the theory,  $\chi$  establishes a first order relation with the reciprocal of the temperature - this being confirmed by a number of authors (Janssens and Van den Mooter, 2009 , Marsac *et al.*, 2010 , Rumondor and Taylor, 2009). Further, these authors used a first order relation to extrapolate the values of  $\chi$  below the melting point of the crystalline components (generally at pharmaceutical stability temperatures) or below extrusion temperatures. It is apparent that once the relationship between  $\chi$  and  $1/T$  is established, the values of  $\chi$  obtained from these relations can be further utilised in FECD and the second derivative of  $\Delta G$  can be utilised to generate a polymer-plasticiser miscibility diagram. Thus, values of  $\chi$  were determined over a range of temperature using two methods:

- a. Extrapolation of equation 4.12 (Tian et al., 2013)

- b. Combining two parts of  $\chi$  obtained at room temperature (Table 4.5) and near the melting point region (by an MPD approach) to quantify terms A and B in equation 4.12 (Zhao et al., 2011).

**Approach (a):** Initially the phase diagram was constructed using method (a) where  $\chi$  obtained by equation 4.10 was rearranged and plotted against the reciprocal of temperature. Careful observation of MPDs of independent blends of PEG and CA suggested that for compositions less than 0.30 and 0.40 volume fractions of PEG and CA respectively did not show any melting endotherms. Similar observations were noted in the case of IBU-HPMCP and IBU-HPMCAS at 0.55 and 0.40 volume fractions of IBU. This phenomenon can be described using an upper critical solution temperature (UCST) approach (Tian *et al.*, 2013).

According to the IUPAC Gold Book and Work *et al.*, (2004) a UCST is defined as the "critical temperature above which a mixture is miscible" (Work *et al.*, 2004). Polymeric blends generally show two transitions between single and two phase states where these states are highly dependent on the enthalpy interactions between the two components. If unfavourable, the mixture displays a UCST and compositions of the blend will be immiscible at lower temperatures while miscibility is observed at higher temperatures due to reduced enthalpic contributions.

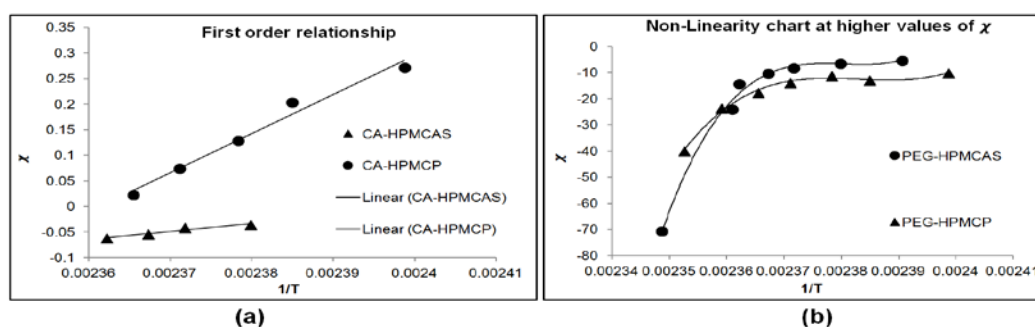


**Figure 4.9: (a) First order linear and (b) non-linear relationship between interaction parameter and  $1/T$ .**

Equation 4.12 was further utilised to investigate the first order relationship. Rearranging the equation 4.10 provided some important clues about linear relationship between  $\chi$  and  $1/T$ . In the case of blends of PEG, the linear relationship was observed in the concentration range of 0.3 - 0.7 while for CA-HPMCAS and CA-HPMCP, 0.65 - 0.85 and 0.3 - 0.7 volume fractions showed linear relationships. A representative chart describing this first order relationship between  $\chi$  and  $1/T$  is shown in Figure 4.9(a). Additionally, a non-linear relationship was also noted, especially at high temperatures and concentrations of crystalline components, which are attributed to higher values of interaction parameters the near melting point of plasticisers (Figure 4.9b). Similar non-linearity has been reported for HPMCAS-Felodipine, Soluplus-Felodipine by Tian and co-workers as well as Zhao and co-workers. Therefore, by utilising the rationale of equation 4.12, linear equations of polymer-plasticiser interactions were extrapolated to pharmaceutical stability temperatures and their respective endothermic-enthalpic constants were determined and presented in Table 4.7.

**Table 4.7: Constants A and B determined using equation 4.12.**

Name	Volume fraction range	Equation	A	B	R <sup>2</sup>
HPMCAS-PEG	0.30 - 0.70	$y = 19487x - 63.366$	-63.36	19487.0	0.8674
HPMCP-PEG	0.30-0.65	$y=42305.2x - 132.16$	-132.16	42305.2	0.9054
HPMCAS-CA	0.65-0.85	$y = 2123.5x - 5.0787$	-5.07	2123.5	0.9734
HPMCP-CA	0.30 - 0.70	$y = 7632.1x - 18.022$	-18.02	7632.1	0.8674
HPMCAS-IBU	0.40-.065	$y = 9014.1x - 26.08$	-26.08	9014.1	0.9895
HPMCP-IBU	0.55-0.80	$y= 11640x-33.46$	-33.46	11640.0	0.9934

**Table 4.8: Comparison of derived constants A and B obtained by the two approaches of investigating of  $\chi$ .**

Name	Interaction parameter equation based on solubility parameter (equation 4.7)		Interaction parameter equation based on extrapolation method (equation 4.12)	
	$\chi = 32515/T - 105.71$	$\chi_{@25^{\circ}\text{C}} = 3.4$	$\chi = 19487/T - 63.36$	$\chi_{@25^{\circ}\text{C}} = 2.03$
HPMCAS-PEG	$\chi = 40703.15/T - 134.82$	$\chi_{@25^{\circ}\text{C}} = 1.76$	$\chi = 40334/T - 131.75$	$\chi_{@25^{\circ}\text{C}} = 3.59$
HPMCAS-CA	$\chi = 4478.88/T - 11.83$	$\chi_{@25^{\circ}\text{C}} = 3.1$	$\chi = 2123.5/T - 5.0787$	$\chi_{@25^{\circ}\text{C}} = 2.04$
HPMCP-CA	$\chi = 5854.85/T - 14.44$	$\chi_{@25^{\circ}\text{C}} = 5.20$	$\chi = 7632.1/T - 18.022$	$\chi_{@25^{\circ}\text{C}} = 7.58$
HPMCAS-IBU	$\chi = 29329/T - 93.56$	$\chi_{@25^{\circ}\text{C}} = 4.85$	$\chi = 9014.1/T - 26.08$	$\chi_{@25^{\circ}\text{C}} = 4.16$
HPMCP-IBU	$\chi = 20284.5/T - 62.08$	$\chi_{@25^{\circ}\text{C}} = 5.98$	$\chi = 11640/T - 33.46$	$\chi_{@25^{\circ}\text{C}} = 4.60$

**Approach (b):** In the second approach of combining the values of  $\chi$  at room temperature (equation 4.7) and near melting point (equation 4.8), the values of A and B were investigated (see Table 4.8). Based on these values,  $\chi$  was calculated and crossed checked this value against the value of  $\chi$  obtained by an approach (a) or equation 4.12. Comparison between two approaches utilised from calculating  $\chi$  of binary compounds yielded comparable values with a maximum difference of  $\pm 1.5$  between two approaches (see Table 4.8). Further the phase diagrams produced by these two approaches provided similar maximum free loadings values and similar phase diagram zones (discussed later in this section). Therefore, the application of either of the methods in investigating the interaction parameter of polymer-plasticiser thermodynamic studies is observed to equivalent in the current research work.

Considering above observation, equation 4.12 was further utilised and the values of the interaction parameter over a range of temperatures were

determined by this method and used to plot a Gibbs free energy curve using equation 4.11 (Figure 4.10).

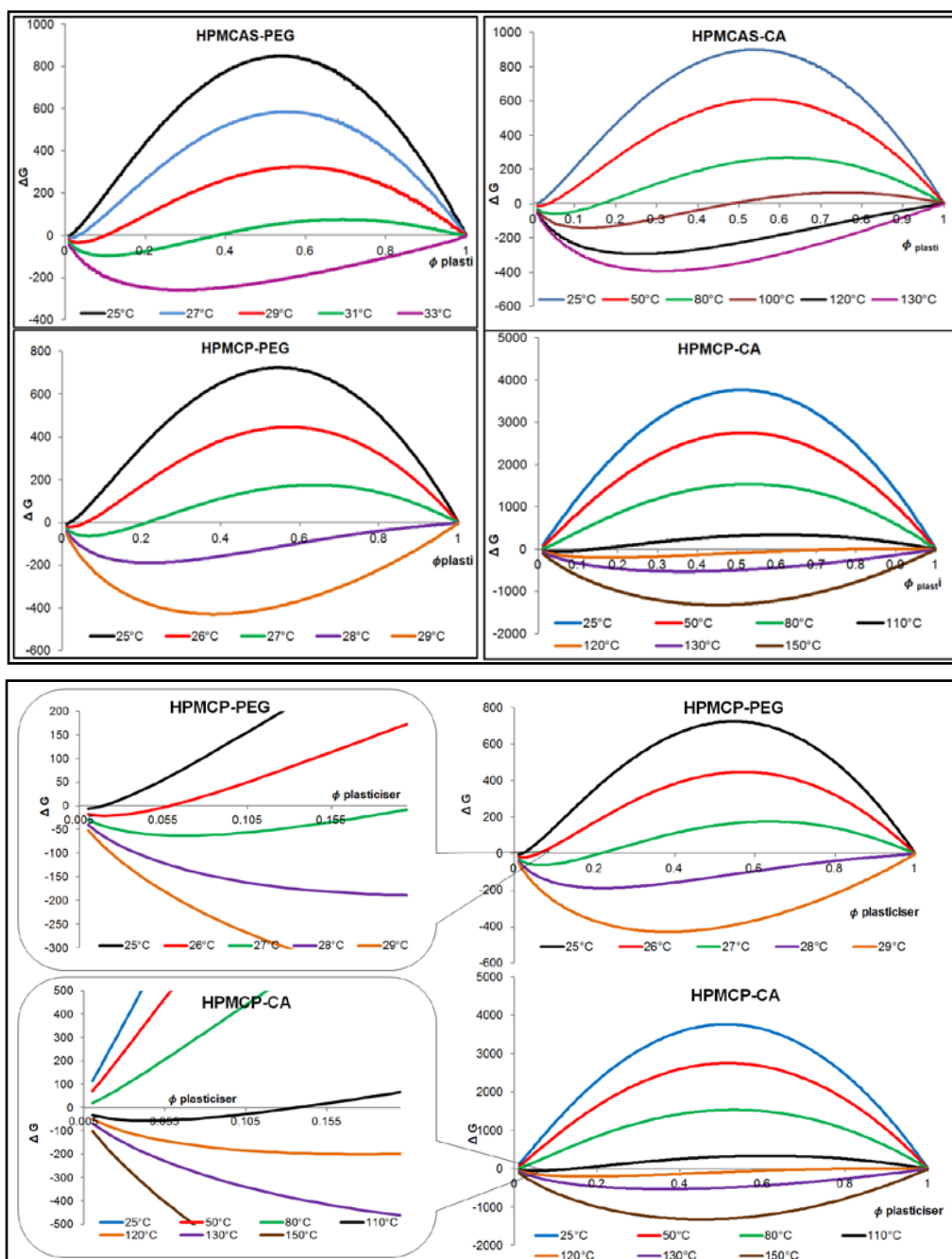


**Figure 4.10: Plots of Gibbs free energy as a function of volume fractions of plasticisers at different temperatures.**

Free energy curve diagrams plotted by this method provided valuable insights about polymer-plasticiser interactions and miscibility between the two components at room temperature. As indicated by the positive values of  $\chi$  of

PEG and CA with their respective blends at 25 °C, it was expected to achieve positive values of Gibbs free energy over the range of concentrations however, at the same temperature blends of PEG showed negative values of  $\Delta G_{\text{mix}}$  up to concentration of ~2% ( $\phi = 0.02$ ) loading with both polymers. This was indicative that at 25 °C miscibility of the PEG with parent polymer can be expected while, at the same temperature, blends of CA even at minimal concentration of 0.5% were immiscible (see Figure 4.10). It is important to note that during practical experiments, 0.5% and 2 % loadings were not actually prepared however the use of mathematical models enables this determination.

A trend was observed where values of  $\Delta G_{\text{mix}}$  decreased with increasing temperature. However, a semi-circular shape of the  $\Delta G_{\text{mix}}$  curve changed to a sigmoidal shape with increase in temperature over a range of concentrations. Thus, the dependency of free energy on temperature and compositions of mixture has been shown justified. Further, it was noted that blends of PEG show negative values of  $\Delta G_{\text{mix}}$  above 33 and 28 °C for HPMCAS and HPMCP samples while similar effects were noted for CA samples above 120 and 130 °C (Figure 4.10). This suggests that the chemical potential of the mixture is significantly dropping than that of the parent molecules favouring miscibility. For instance, beyond 35 and 130 °C for PEG and CA respectively, these are miscible with polymers over the entire range of plasticiser concentration.

Although FECD of PEG and CA suggested approximate temperature profiles where solubility and/or miscibility of these plasticisers with cellulose ester derivative is a maximum, it is important to note that extrusion of HPMCAS and HPMCAS with PEG and CA at 35 and 130 °C is difficult. At high extrusion temperatures, although all ratios of polymeric blends would produce homogenous single phase system, recrystallisation or phase

separation of certain compositions post-processing are most likely to occur due to lack of local stability of the compositions. Therefore, a phase diagram was constructed by calculating the second derivatives of  $\Delta G_{\text{mix}}$  of individual systems and the local stability (spinodal decomposition) was investigated. To further strengthen understanding of recrystallisation behaviour post-process, the  $T_g$  of the mixture was investigated by Fox equations.

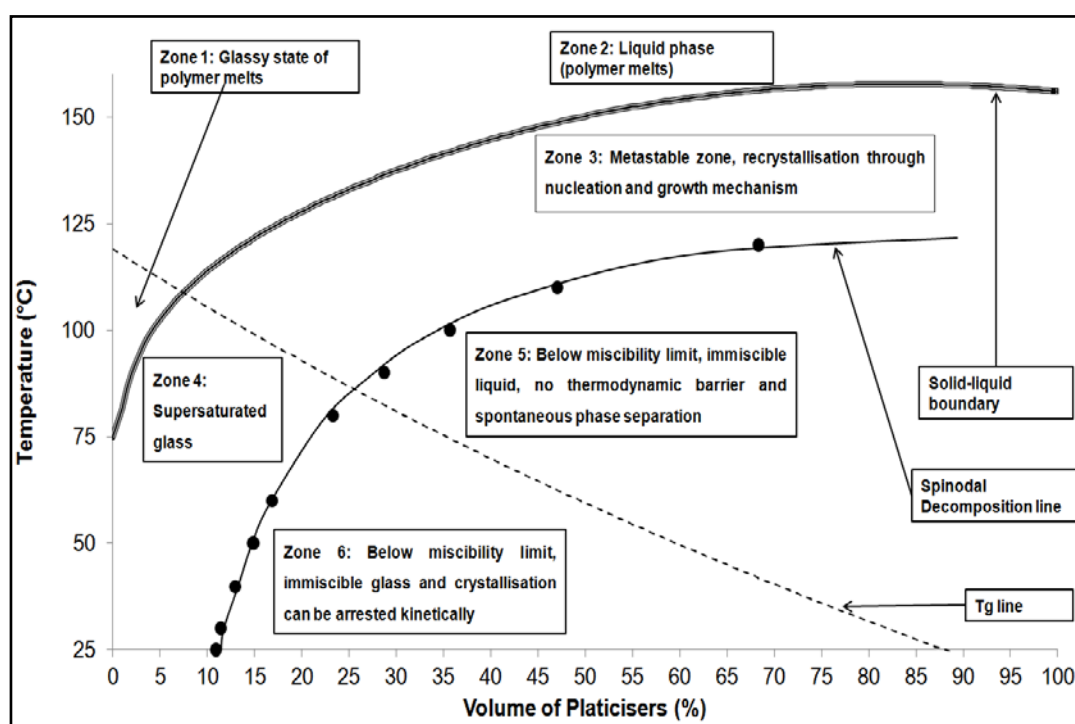


**Figure 4.11: Theoretical solid state solubility-miscibility phase diagram.**

Three lines: solid-solid solubility curve, curves of  $T_g$  and spinodal decomposition line were considered while constructing a phase diagram as discussed below (Qian et al., 2010). Generally, solid dispersions made by HME produce homogenous ASD with a single  $T_g$  temperature. However, in many instances most formulated ASDs fail to maintain amorphicity due to lack of knowledge of metastable compositions and their behaviour with respect to temperature. Therefore the phase diagram requires inclusion of the  $T_g$  curves which clearly distinguish kinetically dependent metastable and thermodynamically stable compositions over relevant pharmaceutical stability

temperatures. As discussed earlier,  $T_g$  and molecular mobility are interrelated where molecular mobility of the material is reduced below  $T_g$  and increased above  $T_g$  i.e., below  $T_g$  the material behaves like a glass and above assumes a liquid-like form. Hence all compositions of polymeric blends below the  $T_g$  line can be termed as glassy whereas above this line they can be considered as liquids (Figure 4.11).

Introduction of the  $T_g$  line in the phase diagram produced six zones as represented in Figure 4.11. Similar zones have been reported in the literature by Qian et al (2010) and Tian et al (2013). Figure 4.11 shows a solid-liquid boundary line above which, at given temperatures, the compositions of two solid materials can be considered as soluble and the compositions in these regions are considered thermodynamically stable. Therefore, zones 1 and 2 represent thermodynamically stable zones where a crystalline entity will not recrystallise upon local fluctuations and even if crystallisation starts, thermodynamic forces will either hinder the process (zone 1, glassy state) or attempt to dissolve the crystalline component in the polymer matrix (zone 2: liquid state). Figure 4.11 also shows a spinodal decomposition line, or miscibility curve line, which represents the supersaturated state of crystalline phase in the amorphous polymer matrix. Typically, the compositions above the spinodal decomposition and below the solid-liquid boundary line represent metastable compositions where recrystallisation can be expected at given temperatures and concentrations.

Pharmaceutically, the composition within zones 3 and 4 are considered as vital since these are zones of metastable compositions where recrystallisation occurs through a nucleation and growth mechanism via various kinetic factors. In this region, a small crystalline nucleus grows and produces more crystals within the polymer matrix by crossing several energy

barriers with the aid of local fluctuations. These local fluctuations are generally attributed to molecular mobility of the crystalline domain and often found above  $T_g$  values. Therefore, the compositions in zone 3 are considered thermodynamically unstable whereas zone 4 represents the zone of supersaturated glass compositions which are considered thermodynamically stable since molecular mobility of the compositions here are kinetically arrested. In summary, a homogenous phase of the mixture can be observed above the polymer-plasticiser solubility line (zones 1 and 2) whereas a metastable phase (zones 3 and 4) can be observed between the region of polymer-plasticiser solubility and the spinodal decomposition line. Below the spinodal decomposition line, all compositions are considered thermodynamically unstable and will spontaneously phase-separate post-extrusion (zones 5 and 6).

To investigate the maximum safe loadings of PEG and CA in HPMCAS and HPMCP polymers, thermodynamic phase diagrams were constructed. Representative charts of these phase diagrams are shown in Figure 4.12 for HPMCP while the entire phase diagrams of polymer-plasticiser and polymer-IBU are produced in section 4.3.1. Phase diagrams of all four mixtures suggested different interactions with the respective polymers (see Figure 4.35, next chapter). In the case of CA-HPMCP at room temperature, the spinodal line begins at a 3.5% concentration meaning this is the maximum loading of CA in HPMCP which can be safely incorporated without a possible chance of phase separation. For the mixture of CA-HPMCAS, the maximum loading of CA was observed to be 12.3%. Similar studies carried out with PEG blends showed 11% and 15% of PEG with HPMCAS and HPMCP respectively can be safely incorporated for stable amorphous dispersions while for mixtures containing Ibuprofen, the maximum safe loadings are 2 and

5% with HPMCAS and HPMCP. CPM showed approx. 4% and 7% maximum safe loading with HPMCP and HPMCAS (Appendix I, Figure 6.1).

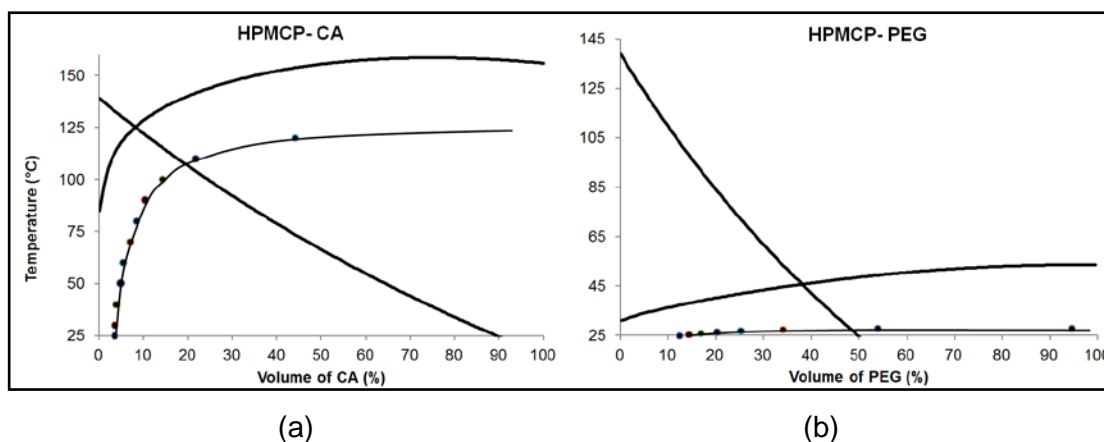


**Figure 4.12: Representative phase diagrams of (a) CA-HPMCP (b) PEG-HPMCP.**

The thermodynamic phase diagrams also provide information about probable extrusion temperatures. The solid state solubility curves suggest the minimum temperature required to form a homogeneous mixture of two solid state components though any temperature above the solid-liquid boundary line cannot be used for extrusion, for example zone 1 which represents the glassy state meaning the viscosity of the polymeric blend would be extremely high and extrusion would not be practically feasible. Hence it was speculated that, for example, extrusion of 5, 10 and 20% CA with HPMCP would require minimum temperatures of 140, 130 and 125 °C and with HPMCAS would require temperatures of 130, 125 and 115 °C. For PEG-HPMCP, it would require 135, 120 and 90 °C and for PEG-HPMCAS, 110, 95 and 80 °C. For CPM-HPMCP, see Appendix.

#### **4.1.3 Polymer melt rheology**

The thermal and rheological properties of polymeric materials determine the ability of the melt to mix and extrude through the die hence the flow behaviour over a range of shear rates should be quantified prior to HME. HME runs on the principles of shear deformation and investigations of shear

thinning as well as deformation can be investigated at laboratory conditions prior to melt extrusion by means of low shear rate (rotational rheology) and high shear rate (capillary rheology) studies. Hence an investigation of polymer melt rheology of both pure and blends of polymers was attempted in order to correlate rheological properties to the melt extrusion process.

#### 4.1.3.1 *Rotational rheology of pure polymers*

- *Strain Amplitude sweep*

This test varies the applied strain at a constant frequency and is carried out to identify the maximum strain value of the linear viscoelastic (LVE) range. Reliability of visco-elastic data can only be ensured when a polymer is investigated in its LVE range where the deformation of the material is reversible. Literature suggests that the polymer processed within its LVE range does not undergo structural changes while beyond this structural breakdown may be possible (Mezger, 2006) and the results of melt rheology can only be understood using complex mathematical derivative equations still under development (Shau-Tarnng Lee and Ramesh, 2004). These equations are generally not suggested for use for polymer blends and composites. It is generally considered that longer the length of LVE, in particular in terms of constant storage modulus ( $G'$ ), the better is the stability of the sample as structural properties of solid materials are related to their elasticity. In the current investigation, different grades of HPMCAS and HPMCP are tested for LVE ranges at a range of temperatures.

Figure 4.13 shows amplitude sweep results for HPMCAS and HPMCP investigated at 150, 175 and 200 °C. It was noted that both HPMCAS and HPMCP polymers show the dominance of  $G'$  over  $G''$  (loss modulus) when processed at 150 °C. However, the gap between  $G'$  and  $G''$  was reduced at

175 °C followed by dominance of  $G''$  over  $G'$  with further increase in temperature. For HPMCP-HP50 and HP55 polymers more interesting behaviour was observed, i.e very short LVER  $<0.1\%$ . A possible explanation is proposed for this. When the samples of HPMCP were recovered after the test at 150 °C, the samples observed to be incompletely melted and portion of solid powdered polymer was dragged in the melt causing shortening the LVER values. Moreover, HPMCP tested at 200 °C showed equivalent values for  $G''$  and  $G'$ . This is attributed to a typical polymeric behaviour which exists at the borderline between liquid and solid also known as 'gel point' behaviour (Mezger, 2006).

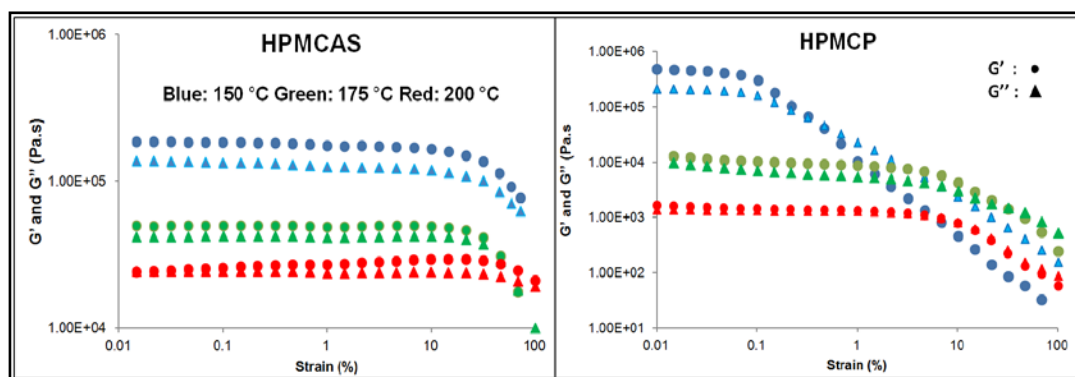


**Figure 4.13: Representative graphs for strain amplitude test.**

The maximum limiting strain value for the LVE region for virgin HPMCAS polymers was found to be 5-10% over the range of temperature under study while the maximum limiting values for HPMCP polymers were found to be 0.1 % at 150 °C and 5% at 175 °C and 200 °C. The shorter LVE range for HPMCP polymers at 150 °C may be attributed to a higher glass transition temperature ( $T_g = 135-145$  °C) compared with HPMCAS ( $T_g = 118-120$  °C). Moreover, it was observed that HPMCP only partially converted into its molten state with some of solid material remaining resulting in a significant reduction in LVE range when processed at 150 °C.

- Frequency Sweep (FS)

In this test, shear rate (frequency) was varied while the strain amplitude was kept constant. Measurement of shear viscosity using rotational rheometers can be performed using either steady shear rate or dynamic frequency sweep experiments however, the viscosity values calculated with steady shear rates are valid only up to  $1\text{-}5\text{ s}^{-1}$  and utilisation of this method beyond these values is described as debatable (Vlachopoulos and Strutt, 2003) while dynamic frequency sweeps can deliver precise information at shear rates up to  $500\text{ s}^{-1}$  (Mezger, 2006). Therefore dynamic FS tests were utilised in the current research work, these achieving shear rates typical of low speed extrusion. From the amplitude sweep tests, different LVE regions for the samples of HPMCAS and HPMCP were noted when tested at different temperatures. However, for convenience, and to allow direct comparison, the instrumental parameters were kept constant for each polymer and FS tests were carried out at a strain value of 0.1 %.

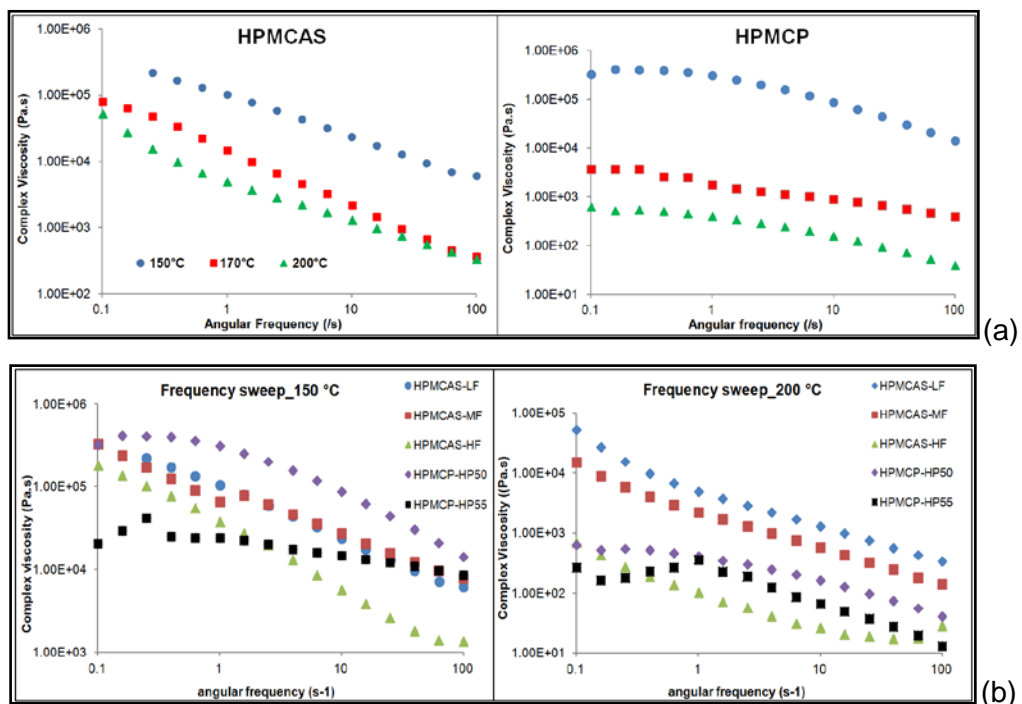


Figure 4.14: Representative graphs for frequency sweep test.

Sweeps for virgin HPMCAS and HPMCP were performed at the same temperatures described in the amplitude sweeps. It was noted that the complex viscosity of all samples increased at lower frequencies. In other words, both polymers (all grades) showed a decrease in polymer melt viscosity with increasing frequency (Figure 4.14b). Complex viscosity studies performed with different grades of HPMCAS and HPMCP suggested a trend in their melt viscosity values and the order was found to be HPMCAS-L > M > H and HPMCP-HP50 > HPMCP-HP55 over the range of temperatures. These correlate with percentage of acidic substitution in the individual polymer. It was noted that HPMCAS-L grade contains high succinoyl ratio and lower acetyl ratio while this ratio is reversed in the HPMCAS-H grade. Since acetic acid can impart a significant plasticisation effect the melt viscosity rank of L > M > H can be justified. Similarly in HPMCP, phthalic acid derivatives are recognised as plasticisers in various melt process (Wilson, 1996), increasing substitution of phthalyl moieties can reduce the melt viscosity of polymer as seen from the curves for HPMCP-HP50 (22% phthalyl substitution) being greater than for HP55 (33% substitution).

These results provide valuable information about melt viscosities of the individual polymers. At lower temperatures, the melt viscosity of HPMCP-HP50 dominates over HPMCAS however, with rise in temperature and beyond 175°C, a significant drop in the viscosity of HPMCP was observed. Interestingly, at lower frequencies, the melt viscosity of both grades of HPMCP was observed to be nearly independent of frequency. This phenomenon is generally known as the Newtonian plateau or indicative of a zero shear viscosity ( $\eta_0$ ). With increasing shear rate a shear thinning region was observed which can be quantified using a shear thinning index given by a simple power law model. However, HPMCAS did not exhibit this

Newtonian plateau within the shear rate range tested and only the shear thinning region was observed (Figure 4.14a, b).

Despite knowing that below 150 °C HPMCP would not show melting phenomenon, frequency sweeps of HPMCP were conducted at 135 and 140 °C. HPMCP showed maximum viscosity values in the range of  $10^9 - 10^{10}$  Pa.s qualitatively agreeing that melt viscosities of thermoplastic polymers near to or below  $T_g$  can reach up to  $10^{12}$  Pa.s (Hancock *et al.*, 1999 , Baird and Taylor, 2012). It is important to note that  $T_g$  of HPMCP is in the range of 135-145 °C and thus, high melt viscosity values ( $10^6$  Pa.s) at 150 °C can be justified.

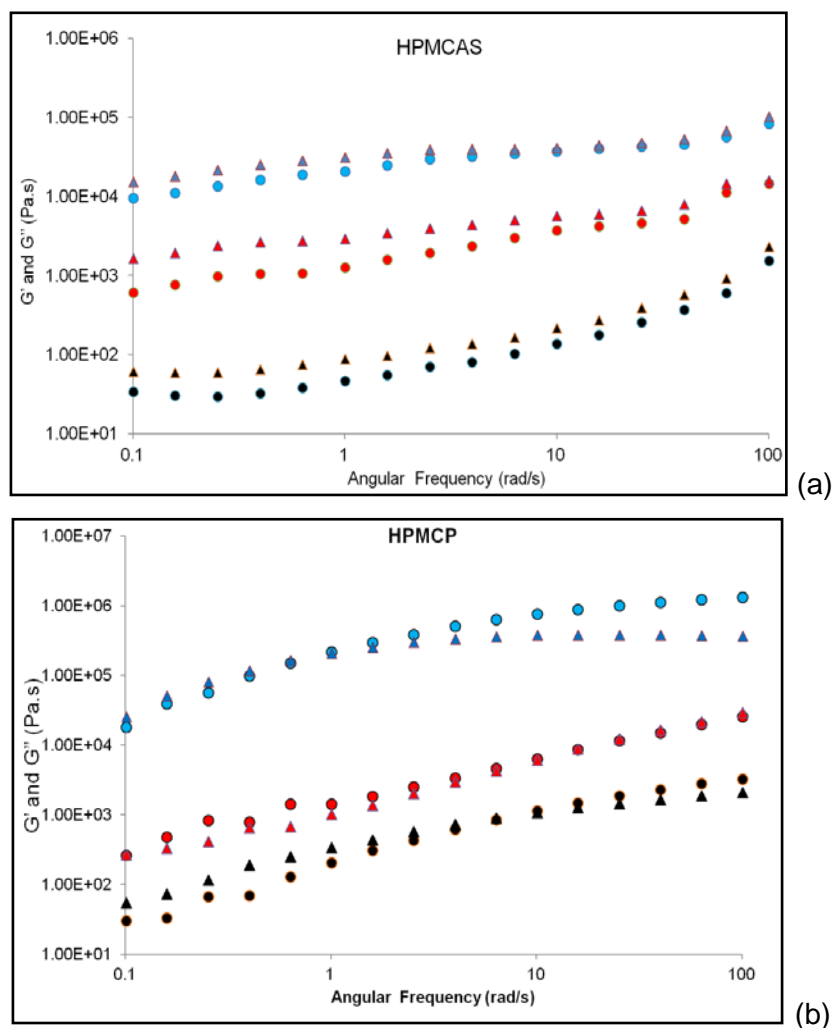


**Figure 4.15: Frequency sweep test (a) HPMCAS (B) HPMCP.**

$G'$ : Circle and  $G''$ : triangle; Blue (150°C), Red (175°C) and Black (200°C)

The important moduli,  $G'$  (storage or elastic modulus) and  $G''$  (loss or viscous modulus) were investigated for their characteristic crossover points and relative dominance as shown in Figure 4.15. The  $G'$  and  $G''$  curves for HPMCAS at lower temperature exhibited a crossover point at approximately 5 rad/s and the dominance of  $G''$  over  $G'$  was noted before crossover point. However, when the temperature was increased from 150 to 200 °C, a shift in the crossover points was noted towards higher frequency values and mainly dominance of  $G''$  over  $G'$  was noted at higher temperatures. Interestingly, samples of HPMCAS beyond 175 °C did not show crossover points within the tested range of shear rates indicate this polymer melt is behaving like a viscoelastic fluid (Figure 4.15a).

Similar investigations were carried out for HPMCP samples (Figure 4.15b). At lower frequencies (up to 5 rad/s) and up to 175 °C, the values of  $G'$  and  $G''$  lie very close to each other and multiple crossover points were noted in these regions. A precise dominance of either of the moduli was not recorded for HPMCP up to 175 °C while at 200 °C a crossover point with dominance of  $G''$  over  $G'$  at 5 rad/s was observed. This was the indication that entanglements between the polymeric chains of HPMCP at molecular level were significantly different than for HPMCAS and warranted further investigation. Further, it is thought that to support this mechanism a 3D molecular architecture of these two polymers should be investigated but such a task is currently it is beyond the scope of this work.

Generally for visco-elastic polymers, at low strain rates  $G''$  dominates while at higher strain rate  $G'$  dominates and theoretically this dominance is indicative of entanglements between the side chains or linear chains of the polymer. Crossover points are generally defined as the point at which the values of  $G'$  and  $G''$  become equal and, from structural property perspectives,

defines the beginning of the rubbery plateau region. The results of  $G'$  and  $G''$  for HPMCAS clearly suggested that samples of HPMCAS followed the characteristic phenomenon of thermoplastic polymers showing dominance of  $G''$  over  $G'$  at lower frequencies and  $G'$  over  $G''$  at higher frequencies at all investigated temperatures; whereas in the case of HPMCP samples this phenomenon was observed only in the case of higher temperature (200 °C).

Occurrences of multiple crossover points observed in the case of HPMCP were initially thought to be because of instrument noise however, similar results were obtained even after repeating experiments multiple times. Then it was thought that the reason could be attributed to some melting behaviour of the polymer solids entrained in the non-homogeneous mixture. A non-homogeneous polymer melt of HPMCP was indeed noticed at 150 °C, however beyond 160 to 180 °C complete molten behaviour was noticed and still despite of it multiple crossovers were obtained. This indicated that below 180 °C, chain entanglements of HPMCP could be following a different mechanism than for a typical thermoplastic polymer. It was speculated that the close values of  $G'$  and  $G''$  showing multiple crossovers are result of interlocking and inter-breaking mechanisms of polymeric side chains forming either weak network between the chains of HPMCP or generation of a structure with no shear dominance of  $G'$  or  $G''$ . Thus, it was believed that physical bond formations between the chains of HPMCP are simultaneously associated with the bond breaking phenomenon attributed to a complex entanglement-disentanglement processes.

The crossover point not only provides information about molecular entanglements but allows quantification of a 'characteristic relaxation time'. This is generally calculated by reciprocating the value of frequency at which the crossover occurs. This time has great importance in rheology since it

correlates with the time to return to equilibrium in response to a sudden disturbance, i.e., a time scale for a system to relax after deformation. In the case of HPMCAS at 150 °C, the crossover frequency was observed around 5 rad/s corresponding to a characteristic relaxation time of 0.2 s while at 175 °C it was noted to be 0.01 s attributed to the crossover frequency at 100 rad/s. Similarly, for HPMCP samples the relaxation time was evaluated. At 150 and 175 °C, since multiple crossover points were observed, it was difficult to determine a single relaxation time however, at 200 °C, the relaxation time was calculated to be 0.1 seconds.

- *Modelling of rheology data by Arrhenius Kinetics*

FS tests for HPMCAS and HPMCP provided relevant information about temperature dependent melt viscosity and zero-shear rate melt viscosities. To investigate these effects on a much broader scale, HPMCAS and HPMCP were further tested for their complex viscosity data over the range of temperatures between 160 - 200°C with an increment of 10 °C as shown in Figure 4.16a. HPMCAS showed shear thinning region at all temperatures whereas a Newtonian plateau (see figure 4.16 a circled region) was observed in the case of HPMCP samples (Figure 4.16a). Moreover, the complex viscosity of polymers reduced by a factor of 2.5 to 3 when the temperature was increased from 160-200 °C. These effects strongly supported the concept that "viscosity is a strong function of temperature" (Advani and Sozer, 2012) and to investigate this temperature dependent viscosity phenomenon, zero shear viscosity was modelled using Arrhenius kinetics. The viscosity at low shear rate or the values determined at the beginning of the Newtonian plateau were considered as zero-shear rate viscosity values and the Arrhenius relationship was quantified using equation 4.13:

$$\log \eta_0 = \log A - \frac{Ea}{RT} \quad \text{Equation 4.13}$$

Where  $A$  is the pre-exponential factor,  $E_a$  is the energy of activation,  $T$  is the absolute temperature and  $\eta_0$  is the viscosity at zero shear-rate.

A linear trend was observed between zero shear-rate viscosity and reciprocal of temperature (Figure 4.16b) and the slope of the curve was utilised to calculate the activation energies ( $E_a$ ). Using this expression, the  $E_a$  of HPMCP was noted to be  $104.09 \pm 1.56$  kJ/mol with its regression value,  $r^2 = 0.9953$  (Figure 4.16b and Table 4.9). To the author's knowledge, this is the first report where the activation energy of HPMCP in its melt form is discussed. Such a relationship for HPMCAS polymers was recently investigated by Sarode and co-workers and values of  $E_a$  for viscous flow of HPMCAS are reported in the range of 126-137 kJ/mol based on a Cross model approach (Sarode *et al.*, 2014).

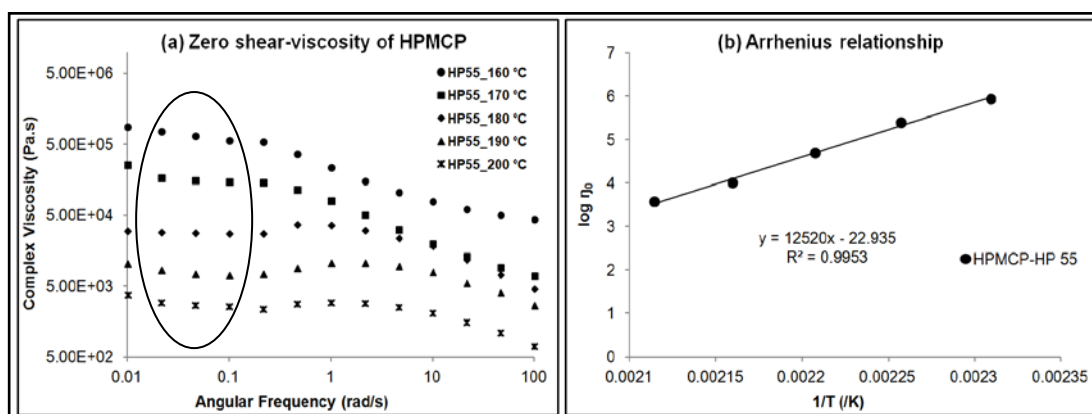


**Figure 4.16: Complex viscosity results and Arrhenius relationship for HPMCP.**

According to Sarode *et al.*, the Newtonian plateau of HPMCAS can be observed when shear rate reaches to  $0.001$  s<sup>-1</sup>. This correlates with the observation of shear thinning behaviour of HPMCAS at the shear rate of  $0.1$  s<sup>-1</sup> in the current research work. FSs test running at  $0.001$  s<sup>-1</sup> possess serious limitations as far as time required to complete these tests are concerned. During investigations it was observed that FS tests ran between the angular frequencies  $0.1$ -  $100$  rad.s<sup>-1</sup> and  $0.01$ -  $100$  rad.s<sup>-1</sup> approximately

took 20 and 70 minutes respectively to complete whereas it is speculated that to investigate melt viscosity between 0.001-100 rad.s<sup>-1</sup> would take certainly more than 4 hours while the thermal stability of these polymers over this period at very low shear rates is ambiguous and discussed very sparsely in the literature. Considering these facts the viscosity values obtained at 0.1 rad/s were utilised to investigate the activation energy for HPMCAS. This consideration provided a value for Ea of 13.65 kJ/mol – around 10% of the values reported by Sarode et al., 2014 (Table 4.9). Since HPMCAS did not show typical Newtonian behaviour at given frequency values and to investigate typical melt behaviour of Newtonian behaviour followed by shear thinning region over the range of 10<sup>-3</sup> to 10<sup>3</sup> time-temperature superposition study was conducted.

**Table 4.9: Energy of activation for polymer-melt viscosities.**

Name	Equation	Ea (kJ/mol)	r <sup>2</sup>
HPMCP	$y = 12520x - 22.935$	104.0913 ± 1.564	0.9953
HPMCAS	$y = 1642.8x + 1.5483$	13.65 ± 0.2354	0.9868

- *Modelling of rheology data by time temperature superposition (TTS)*

The shifting of crossover points towards higher frequencies with increasing temperature allows the common use of TTS in rheology. Due to the possibility of the thermal degradation of HPMCAS and HPMCP over long period of time at elevated temperatures, shear rates below 0.01 rad.s<sup>-1</sup> were not examined, instead melt properties at frequencies lower than 0.1 rad/s were determined by TTS studies.

Melt rheology of the polymer is significantly dependent on two parameters, time and temperature - the basis of TTS is projected on these two parameters. Typically, when a polymer is heated at elevated

temperatures and at low shear rates, it experiences softening of polymer chains because of increasing molecular mobility (values of  $G'$  decreases). In other words, the deformation takes place over a relatively long period of time. Similarly, when the polymer melt is exposed at relatively low temperatures and high shear rates, a large deformation over the shorter period of time can be expected (values of  $G''$  decreases), i.e., the first condition brings softening while the second condition brings rigidity.

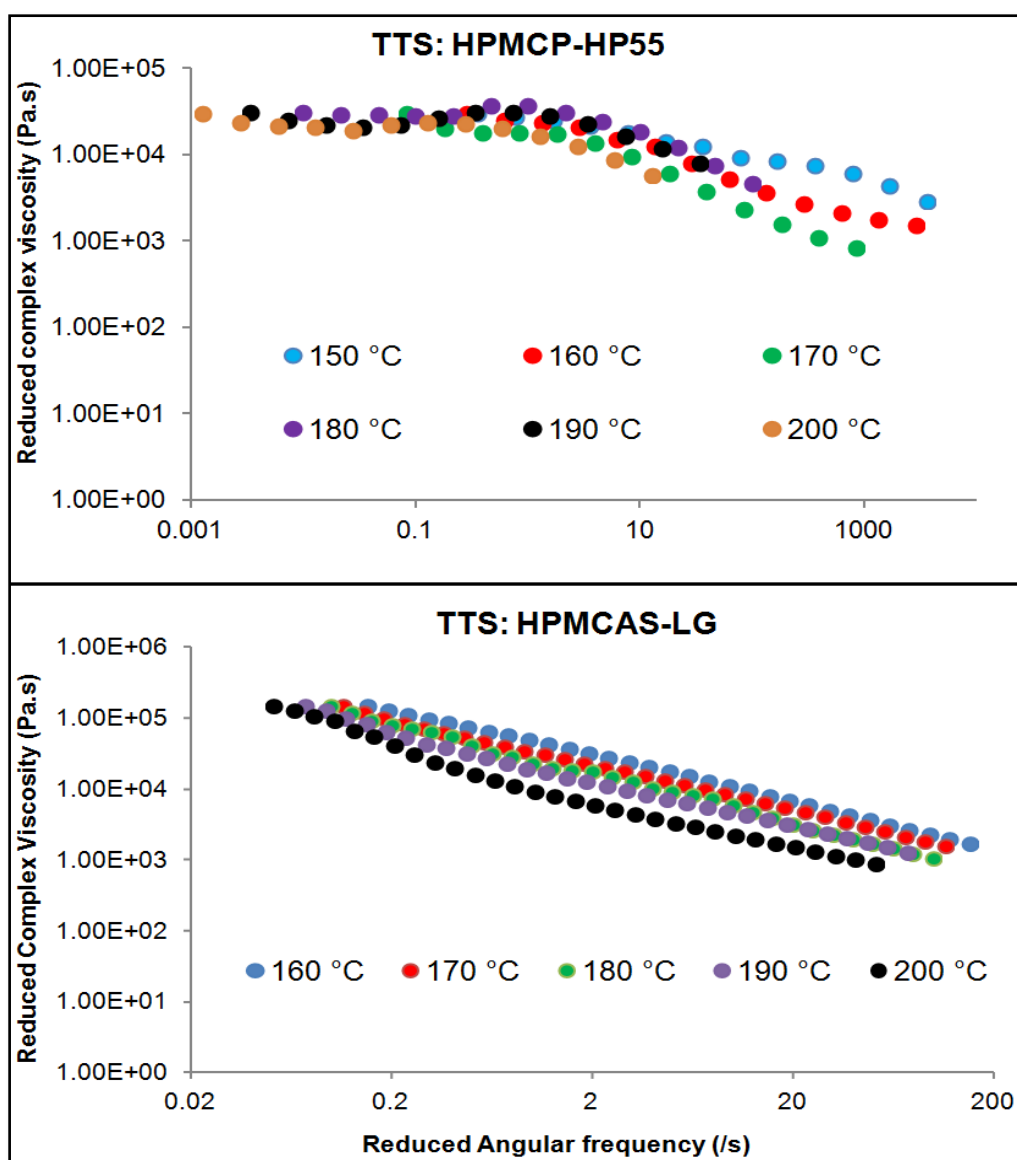


Figure 4.17: TTS curves for HPMCP and HPMCAS.

TTS tests for HPMCAS and HPMCP were investigated based on the Williams-Landel-Ferry (WLF) model. According to this model the 'vertical shift' or 'temperature shift' ( $a_{T1}$ ) factor can be calculated based on the corresponding zero shear viscosity values of polymeric melts at different temperatures (equation 4.14).

$$a_{T1} = \frac{\eta_T}{\eta_{T_{ref}}} \quad \text{Equation 4.14}$$

$\eta_0$  values at a range of temperatures were determined by FS tests. The master curve was plotted from 150 to 200 °C with 180 °C being kept as a reference temperature (Table 4.10). The calculated shift factor was then used to calculate the reduced frequency ( $\omega_{r1}$ ) and reduced viscosity ( $\eta_{r1}$ ) using equation 4.15.

$$\omega_{r1} = \omega * a_{T1} \quad \text{and} \quad \eta_{r1} = \frac{\eta_T}{a_{T1}} \quad \text{Equation 4.15}$$

**Table 4.10: Shift factor calculations for HPMCP and HPMCAS.**

HPMCP						
Name	1	2	3	4	5	6
T (°C)	150	160.00	170	180	190	200
$\eta_0$	1.08E+06	8.80E+05	2.54E+05	3.00E+04	1.04E+04	3.83E+03
$a_{T1}$	35.96	29.33	8.466	1	0.3466	0.1276
HPMCAS						
Name	1	2	3	4	5	
T (°C)	160	170	180	190	200	
$\eta_0$	2.29E+05	1.72E+05	1.49E+05	1.12E+05	7.75E+04	
$a_{T1}$	1.5316	1.15165	1	0.7469	0.5189	

A graph of  $\eta_{r1}$  versus  $\omega_{r1}$  was plotted. When a logarithmic form of reduced frequency values were considered, it was observed that negative

values of  $aT_1$  indicated a shift of the viscosity curve towards the left side of the reference temperature while a right shift was indicative of positive values of  $aT_1$  (Figure 4.17). A clear expansion of polymer-melt viscosity of HPMCP over the range of frequency ( $10^{-3}$  to 103 rad/s) was noted when the TTS graph was investigated. This graph suggested that this polymer will produce Newtonian behaviour from 0.001 to 0.1 rad/s followed by a shear thinning region at higher frequencies. Similar studies were performed with HPMCAS however the projection of frequency was expanded only between 0.02 - 200 rad/s and at/below 0.02 rad/s it was believed that Newtonian behaviour will begin. This modelling was comparable with the observations of FS where HPMCAS failed to show Newtonian plateau until 0.01 rad/s.

#### *4.1.3.2 Capillary rheology of pure polymers*

Flow properties of different grades of pure polymers under high shear rate were investigated by capillary rheometer. Here, the material was subjected to high pressure and temperature during an equilibration time whilst it melted prior to the melt being forced through capillary dies at a range of piston speeds while the melt pressure drop was measured through long and short orifice capillary dies at different flow rates in order to calculate apparent shear rate, shear stress, and shear viscosity. Capillary rheology data of virgin polymers was used to evaluate pressure / time curves, shear viscosities and to allow power law studies of the melts. Three temperatures, 150, 175 and 200 °C were used similar to the FS test of rotational rheometry.

Initially melt stability of polymers with increase in steady shear rate was studied with the help of pressure versus time graphs. Capillary rheology works on the principle of piston displacement to increase the shear rate (piston speed) which leads to a linear increase in the melt pressure across the capillary dies can be observed. The structure of the steady shear rate test

was designed in five distinct stages in which the shear rate was increased from 50 to 2500 s<sup>-1</sup> and at every stage; the shear rate was maintained constant over a minute.

Figure 4.18 shows a characteristic pressure against time chart for different grades of HPMCAS and HPMCP polymers. Earlier, it was observed that both polymers produce significantly high values of viscosity at 150 °C and when the same temperature was utilised at high shear rates, enormous pressure generation was noted. In particular with HPMCP polymers, the pressure developed was so large (more than 30000 psi) that it resulted in failure of the piston utilised in capillary rheometry. This indicated that utilisation of HPMCP at 150 °C imparts significant pressure generation and if ignored will damage HME screws and motor if processed alone. In other words, extrusion of HPMCP between the temperatures of 150-160 °C can be possible only when minimum screw speed and high shear screw configuration is used. Similar statements will be applicable to the blends of drug-HPMCP mixtures having melting point of drug > 150 °C. Considering these facts and in order to reduce further damage to the capillary instrument, melt viscosity of virgin polymers was investigated only at 175 and 200 °C.

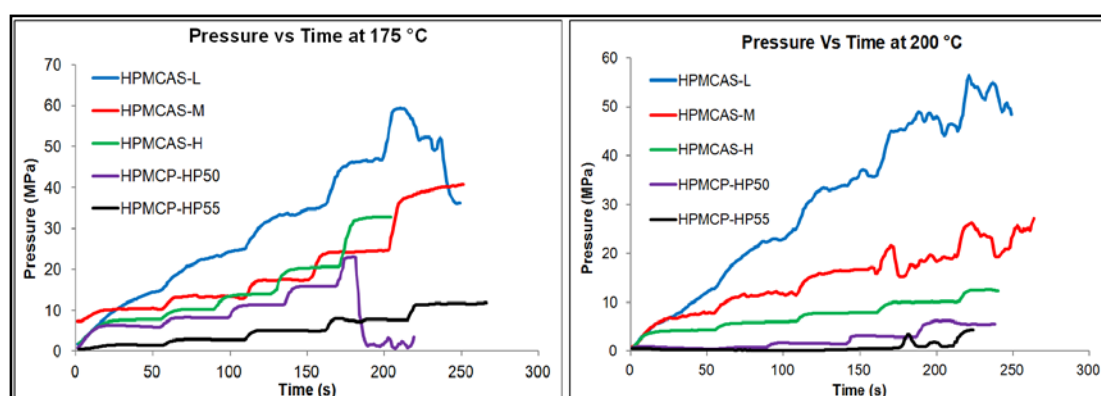


**Figure 4.18: Pressure drop for HPMCAS and HPMCP polymers.**

All grades of polymers showed increases in pressure with increase in shear rate in a steady shear rate constant test. However, noisy lines

especially during the steady phase of shear rates were noted in some of the samples at 175 and 200 °C. HPMCAS-L grade showed a constant increase in the values of pressure with increase in shear rate. However the sample did not attain any equilibrium stage and beyond 200 seconds (at highest shear rate) poor melt stability was noted. In contrast HPMCAS-M and H grades showed relatively smooth flow of pressure versus time curves at 175 °C. Similar observations were made at 200 °C for the same grades though significantly noisy data were noted. Smooth lines of melt pressure with increase in shear rate by attaining equilibrium stage over the period of time are generally indicative of the stability of polymer melts. Thus, from these results it was noted that the melt stability for HPMCAS was in the order of H > M > L. Similar studies conducted for HPMCP showed that melt stability of HPMCP was relatively stable compared with HPMCAS at both temperatures though for the HP50 grade at 175 °C at high shear rates, there was significant pressure drop was noted due to high pressure generation of more than 30,000psi or 206.84 MPa (Figure 4.18). In summary the measured pressure was observed to be in the order of LF > MF > HF > HP50 > HP55 whereas the melt stability was in the order of HPMCAS-H > HPMCP-HP55 ≥ HPMCP-HP50 > HPMCAS-M > HPMCAS-L.

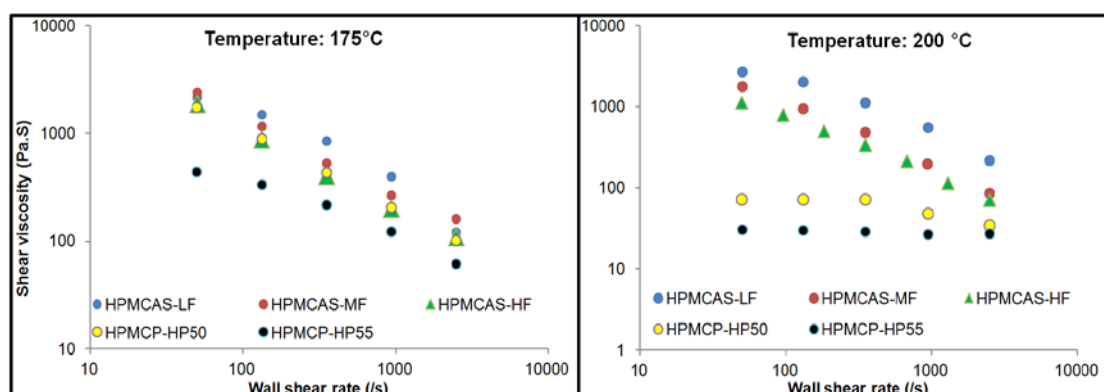


**Figure 4.19: Temperature dependent shear viscosity of virgin polymers.**

The relationship of shear viscosity with wall shear rate was plotted for virgin polymers processed at 175 °C and 200 °C (Figure 4.19). All grades of HPMCAS and HPMCP exhibited decrease in melt viscosity with increase in shear rate as well as with increase in temperature - indicative of shear thinning behaviour. It was observed that shear viscosity of both polymers at 175 °C linearly dropped with shear rate with higher melt viscosities for HPMCAS compared to HPMCP polymers. Similar results were obtained when the polymers were studied at 200 °C. However, in the case of HPMCP-HP55, the viscosity values at 10 and 100 s<sup>-1</sup> shear rates looked to be constant and beyond the values of 100 s<sup>-1</sup>, a marginal drop was noted at 175 °C whereas at 200 °C both grades showed constant viscosity values until ~1000 s<sup>-1</sup> shear rate. Moreover, the viscosity values observed were significantly lower than for HPMCAS. These studies indicated that polymer melt viscosity of HPMCAS is significantly higher than that of HPMCP especially at elevated temperatures. These results are comparable with the results of rotational rheology studies.

The power law index was investigated using equation 4.16:

$$\eta = K * (\text{shear rate})^{n-1} \quad \text{Equation 4.16}$$

**Table 4.11: Power law index and consistency index for virgin polymers.**

Polymer	Power law		r <sup>2</sup> value	
	175 °C	200 °C	175 °C	200 °C
HPMCAS-LF	0.42	0.44	0.9610	0.9568
HPMCAS-MF	0.24	0.25	0.9948	0.9447
HPMCAS-HF	0.23	0.30	0.9934	0.9651
HPMCP-HP50	0.26	0.87	0.9979	0.9861
HPMCP-HP55	0.56	0.55	0.9855	0.8368

The power law index ( $n$ ) describes the shear thinning or thickening nature of the polymer and is calculated from the gradient of the log shear stress versus log shear rate plot.  $K$  is the consistency index of the melt and is calculated from the intercept of log shear stress against log shear rate. Power law indices less than one indicate shear-thinning behaviour while  $n > 1$  indicates shear thickening. From Table 4.11 it can be seen that all materials underwent shear thinning. The  $r^2$  values were calculated up to shear rate  $1000 \text{ s}^{-1}$  to investigate the validity of power law model with processed polymers. Except HPMCP-HP55 processed at 200 °C the calculated power law index and their relative regression coefficient values were greater than 0.94 while the  $r^2$  value of HPMCP-HP55 at the same temperature showed 0.83 indicating a slight deviation from power law. This deviation was attributed to equivalent melt viscosity values of HPMCP-HP55 at 200 °C over the range of wall shear rate.

#### 4.1.3.3 *Shear rheology of polymer blends (plasticisers and a model drug)*

The results of both rotational and especially capillary rheometer suggested that virgin polymers are high viscosity polymers and they cannot be processed below 150 °C in melt extrusion process unless polymers are subjected to high shear screw configuration with slow screw speeds. In such cases plasticisers may be used to reduce processing temperatures and melt viscosities. Since the plasticisers TEC, CA and PEG are noted to influence the thermal and thermodynamic properties of virgin polymers, investigating their behaviour, role and effects on polymer melt studies was one of the primary aspects of the current study. The major focus of this study was to investigate and manipulate the visco-elasticity of the parent polymers for their suitability in melt processing as well for maintaining physico-chemical stability of the polymer blend. A model drug, Ibuprofen, was utilised with the polymer

and its influence on melt stability of the drug-polymer complex was also determined to anticipate flow properties or melt stability of mixture during processing as well as to decide processing conditions for HME process.

- *Rotational rheology*

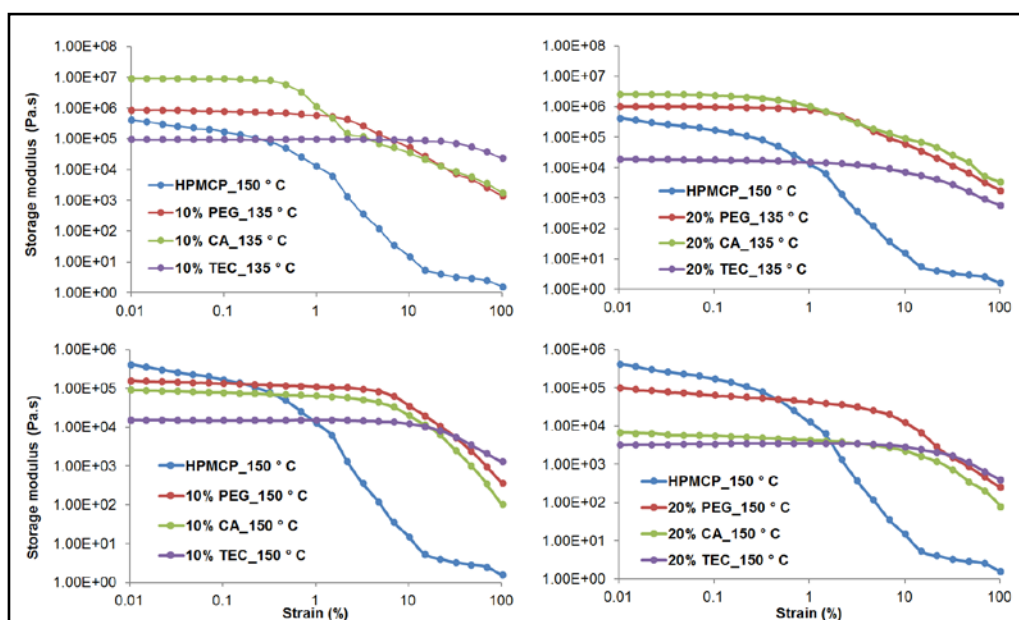


**Figure 4.20: Amplitude sweep of blends of HPMCP.**

Physical mixtures of TEC, CA and PEG (10, 15 and 20% w/w) were prepared with HPMCP-HP55 and the mixtures were subjected to amplitude and frequency sweeps at 135, 140 and 150 °C. Figure 4.20 shows results of amplitude sweep tests for the blends of HPMCP. In the case of HPMCP-HP55, the maximum limiting value at 150 °C was close to 0.1% however, with 10% plasticiser the extent of the LVE expanded and, at 135 °C, the maximum limiting value was in the order TEC (10%), PEG (5%) and CA (1%). Similar results were observed when the concentration of plasticiser and temperature was increased. It is interesting to note that the LVE of blends of TEC improved marginally over the concentration and temperature gain whereas that of for PEG and CA, the LVE improved with percentage plasticiser content and LVE of the polymeric blends of PEG and CA was increased to maximum 10-12 % of strain values.

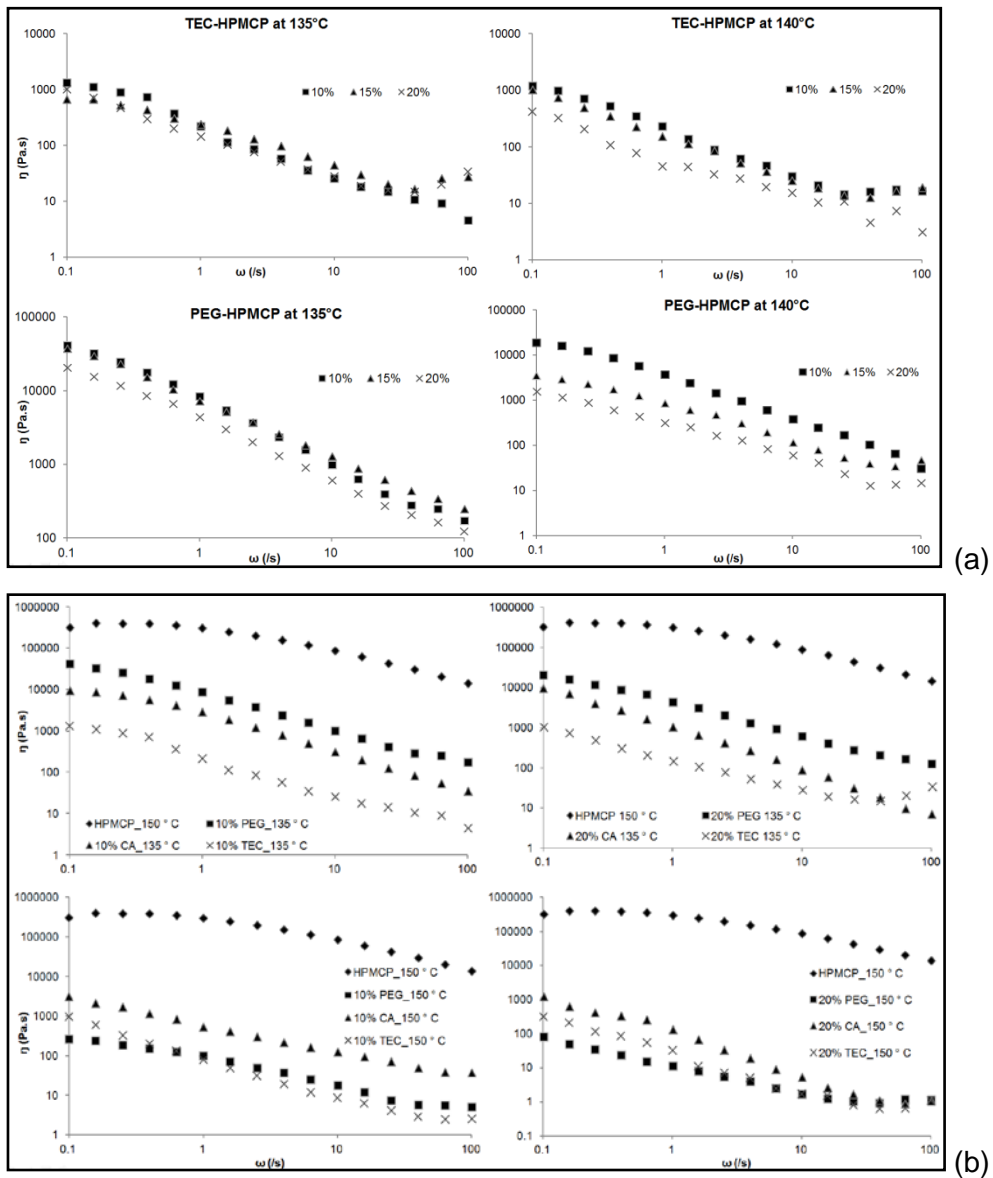


**Figure 4.21: Effects of plasticisers on polymer melt viscosity.**

Figure 4.21 shows complex viscosity data for similar blends at the same temperature profiles from FS tests. As discussed earlier, the polymer melt viscosity of HPMCP was largest at 150 °C, however, 10% plasticisation made a significant impact in lowering the viscosity of the polymer. Broadly, the viscosity of HPMCP blends dropped with increase in plasticisers' concentrations, angular frequency, and temperature. However, FS of some of the blends produced some interesting results. For instance, at the respective temperatures, the influence of TEC loadings on polymer melt viscosity was insignificant (Figure 4.21a). Similar results were obtained with

blends of PEG however, except for 135 °C, distinct viscosity differences were noted between 10, 15 and 20% loadings at 140 and 150 °C (Figure 4.21b).

Further, it was observed that at 10% and 135 °C the viscosity of the PEG-HPMCP was greater than the viscosity of TEC-HPMCP. Similar results were observed with 20% loading at 135 °C. However, at the same concentration and 150 °C, the viscosity of both materials was observed to be only marginally different especially beyond the angular frequency  $1 \text{ s}^{-1}$ . Another important point was noted whereby, despite the concentrations of TEC and CA, a Newtonian plateau was observed at 135 °C and with increasing temperature this plateau disappeared. This observation was not noted in the blends of PEG, these exhibiting shears thinning behaviour over the entire temperature and concentration ranges studied.

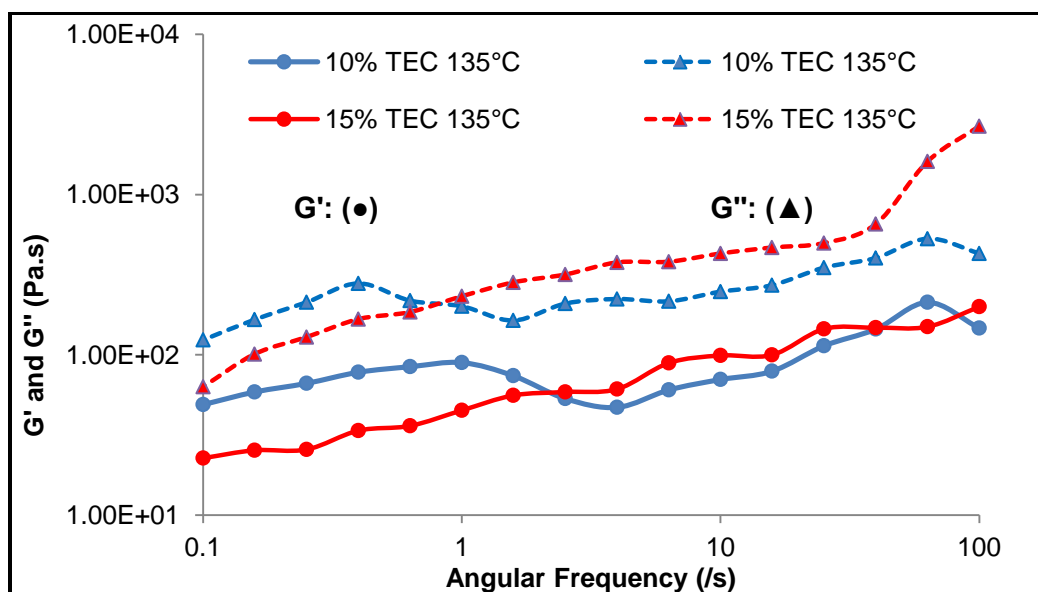


**Figure 4.22: Shift of cross over points towards higher frequency.**

FS curves particularly,  $G'$  and  $G''$  curves for three plasticisers with their respective concentrations and temperatures were further investigated - a representative figure is shown in Figure 4.22. In the case of TEC blends with

both polymers,  $G''$  dominated over  $G'$  and crossover points was not observed. Further, it was noted that with the TEC blends, polymer relaxation time can be decreased. Similarly in the case of PEG blends, it was noted that 10% PEG blend processed at 135 °C exhibited a crossover point at the angular frequency of  $7 \text{ s}^{-1}$  and beyond this point the blend started gaining rigidity. However, with 15% and 20% PEG-2000, the crossover point was shifted to higher angular frequencies greater than  $100 \text{ s}^{-1}$  indicating the ability of PEG-2000 to decrease the relaxation time for the polymer complex. Compared to the  $G'$  and  $G''$  values of PEG and TEC, viscous and elastic moduli of the blends of CA showed significant fluctuations in their characteristic graphs. There was overall a non-satisfactory response noted believed to be attributable to instability or incompatibility of CA with HPMCP-HP55 polymer irrespective of applied concentration and temperature. These observations are later cross-checked with capillary rheology experiments.

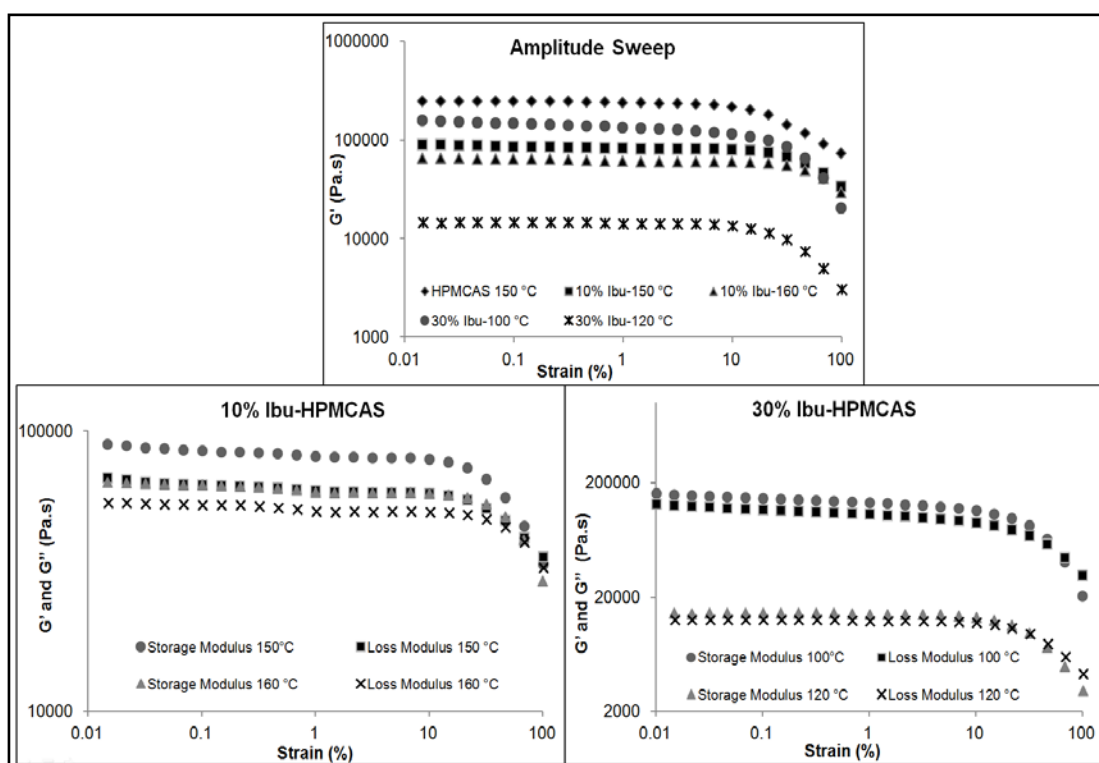


Figure 4.23: Amplitude sweep tests for drug-polymer complex.

In the second experiment, the effect of the model drug Ibuprofen (IBU) with HPMCAS-LF grade polymer was investigated (Figure 4.23). Ibuprofen was loaded with the polymer in 10 and 30 % ratios. Earlier, the LVE region of HPMCAS at 150 °C and 160 °C was observed to be limited at 5 - 8 % of strain amplitude and similar values were observed with 10 - 30% drug loadings at relatively lower temperatures. This suggested that the viscoelasticity of the drug-polymer complex can be modified according to processing conditions as well as with percentage drug loadings. Moreover, it was interesting to note that with 10 % IBU loading at 150 °C, G' dominated over G'' which is generally observed in many polymeric systems though with increase in temperature of 10 °C, the difference between G' and G'' significantly reduced. Similar results were obtained with 30% loadings at 100 °C while at 120 °C, the polymer melt showed 'gel point' properties (Figure 4.23).

Once the LVE values had been calculated, the complex viscosity of the drug-polymer complexes was determined from FS tests. Figure 4.24 shows viscosity and storage and loss modulus values from these tests. At low frequencies, the viscosity of virgin HPMCAS-LF was found to be more than  $10^6$  Pa.s at 150 °C. However, with 10% drug loading at the same temperature, the viscosity was found to reduce to approximately  $10^4$  to  $10^3$  Pa.s. This was attributed to the plasticisation effect of Ibuprofen on the HPMCAS. The melting point of Ibuprofen is 76 °C and DSC thermograms confirmed this plasticisation by demonstrating the shift of  $T_g$  of HPMCAS-LF from 120 °C to 65 °C. Moreover it is interesting to note that the viscosity values of 30% Ibuprofen with HPMCAS-LF processed at 100 °C and 10 % Ibuprofen in HPMCAS-LF processed at 150 °C have similar values demonstrating that viscosity is an entirely temperature and concentration dependent phenomenon. With 30% Ibuprofen loading, processing temperatures at 100 °C will be inclined to produce higher torque or might

even cause melt instability. Further crossover studies of frequency sweep based  $G'$  and  $G''$  suggested that the relaxation time of these mixtures can be significantly reduced to 0.01 s by the addition of 10% ibuprofen, and mixtures of 30% did not exhibit any crossover points even at low processing temperatures suggesting plasticisation by the drug for these two polymers (Figure 4.25).

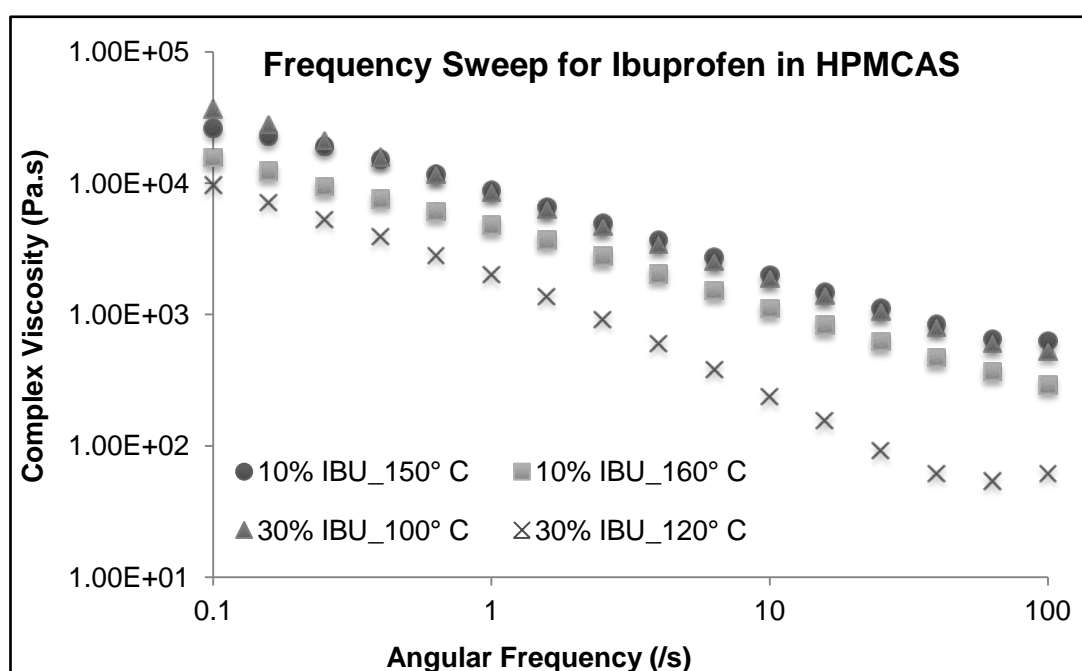


Figure 4.24: Complex viscosity values for IBU-HPMCAS compositions.

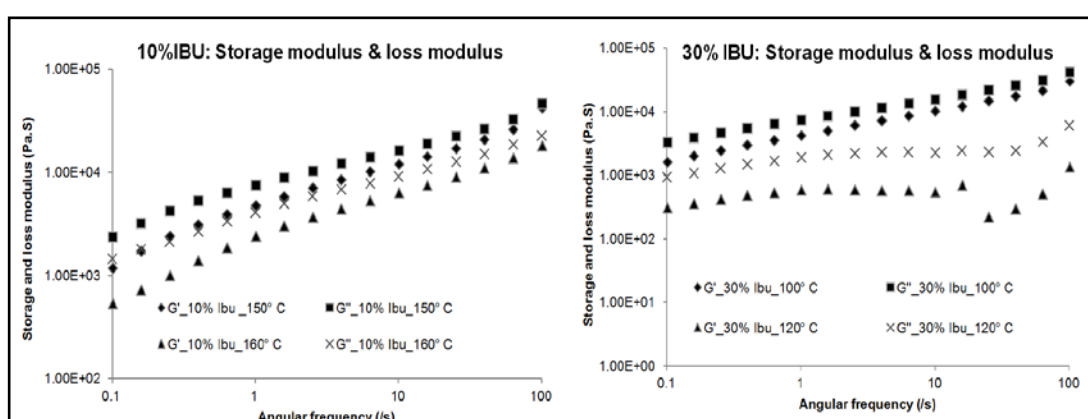


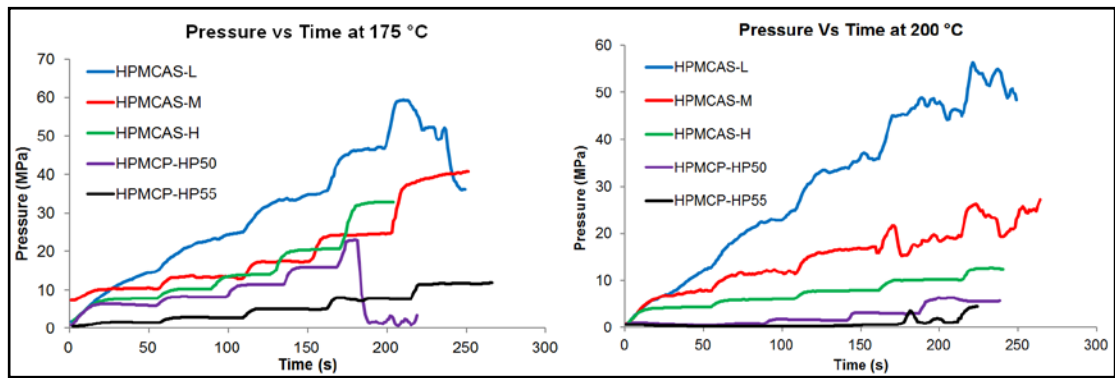
Figure 4.25: Storage and loss moduli of IBU-HPMCAS samples.

With these additives the crossover points of polymer complexes shifted significantly to the higher frequencies with a dominance of  $G''$  over  $G'$  which

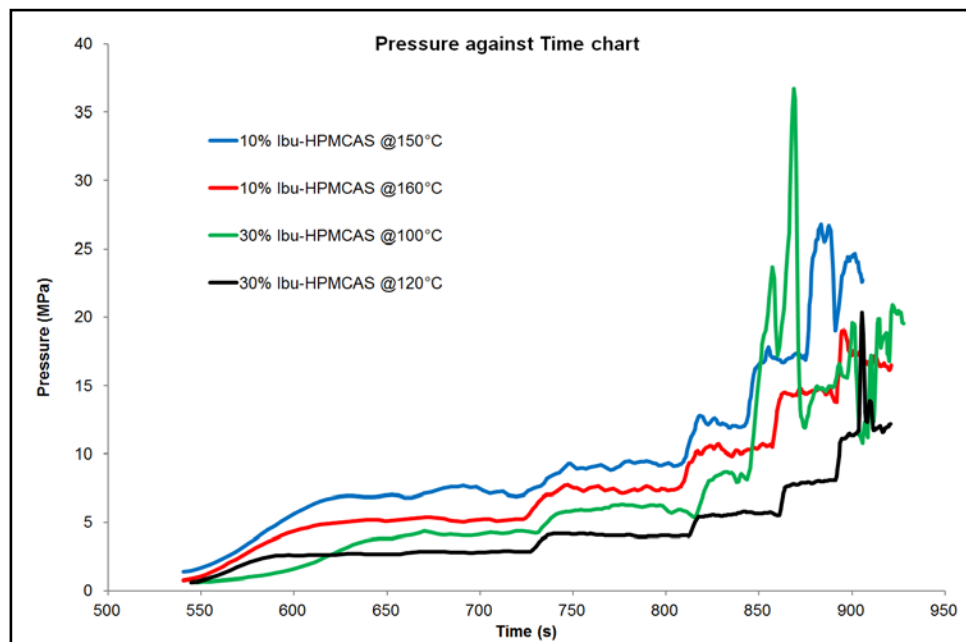
clearly indicated that plasticisation has important role to play not only in reducing the melt viscosity of the polymer but also reducing the relaxation time of the parent polymer. At lower frequencies, the polymers show more entanglements and forms a temporary entanglement network which reduces molecular mobility (intermolecular sliding phenomenon) due to intermolecular chain interactions. The relative motions between these chains generate frictional heat (Mezger, 2006 , Winter, 1994 , Wool, 1993). As a consequence, viscous behaviour dominates over elasticity. Moreover this behaviour causes the molecules to relax slowly (Mezger, 2006). In other words, at higher frequencies polymers entanglements show more rigidity whereby molecules store the deformational energy which is lost during the relative motion of the molecule and hence elastic modulus dominates over viscous modulus. Plasticisers typically works by this mechanism and thus it was believed that  $G''$  of polymeric blends dominated significantly over  $G'$ . From the figure 4.25, it can be observed that crossover point occurs at  $100 \text{ s}^{-1}$  at  $150 \text{ }^\circ\text{C}$  for 10% Ibu-HPMCAS and it is believed that frequencies  $> 100 \text{ s}^{-1}$  crossover point can be expected for 30% Ibu loadings however since rotational rheometer is limited upto  $100 \text{ s}^{-1}$  frequencies, precise values could not achieved.

- *Capillary rheology*

Blends of HPMCP and plasticisers were investigated in capillary rheology at relatively high shear rates using a similar methodology as for the pure polymers described earlier.



(a)



(b)

**Figure 4.26: Pressure versus time graphs (a) comparison at 140 °C for polymer-plasticisers and (b) IBU-HPMCAS compositions.**

Figure 4.26 provides representative pressure versus time curves for blends of TEC and CA with HPMCP analysed at 140 °C. It was noted that blends of TEC and PEG produced relatively smooth curves of long die pressures with increasing wall shear rates. However, blends of CA produced noisy traces compared with virgin HPMCP and the other two blends. Moreover, the measured pressure across the long length of the die of TEC and PEG blends showed a linear drop with increase in their loadings whereas for CA blends, the measured long length die pressures were found to be approximately equivalent, especially at high wall shear rates. These

studies indicated melt stability of TEC and PEG with the blends of HPMCP was relatively better than melt stability of HPMCP while instability occurred in the case of blends of CA. Furthermore, the extrudates obtained with the blends of CA were inconsistent and the melt was extruding out of the capillary die with a cracking noise. The fluctuation in the pressures indicates that plasticiser is non-homogeneous with polymer as far as melt stability is concerned.

The characteristic pressure drop–time curves obtained for HPMCAS melts containing 10 % and 30 % Ibuprofen at different temperatures are shown in Figure 4.26b. It was observed that the time required for attaining the equilibrium at the first stage increased with the viscosity of melt. With 10% ibuprofen at 150 °C, the long die pressure drop was found to be greater than at 160 °C due to the effect of temperature on viscosity. Similar effects were observed for HPMCAS with 30 % Ibuprofen at 100 °C and 120 °C temperatures. The pressure data for 30% Ibuprofen in HPMCAS at 100 °C shows a noisy baseline indicating unstable flow possibly due to incomplete melting. However, with the same concentrations at 120 °C changes in pressure are more distinct at each flow rate suggested that steady flow had been achieved. Overall, by comparing these graphs it was understood that melt stability of materials inside the capillary rheometer (and subsequently at melt extruder) can be carefully monitored with either selection of proper plasticiser concentration along with the processing conditions.

Further to these pressure / time curves, the shear viscosity of these blends was investigated and shear viscosity against wall shear rate curves for blends of plasticisers suggested shear thinning behaviour of the polymers with respect to increase in shear rate, temperature and plasticiser loadings. However, with exception of TEC and PEG blends with HPMCP (Figure 4.27),

the concentrations of CA were observed to be inconsistent with a viscosity drop. The viscosity reduced with increase in the temperatures attributed to formation of a non homogenous mixture (Figure 4.27). Similar studies were performed for 10% and 30% Ibuprofen. HPMCAS polymer was tested at 175 °C and the viscosity was high compared with systems containing 10 and 30% ibuprofen; lower temperatures were not possible for the pure polymer. Results showed a clear decrease in shear viscosity with increasing shear rate in all cases, suggesting shear thinning behaviour.

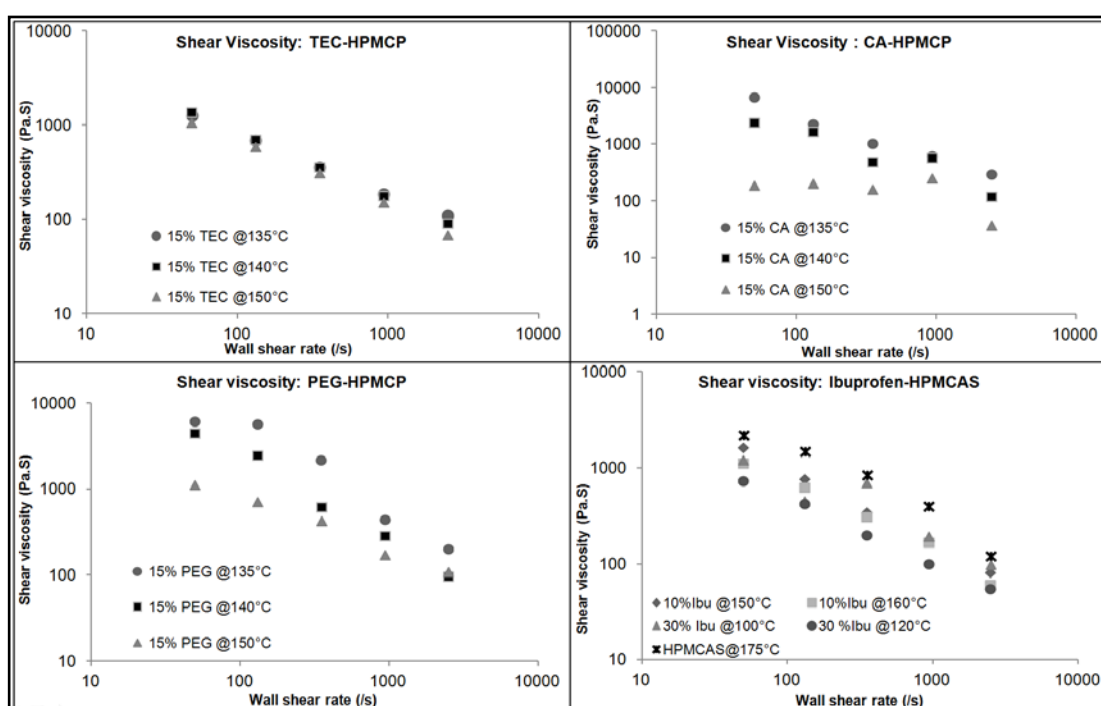


**Figure 4.27: Graphs showing linear dependence of viscosity.**

In light of experimental findings with plasticisers, experimental data of apparent viscosity of blends of polymers were investigated for power law fitting and the power law index was calculated along with their coefficient of regression ( $r^2$ ) for three concentrations and temperatures (Table 4.12). It was interesting to note that among the three plasticisers; only TEC and PEG appeared to be suitable for describing the statistical significance of power law modelling where the  $r^2$  values were more than 0.90 whereas  $r^2$  values of

blends of CA were observed to be less than 0.70. Similar results were obtained in the case of blends of Ibuprofen-HPMCAS ( $r^2 > 0.9800$ ) except for 30% drug loading processed at 100 °C ( $r^2 = 0.6802$ ), which supported the assumption of melt instability issue observed in the pressure plots. An important observation was noted in the case of blends of CA especially at 15 and 20% loadings for 135 and 140 °C processing temperatures. The blends of 15 and 20% CA produced power law index close to 1 value, which suggested shear thickening behaviour, deviating from shear thinning behaviour of polymer melt. Thus, based on these observations, it was noted that addition of citric acid cannot be a choice of plasticiser to modify melt rheology of both polymers as it can destabilise the melt properties of cellulose derivatives during extrusion.

**Table 4.12: Calculated power law index for plasticised polymer.**

Plasticiser	Loadings (%)	Power law index (n)					
		100 °C	120 °C	135 °C	140 °C	150 °C	160 °C
TEC	10	-	-	0.26	0.311	0.26	-
	15	-	-	0.36	0.30	0.32	-
	20	-	-	0.31	0.27	0.50	-
PEG-2000	10	-	-	0.11	0.10	0.11	-
	15	-	-	0.10	0.10	0.38	-
	20	-	-	0.1	0.19	0.41	-
CA	10	-	-	0.23	0.32	0.31	-
	15	-	-	0.81	0.82	0.58	-
	20	-	-	0.83	0.72	0.59	-
Ibuprofen	10	-	-	-	-	0.23	0.34
	30	0.48	0.31	-	-	-	-

- *Cox Merz rule*

The primary interest for investigating the polymer melt rheology was to understand the effect of shear rate on shear viscosity of samples over the ranges of temperatures with or without the presence of plasticisers. Generally capillary rheometry is considered as a preformulatory tool for melt extrusion studies since similar shear rates are generally applied in extrusion. However, with capillary studies it is generally difficult to perform the shear viscosity test at low shear rates ( $< 10 \text{ s}^{-1}$ ) and at low temperatures due to the probability of high pressure generation. Therefore, these studies are generally performed on a rotational rheometer where shear rate (frequencies) can be varied between 0.001 to 100  $\text{s}^{-1}$ . Since neither of the techniques cover the entire range of shear rate i.e. 0.001 to 100,000  $\text{s}^{-1}$ , visualisation of melt flow over the range of shear rates becomes difficult.

To overcome these difficulties and predict melt properties of the polymer samples both at low and high shear rates, Cox and Merz (Cox and Merz, 1958) derived an equation which links complex viscosity obtained from rotational to steady shear rate-viscosity obtained from capillary rheometers:

$$|\omega \rightarrow 0(\eta^* \omega) = |\gamma \rightarrow 0 \eta(\dot{\gamma}) \quad \text{Equation 4.17}$$

For both polymeric samples and their blends, the data of rotational rheometry and capillary rheometry was modified according to the above equation and the Cox-Merz rule was investigated (Figure 4.28). From this figure it can be seen that the data of both HPMCAS and HPMCP did not align with observed rotational and capillary viscosity measurements at 175 and 200 °C. However, with plasticisers, TEC and PEG, the viscosity values of capillary were observed close to that of rotational rheology measurements. Moreover, when Cox Merz rule was investigated for blends of CA, significant difference

between rotational and capillary viscosity measurements was observed (Appendix I, Figure 6.2).

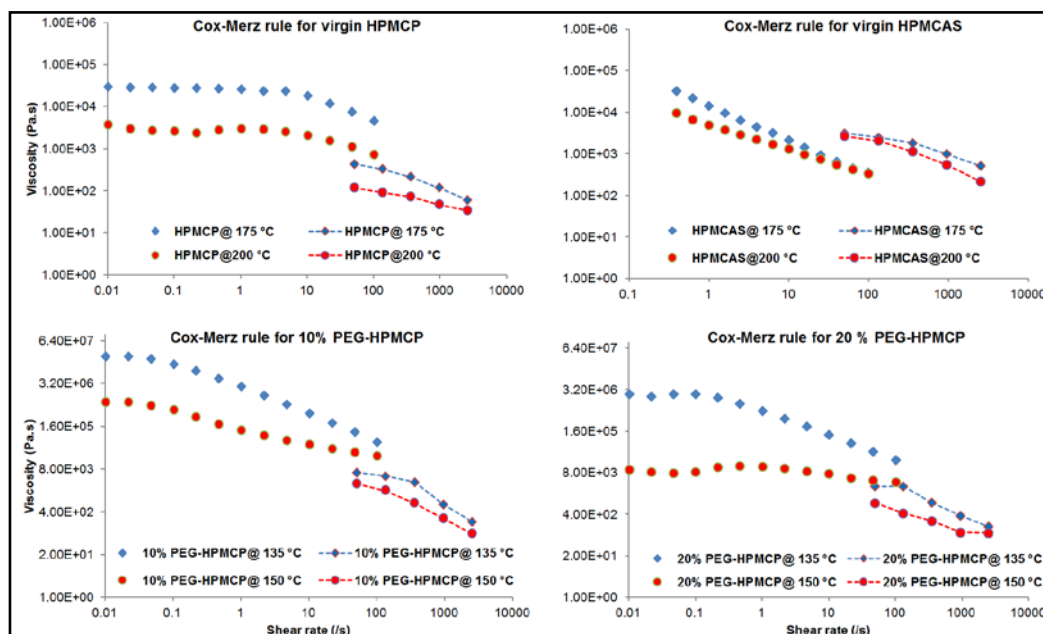


**Figure 4.28: Applications of Cox-Merz rule.**

Applicability of this rule generally holds true for most of the polymeric melts and dilute polymeric solutions containing linear branching. However literature reports suggest that deviations from this rule can also be expected especially at the higher frequencies or high shear rates (Rao, 2010 , Kulicke and Porter, 1980 , Tant et al., 1997). Moreover, certain reports suggest that difference in rotational and capillary viscometric data employed in the Cox-Merz rule could be attributed to thermal and mechanical degradation of the materials (Albertsson, 2001 , Gruber and O'Brien, 2005). As discussed earlier, higher processing temperatures of HPMCAS and HPMCP are detrimental to polymeric thermal stability and thus degradations of these polymers resulting in variation in viscosities are one of the possible reasons for deviations from the Cox Merz rule.

#### **4.1.4 Thermo-chemical stability of pure polymers**

Solid state polymers undergo changes in structural features when they are exposed to heat related to the chemical composition of the polymers. While the pharmaceutical industry is extremely cautious about degradation of APIs little effort has been spent in the characterisation of pharmaceutical polymers since conventionally polymers are considered as inert. Moreover, less attention has been given to the fundamental chemical properties of polymers especially, when they are used in the process of HME. Few researchers have suggested a relationship between thermal degradation, degradation products, mechanism and end properties of polymers during HME process. It is more evident that predictions of these properties for certain temperatures over relevant time scales would provide valuable information for precise engineering of materials and therefore, the probability of incompatibilities or formulation failures can be reduced.

##### *4.1.4.1 Polymer chemistry and structural features*

Thermal properties of both polymers HPMCAS and HPMCP, showed two-step degradation transitions in which first degradation transition was correlated to the loss of acidic substitutions. However, the thermal stability of polymer / materials in the temperature range between  $T_g$  or  $T_m$  and onset of degradation temperatures for HME process should also be investigated. These changes, if they occur, should be screened prior to extrusion studies for all possible degradation products. This gives formulators a 'flavour' of the chemical stability of samples for process optimisation. Here we examine the thermo-chemical properties such as degradation of polymers upon isothermal exposures through FTIR, HPLC and MS.

- *FTIR studies*

Initially, the FTIR spectra of both virgin polymers were investigated for their characteristic functional group IR absorptions and these absorptions were carefully compared against the isothermally exposed samples of polymers. Since authors Zedong Dong and Choi (2008) suggested succinic acid is generated from HPMCAS when exposed to oven temperatures. Considering these facts thermo-chemical changes should be reflected in FTIR studies. Investigation of such studies by FTIR is a practical approach to investigate structural changes. Virgin samples of both polymers were subjected to isothermal temperatures over 30 minutes (140, 160, 180 and 200 °C) and studied using FTIR.

Being ester derivatives, FTIR spectra of both virgin HPMCAS and HPMCP showed the characteristic carbonyl functional group of ester at approximately  $1736.03\text{ cm}^{-1}$  for acetate succinate derivatives and  $1721.19\text{ cm}^{-1}$  for phthalate derivatives (Figure 4.29). Since, ester bonds are known for their thermolability, considering these peaks as a reference, the heated samples of polymers were compared against the reference peak.

Infrared spectroscopy of virgin HPMCAS showed a strong band at  $1736\text{ cm}^{-1}$  corresponding to vibrations of acetyl and succinoyl (-COO-) functional groups and formation of new IR absorptions was speculated based on the hydrolytic cleavage of acetate and succinate moieties. However, despite exposing the samples of HPMCAS to three temperatures over a period of 30 minutes, only marginal changes were noted, though IR absorption bands were shifted towards higher wave numbers compared with the reference band at  $1736\text{ cm}^{-1}$  (Figure 4.29). Additionally, IR spectra of heated samples of HPMCAS produced a small and broad band at the wave number  $3500\text{ cm}^{-1}$  indicating formation of hydroxyl moieties. An interesting observation was

noted between the regions of 2800-2900  $\text{cm}^{-1}$  which corresponds to aromatic and aliphatic -CH stretching. FTIR spectrum of virgin HPMCAS showed relatively broad peaks between the regions of -CH stretching however, thermally exposed samples of HPMCAS showed sharp bands between these regions suggesting strong interactions between the functional groups of HPMCAS (Figure 4.29).

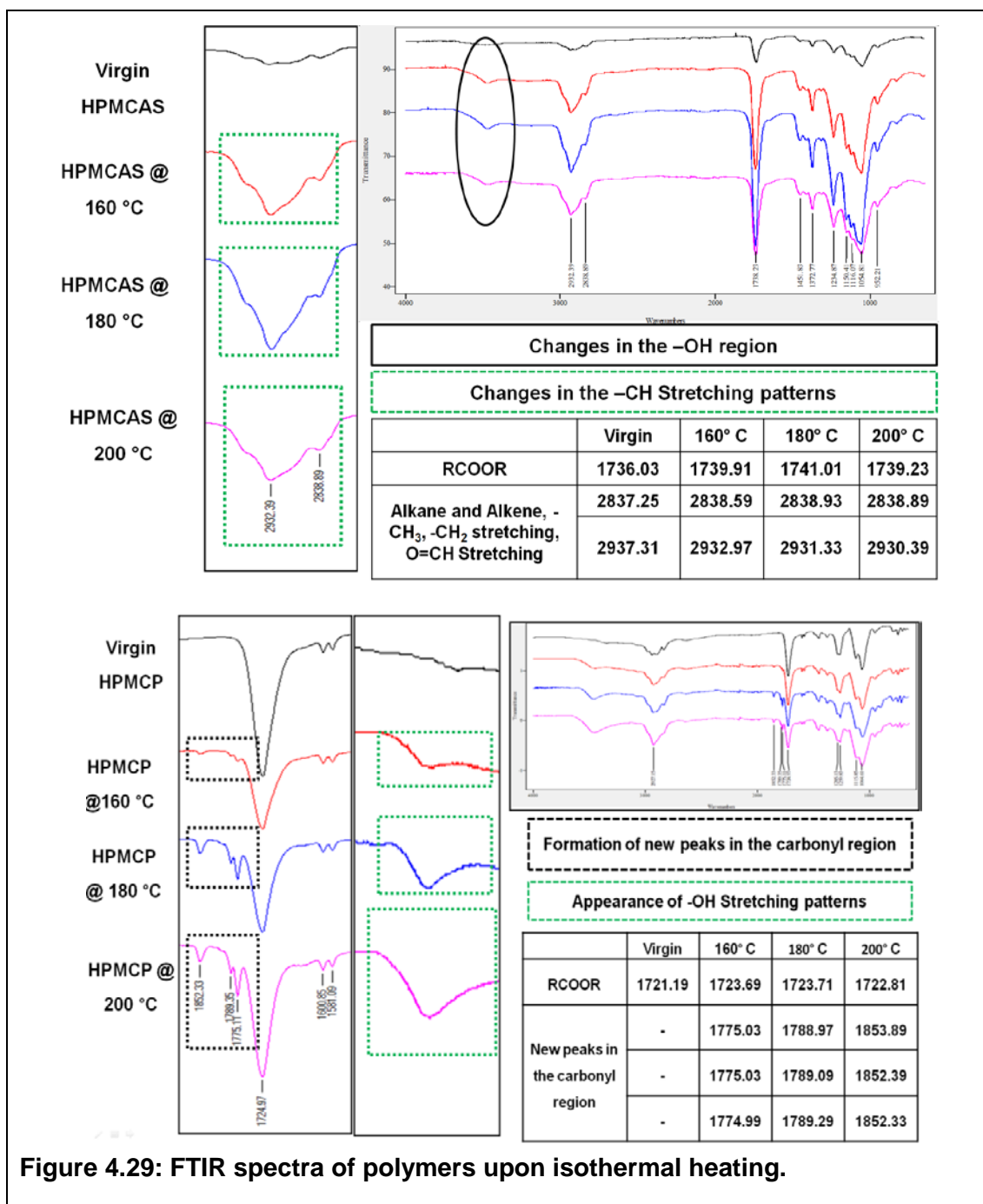


Figure 4.29: FTIR spectra of polymers upon isothermal heating.

Similar comparisons were made between virgin and thermally exposed samples of HPMCP. In the case of HPMCP polymers were compared to reference peak at  $1721.19\text{ cm}^{-1}$  and three new IR bands were observed in the region of  $1775$  to  $1860\text{ cm}^{-1}$  with the heated samples of HPMCP polymer. These results indicate the formation of new compounds during thermal exposure. Moreover, the bands in the region of  $1775$  to  $1860\text{ cm}^{-1}$  suggest newly formed compounds possessing carbonyl functional groups, the intensity of these three bands increased with the exposed temperatures. These absorptions peaks were further compared against the FTIR spectrum of standard phthalic acid and it was noted that, apart from the known characteristic absorption band of phthalic acid, a few unknown bands were also generated which were absent both in phthalic acid (PA) and pure samples of HPMCP. This study indicated that the degradation of HPMCP involves the production of different entities apart from its primary degradation product, PA.

In summary, FTIR studies observed in the case of HPMCAS did not provide a clear idea (just speculation based on formation of-OH bands) about hydrolytic cleavage at the site of the ester bonds however, in the case of HPMCP; it suggested degradation at the ester sites.

- *High performance liquid chromatography (HPLC)*

Generally, any chemical changes happening to materials during processing, including degradation, result either in production of new compounds or decrease in the contents of the parent compounds. These chemical changes are generally mapped qualitatively and quantitatively by means of analytical techniques including HPLC.

A new HPLC method was developed for characterisation of degradation products of both polymers since other methods reported in the literature involve basic tests which are usually used for bench top quality control measurements. For example, in a recent paper, stability assessments of HPMCAS was analysed by HPLC where the extrudate samples of HPMCAS were completely hydrolysed in sodium hydroxide solutions and quantified against manufacturer's specifications to measure the loss of acidic content during processing (Sarode et al., 2014). However, utilisation of such methods in day to day analysis would limit access to few important data called "impurity profiling" which is the most important parameter in pharmaceutical formulations. Moreover, for complex ester derivatives such as HPMCAS and HPMCP where a precise degradation mechanism is unknown, hydrolysing the entire polymer for estimating percent degradation of the polymer will limit the qualitative-quantitation of the other potential degradants and thus, incompatibility reactions during HME.

FTIR studies clearly suggested the formation of new compounds upon application of thermal energy to HPMCP so that characterisation of HPMCP for only its primary degradation product (phthalic acid) by hydrolysing the entire polymer will not only limit the potential incompatibility studies but would also underestimate the probability of finding additional degradation products of polymers. Moreover, there are few reports suggesting chemical incompatibilities of HPMCP polymers with added drugs, possibly due to the lack of a precise method of analysis other than hydrolysis. Therefore, there is a scope to develop a method which can potentially help in analysing degradation products of both polymers without hydrolysing the entire polymer.

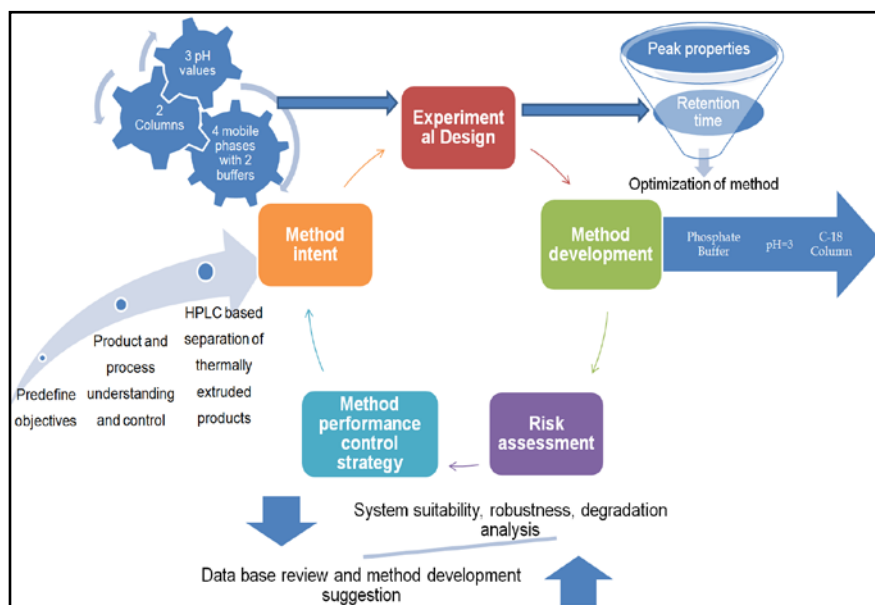


**Figure 4.30: HPLC method development and validation, a QbD like approach.**

The HPLC method was developed in a systematic way as shown in Figure 4.30. Different sets of parameters were utilised. The design of the experiment was composed of two buffers  $\text{KH}_2\text{PO}_4$ , and  $\text{Na}_2\text{HPO}_4$ , pH values (pH = 3, 4 and 5), and columns (C8 and C18). Since, polymers are soluble at  $\text{pH} > 6$  and could possibly cause hydrolysis of polymer melt extrudates, care was taken during method development. Hence, in the current method, all polymeric samples and standards were dissolved in methanol rather than dissolving in water at  $\text{pH} > 6$

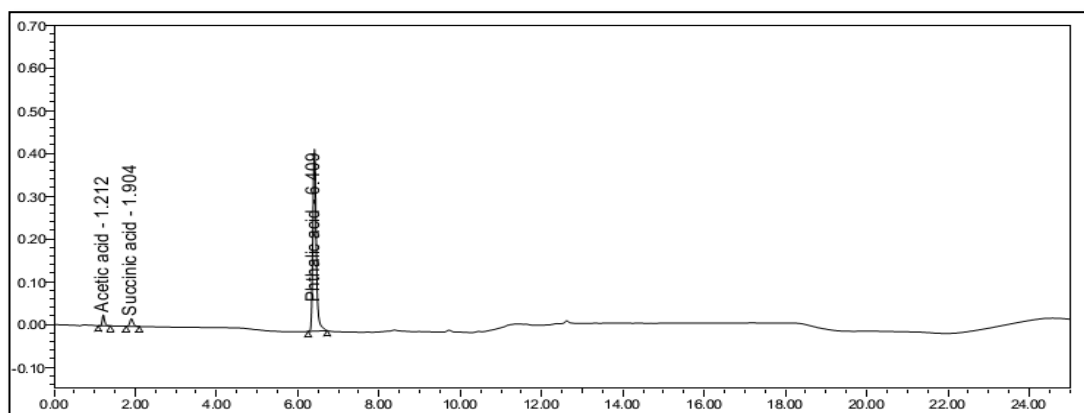


**Figure 4.31: Resolution solution of AA, SA, and PA in a gradient method.**

Various attempts were made to investigate and develop a method in the isocratic mode for qualitative analysis of these three primary degradation products over a range of columns and mobile phases. However, certain parameters of system suitability such as peak properties, plate counts, tailing properties, peak resolutions were non-satisfactory and unfit according to ICH guidelines. Therefore, a gradient method was investigated and a mobile phase containing phosphate buffer (0.05M) and methanol was selected based on acceptable system suitability values. A typical chromatogram of the pure AA, SA and PA sample obtained using the optimised method is shown in Figure 4.31. This method resolved AA, SA in less than 5 minutes and less than 10 minutes for PA.

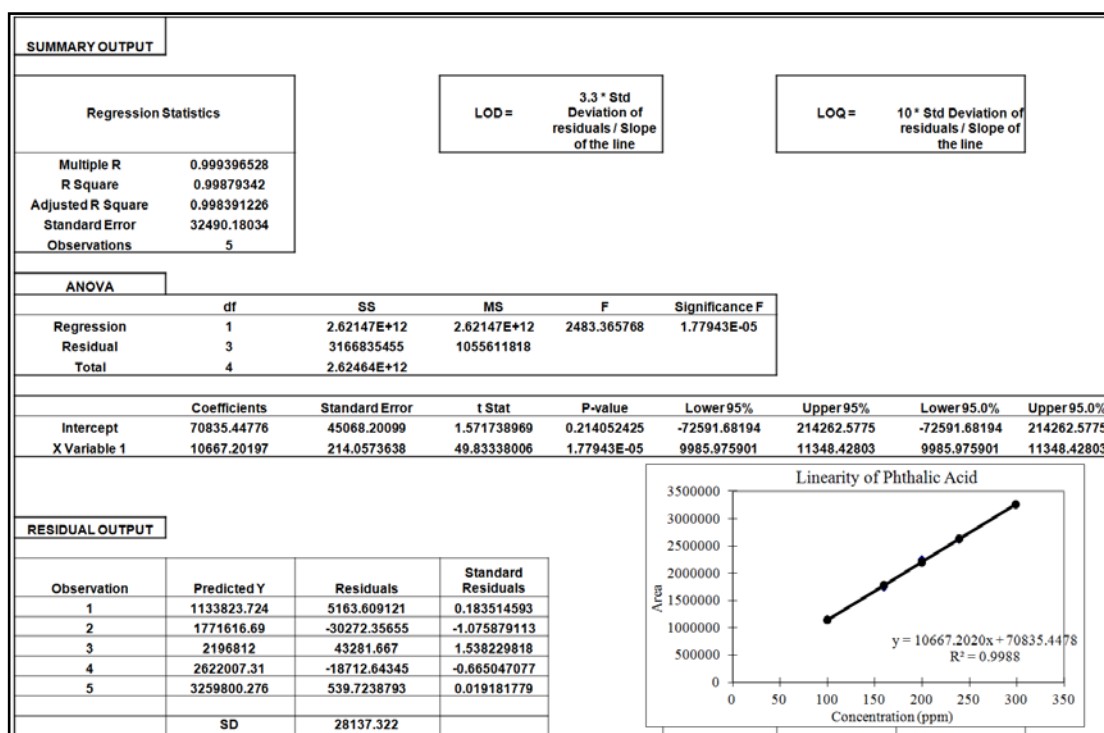
**Table 4.13: Linearity, LOD and LOQ for AA, SA and PA.**

Name	Linearity	LOD µg/mL	LOQ µg/mL	System suitability	Theoretical plates	Tailing factor	Recovery (%)
AA	0.9997	4.07	12.33	0.3026	4096	1.20	99-101%
SA	0.9995	5.51	16.72	0.4040	3226	1.10	98-102%
PA	0.9988	8.74	26.37	0.8040	5323	1.15	100-101%
Criteria	≥0.9	NA	NA	≤ 2.0% RSD	≥ 2000	≤ 2.0	90-110%

Recovery test was performed at n=4, Limit of detection: LOD, Limit of Quantitation : LOQ

During validation, a calibration curve was constructed by plotting mean area for respective impurities against their concentration and results were observed to be linear with a coefficient of regression  $\geq 0.99$ . The LOD of analyte was found to be 4, 5 and 8 µg/mL for AA, SA and PA respectively (Table 4.13 and Figure 4.32). Moreover, non-interfering peaks of AA, SA and PA in a resolution solution proved the selectivity of the method (Figure 4.31). A precision study was carried out to investigate the closeness of the method

by employing a number of different samples of extrudates. The relative standard deviation (RSD) values of system, method and intermediate precision suggested that the method was highly reproducible. The robustness of the method was validated by change in flow rate ( $1.0 \pm 0.1$  ml/min), change in pH of the mobile phase ( $\text{pH} = 3.0 \pm 0.2$ ) and change in the column serial number. Non-significant difference was noted when the method was exposed to small variations of robustness. The percent RSD values in all cases of robustness parameter were observed to be less than 2 with tailing factor less than 1.3 and theoretical plates more than 3000 (Table 4.13). Additionally, percent recovery values obtained by spiking known concentration of impurities of AA, SA and PA in the extrudates of polymers showed that the proposed method is accurate for estimation of impurities from HPMCAS and HPMCP based on nearly 100% recovery of spiked compounds.



(a)

Date		24/09/2012		
PARAMETER		High pH (2.1)		
Preparation of Standard solution				
	Potency %	Weight in mg	Dil. 1 in ml	
Acetic acid	99.7	98.50	100	
Succinic acid	99	98.87	100	
Phthalic acid	99.5	100.32	100	
		in ml	Dil. 2 in ml	
		10	50	
		10	50	
		2	50	
Standard Solution				
System suitability solution				
	Area of Injection-1	Area of Injection-2	Area of Injection-3	
Acetic acid Area	57407.00	96772.00	57055.00	
Succinic acid Area	192289.00	102082.00	191762.00	
Phthalic acid Area	2460343.00	2455032.00	2459577.00	
	Area of Injection-4	Area of Injection-5	Mean	
	57042.00	97323.00	97155.00	
	102054.00	188.2273	195.1912	
	2457624.00	2371.5766	0.2905	
			0.1844	
			0.0963	
Sample preparation				
Acetic acid				
Batch No	Wt. Sample(mg)	Dil. 1 in ml	Volume Taken	
A	300.12	100.00	5.00	
B	300.25	100.00	5.00	
			Dil. 2 in ml	
			10.00	
			10.00	
			10.00	
Phthalic acid				
Batch No	Wt. Sample(mg)	Dil. 1 in ml	Volume Taken	
A	100.32	100.00	5.00	
B	100.06	100.00	5.00	
			Dil. 2 in ml	
			10.00	
			10.00	
			10.00	
Area				
Batch	Acetic acid		Succinic acid	
	A	B	A	B
1	4951.0000	4572.0000	16049.0000	15944.0000
2	4891.0000	4657.0000	16229.0000	16073.0000
Amount found 1	0.6729	0.5157	2.8723	2.9579
Amount found 2	0.6589	0.5214	2.8955	2.8745
Mean	0.6659	0.5214	2.8839	2.9662
SD	0.0099	0.0081	0.0118	0.0530
RSD	1.4877	1.3025	0.7806	0.5018

Date		24/09/2012		
PARAMETER		Low flow (0.5ml/min)		
Preparation of Standard solution				
	Potency %	Weight in mg	Dil. 1 in ml	
Acetic acid	99.7	99.85	100	
Succinic acid	99	100.01	100	
Phthalic acid	99.5	100.09	100	
		in ml	Dil. 2 in ml	
		100	50	
		100	50	
		2	50	
Standard Solution				
System suitability solution				
	Area of Injection-1	Area of Injection-2	Area of Injection-3	
Acetic acid Area	108786.00	108390.00	108312.00	
Succinic acid Area	113645.00	112661.00	113063.00	
Phthalic acid Area	2731131.00	2715082.00	2675307.00	
	Area of Injection-4	Area of Injection-5	Mean	
	113400.00	113400.00	108357.00	
			270.5991	
			0.2498	
			0.3367	
			0.8968	
Sample preparation				
Acetic acid				
Batch No	Wt. Sample(mg)	Dil. 1 in ml	Volume Taken	
A	300.15	100.00	5.00	
B	300.18	100.00	5.00	
			Dil. 2 in ml	
			10.00	
			10.00	
			10.00	
Phthalic acid				
Batch No	Wt. Sample(mg)	Dil. 1 in ml	Volume Taken	
A	100.14	100.00	5.00	
B	100.03	100.00	5.00	
			Dil. 2 in ml	
			10.00	
			10.00	
			10.00	
Area				
Batch	Acetic acid		Succinic acid	
	A	B	A	B
1	25577.0000	25500.0000	18875.0000	18114.0000
2	25668.0000	25597.0000	18955.0000	18283.0000
Amount found 1	3.1315	3.1210	2.1984	2.8105
Amount found 2	3.1411	3.1337	2.1772	2.1362
Mean	3.1366	3.1277	2.1533	2.1204
SD	0.0072	0.0084	0.0511	0.0139
RSD	0.2291	0.2685	2.3515	0.6367

(b)

Figure 4.32: A representative chart showing statistics utilised during validation (a) LOD-LOQ (b) robustness parameter.

- Mass spectroscopy (MS)

FTIR analysis of isothermally exposed samples of both polymers yielded some idea about polymer degradations at the ester sites. In initial attempts for finding degradation products of polymers, mass spectroscopy was utilised to study the characteristic molecular fragmentation patterns of different degradation products.

A mechanistic approach of time of flight was utilised in the MS studies and different molecular fragments obtained from the polymers were investigated. The analysis was performed in a positive ion mode. Isothemally heated samples of both polymers were subjected to MS independently and molecular fragmentation patterns were investigated. The resulting spectra of these samples produced valuable information about the probable degradation products of HPMCAS and HPMCP. Data suggest traces of succinic acid, formaldehyde and succinic anhydride present in the case of HPMCAS.

HPMCP produced phthalic acid, fragments of benzene, aliphatic-aromatic chains as well as alkene chains. Detections of higher molecular weight compounds was unachievable in the current investigation (entire spectra was not obtained and gave limited information) due to limited maximum detection limit of the in-house spectrophotometer (up to Mw = 2000 Da). Further, it was interesting to note that mass spectra of thermally exposed samples of HPMCAS up to 180 °C did not show a presence of these degradation products indicating degradation of HPMCAS was still incomplete below 180 °C. This observation is in contrast to that of Zedong Dong, 2008. However the possibility of succinic acid being released below 180 °C is still acknowledged

#### **4.1.5 Summary**

Preliminary studies of thermal, thermodynamic melt rheology and thermo-chemical properties of virgin polymers, plasticisers and APIs provided valuable information about thermal material properties. Firstly, thermal studies are discussed. TGA provides degradation temperatures of materials and degradation patterns of materials suitable for screening via derivative weight loss curves. For example, TGA of HPMCAS initially looked to be a single step degradation transition however producing derivative curves allowed two peaks to be observed distinctly. Similarly, derivative weight loss of CPM suggested that fluctuations in curve patterns indicative of chemical changes in CPM before its degradation temperature. Thus, the previous assumption of TGA providing an apparent degradation temperature was justified and further confirmed when isothermally exposed samples of polymer below polymer's conventional degradation temperatures showed generation of degradation products as seen in FTIR and MS studies.

During thermodynamic studies, it was observed that both polymers are well designed for manufacturing ASDs. For instance, they are high  $T_g$

polymers, possess better miscibility and solubility profiles for a variety of API and plasticisers based on their solubility parameter values. Note that most of the poorly water soluble APIs are observed to possess  $\delta$  values in the range of 20-30. These combined beneficial properties aid in producing and maintaining ASD. Further, the ability of plasticisers to form strong or weak glassy state and their maximum safe loading values without chances of recrystallisation or phase separation was investigated. PEG provides a maximum safe loading up to 10-12 % whereas applications of CA as a plasticiser for these two polymers in the manufacturing of ASDs can be ambiguous and great care should be taken during extrusion and later stability studies.

Comprehensive melt rheology was investigated for fundamentals of rheological properties of both pure and blends of polymers for their suitability as well as flow characteristics in extrusion. Rotational and capillary rheology studies of virgin and plasticised polymers provided valuable insights of mechanical properties. LVE regions of all polymers were determined showing linear viscoelastic range of HPMCAS was observed to be extensive compared with HPMCP at all investigated temperatures. FS tests suggest that HPMCAS is more viscous than HPMCP and even at low shear rates of 0.01 and 0.1 rad/s the polymer exhibits shear thinning while HPMCP shows a Newtonian plateau at low shear rates. Investigations of  $G'$  and  $G''$  indicate multiple crossover points and correlate their relationship with the formation of a weak network among the polymeric chains. In terms of plasticiser addition, it was noted that TEC and PEG would be better choices compared to CA since CA yields unstable melt flow. Capillary rheology investigation of virgin polymers revealed high amount of pressure generation across the long and short die length at higher shear rates at 150 °C suggesting that, although this temperature is well above the glass transition temperature of the parent

polymers, extrusion will be difficult leading to high levels of torque generation inside the extrusion barrel and thus potential damage. Capillary studies showed real time melt stability at high shear rates where all grades of HPMCAS looked to be stable even at maximum processing temperature. However, plasticisation of polymers produced significant impact on the melt stability of formulations especially with TEC and PEG blends, as shown in the rotational investigations.

Thermo-chemical studies showed that these polymers are expected not only to produce known degradation products of succinic-acetic and phthalic acids but are also capable of producing unknown degradation product which should be screened for post extrusion studies for potential incompatible reactions. Moreover, it was also noted that thermo-chemical stability of these two polymers can be compromised as a function of temperature. Thus, it demands extensive attention especially for API-polymer chemical interactions during and/or post extrusion. Further, it is also advised that thermo-chemical analysis of melt extrudates should not only be limited for percentage assay values of APIs but should also be screened for chemical reactions between the degradation products of polymers and the pure API.

## **4.2 Hot melt extrusion and processing attributes**

Here the influences of polymeric properties on HME processing conditions and vice versa are discussed. For example, preliminary studies suggest that both HPMCAS and HPMCP are highly viscous polymers hence the influence of this viscosity on screw speeds, set temperatures, torque generation and motor overload must be considered. In addition the influences of these processing parameters on the polymeric properties such as activation energy of melt, melt flow behaviour inside extruder (smooth or unstable) are discussed briefly.

### **4.2.1 Influence of pure and blend polymeric properties on processability**

Different grades of HPMCAS and HPMCP polymers were extruded between temperatures of 150 and 200 °C at three screw speeds 20, 80 and 100 rpm with motor load in terms of torque generation being measured. Based on the  $T_g$  values of the pure polymers, (HPMCAS < HPMCP) improved processability of HPMCAS was speculated at higher temperatures over HPMCP. Preliminary studies showed the melt viscosity of HPMCAS to be considerably > HPMCP even at higher extruding temperatures, hence a study of the influence of screw speeds on generation of torque (at die zone) over the range of temperatures at different polymeric grades was commenced. Similarly, blends were investigated and their processability studied.

Table 4.14 shows the effects of temperatures and screw speeds on the generation of torque inside extruder barrel for pure polymeric samples. As preliminary studies suggested, both polymers were observed to be extremely difficult to extrude at temperatures less than 160 °C at the possible screw speeds and those less than 10 rpm yielded melt extrudates with maximum torque (close to 95%) with residence time  $\approx$  25 min. Polymers processed



extruder with torque values varying between 20-50% at 150-180 °C. This was attributed to plasticiser induced reduction in cohesive interactions between the long chains of the polymers. Figure 4.33 shows the effect of plasticisers on torque reduction with respect to temperature and concentration. From the Figure 4.33, it can be seen that PEG provides significant plasticisation for HPMCP allowing blends to be processed at 120 °C with a maximum torque. Similar results were obtained for PEG-HPMCAS blends but data is not shown here.

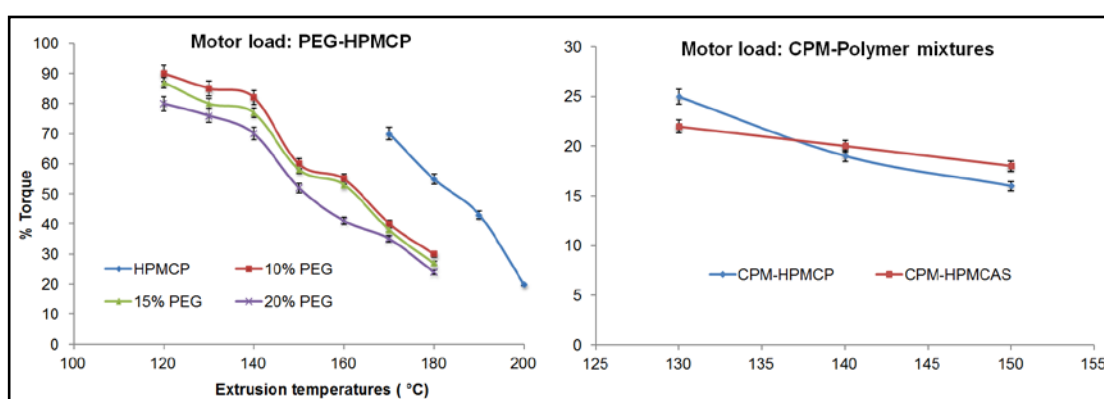


**Figure 4.33: Percentage torque versus extrusion temperatures for samples**

Further, the blends achieved 50% of the torque at 150 °C with HPMCP and 130 °C with HPMCAS while the pure polymers overloaded the extruder motor. These observations coincided with the rheological studies where preliminary studies reached up to the temperatures of 130 °C (See section 4.1.3.3, Capillary rheology data). Similar studies carried out for the blends of CPM with both polymers. Two observations were noted. Firstly blends of CPM with both polymers reduced the torque values significantly compared with PEG blends suggesting CPM provides greater plasticising activity than PEG. Secondly CPM-HPMCP blends produced % torque value of 25% at 130 °C which linearly decreased to 15% at 150 °C. While blends of CPM with HPMCAS produced torque values between 21 to 18% when processing temperature was increased from 130 to 150 °C. An interesting observation

was noted during extrusion of CPM with both polymers. CPM-HPMCP produced intense dark brown coloured extrudates especially at 150 C whereas the CPM-HPMCAS produced extrudates of less intense colour.

#### 4.2.2 Polymer melt flow behaviour inside extruder

Preliminary studies of capillary rheology provided a flavour of polymer melt flow and its stability at high shear rate. However, shear stresses and shear rates inside an extruder are not constant due to the nature of the flow paths seen by different parts of the melt.

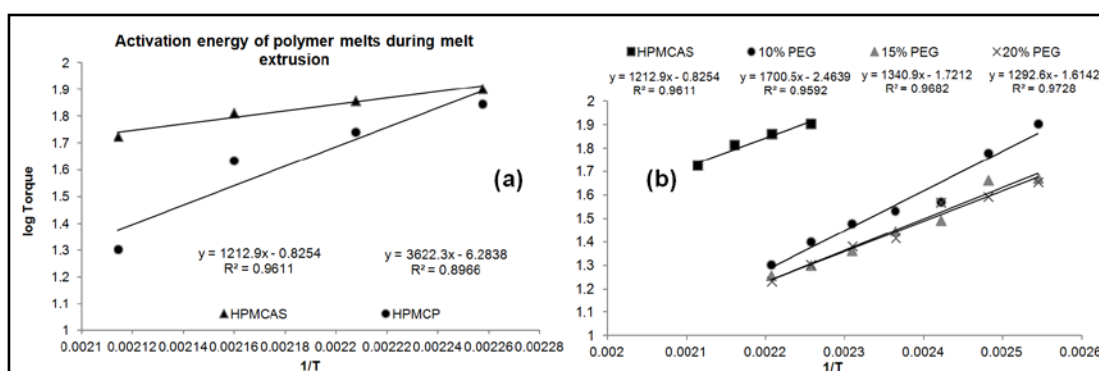


**Figure 4.34: Activation energy plots of (a) pure and (b) polymer blends.**

The majority of thermoplastic materials exhibit non-Newtonian flow behaviour in which the temperature dependent melt viscosities are dependent on chain entanglements, molecular weight and its distribution, and plasticiser loadings. Since temperature dependent melt viscosity is a function of the Arrhenius equation (as discussed earlier) then by correlating extruder torque values to viscosity the Arrhenius activation energies can be recovered by plotting log torque against the reciprocal of temperature as for equation 4.18 (Schilling, 2009 , Goodrich and Porter, 1967 , Menon *et al.*, 2006). 500 gm samples of HPMCAS-LG and HPMCP-HP55 were processed over the range of temperatures at the same screw speeds at least ten times and average

values of torques were taken into the consideration - the values of torques were considered only when reproducible torque values were received.

$$\log \eta \sim \log T_q = \log A - E_a/RT \quad \text{Equation 4.18}$$

From the Figure 4.34, a linear relationship can be seen between the torque values and reciprocal of temperature.  $E_a$  values were calculated from the slope of the line. For pure polymers, the flow activation energy was observed to be 30.11 and 10.08 kJ/mol for HPMCP and HPMCAS respectively between the temperature range 170-200 °C (Table 4.15). It was interesting to see that HPMCP produced higher values of  $E_a$  than that of HPMCAS which suggests that despite possessing only one substituent, phthalic acid, HPMCP still requires more energy to make polymer melt flow compared with bi-substituted HPMCAS polymers. When blends of PEG as well as CPM were investigated, PEG-HPMCP produced relatively similar values of  $E_a$  whereas PEG-HPMCAS showed a trend in lowering  $E_a$  values (Table 4.15). This was attributed to increase in molecular mobility. Similar studies were performed with citric acid blends and in all cases  $E_a$  of the blends was equivalent to that of the parent polymers. It was thought that this can be attributed to poor plasticising effect of citric acid compared with PEG, resulting incomplete melt formation with both polymers below 160 °C. This was the maximum processing temperature since above 160 °C CA was degraded.

Earlier in the preformulation studies, Arrhenius kinetic values of  $E_a$  calculated at zero-shear rate for HPMCAS produced values of approximately 13 kJ/mol where it was attributed to lack of Newtonian plateau and the complex viscosity values were actually co-related to non-Newtonian viscoelastic region. Comparing these values with the  $E_a$  calculated for melt extrusion process (i.e. 10.08 kJ/mol), it can be seen that these values are

comparable and difference in their values by 3 kJ/mol can be attributed to combined effect of temperature and shear which is enormous in the case of HME compared to rotational rheometer. Thus the validity of rotational as well as capillary studies as preformulatory tool for HME studied of HPMCAS and HPMCP was justified. Blends of CPM and IBU also provided similar results and lower activation energy with both polymers. However, for 30% IBU processed above 120 °C, the viscosity was virtually independent of screw speed (torque < 1-2%) and collection of such these samples difficult.

**Table 4.15: Flow activation energy of polymers during extrusion.**

<b>Name</b>	<b>Ea (kJ/Mol)</b>
HPMCP	30.11 (170-200 °C)
10% PEG	11.85 (120-180 °C)
15% PEG	12.19 (120-180 °C)
20% PEG	12.69 (120-180 °C)
20% CPM	13.75 (130-150 °C)
HPMCAS	10.08 (170-200 °C)
10% PEG	14.13 (120-180 °C)
15% PEG	11.14 (120-180 °C)
20% PEG	10.74 (120-180 °C)
20% CPM	6.17 (130-150 °C)

#### **4.2.3 Summary**

By looking at the material properties and processability of cellulose ester derivatives in HME, important insights and correlation with preformulatory studies were noted. When processed in HME with a linearly increasing temperature distribution from zones 2 to 6 and then maintaining a constant maximum temperature provided better processability despite a variety of

blend concentrations. Further, although the difference in  $T_g$  of HPMCAS and HPMCP is greater than 25 °C, the processing temperatures of both polymers were found to be similar – this was also found applicable to their blends with PEG and TEC (see Appendix I, Figure 6.3). Since torque values (pressure or shear stress) are representative of temperature dependent melt viscosity values, energy of activation was calculated by comparing torque values with Arrhenius equation (see equation 4.18). Compared with other polymers such as Eudragit® S100 ( $E_a > 106$  kJ/mol) or HPMC, both HPMCP and HPMCAS provided approximately 1/10<sup>th</sup> lower values of  $E_a$  than other melt extrusion polymers to overcome viscosity barrier for extrusion process. This suggests easier processability of HPMCP and HPMCAS. Inclusion of plasticisers further reduces  $E_a$  and improves processing time and efficiency. However, it is essential to note that polymer-plasticiser compatibility is an important factor in extrusion. Over all this study showed that HPMCAS possesses relatively easy and stable processability suited to HME compared to HPMCP and with the addition of plasticisers this can be reproduced at lower processing temperatures.

### **4.3 Characterisation of polymer melt extrudates**

This chapter provides results probing thermodynamic, rheological and thermo-chemical properties of HPMCAS and HPMCP polymer melt with plasticisers and model APIs in extrudates. Firstly, the thermodynamic properties of melts are discussed, comparing theoretical phase diagrams with empirical melt extrudates and their related stability studies, as determined by DSC, XRD and Dynamic Vapour Sorption (DVS) studies. Secondly, the melt rheology of the polymer extrudates is discussed prior to investigations of the thermo-chemical stability of melts with respect to polymer degradation products, unknown impurities and polymer-API- chemical compatibility with or without use of plasticisers. Further, chemical analogues of model APIs which could face incompatibilities with these polymers are also discussed in the last section.

#### **4.3.1 Thermodynamic approaches**

Initial studies of fragility index, Fox equation modelling and the thermodynamics of miscibility provided valuable information about thermodynamic properties of polymer-plasticiser or polymer-API mixtures. In order to validate these theoretical aspects extrudates were validated for physical stability against thermodynamic phase diagram.

Earlier, thermodynamic phase diagrams of blends of PEG with HPMCAS and HPMCP suggested that at 25 °C, loadings of PEG up to 10 and 12% w/w will remain as super saturated glasses and 15, 20% of PEG loadings will lie in the metastable and unstable regions. Similarly, 10% CA will produce a thermodynamically stable amorphous blend with HPMCAS whereas 3% of CA loadings were feasible with HPMCP polymer at 25 °C. Hence, three compositions of 10, 15 and 20% (w/w) of plasticiser loading were investigated

using HME and extrudate strands of independent polymeric samples were exposed to open tray stability conditions (i.e. variable temperature and humidity conditions). These compositions were selected specifically based on the binodal and spinodal decomposition curves so that stable, metastable and unstable compositions could be investigated and compared for phase diagram validation.

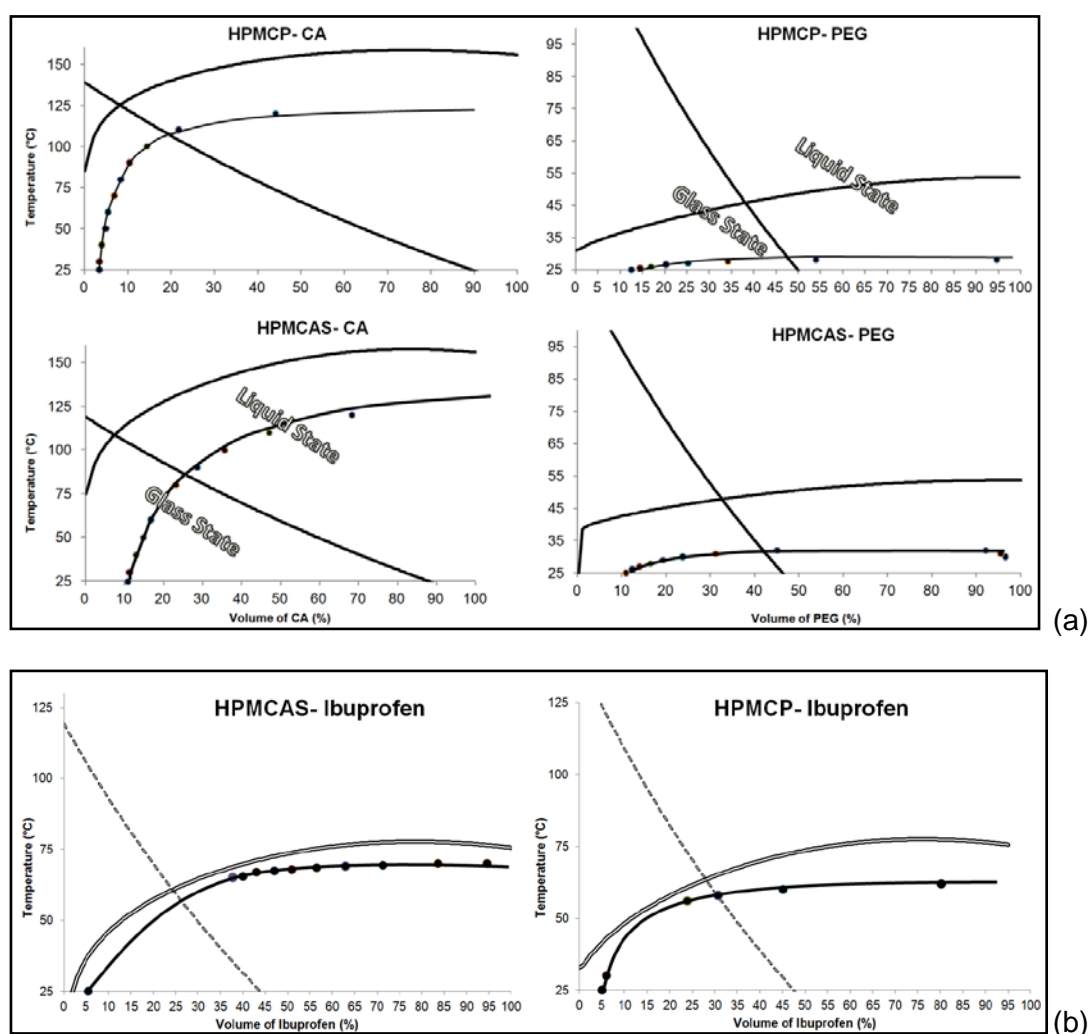


**Figure 4.35: Thermodynamic phase diagrams of (a) polymer-plasticiser and (b) IBU-polymer mixtures.**

Polymer melt extrudates of blends of PEG with both polymers are discussed first. All three compositions of PEG loadings processed at 140 °C were considered since this temperatures lies above the polymer-plasticiser solubility curve (Figure 4.35a). Here processing of these blends proved

feasible without any processing errors. Post extrusion, melt extrudates of these 3 compositions were divided for three time points: initial ( $t_0$ ), 12 months ( $t_{12}$ ) and 24 months ( $t_{24}$ ) and physical stability of melt extrudates was screened. To investigate the influence of downstream processes on physical stability, extrudates were stored in two forms - (a) extrudate strands (b) pelletised chip.

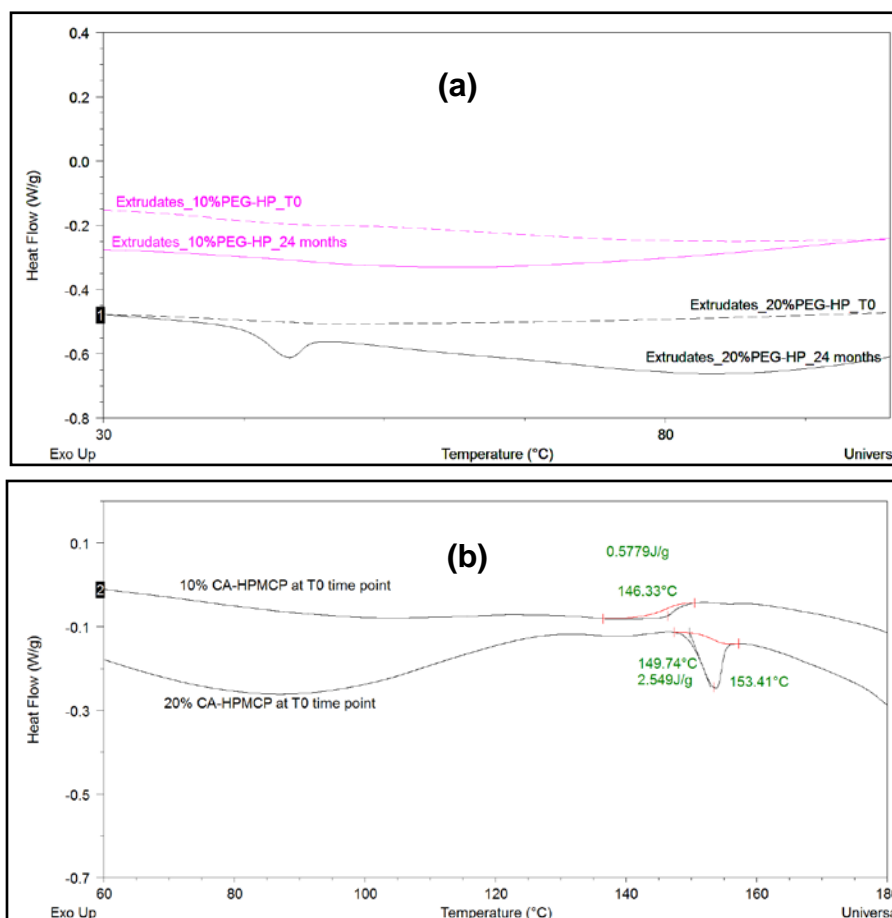
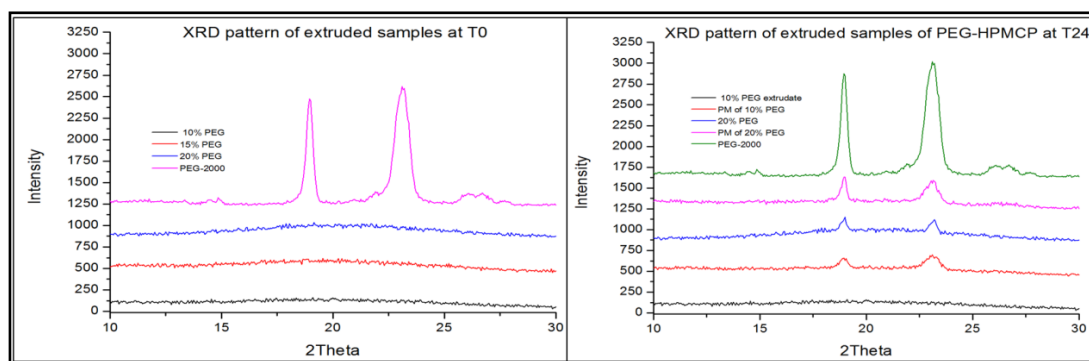


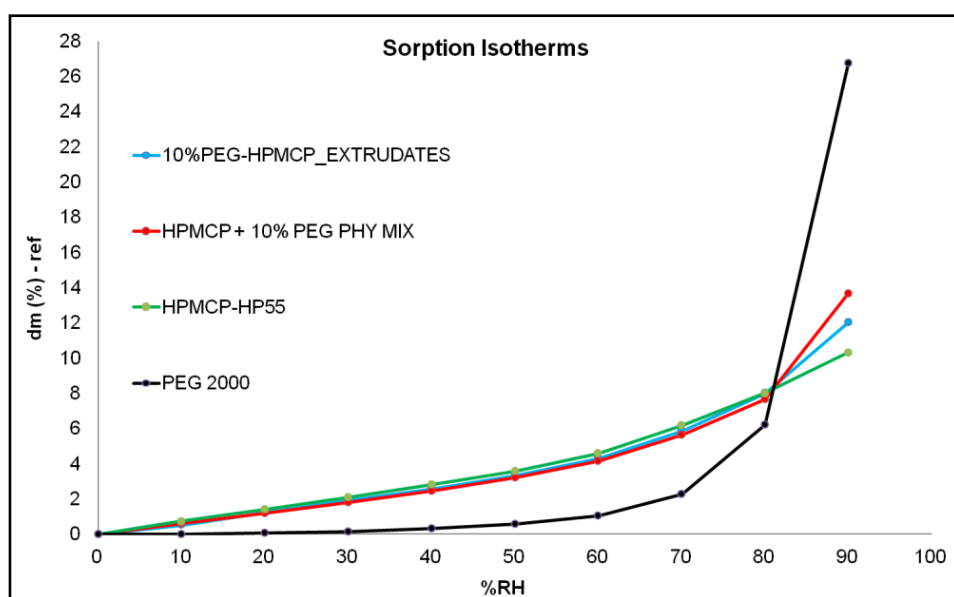
**Figure 4.36: DSC thermograms of melt extrudates of (a) PEG-HPMCP (b) CA-HPMCP during stability studies.**

Polymer melt extrudates of PEG with HPMCAS and HPMCP did not exhibit the melting endotherm of PEG in DSC (Figure 4.36a) and along with X-ray diffraction (XRD studies) (Figure 4.37a) confirmed complete amorphisation of all three systems at  $t_0$  conditions. Similar stability studies were then carried out on same melt extrudates at different time intervals at variable temperature and humidity conditions. A representative DSC

thermogram of melt extrudates of PEG-HPMCP (10 and 20% loadings) investigated over the period of time is shown in the Figure 4.36. It was observed that despite a range of temperature and humidity exposures in an open tray environment 10% PEG loadings remained amorphous over 2 years whereas 15 and 20% of PEG loadings concentrations showed endothermic events at the end of 2 years. Moreover, the melting endotherms of PEG of 15 and 20% PEG produced  $\Delta H = 0.6949$  and  $1.398$  J/g which confirmed the existence of semi-crystalline PEG. XRD patterns of these melt extrudates confirmed the presence of characteristic peaks of PEG at 18.8 and 23.2 respectively (Figure 4.37).



(a)



(b)

**Figure 4.37: A representative figures of (a) XRD of melt extrudates of PEG-HPMCP upon stability (b) effect of moisture on 10% PEG mixtures**

According to phase diagrams (Figure 4.35a), concentrations up to 10% were in the safe zones of zone 4 at 25 °C whereas, at the same conditions, 15 and 20% loadings were lying in the zone of 6 which is considered part of the spinodal decomposition zone. However, since this region comes under the glass transition curve, kinetic displacements, especially molecular mobility, is kinetically arrested and here the glass forming ability (fragility) of the crystalline compound as well as polymer viscosity may play a dominant role in the extent of recrystallisation or phase separation as a function of time. Thus, while considering enthalpy values of recrystallised PEG at the end of 24 months, it can be seen that values are very low compared with pure PEG (100%,  $\Delta H = 170.4 \text{ J/g}$ ). These results support the assumption of kinetic anticipations in zone 6 due to both strong glass forming ability and high polymer melt viscosity.

It can be debated that the above phase diagram does not take into account moisture uptake by melt extrudates, one of the prime factors for recrystallisation (Sarode, 2010 , Yoshinari *et al.*, 2002 , Rumondor *et al.*, 2009a , Huang and Dai, 2014). In order to validate the effect of moisture on the recrystallisation behaviour of the PEG in its 10% loadings, DVS studies were conducted for both HPMCP and HPMCAS samples. According to literature reports on DVS, when an amorphous state (prepared from its crystalline state) of samples is exposed to moisture, it results into weight gain and the process continues as the % moisture level increases. However, in between if amorphous state shows a sudden loss in weight, it generally indicates phase transformation i.e amorphous to crystalline (Hunter *et al.*, 2010). Thus, it was speculated that melt extrudates of 10% PEG samples would provide similar results upon exposure to 90% moisture. However no sudden loss of water was observed in the melt extrudates of 10% PEG confirming the absence of recrystallisation as a function of humidity (Figure

4.37b). In order to provide more kinetic displacements, 10% of PEG extrudates were milled and samples screened using DSC, XRD and DVS. No sign of recrystallisation or phase separation was observed. Thus, the predictions made for the phase diagram of maximum safe loadings of PEG in HPMCP up to 12% was justified and confirmed with these studies. Similar results were obtained for HPMCAS blends and 10% maximum loadings of PEG confirming it as a safe concentration for melt extrusion.

Similar studies were conducted for the blends of CA and Ibuprofen. Extrusion studies involving CA were carried at 140 °C and melt extrudates of these samples were subjected to DSC. All three compositions (10,15 and 20% CA) showed melting endotherm at the initial time points (Figure 4.36b) indicating spontaneous phase separation of plasticiser from polymer and confirming that neither of the compositions survived system re-equilibration upon die exit resulting into decomposition into crystalline phases. Moreover, the fragility parameter for CA showed that it forms a poor glass and melt viscosity of its polymeric blends was poor compared to PEG blends, hence this kinetic arrest did not occur. Further, it was thought that the processing temperature of 140 °C could be responsible recrystallisation due to insufficient melting. Therefore, the processing temperature was increased to 150 and 160 °C and extrudates of CA were investigated for stability studies. However, it was noted that blends of CA with both polymers processed at 150 and 160 °C produced degradation of CA due to high shear and temperature thus stability studies of these extrudates were not studied further.

Extrudates of IBU (10 and 30% loadings) were investigated. At  $t_0$ , all processed samples showed amorphisation of Ibuprofen (Figure 4.38) and the 10% loaded blend remained amorphous until the first month time point whereas 30% Ibuprofen extrudates produced recrystallisation within a day

(Figure 4.38). As can be seen from the phase diagram, none of the investigated loadings of Ibuprofen were stable at 25 °C and the phase diagram predicted its spontaneous phase separation upon extrusion which resulted very quickly in the case of 30% loading while the 10% loading sample took a longer time to recrystallise. All these phenomena can be again related to polymer melt viscosity and the fragility of IBU. Preliminary studies showed that IBU produces lower values of polymer melt viscosity due to its significant plasticisation effect and it is expected that polymer melt viscosity of 30% < 10% IBU. Additionally the fragility parameter ( $m_1$ ) of IBU ( $m_1 = 60$ ) was close to the border line of strong glass formation i.e.  $m_1 < 70$ .

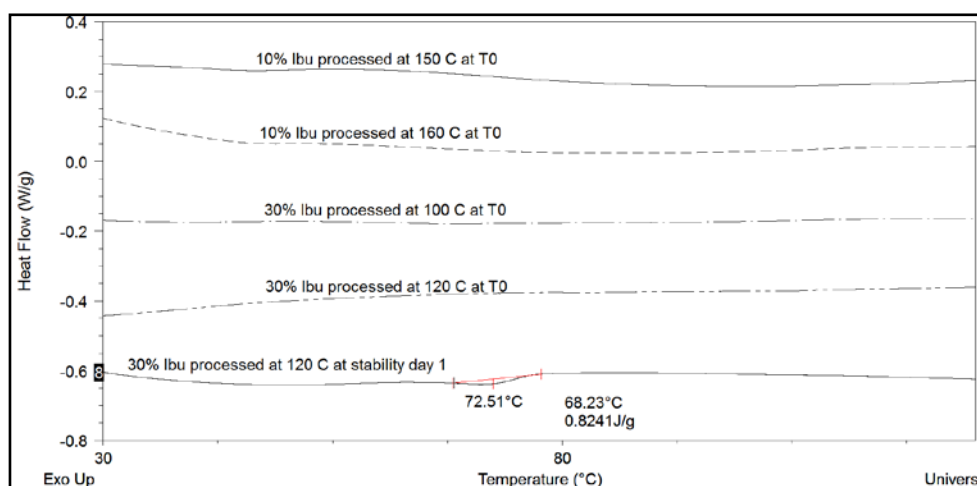


**Figure 4.38: DSC thermograms of blends of Ibuprofen post extrusion.**

### **4.3.2 Polymer melt rheology**

Investigations of melt viscosity not only provide insights of flow properties of materials but also allow judgement about post-process polymer degradation since viscosity is a strong function of molecular weight. Thus, any change in viscosity with respect to shear-temperature and their effects on molecular weight of the polymer can be generalised. Preliminary studies of both polymers suggested chemical changes upon isothermal heating for 30 minutes and these effects might be enhanced with thermo-mechanical forces.

It is important to note that although the residence time more than 15-20 minutes are not generally suggested for pharmaceutical extrusions (Singhal *et al.*, 2011 , Jani, 2015 , Fule and Amin, 2014); materials passing through isothermal zones of temperatures and screw configured shear could produce degradations. Thus, mechanical degradation of the polymer can be expected. These degradations can be probed via rheology comparing data for melt extrudates with that of preformulatory data.

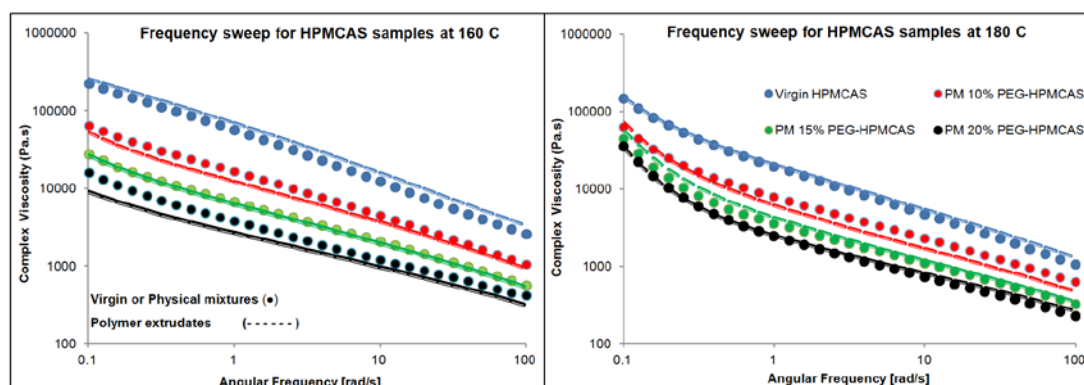
#### 4.3.2.1 *Complex viscosities of pre and post extruded materials*

Previous studies of polymer blends suggested that out of three model plasticisers, TEC and PEG provide better melt stability to both polymers however, due to the possibility of evaporation of liquid TEC at the higher extrusion temperatures, PEG blends were considered as a choice of plasticiser for HME processing hence discussions are restricted to the studies of PEG blends.

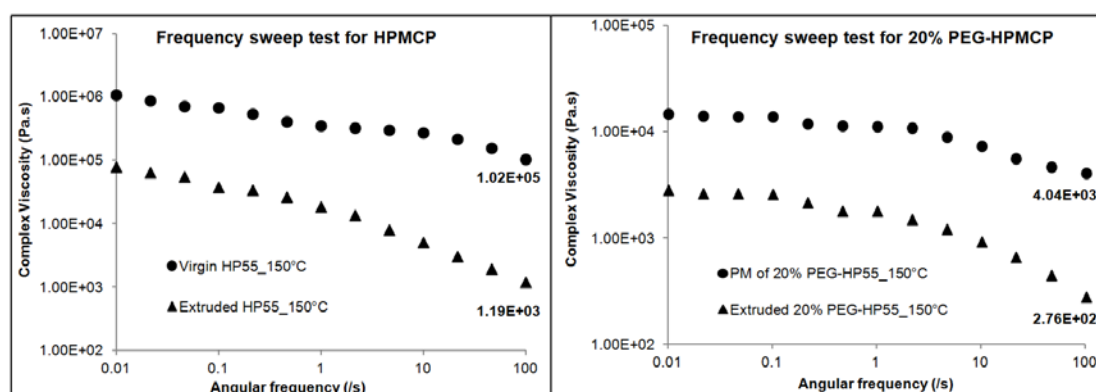
Complex viscosity of pure and blended polymers (with PEG) was investigated against melt extruded polymers. In all cases, the residence time of extrusion of virgin and blends of polymers was observed to be less than 15 minutes. Strands of extrudates were pelletised and subjected to frequency sweep tests. Figure 4.39(a) shows a comparison of viscosities for HPMCAS and its PEG blends pre- and post-extrusion. It was observed that the viscosity values of HPMCAS and its blends were comparable at the investigated temperatures from 150-180 °C and viscosity measurements at 0.1-100 rad.s<sup>-1</sup> were also found to be similar. Generally, the viscosity values of polymer melt in their pre- and post-extrusion forms exhibit differences in values however; differences will be small unless materials show thermal or mechanical degradation during extrusion (Crowley *et al.*, 2004 , Elaine Kenny, 2013). From figure 4.39 it can be seen that pure and blends of HPMCAS polymers

were relatively stable post extrusion process, producing similar complex viscosity values at all processing conditions. Further, it is worth to mention here that despite the use of a plasticiser, it was initially assumed that pre and post extrusion complex viscosities would vary significantly since intensities of shear rate and stresses involved in the case of HME are significantly higher than that of the frequency based tests of rotational rheometer. However, the values of both sets of samples lie within 0.5 - 1% proximity. Thus, mechanical degradation was speculated to be minimal in terms of bulk rheology.

Similar results were obtained with the blends of Ibuprofen and mechanical degradation of these samples was again shown to be minimal.



(a)



(b)

**Figure 4.39: Complex viscosity comparison between of pre and post processed materials of (a) HPMCAS and (b) HPMCP.**

Compared with the above samples, virgin and extrudate of HPMCP showed notable viscosity differences (Figure 4.39b). Polymer melt viscosity of

virgin HPMCP at 150 °C at the angular frequency of 100 rad/s produced a value of  $1.2 \times 10^5$  Pa.s whereas melt extrudates (from 150 °C trial) gave  $1.19 \times 10^3$  Pa.s. These results indicated that the viscosity values of the virgin HPMCP-HP55 after extrusion were 100 times lower than before extrusion at both higher and lower shear rates (Figure 4.39b). Additionally, the viscosity differences between blends of HPMCP pre- and post-extrusion reduced with increase in the concentration of PEG. For instance, the viscosity gap between physical mixtures and extrudates of 20% PEG differed by 10 times compared to 100 times for the pure polymer (Figure 4.39b). However, still the values between blends of pre-post samples were significantly higher compared with HPMCAS samples thought to be a result of thermal or mechanical degradation. Nevertheless, PEG not only aids processing of HPMCP at lower temperature by reducing melt viscosity but also provides a stabilising effect since the difference between pre- and post- process viscosities of pure polymer was reduced.

To investigate this effect, melt viscosities of HPMCP were further investigated for reduced complex viscosity (see equation 4.19).

$$\eta_{reduced} = \frac{\eta}{\eta_0} \quad \text{Equation 4.19}$$

The reduced complex viscosity of HPMCP and its blends when compared at 150 °C, the decay rate of the plasticised polymer was observed to reduce significantly over the shear rate of 0.01 to 100 s<sup>-1</sup>. It was noted that the viscosity of pure polymer reduces to 50% at 0.1 rad/s whereas with 10, 15 and 20% blends, it requires approximately 1, 5 and 7 rad/s angular frequencies. Further, a comparison between the slopes of these samples produced an order, 20%PEG-HP < 15%PEG-HP < 10%PEG-HP < HPMCP (Figure 4.40) confirming this stabilising effect of PEG on HPMCP polymers.

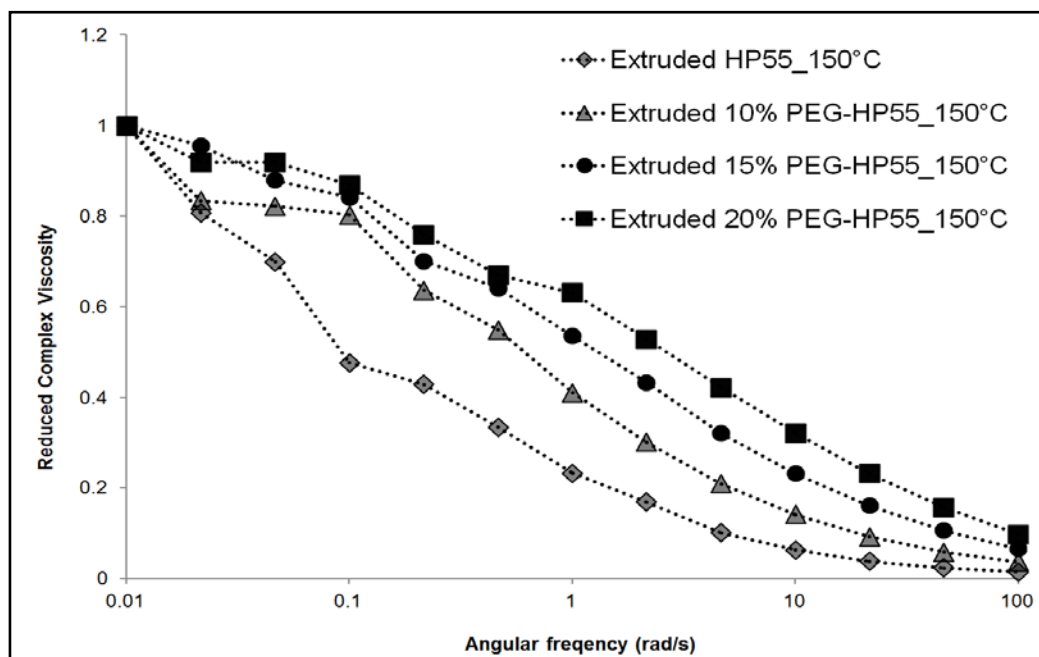


Figure 4.40: Decay rates of polymeric samples.

#### 4.3.3 Thermo-chemical stability of melt extrudates

Chemical incompatibility of excipients or chemical reactions of degradation products of API and/or excipients producing lethal effects have been known to the pharmaceutical world for a long time (Wu *et al.*, 2011b , Wyttenbach *et al.*, 2005 , Bharate *et al.*, 2010). Thus, regulatory bodies across world demand communications from formulators to report every single interaction of API(s) occurring within the formulation, making sure of the safety and efficacy of the product. Over the years, these interactions have mainly focused on degradation products of the API however; recently developments in WHO and ICH guidelines, quantification of degradation products of excipient and their interactions with APIs are highly encouraged (WHO, 2009). Moreover, the European Medicine Agency (EMA) has recently raised concerns about certain phthalate derivatives such as "Dibutyl phthalate (DBP), Diethyl phthalate (DEP), Polyvinyl acetate phthalate (PVAP), Cellulose acetate phthalate (CAP) and HPMCP" for their use in food products as well as in pharmaceutical dosage forms (European-Medicines-Agency, 2014) due

to their possible toxicity profiles. According to the EMA, DBP and DEP have shown human toxicological effects related to the reproductive system and thus, EMA has capped their maximum exposure limit in their latest guidelines. Further, it was also noticed that although till this date EMA has not suggested any restrictions over the usage of HPMCP in pharmaceutical formulations, evaluation of degradation products of HPMCP during extrusion should be strongly pursued since the probability of its degradation is highest in HME.

To investigate this, the degradation products of the pure polymer post-extrusion were investigated and a quantitative estimation with respect to temperature and shear was mapped. Then, chemical incompatibility studies between blends of Chlorpropamide-Polymer (with/without plasticisers) and Ibuprofen blends were investigated extensively. These properties were outlined by means of HPLC, FTIR, NMR and GC-MS techniques.

#### *4.3.3.1 Structural elucidation of degradation product (publication I)*

Polymer melt extrudates, processed at a range of temperatures were subjected to a previously developed-validated HPLC method and respective degradation products: acetic acid (AA), Succinic acid (SA) and Phthalic acid (PA) were screened along with other degradation products. In all cases, AA, SA and PA peaks were noted in HPLC analysis however; the extrudates of HPMCP produced a well-resolved, non-interfering peak of an unknown impurity (Figure 4.41) at 8.3 minutes. The unknown impurity was observed repeatedly in all HME samples but not in the virgin polymer.

Previous reports of HPMCP degradation have not discussed any such impurity other than PA. Hence an experiment was conducted where the influence of temperature alone (isothermal effect) was checked for appearance of this unknown compound. Isothermally heated samples of

HPMCP were subjected to HPLC studies and resulted in producing the same unknown impurity at 8.3 minutes. Therefore, endeavours were made to recover and elucidate the unknown impurity of HPMCP.

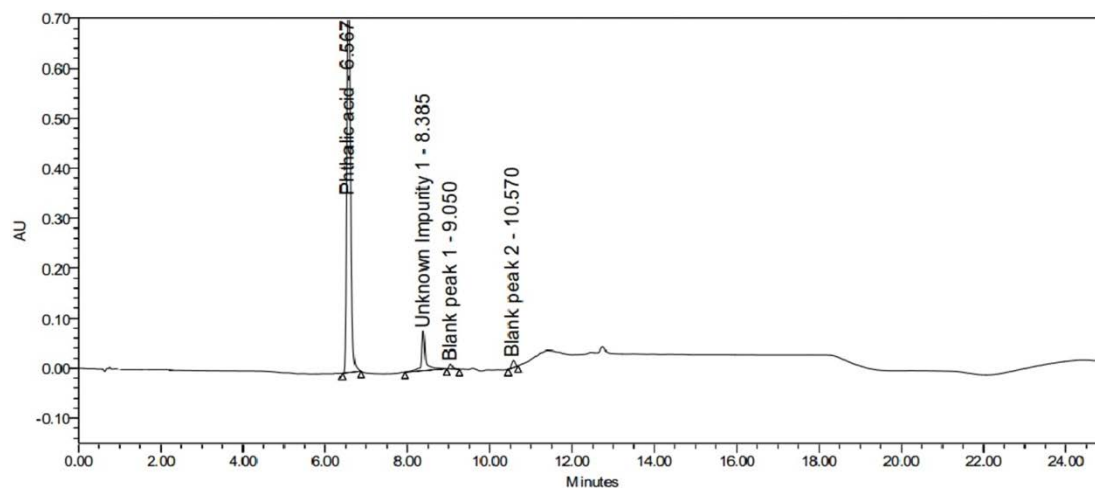


**Figure 4.41: HPLC chromatogram of HPMCP polymer extrudates.**

To extract the unknown impurity (Cryst-A), a procedure mimicking preparative HPLC (Vasu Dev *et al.*, 2009) was initially used however, the quantity of Cryst-A so obtained was too low to elucidate and quantify. Therefore, another approach was utilised. Since, isothermally heated samples of TGA showed the presence of an unknown impurity, in one of the attempts of extracting Cryst-A, HPMCP (~0.50 g) was kept in different sets of glass vials covered with aluminium foil and independent samples were heated for over half an hour in an oil bath to different temperatures from 150-200 °C with an increment of 10 °C. Colourless crystals were observed to be deposited at the mouth and inner side of each glass vial (Figure 4.42a). Generation of these crystals was thought to be vapour phase condensed crystals of PA and when subjected to HPLC analysis, the retention time of vapour phase condensed crystals matched with that of Cryst-A. Thus, extraction of Cryst-A was believed to be successful. In order to maximise production of the Cryst-A, HPMCP was subjected to a condensation apparatus (Figure 4.42b) and approximately 2 - 3 g of polymeric sample was used at different temperatures

to collect Cryst-A for its structural elucidation. Structural elucidation of Cryst-A was performed using FTIR, NMR, GC and mass spectroscopy.

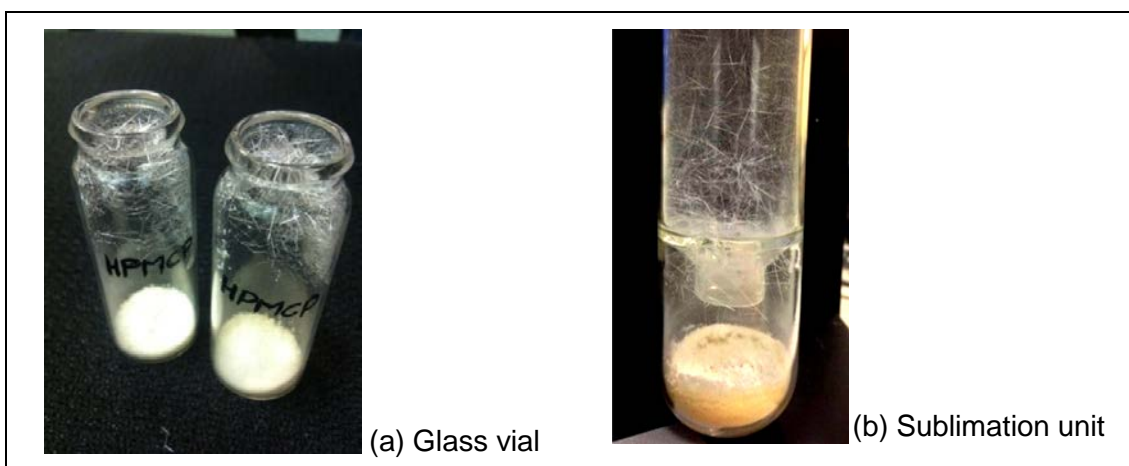


**Figure 4.42: Sublimation product of HPMCP.**

FTIR of the Cryst-A was investigated for its typical characteristic wave numbers and finger print regions which then compared against standard IR absorption values of different sets of functional groups, given in different textbooks (Larkin, 2011 , Stuart, 2005b , Stuart, 2005a). Initially FTIR of Cryst-A was compared against standard crystals of PA to investigate similarities or dissimilarities between the two compound spectra. IR of Cryst-A showed strong absorption peaks of alkane-alkene stretching bending values along with carbonyl (C=O) stretching peaks. The FTIR spectrum of Cryst-A showed intense peaks at 1761, 1792 and 1853  $\text{cm}^{-1}$  indicating the presence of a carbonyl (-C-O-O-C) functional in the structure (Figure 4.43). Moreover, the characteristic stretching and bending vibrations of alkenes were recorded at 1359 and 1365  $\text{cm}^{-1}$ . However, when the fingerprint region of the Cryst-A was considered based on the strong peak at 906  $\text{cm}^{-1}$  the structure was speculated to possess an anhydride functional group (C-O-C group).

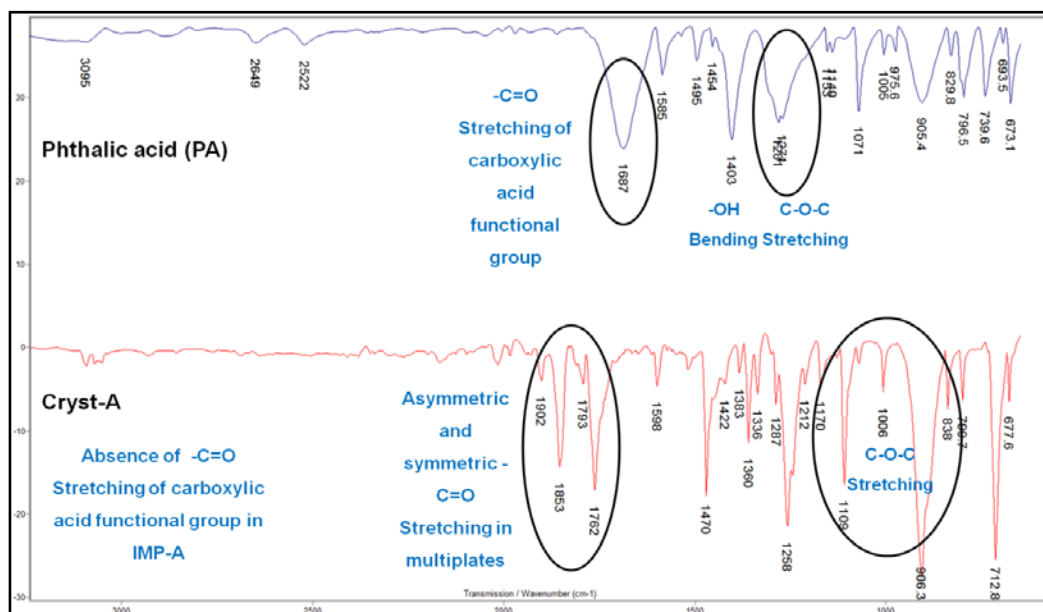


**Figure 4.43: Infra Red spectroscopy of Cryst-A.**

Further, both Cryst-A and PA were subjected to proton ( $^1\text{H-NMR}$ ) and carbon NMR ( $^{13}\text{C-NMR}$ ) spectroscopy. The compounds were dissolved in acetone- $d_6$  (deuterated-acetone) and scanned for 128 as well as 1024 spins for  $^1\text{H-NMR}$  and  $^{13}\text{C-NMR}$  respectively. Figure 4.44 represents typical  $^1\text{H-NMR}$  spectra of both compounds. In the case of Cryst-A, multiplicities in chemical shifts were recorded in the range of  $\delta$  7.9 to 8.13 ppm which is the characteristic region of aromatic protons. Similarly, values were recorded for PA where the characteristic chemical shifts of aromatic protons, particularly, protons associated with carbons C3, C4, C5, C6 of PA was observed between  $\delta$  7.6 to 7.86 ppm (Figure 4.44). When compared, these chemical shifts were marginally separated however clear distinctions between the two components were noted suggesting the different chemical nature of the two compounds. Further,  $^1\text{H-NMR}$  spectra of both PA and Cryst-A recorded a common chemical shift between  $\delta$  2.6 to 2.10 ppm (multiplicity) which was attributed to protons of the acetone- $d_6$  solvent.

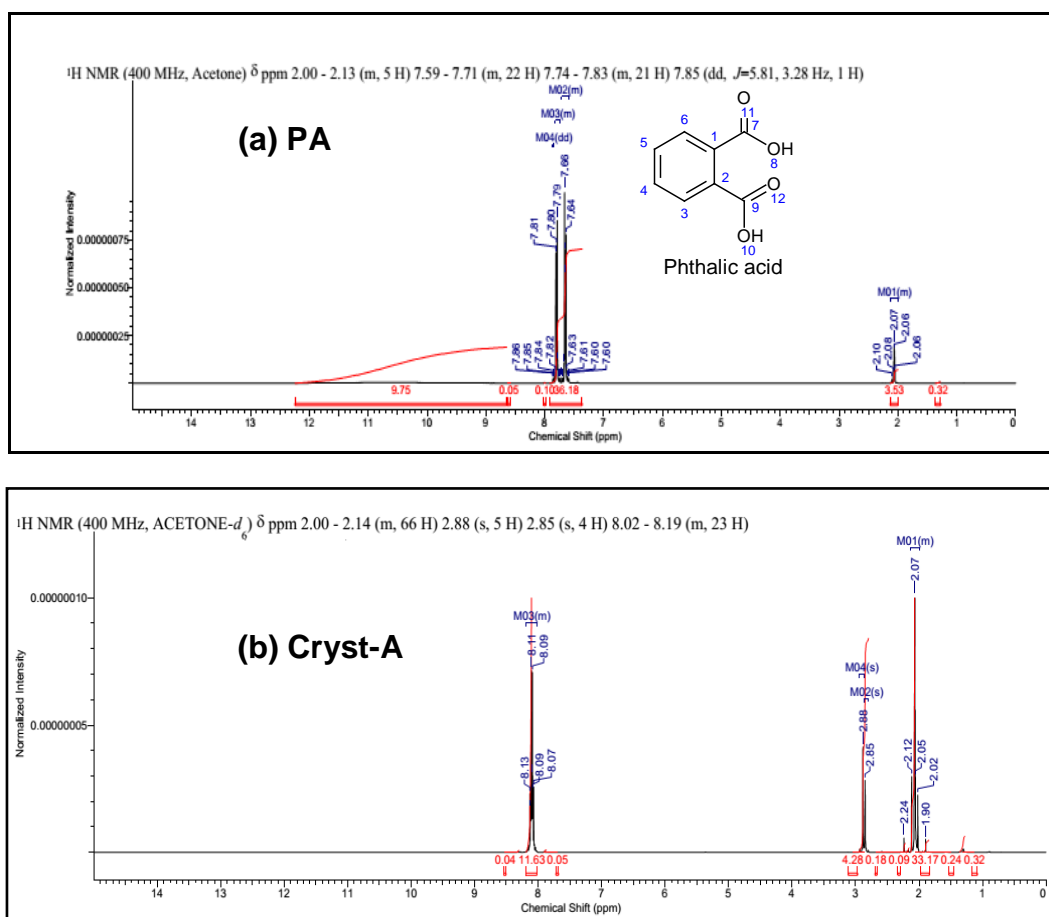


**Figure 4.44: <sup>1</sup>H-NMR spectra of (a) PA and (b) Cryst-A.**

Additionally, a chemical shift was observed at  $\delta$  2.85 ppm (Figure 2b), which was not recorded in the case of <sup>1</sup>H-NMR of PA. This was attributed to the presence of moisture within the acetone-*d*<sub>6</sub>. The NMR sample solution of PA was prepared with freshly opened NMR grade acetone-*d*<sub>6</sub> while the solution of IMP-A was prepared later. It was further confirmed by a blank reading of acetone-*d*<sub>6</sub> itself where the chemical shift at  $\delta$  2.85 ppm was noted. In order to eliminate the error of moisture sensitivity of acetone-*d*<sub>6</sub>, *d*<sub>6</sub>-DMSO solvent was utilised and explanation of these results can be found in the published article (Karandikar et al., 2015).

<sup>13</sup>C-NMR analysis of both compounds showed similarities in their spectra Figure 4.45. Chemically, phthalic acid contains eight carbon atoms where half of them are equivalent in nature. Generally, each unique carbon

produces a separate line in  $^{13}\text{C}$ -NMR spectra however; an equivalent carbon atom present in the structure duplicates and gives the same line. Thus, although PA possesses eight carbon atoms, only four lines were produced in  $^{13}\text{C}$ -NMR (Figure 4.45). Similar to PA, Cryst-A showed four lines with values close to the values of PA however the pattern of both spectra was entirely different indicating that either Cryst-A possesses a similar number of carbon atom as PA or only four carbons are present in the structure.

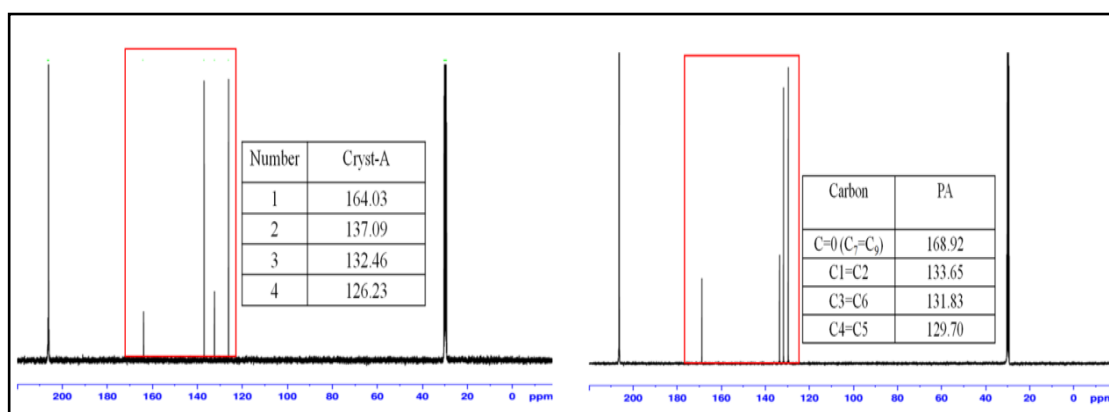


**Figure 4.45:**  $^{13}\text{C}$ -NMR of PA and Cryst-A.

FTIR and NMR investigations suggested that Cryst-A might possess the anhydride functional group and equivalent number of carbon atoms in its structure. Therefore, gas chromatography integrated with mass spectroscopy (GC-MS) was utilised for a precise mass fragmentation pattern of Cryst-A. Cryst-A was dissolved in methanol and subjected for GC analysis. A typical chromatogram of GC is presented in Figure 4.46 showing three characteristic signals at 11, 14 and 16 min in which signal of 14 min was observed with maximum abundance. This signal was attributed to Cryst-A and signals at 11 and 16 minutes were believed to be another two unknown impurities. Thus, mass fragmentation patterns for the individual GC peaks were then analysed.

It was observed that the peak eluted at signal 14 minute possessing mass to charge value ( $m/z$ ) 149, decarboxylated to give a fragment of 104 followed by loss of alkynes moieties to produce a molecular fragment of

benzene ( $m/z=76$ ). When compared, this fragmentation pattern matched with that of phthalic anhydride (PAH) which was confirmed against the standard crystals of PAH. To validate presence of Cryst-A as crystals of PAH, a series of tests were conducted. Initially, a standard PAH solution injected into HPLC produced its retention at 8.3 min exactly at the retention time of Cryst-A and UV spectra of both compounds matched in photodiode array (PDA) detection. Second confirmatory test was performed based on the melting points of both compounds and Cryst-A and PAH produced similar melting points in DSC (MP = 129 -130°C). Thus, Cryst-A was confirmed as a crystal of PAH so two major degradation products, PA and PAH are noted.

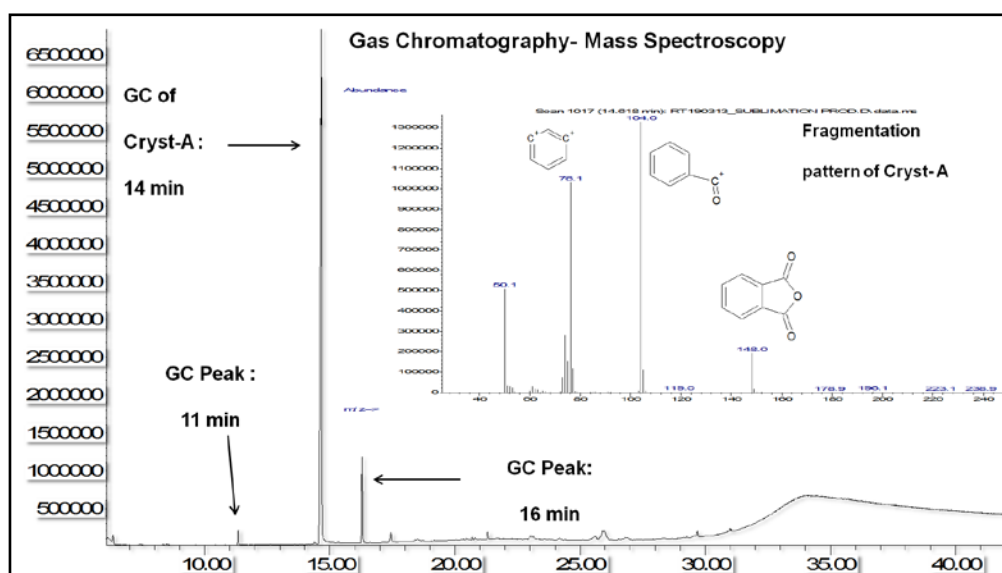


**Figure 4.46: GC-MS of Cryst-A and the fragmentation pathway of Cryst-A.**

Further to these structural investigations, focus then shifted to the two other signals obtained in the chromatogram of GC and their mass fragmentation patterns were studied in detail. Upon comparison with structural data bases, it was found that the two associated impurities were methyl benzoate and phthalic acid dimethyl ester at 11 and 16 min respectively. Appearances of methyl benzoate and phthalic acid dimethyl ester impurities were exceptional in the current study because none of the above analytical techniques except GC-MS showed their presence in the

Cryst-A solutions. Therefore, efforts were made to understand their occurrence in the GC-MS solutions.

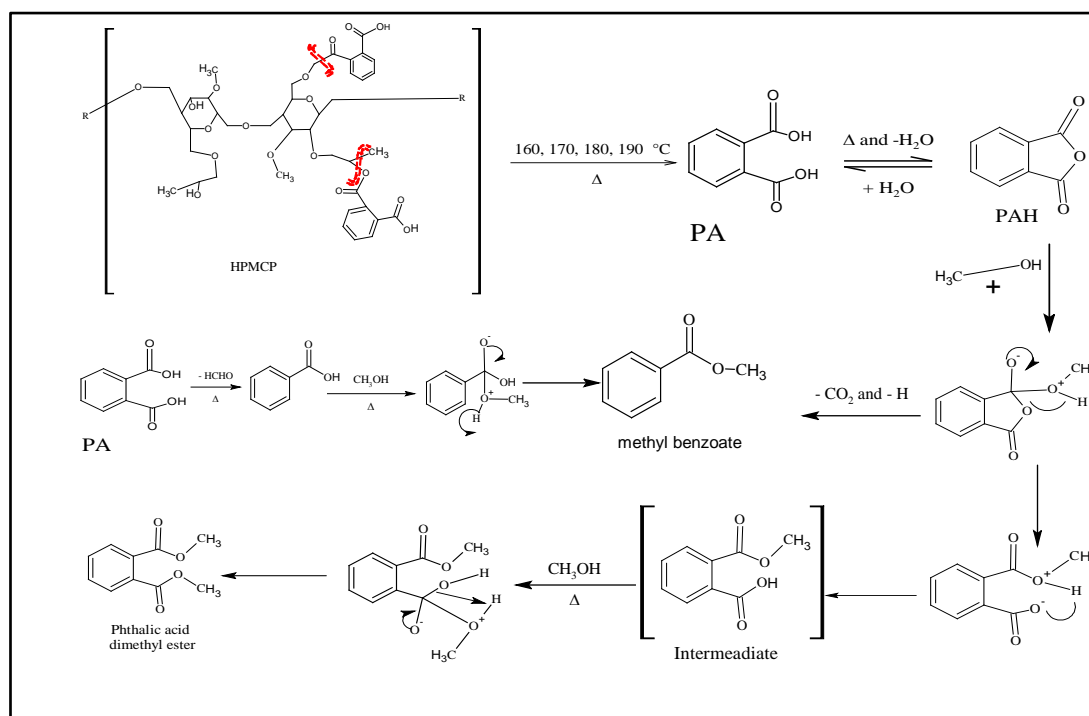


**Figure 4.47: Schematic representation of formation of environmental related impurity below onset degradation temperature of HPMCP.**

From literature reports and the chemical reactivity of PAH, it was noted that PAH is highly sensitive to water and different solvents undergoing various reactions from hydrolysis to ring opening to form its derivatives. Moreover, it can react with different range of alcohols to produce phthalate esters at higher temperatures (Cooksey, 2010). Since during analysis, Cryst-A was dissolved in methanol and heated to more than 200°C prior to injection to gas chromatography, it was speculated that trace amounts of PAH may have reacted with methanol. Formation of these two compounds at the higher temperatures with a limited time of exposure (practically fractions of seconds) clearly indicated the chemical sensitivity of PAH. Since these two impurities were not directly related with thermal degradation of HPMCP, they were termed as 'analytical-environmental related impurities'. Further, it was

observed that these impurities can be formed directly from PA and thus an attempt was made to propose a reaction mechanism of the formation of analytical-related impurities – see Figure 4.47.

Structural elucidation studies of polymer degradation provided important information about all possible degradation products of both polymers during their extrusion within extrusion temperatures of 150-200 °C. Therefore, to quantify these degradation products, the effect of temperature alone (isothermal TGA) and influence of processing (screw speed and temperature) on thermo-chemical stability of polymers was investigated.

#### *4.3.3.2 Thermo-chemical stability: Effect of temperature*

Virgin samples of HPMCAS and HPMCP were exposed to isothermal TGA temperatures between 150-200 °C for 30 minutes and leftover samples from the TGA pans were analysed by HPLC for their respective degradation products. HPLC analysis of thermally exposed samples of HPMCAS did not show AA and SA peaks in the chromatograms however samples of HPMCP did show PA and PAH peaks at all investigated temperatures. During isothermal analysis, HPMCAS recorded marginal TGA weight loss at investigated temperatures. Thus, the absence of AA and SA peak in the samples of HPMCAS was speculated to be result of either their generation below limit of detection of HPLC method or evaporation of these samples (Boiling point of AA > 118 °C) during isothermal heating. Degradation products of HPMCP were further quantified.

Figure 4.48a shows three readings: total weight loss of polymer and quantitative estimations of PA as well as PAH upon isothermal exposure. A linear followed by a nonlinear polymer weight loss was observed between 150 to 180 °C and > 180 °C respectively. However, despite these linear and non-

linear results, the degradation of PA and PAH increased linearly and the sum of two known impurities was observed to be 3.9, 5.6, 7.8 10.1 and 11.4 % at the respective temperatures (Figure 4.48a). A comparison between the sum of percentage impurities of PA and PAH showed an interesting relationship with the total weight loss of the polymer at each temperature measurement. At every temperature, the sum of impurities and total polymer weight loss differed by a factor of 1.5 to 2 indicating that degradation of the polymer must be associated with evaporation of small molecules along with generation of PA and PAH not recorded in HPLC. Thus, the hypothesis of evaporation of small molecules during isothermal heating below HPMCP's conventional degradation temperature seems proven.

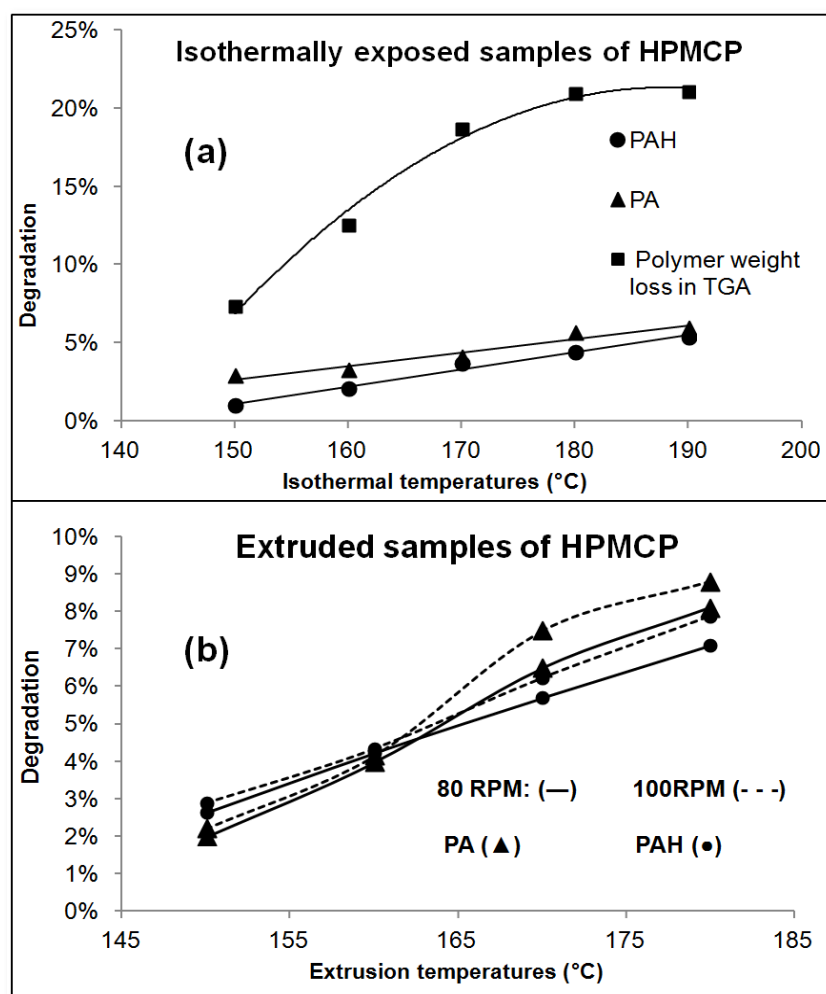


Figure 4.48: Quantification of degradation products of HPMCP.

#### 4.3.3.3 Thermo-chemical stability: Effect of shear and temperature

The combined effect of shear and temperature on polymer degradation was investigated by processing polymers at two screw speeds (80 and 100 rpm) over the maximum barrel temperatures (150 - 180°C). Figure 4.48b shows effect of screw speed on degradation of HPMCP polymer. Degradation of HPMCP into PA and PAH increased when the screw speed of extruder was changed from 80 to 100 rpm suggesting impact of shear on the degradation of polymer. Moreover, at lower extrusion temperatures (150 to 170 °C) and at the same screw speeds, the percentage degradation of PA < PAH while at the higher temperatures (180 and 190 °C) percent degradation of PA > PAH (Figure 4.48b). Similar studies were performed for HPMCAS polymer with a marginal difference between acidic contents of AA and SA noted (Table 4.16). Thus, thermo-mechanical stability of HPMCP was found poor compared to HPMCAS.

**Table 4.16: Degradation products of polymers upon extrusion.**

Extrusion temperatures (°C)	Phthalic acid		Phthalic anhydride		Acetic acid		Succinic acid	
	80 rpm	100 rpm	80 rpm	100 rpm	80 rpm	100 rpm	80 rpm	100 rpm
150	1.99%	2.20%	2.62%	2.89%	0.10%	0.10%	0.49%	0.50%
160	3.98%	4.16%	4.23%	4.35%	0.13%	0.13%	0.46%	0.46%
170	6.50%	7.50%	5.70%	6.23%	0.13%	0.13%	0.47%	0.47%
180	8.10%	8.80%	7.10%	7.89%	0.13%	0.13%	0.46%	0.47%

#### 4.3.3.4 Drug-polymer chemical compatibility studies during HME

Chemical compatibility studies of HPMCAS and HPMCP with the model API containing free reactive functional groups is discussed in this section.

Degradations of API during shear and temperature fields encountered in HME are generally reported in the literature (Crowley et al., 2007b , Repka et al., 2007). However, the influence of these forces on excipients forming excipient's degradation products and their reactions with API are rarely studied. While estimation of API degradations during processing is mandatory, estimation of potential chemical interactions between excipient-API or degradation products of the excipient and API during extrusion should also be studied. More importantly such studies should be performed with the excipients such as HPMCAS and HPMCP, where acidic degradation products can possess the ability to react with analytical solvents but can also react or deteriorate the chemical structure of an API.

So far only one report has been published in the literature which suggest potential incompatibility of HPMCAS during HME (Zedong Dong and Choi, 2008). To investigate more such studies two model drugs having different free functional groups were studied. Based on these studies, suitability of these polymers with the chemical analogues of these API is also discussed.

- Chemical incompatibility: Zedong Dong and Choi (2008) paper discussion

A chemical incompatibility of HPMCAS with the API containing free hydroxyl group was investigated by Zedong and co-worker (Zedong Dong and Choi, 2008). According to the authors, it was hypothesized that degradation of HPMCAS resulting in production of succinic acid (SA) would react with the free hydroxyl group of the API and esters of SA-API will be generated. The authors performed two experiments: firstly, physical mixtures of SA and API were subjected to oven temperatures at 140 °C for an hour and samples were analysed by LC-MS. In the second experiment, the powdered extrudates were stored in an oven at 140 °C and samples were analysed in LC-MS at the

intervals of zero, first, third and fifth hours. During the analysis of first experiment, the authors confirmed the formation of an esterification reaction between the virgin SA and the API. However, when similar studies were conducted for melt extrudates samples investigated at the interval of zeroth hour did not form ester derivatives while samples investigated at the rest of time intervals produced ester derivatives.

It is important to note that despite these important communications, the report was observed to be seriously limited especially in terms of temperature conditions at which the post extrudate samples were stored. The incompatibility studies carried out in their research clearly suggested that melt extrudates did not produce any incompatible reactions at the initial stages (zeroth time point) and the temperature (140 °C) at which these extrudates were stored is indeed impractical to investigate post extrusion stability studies. Conversely, from these observations one can debate that esterification reaction between degradation products of HPMCAS and API would occur only when residence time of their extrusion exceeds > 1 hour. However, this report hints at a possible outcome of chemical incompatibility reactions during extrusion.

- Extrusion studies with model APIs: Chlorpropamide and Ibuprofen

Considering the facts of the above study, a new study was designed where two model APIs: ibuprofen and chlorpropamide were selected. Being BCS class II drugs, apart from their solubility studies, chemical compatibility with the cellulose ester derivatives was specifically focused on since these two model APIs contains free chemical functional groups which may take part in reactions during HME. Moreover, although both IBU and CPM have been on the market for quite a long time, chemical compatibility of IBU during melt extrusion has been sparsely studied (Fathy, 2006 , Heintz, 2014) while, to the

author's knowledge, extrusion studies of CPM have not been conducted despite its inclusion in the patents of hot melt extruded pharmaceutical dosage forms (McGinity, 2002 , Crowley et al., 2007a)

Physical mixtures of chlorpropamide (CPM) with HPMCAS and HPMCP were prepared in the ratio of 1:4 w/w (API: polymer) by grinding in a mortar and pestle while 10 and 30% Ibuprofen mixtures (w/w) were prepared for chemical incompatibility studies. These mixtures were further extruded at the set temperatures given in the experimental section. In all cases, the residence time observed to be less than 10 minutes. The chemical incompatibilities of API-polymer extrudates (CPM and IBU) was investigated for percentage API assay, impurity qualification-quantification and potential chemical incompatible reactions during the extrusion process by means of HPLC and GC-MS.

For CPM, the melting point of the API was observed to be in the range of 123 - 128 °C. Literature reports suggest that CPM has 5 polymorphs (forms I to V) where form III is the commercially available form as used in the current investigation (Drebushchak et al., 2008 , Popescu et al., 2009). The DSC thermogram of CPM showed 2 melting endotherms at 124 and 128 °C whereby form III converts to form I and melts at 128 °C (Figure 4.49) (Drebushchak et al., 2008). Moreover, the onset degradation temperature of CPM was observed to be in the range of 155 to 170 °C where the isothermal weight loss of HPMCP was noted. Therefore, melt extrusion of CPM was performed between 130 to 150 °C and HPLC analysis performed. USP monograph suggests that CPM is associated with 2 related impurities, Impurity A (4-chlorobenzenesulfonamide) and Impurity B (1,3-dipropylurea) (USP-29) and these two were also monitored by HPLC.

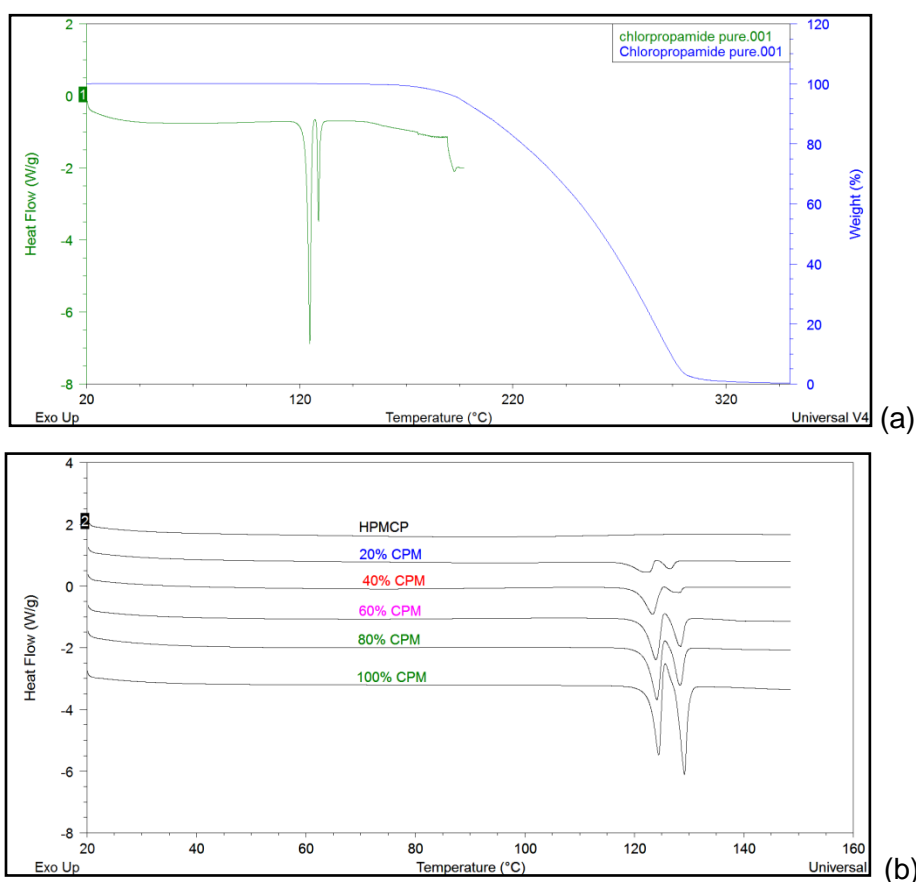


**Figure 4.49: (a) Thermal properties of CPM (b) components miscibility by DSC.**

Blends of CPM were investigated on the same platform of quantitative estimation of degradation products of HPMCP. During analysis, a solution containing known concentrations of AA, SA, PA, PAH, Impurity A&B and CPM was injected into the HPLC and quantitative estimations were carried out against these known concentrations. A comparison between a standard solution, physical mixture, thermally exposed and melt extruded samples of CPM-HPMCP is presented in the Figure 4.50. A physical mixture of 20% CPM in HPMCP and HPMCAS was initially investigated for its mixture uniformity. From table 4.17 and 4.18, it can be seen that physical mixtures of CPM with HPMCP and HPMCAS produced assay values 95.45 and 98.66% respectively without the appearance of unknown peaks in the HPLC chromatogram. This clearly indicated that content uniformity as well as miscibility of CPM with both polymers was reasonable as confirmed by

crossed check against its DSC thermograms (Figure 4.49b melting point depression).

Similar to the untreated physical mixtures, when TGA exposed samples were investigated by HPLC a significant amount of known and unknown peaks were recorded with increase in temperature. For instance, TGA exposed samples of 20% CPM-HPMCP produced known impurities (PA, PAH and CPM-impurity A) at their respective retention time (Rt) whereas four unknown impurities were recorded at 9.8, 10.8, 11.6 and 13.8 minutes respectively. It was noted that the sharp peak of CPM was split into two with increase in temperature and impurity at Rt 11.6 min and also increased significantly with increase in temperature (Figure 4.50a). Similar results were obtained with HPMCAS samples where unknown peaks were noted at 10.8, 12.2 and 12.6 minutes without the appearance of AA, SA peaks and most importantly peak doubling was not recorded with CPM-HPMCAS samples.

Melt extruded of similar mixtures were subjected to HPLC and degradation products of both materials were studied as shown in Figure 4.50 and Figure 4.51 for CPM-HPMCP and CPM-HPMCAS respectively.

In the case of CPM-HPMCP samples, melt extrudates of CPM-HPMCP provided unknown impurities at Rt 9.5, 10.8, 13.8 min (Figure 4.50b) whereas melt extrudate samples of CPM-HPMCAS produced new unknown impurities. Quantitative analysis of the API as well as impurities was calculated for percentage assay values. Table 4.17 and 4.18 show calculated values for percentage drug and impurity profiling of CPM with different blends.

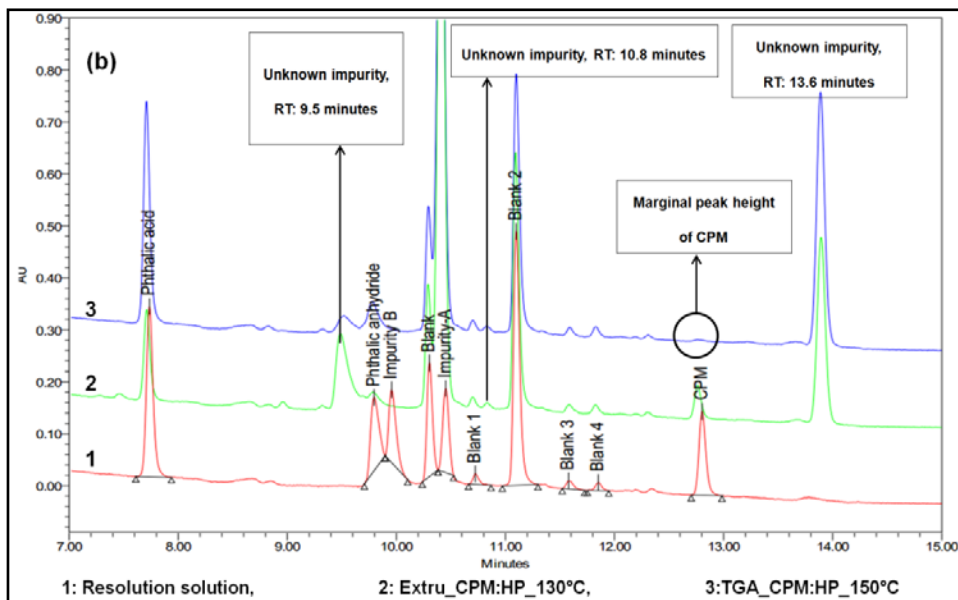
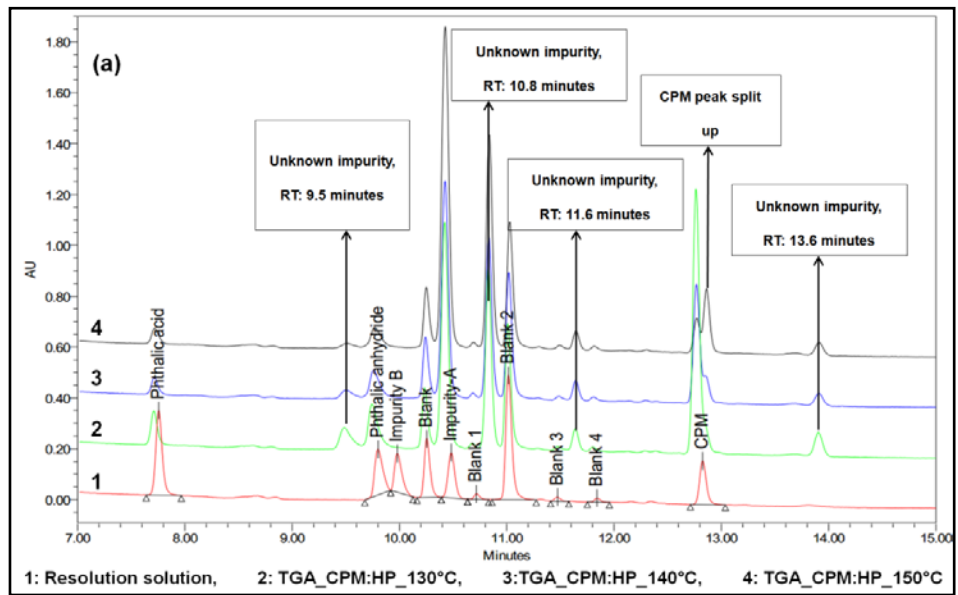


**Figure 4.50: Chromatograms of CPM-HPMCP (a) TGA (b) Melt extrudates.**

Interesting observations were noted upon comparing the results of melt extrudates against TGA samples of CPM blends. Firstly, CPM-HPMCP is discussed for which significant process dependent degradations were noted. Assay of CPM dropped from 29 to 2 % in the TGA exposed samples while melt extrudates of the same mixtures over the range 130 - 150 °C produced assay of 3 to 0.5% (Table 4.17). Further, unknown impurities at Rt 9.5 and 13.8 minutes decreased from 3% to 0.9% whereas the impurity at 10.8

minutes increased from 16% to 24% with increase in TGA temperature (Figure 4.50a). While melt extrudates of CPM-HPMCP investigated for unknown impurity at Rt 9.5 decreased from 13 % to 2 % and impurity at 13.8 minutes increased from 24 to 36 % while the impurity at 10.8 minutes remained relatively constant between 0.45 and 0.48 % with increase in extrusion temperatures. TGA exposed samples of CPM exhibited the peak split phenomenon in HPLC chromatograms however, the melt extrudates of the same samples did not show this. Moreover, with increase in extrusion temperature, peak height of CPM reduced significantly and at maximum extrusion temperature, marginal CPM peak was noted indicating complete degradation of an API during processing (Figure 4.50b and Table 4.17).

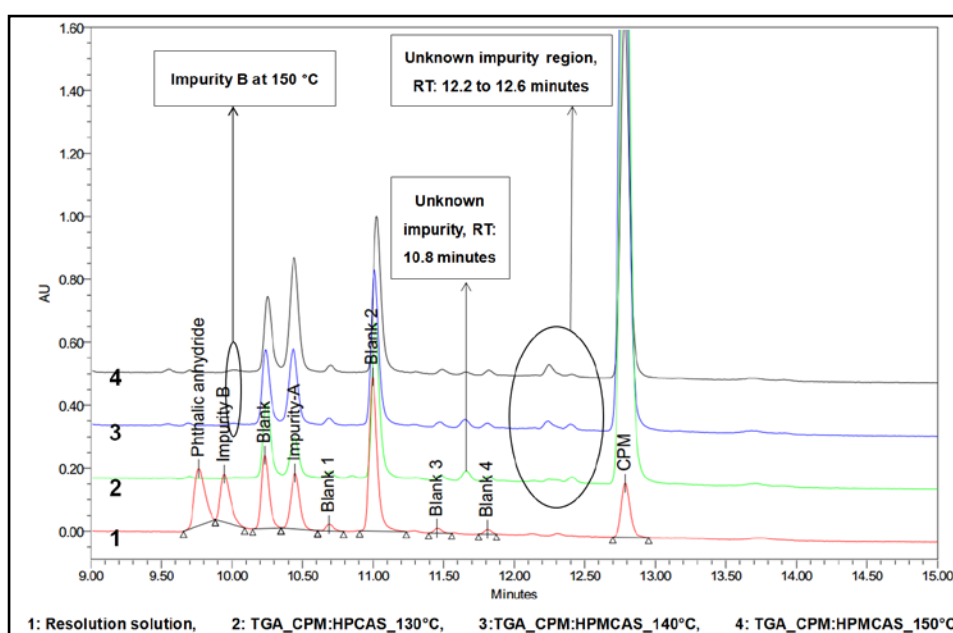


**Figure 4.51: Chromatograms of TGA exposed CPM-HPMCAS.**

Similar to the CPM-HPMCP mixtures, quantitative estimation of CPM-HPMCAS was carried out. It was illustrated that percentage assay of CPM in thermally exposed samples of HPMCAS mixtures was reduced from 55 to 48% from 130 to 150 °C treated samples whereas extrusion carried out in the same temperature range produced assay drop from 48 - 25 %. Moreover, it was noticed that samples of CPM-HPMCAS produced fewer unknown

impurities and their percentage content was significantly lower than unknown impurities of HPMCP (Table 4.17 and 4.18). The sum of unknown degradation products obtained with HPMCAS mixtures was found to be 1/10th of that of HPMCP mixtures and thus, incompatible reactions of CPM with HPMCAS were speculated to be lower compared with HPMCP.

**Table 4.17: HPLC analysis CPM-HPMCP samples.**

Name	CPM (%)	CPM-A (%)	PA (%)	PAH (%)	Total Unknown impurities (%)
PM_CPM: HP55	95.45	0	2.22	0.5	0
TGA_CPM:HP55@130 °C	28.91	21.32	1.87	5.21	24.55
TGA_CPM:HP55@140 °C	12.87	29.65	1.41	5.17	29.09
TGA_CPM:HP55@150 °C	1.89	38.5	1.23	3.41	34.44
Extru_CPM-HP55@130°C	3.54	71.09	4.81	1.055	38.9
Extru_CPM-HP55@140°C	1.51	73.34	10.71	3.03	39.43
Extru_CPM-HP55@150°C	0.5	70.91	12.68	4.94	40.92

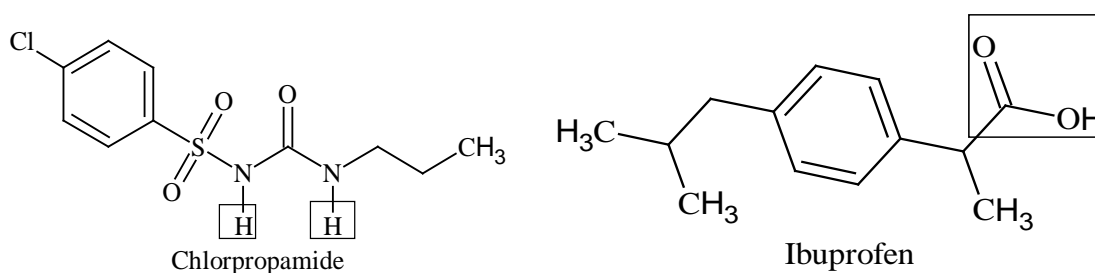


**Figure 4.52: Chemical structure of Chlorpropamide and Ibuprofen**

Further, an important observation noted in these mixtures was the presence of CPM impurity B. CPM-B was recorded in the case of HPMCAS samples especially at higher temperatures of 140 and 150 °C in both heating techniques while, in the case of the HPMCP samples, this impurity was not recorded at all. Thus, it was thought that generation of CPM-B was either

inhibited by HPMCP or that this impurity may have reacted with PA or PAH producing further unknown impurities.

**Table 4.18: HPLC analysis CPM-HPMCAS samples.**

Name	CPM (%)	CPM-A (%)	CPM-B (%)	Total Unknown impurities (%)
PM_CPM:LG	98.66	0	0	0
TGA_CPM:LG@130 °C	55.76	2.73	0	1.27
TGA_CPM:LG@140 °C	50.46	4.72	0.43	1.73
TGA_CPM:LG@150 °C	46.46	13.74	1.8	2.66
Extru_CPM-LG@130°C	48.03	18.65	0	1.88
Extru_CPM-LG@ 140°C	43.65	30.45	0	2.45
Extru_CPM-LG@150°C	25.64	43.31	1.73	6.14

Quantitative estimation of assays of percentage drug and impurity profiling provided valuable information about drug-polymer interactions and the effects of processing parameters on chemical stability of polymeric samples. Occurrences of known impurities of polymer and API clearly indicated that both materials degrade between 130-150 °C. Nonetheless, occurrence of unknown impurities in these samples was indicative of chemical interaction between the two components. It was thought that formations of unknowns are attributed to two conditions: (a) degradation of CPM into its small molecular fragments or (b) thermally assisted chemical reactions between degradation products of individual materials forming new compounds. To investigate the first possibility, TGA exposed samples of pure CPM were subjected to HPLC analysis and except for impurity A (4-chlorobenzenesulfonamide), other peaks were not recorded in HPLC. Thus, the formation of unknown compounds due to degradation of CPM into its small molecular fragments (except impurity-A) was eliminated. It was also

found that the thermal stability of CPM was compromised at the higher temperatures of TGA (140 and 150 °C) proving that impurity-A is a thermal degradation product of CPM.

HPLC analysis of TGA treated samples and extrudates of CPM provided valuable information about quantification of degradation products of both an API and polymers. DSC studies suggested that CPM will be miscible with the polymer (Figure 4.49b) and CPM will act as plasticiser (in the case of HPMCP) during melt extrusion due to its lower melting point than T<sub>g</sub> of HPMCP. Moreover, CPM possess 2 free hydrogen and 3 oxygen atoms which can take part in hydrogen bond interactions with acceptor (H sites) and donor sites (O sites) of HPMCAS and HPMCP aiding in the stability of the dispersion (Figure 4.52). Thus, it was speculated that degradation of polymer itself will reduce and probability of generation of impurities will also reduce. However, by looking at the assay values of CPM and percentage unknown impurities, the assumptions of reductions in degradation differed noticeably. Moreover, production of large quantities of unknown compounds during extrusion of CPM was indeed alarming for its suitability in melt extrusion as well as with these polymers. Hence investigations elucidating these unknown impurities using GC-MS were conducted.

A GC-MS spectrum of extrudates of CPM-HPMCP is shown in Figure 4.53 showing seven well resolved peaks in the chromatogram. These peaks were analysed for their fragmentation patterns and compared against the standard data base of NIST (NIST, 2011). Upon GC-MS, Benzoic acid methyl ester (R<sub>t</sub> = 7.6 minutes), Phthalic acid (R<sub>t</sub>: 10.89 minutes), Methyl, 4-amino-3-methoxybenzoate (R<sub>t</sub> = 11.89 minutes), N-n-Propylphthalimide (R<sub>t</sub> = 14.03 minutes), CPM-A (R<sub>t</sub> = 15.8 minutes), Dimethylphthalate (R<sub>t</sub> = 16.9 minutes) and Phthalic acid-diamide, N,N'-diisopropyl (R<sub>t</sub> = 19.7 minutes) were noted

(Figure 4.54a). Similarly, melt extrudates of CPM-HPMCAS were also analysed and GC spectrum of the sample is presented in Figure 4.53b. The GC spectrum of CPM-HPMCAS produced six well resolved peaks and GC-MS studies (Figure 4.54b) revealed the presence of succinic anhydride (Rt = 6.39 minutes), succinic acid dimethyl ester (Rt = 6.66 minutes), succinic acid, monomethyl ester (Rt= 7.9 minutes), N-propylsuccinimide (Rt = 9.4 minutes), N-n-Propylphthalimide (Rt = 13.91 minutes) and CPM-A (Rt = 15.8 minutes).

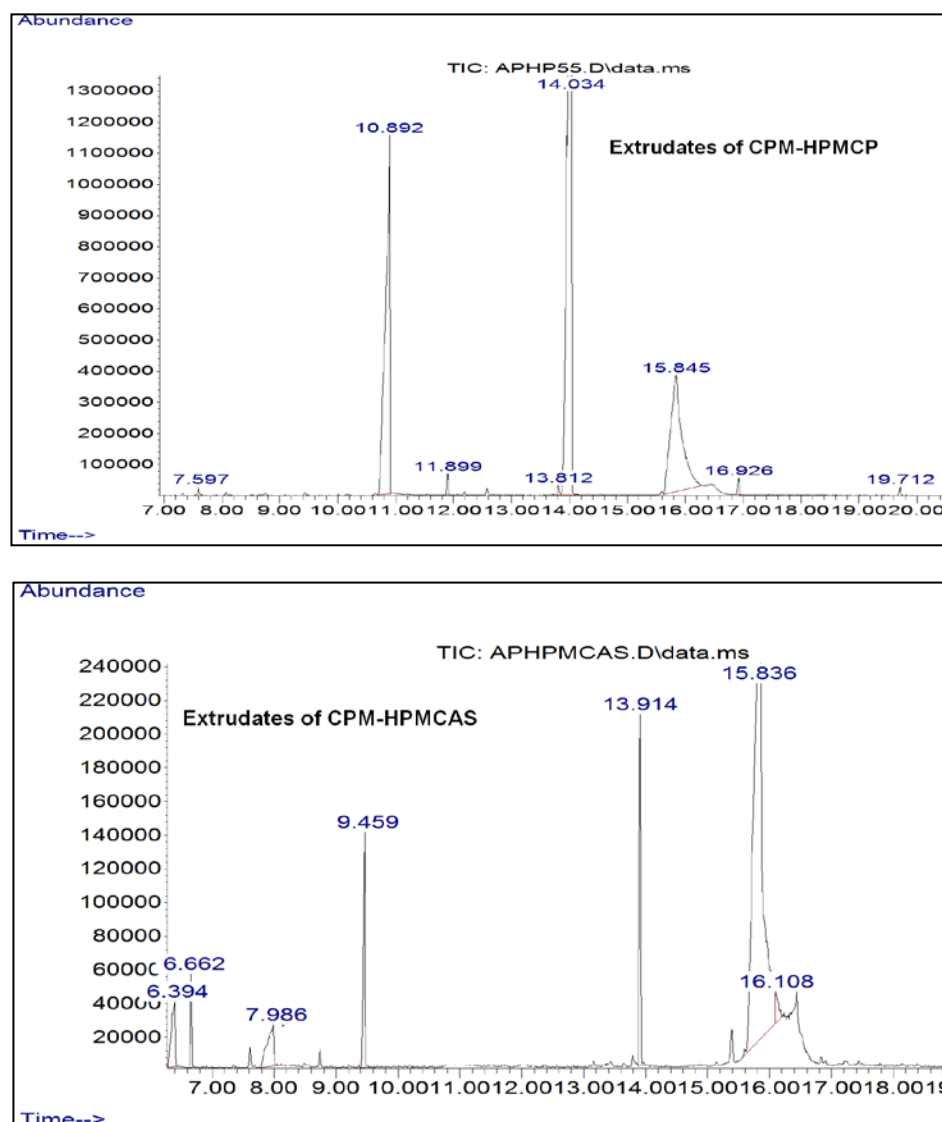


**Figure 4.53: GC spectra of extrudates of CPM.**

Structural elucidation of unknown impurities of CPM-HPMCP and CPM-HPMCAS by GC-MS provided critical information about degradation products

and chemical reactions between the degradation products of both API-polymers. However, since the current studies were not only limited to distinguish degradation products of these melt extruded system, discussions related to the degradation mechanism of CPM and mechanism of unknown formations were further extended.

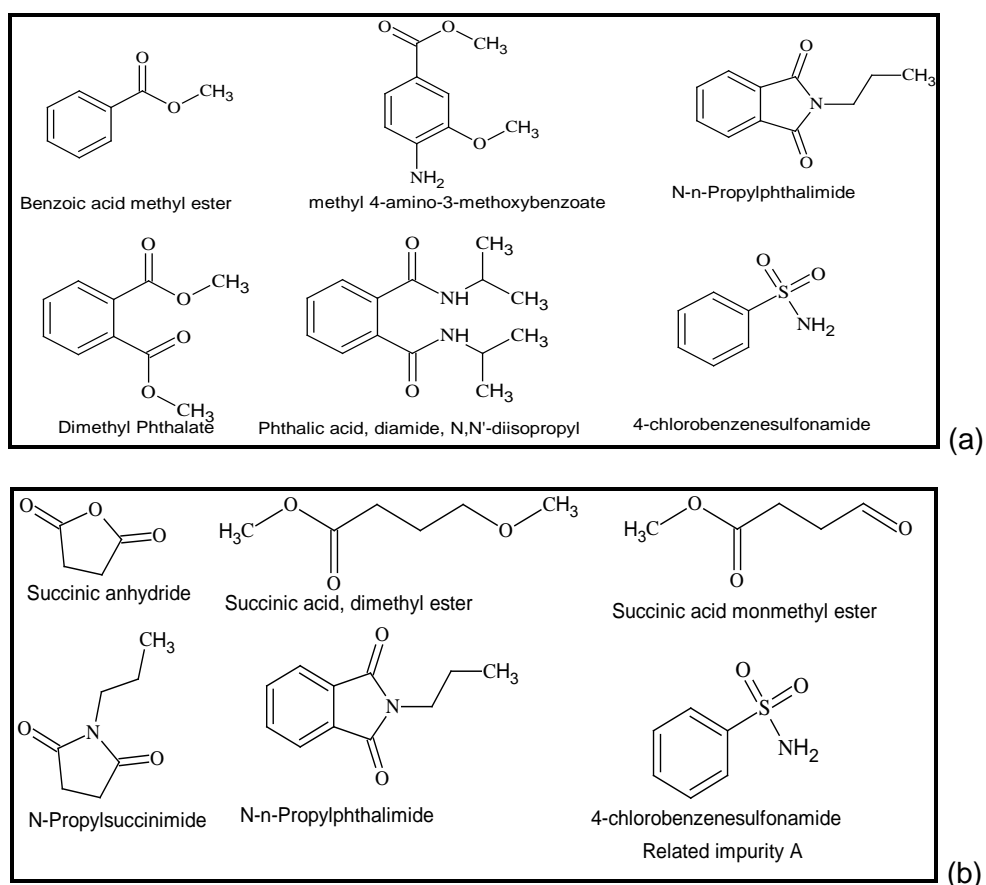


**Figure 4.54: Unknown impurities (a) of CPM-HPMCP (b) CPM-HPMCAS**

Structurally, CPM possesses the highly electron deficient carbon atom of urea due to its surrounding environment of electronegative groups such as nitrogen and oxygen (Figure 4.55, red marked). Thus, any nucleophile attacking this carbon atom will result in the breakdown of the molecule with the release of carbon dioxide. Literature reviews suggest that CPM undergoes hydrolysis when it comes into contact with water molecules resulting in production of CPM related impurity-A (CPM-A) and carbon dioxide where water acting as a nucleophilic agent initiates further reactions

(Degradation scheme A) (Figure 4.55) (Kaistha, 1969). Moreover, it was also found that the production of the related impurity B (CPM-B) and formation of butan-1-amine is also based on the pH of hydrolytic medium (Kaistha, 1969) (Degradation scheme B) (Figure 4.55). Considering these facts and analogues to the aqueous hydrolysis mechanism discussed by Kaistha (1969), a relevant mechanism for formation of CPM-A and CPM-B in the melt extrudates of cellulose ester derivatives is proposed.

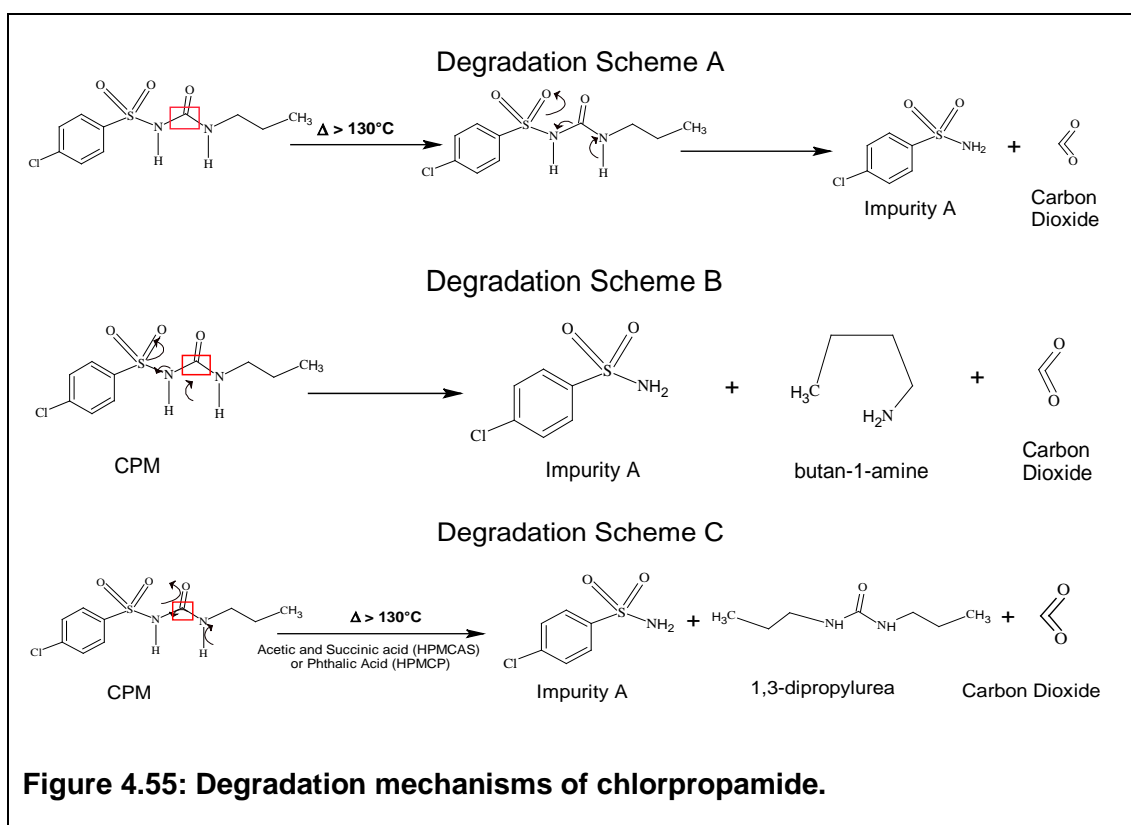


**Figure 4.55: Degradation mechanisms of chlorpropamide.**

HPLC analysis of TGA exposed samples of pure CPM produced only CPM-A however, when CPM mixtures with these two polymers was subjected for TGA studies, CPM-A along with traces of CPM-B was found during HPLC analysis. Moreover, the content of CPM-B was increased when the samples were shifted from TGA treated samples to extruded studies. While moisture uptake by polymers could be responsible for hydrolysis of CPM to CPM-A and CPM-B in all studies this possibility was minimised using vacuum oven drying at temperatures higher than the boiling point of water. Hence, it was thought

that similar to the degradation of HPMCAS and HPMCP, shear and temperature forces are the predominant forces involving hydrolysis of CPM. Further, it was anticipated that the acidic moieties released from the polymers during extrusion producing local acidic environment could be responsible for generation of CPM-B impurity. Therefore, a schematic degradation mechanism of CPM in the presence of degradation products of HPMCAS and HPMCP was designed. It is presented in figure 4.55 - degradation scheme C).

According to degradation scheme C, it was expected to generate impurity B in the melt extrudates of both polymers however, as discussed previously it appeared only in the cases of HPMCAS samples. Therefore, more detailed investigations of the CPM-HPMCP samples were undertaken. Initially the non-appearance of CPM-B in HPMCP samples was attributed to either (a) evaporation of the CPM-B during thermal processing or (b) degradation of CPM-B to further small molecules during extrusion or (c) reactions of CPM-B with degradation products of HPMCP. To investigate these possibilities, structural features of unknown impurities of CPM-HPMCP and chemical reactions of PA and PAH with urea or 1, 3-dipropyl urea was searched through the literature.

The melting point of 1, 3-dipropyl urea was observed to be in the range of 104 to 106 °C further confirmed against literature values (Sigma-Aldrich, 2014). Since processing temperatures of CPM-HPMCP were higher (> 130 °C) than this its generation during degradation of CPM and evaporation of the same, could be one a possibility. However, boiling and/or vaporisation point of the same compound is reported to be 262 °C (Yaws, 2015) and hence evaporation of CPM-B during HME was discarded.

The structural features of unknown compounds provided a comprehensive picture for the reasons for absence of CPM-B in the

extrudates of CPM-HPMCP. It was noted that the structure of N-n-Propylphthalimide (Rt = 14.03 minutes) and Phthalic acid-diamide, N, N'-diisopropyl (Rt = 19.7 minutes) bear the highest resemblance with the structures of PA, PAH and N, N'-diisopropyl. Moreover, a literature search of reactions of Phthalimide by Gabriel synthesis suggested that phthalic anhydride (PAH) interacts with urea at high temperatures to form phthalimide or derivatives of phthalimide (Chemical-Forums, 2011) with the intermediate phthalic acid-diamide, N,N-diisopropyl. The detail mechanism of reactions has been discussed in reports such as Chemical-Forums (2011) and different organic chemistry books or patents (Agusto and Boehme, 1974, Liu and Yuan, 2006). Thus, the hypothesis of either fragmentation of 1,3-dipropyl urea into urea reacting or reactions between degradation products of HPMCP and 1, 3-dipropyl urea producing unknown derivatives are responsible for non appearance of 1, 3-dipropyl urea (CPM-B) in the HPLC samples was justified.

Similar results were obtained with HPMCAS samples where succinic anhydride (SAH) formed during melt extrusion reacted with CPM-B and an n-propyl succinamide impurity was generated (Fokin et al., 1988). Moreover, methyl ester derivatives of both phthalic acid and succinic acids were also noted during GC-MS studies suggesting the potential ability to undergo further reactions.

Reactions of CPM-B with both PAH and SAH were noted in the current studies. However, reasons to find out competitive reactions of CPM-B and PAH to undergo complete derivatisation over CPM-B with SAH is not fully understood at this stage and need to be studied in detail in future works. However, fingerprinting the degradation products of both extrudates was observed to be valuable since incompatible reactions of phthalic acid, phthalic anhydride and succinic acid noted with formation of esters at the extruding

temperature of chlorpropamide, in contrast to the studies of Zedong Dong and Choi.

Ibuprofen (Figure 4.52) mixed samples of HPMCAS and HPMCP were also investigated for potential incompatibility studies. Ibuprofen melts at 75 °C and acts a plasticiser in various polymeric systems (Siepmann *et al.*, 2006a). Ibuprofen was extruded with HPMCAS and HPMCP at two drug loadings (10 and 30% w/w) and extruded at the temperatures of 100, 120 (for 30% w/w), 150 and 160 °C (10% w/w) respectively. The melt extrudates were further analysed using HPLC and GC-MS. Over the range of temperatures and drug loadings of ibuprofen, the percentage assay of an API was 98 to 99% and no additional peaks except PA was noted in the HPLC. Similar results were reproduced using GC-MS which confirmed that ibuprofen did not react with either of the polymers.

#### **4.3.4 Summary**

Characterisation of polymer melt extrudates by advanced analytical techniques specifically focused for thermodynamic, rheological and thermochemical stability properties yielded major insights into the materials' behaviour during the HME process. A correlation between the preformulatory properties, critical attributes observed during HME processing and post-extrusion properties was established which are summarised below.

Thermodynamic investigation of materials, especially their solid state miscibility studies and thermodynamic approaches utilised for constructing the phase diagrams provided very good correlation between pre- and post-extrusion studies. In all cases, PEG was found to be better plasticiser providing maximum safe loading concentration of 10 % with HPMCAS and HPMCP polymers without concerns of phase separation. This study showed

that simple DSC experiments on two component systems can be utilised to construct a phase diagram for HME processing attributes. Further this study also shows that by finding such a homogeneous polymer-plasticiser blend, different drug loadings can be incorporated into the system where the influence of plasticisers on the physical stability of an amorphous solid dispersion (ASD) can be controlled. This opens up an alternative approach for study of complex three component system for ASDs.

Melt rheology studies of extrudates clearly suggested that despite the demanding processing conditions of HME, HPMCAS can withstand and produce equivalent viscosity values post-extrusion compared with its preformulatory whereas HPMCP cannot. This confirmed that HPMCP is more susceptible to mechanical degradation whereas HPMCAS can be safely extruded below 200°C. However, it is important to note that HPMCP's mechanical degradation can be significantly reduced through the inclusion of PEG and thus, overall thermo-mechanical properties of polymers can be improved with PEG compared to TEC whereas CA produces deteriorating effects.

Thermo-chemical stability studies yielded a precise picture of the polymers' suitability with different APIs and plasticisers at the demanding processing conditions of HME. A clear temperature-shear dependence on the chemical stability of both polymers was observed between 150 and 200 °C where HPMCP was significantly compromised despite the use of PEG loadings. Further, HPMCP is noted to produce PAH as an additional degradation product along with PA and chemical reactivity of these compounds found to be sensitive enough to react further with both solvents as well as solid state compounds. Formation of esters or chemically incompatible reactions between degradation products of HPMCAS and

HPMCP with Chlorpropamide suggested that these polymers are unsuitable for extrusion with this API due to unknown toxicological profiles of these impurities. Moreover, these reactions can progress even at pharmaceutical stability temperatures where the possibility of moisture induced hydrolysis cannot be discounted. In contrast, both polymers looked to be quite stable with ibuprofen. Considering the facts of these reactions it is also speculated that drugs analogous to Chlorpropamide such as: Carbutamide, Acetohexamide, Tolbutamide, Glipizide, Glicazide, Glebenclamide, Glibornuride, Gliquidone, Glycopyramide and Glimepiride would produce similar effects with HPMCAS and HPMCP polymer whereas Ibuprofen analogues such as: Flurbiprofen, Ketoprofen, Indoprofen, Fenoprofen and Naproxen would be safe to process with these polymers. Furthermore, active ingredients containing free -OH, -SO<sub>2</sub>N- and -NH<sub>2</sub> could react with degradation products of these polymers and unknown impurities can be expected.

#### **4.4 Polymer degradation mechanism and kinetic modelling**

Ester hydrolysis of HPMCAS and HPMCP during the extreme conditions of HME has been discussed in the literature by few research groups however, the mechanism with which polymers degrade are discussed equivocally. For example, author Zedong Dong and co-workers suggest HPMCAS's degradation via hydrolysis of ester bonds whereas author Hughey and co-workers correlate this due to depolymerisation or cross linking of the polymer at high temperatures (Zedong Dong and Choi, 2008 , Hughey *et al.*, 2010). However, these authors neither established precise degradation mechanisms nor showed rational step by step changes in the chemistry of polymers when subjected to extreme conditions of shear and temperature. Furthermore, in the previous study the extent of degradation was observed to be temperature and time dependent below its onset degradation temperature (200 °C) therefore an attempt was made to investigate degradation of kinetics polymer.

##### **4.4.1 Degradation mechanism (publication I)**

Structural elucidation of both HPMCAS and HPMCP polymers suggests that both polymers hydrolyse into their respective acidic degradation products by the attack of the thermal forces at the site of ester linkages. However, in the case of HPMCP, the polymer not only hydrolyses to PA but further converts to PAH when extruded below its onset degradation temperature. Additionally, both impurities hold the capability to react further either with the solvents or undergo further degradation into their smaller molecular fragments. Similar results can be expected with HPMCAS polymer and chances of succinic anhydride generation cannot be foreseen. Therefore, based on the TGA degradation steps and impurity profiling of independent polymers, a two step decomposition pattern was correlated systematically with its degradation mechanism and is presented in Figure 4.56.

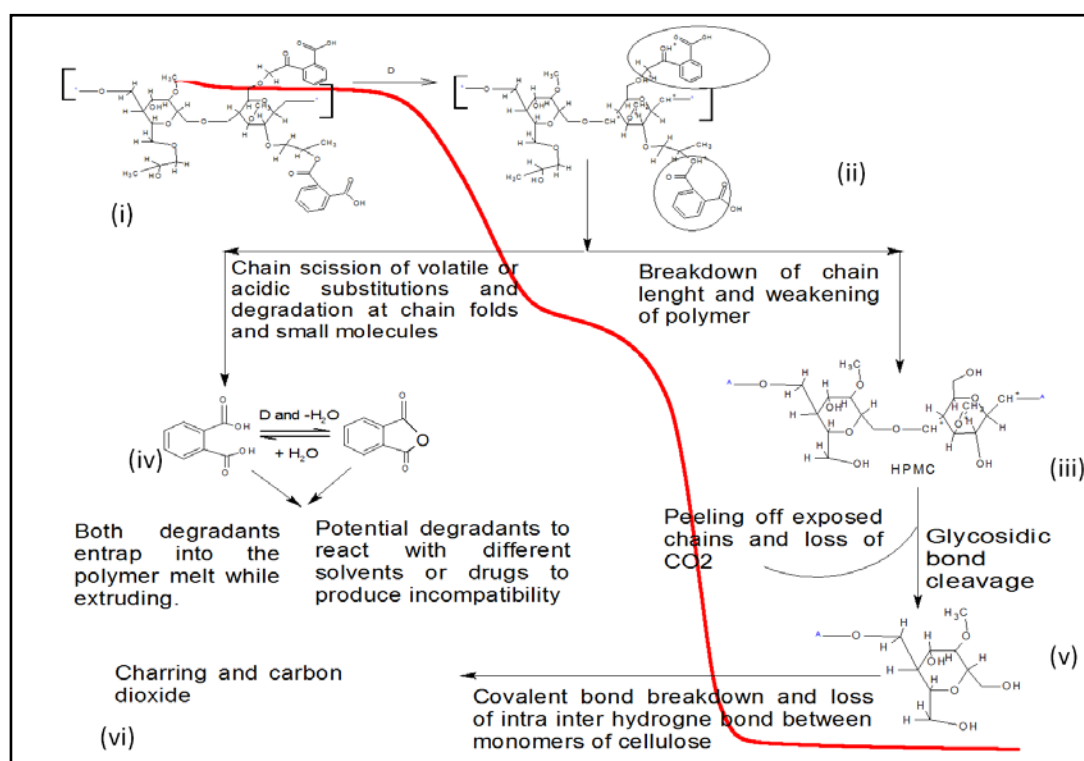


**Figure 4.56: Schematic representation of degradation of HPMCP.**

An outline of the degradation pathway was designed based on the degradation products observed during investigations. As can be seen from the TGA studies, HPMCP polymers showed a two step decomposition curve where the first step belongs to loss of acidic substitutions followed by degradation of the cellulose back bone (HPMC). A schematic representation of degradation behaviour of polymer over the entire range of TGA temperatures is shown. Figure 4.56 (i and ii) shows typical structure of the polymer and reactive sites of HPMCP where the substitutions have been made (marked in circle). Two possible reactions could occur after thermal stress to the polymer; (A) oxidation and chain scission at the sites of ester linkages (B) breakdown of the glycosidic linkages (Karandikar *et al.*, 2015).

Generally, the stability and degradation of the polymer is strongly dependent on the bond strength of the individual chemical entities. In comparison to different chemical reactions or substitutions, ester linkages are

highly susceptible to chemical breakdown to produce subsequent products. It was observed that at high temperature ( $> 160\text{ }^{\circ}\text{C}$ ) long chains of HPMCP started to break at the ester linkages (Figure 4.56ii) forming acidic components (Figure 4.56iii) as well as the formation of small volatile molecules from the degradation linkages leaving the back bone of the polymer to degrade at higher temperatures (Figure 4.56 iv). This back bone ( $\beta$  substituted glucose units) then further degrades at higher temperatures via breakdown of glycosidic linkages. At these conditions, peeling off the alkyl side chain of HPMC can be expected (Figure 4.56 iii, v), turning pure polymer into char or ash (Figure 4.56 vi) at temperatures of  $600\text{ }^{\circ}\text{C}$ . A similar representation of degradation mechanism for HPMCAS is provided in Appendix I, Figure 6.4.

Thermal degradation of polymers, especially ester derivatives generally follows a complex degradation mechanism which involves a series of hydrolytic, oxidative and cross linking events. However, these events can occur both in the presence and/or absence of radical formation; therefore, degradation mechanisms of both polymers must be broadly speculated upon. Fingerprinting of HPMCP produced valuable information about its degradation products: phthalic acid (primary degradation product), phthalic anhydride (secondary degradation product) [similarly succinic acid and succinic anhydride] and several other associated degradation products (formaldehyde, fragments of benzoic acid, benzene ethylene and gases such as carbon-dioxide). Based on this information, a series of consequences were speculated which can be involved during degradation (both thermal and shear induced) of the polymer and are discussed below.

- I. Chain scission or polymer degradation via radical formation process in the presence of oxygen: such reactions are generally known as

homolytic scission reactions and are commonly found in processes involving high temperature and shear (Grassie and Scott, 1988 , Nishida *et al.*, 2009). This can be explained further by dividing degradation stage (A) in to micro degradative stages such as:

- (A1) Initiation of degradation based on bond strength of aromatic esters forming free radicals.
  - (A2) Propagation of hydrolytic reactions through formation of peroxy radical (ROO\*) which can then remove a hydrogen atom from polymer chains.
  - (A3) Acceleration of cascade reactions forming volatile degradants based on their equilibrium vapour pressures.
  - (A4) Chain termination forming acidic-anhydride moieties from the polymer.
- II. Chain scission or polymer degradation via non-radical process during inert environment of TGA (N<sub>2</sub> gas). This process generally involves the formation of substituted six-membered ring intermediate formation of beta glucose units via formation of unsaturated or saturated small end groups of the polymers.

#### **4.4.2 Isothermal degradation kinetics and implications of plasticisers**

Thermal and thermo-chemical investigations of HPMCAS and HPMCP provided valuable insights of material properties especially about a relationship between thermal properties and its associated chemical features or degradations over the range of processing conditions. However, HME being a thermo-mechanical process and generally running in an open environment, the mechanism of cellulose ester degradations in the presence of oxygen may involve processes like oxidation, radical depolymerisation reactions (as discussed above). Thus, degradation of cellulose esters can be considered as thermo-oxidative and/or thermo-hydrolytic processes and

possibilities of following more than one degradation mechanism cannot be precluded in the case of HME.

Studies involving extrusion can begin with investigations of TGA to determine onset degradation temperatures. However, it is important to note these temperatures can be apparent indicators of material degradations and degradations can occur below these values when materials are subjected to isothermal temperatures for a length of time. Similar observations have been noted in the current research work which clearly suggests that thermal degradation reactions are highly temperature-time dependent and these further advances for thermal degradation kinetic studies. Investigation of degradation products or the degradation mechanism of pharmaceutical polymers is by far briefly studied in different research articles. However, investigation of degradation kinetics of pharmaceutical polymers and applications of kinetic studies time have not received due consideration in HME studies. Degradation kinetic studies are generally carried out to anticipate and extrapolate the extent of degradation caused during the steps of different manufacturing processes. Thus, investigations of kinetic studies should also be considered as one of the pre-requisite studies for melt extrusion.

Thermal degradation kinetics is largely explored by TGA techniques where the samples under investigations are continuously measured for its weight loss over the range of the temperatures at a particular heating rate. Once the measurements are made, raw values of the material weight loss can be subjected to equations of kinetics. Thermal degradation kinetics is generally carried out by two modes: an isothermal and non-isothermal mode. Both modes have different advantages and limitations (Dahiya *et al.*, 2008 , Andres *et al.*, 2001 , Abate *et al.*, 2005). However, the isothermal mode is the most preferred mode of kinetic investigations since material conversion and

change in reaction mechanisms can be well explained on the basis of experimental conditions (B. Janković *et al.*, 2008 , Vega-Baudrit *et al.*, 2008). In contrast, in non-isothermal testing, the extent of degradation significantly varies with the change in heating rate and kinetic parameters calculated over time can be prone to some errors (Gupta and Viswanath, 1996 , Dahiya *et al.*, 2008 , Hurduc *et al.*, 2007).

Further, thermal degradation kinetics can also be influenced by the addition of plasticisers in the polymers (Gupta and Viswanath, 1996 , Silva *et al.*, 2010), generally added to reduce processing temperatures. However plasticisers are known to increase molecular mobility of polymers which can reduce  $T_g$  and could also affect the degradation temperature of the parent polymer. This further adds to complexity of degradation mechanism and subsequently the kinetics of degradation the polymer (Gupta and Viswanath, 1996 , Mano *et al.*, 2003).

Currently the two polymers are widely processed with different plasticisers such as TEC or propylene glycol or triacetin (TA), and acetyltriethyl citrate (ATEC) however their influence on degradation temperature followed by degradation kinetics of polymers have not been investigated. Therefore in the current studies, degradation kinetics of pure and blends of polymers (plasticisers only) have been carefully monitored using mathematical models. Firstly, the isothermal polymer weight loss was investigated. Secondly, implications of plasticisers on polymer degradation mechanism and pattern were investigated. Lastly, thermal degradation kinetic studies of pure and blends of polymeric samples were modelled for thermo-mechanical kinetic approaches.

#### 4.4.2.1 Isothermal analysis of polymers and polymeric blends

Independent samples of virgin HPMCP and its respective blends (with PEG and CA) were heated in a TGA furnace from 140 to 200 °C at an increment of 10°C, while similar treatment was given to HPMCAS polymers between 190-260 °C. The sample was held at each temperature for 30 min isothermally and weight loss over the 30 min was measured. This weight loss was then normalised and graphs were plotted. Isothermal weight loss studies of both virgin polymers suggested linear degradations at investigated temperatures however, the patterns of degradation changed to curvilinear (at/beyond 170 and 230 °C for HPMCP and HPMCAS respectively) indicating change in the kinetics of the process (see Figure 4.57). Similar treatment was given to the polymeric blends and remarkable fluctuations in polymeric weight losses of blends were noted. For instance, PEG blends showed decrease in the weight loss compared to the pure polymer with increase in the temperature (Table 4.19) whereas the blends with CA maximised the degradation of both polymers (data not shown here).

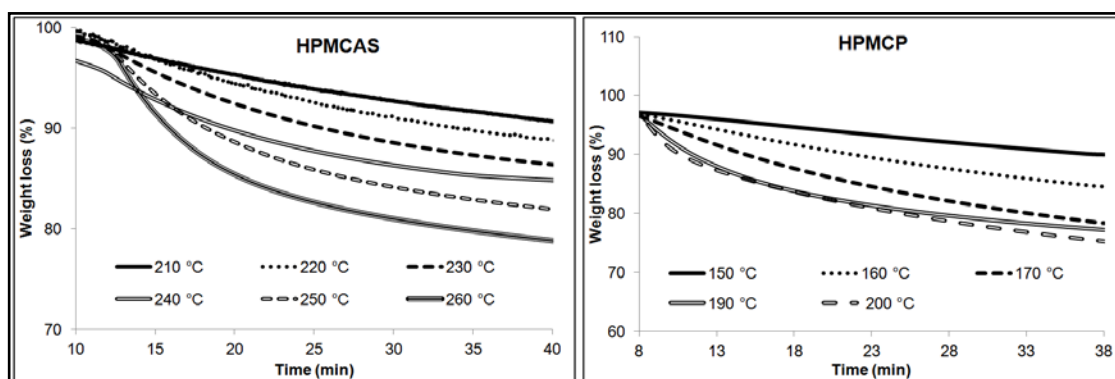


**Figure 4.57: Linear to curvilinear graphs of polymers.**

In another case, particularly for blends of PEG-HPMCP, at initial temperatures, the percentage weight loss was in the order of HPMCP  $\geq$  10% PEG = 15% PEG  $\geq$  20% PEG. However, beyond 170 °C, the weight losses of blends of HPMCP decreased and the order was observed to be HPMCP >

10% PEG >15% PEG >20% PEG whereas for HPMCAS-PEG mixture, the order of degradation was observed to be HPMCAS > 10% PEG > 15% PEG > 20%PEG. Moreover, the curvilinear curves of parent polymers were changed (curvilinear to linear) with the addition of PEG suggesting changes in degradation kinetics of the blends when compared to the pure polymer. For instance at 180 °C, weight loss of pure HPMCP was curvilinear however with increase in PEG content, weight loss was reduced with decrease in curvilinear slope (see Figure 4.58). Similar trends can be seen with HPMCAS and its blends at 250 °C.

**Table 4.19: Isothermal weight loss of materials.**

Temperature		150 °C	160°C	170°C	180°C	190°C
Degradation (%)	HPMCP	7.31%	12.52%	18.68%	20.92%	21.09%
	10% PEG	9.59%	12.71%	16.27%	16.43%	16.33%
	15% PEG	8.61%	13.24%	17.20%	16.2%	16.06%
	20% PEG	6.23%	10.27%	18.26%	17.5%	15.98%
Temperature		210°C	220°C	230°C	240°C	250°C
Degradation (%)	HPMCAS	8.08%	10.74%	12.61%	14.46%	16.72%
	10% PEG	7.66%	8.71%	10.69%	12.03%	13.05%
	15% PEG	5.22%	6.08%	8.33%	10.19%	12.78%
	20% PEG	4.25%	5.71%	8.01%	9.34%	11.7%

To investigate these behaviours, a non-isothermal TGA study was conducted. Figure 4.59 shows TGA thermograms of blends of PEG and CA with respective pure polymers. Marked differences were noted when TGA thermograms were compared. For example, considering TGA thermograms of pure polymers as reference, the blends of PEG showed a right shift (towards higher temperatures) in degradation temperatures whereas blends of CA showed a left shift to the reference degradation temperatures (Figure 4.59).

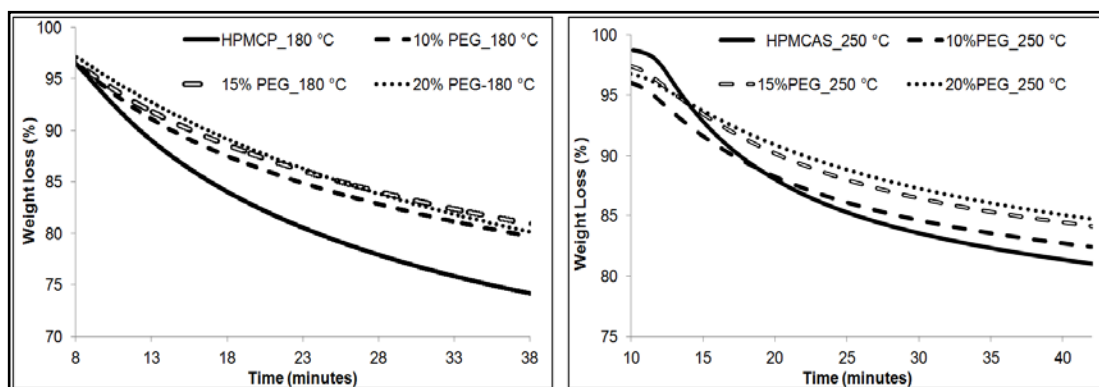


**Figure 4.58: Curvilinear to linear weight loss changes with addition of PEG.**

Non-isothermal analysis of the polymer blends clearly indicated that additives have a marked effect on both degradation patterns as well as on mechanisms of parent polymers. The degradation pattern of blends of PEG remained unchanged and showed distinct two-step decomposition curves as for the original polymers (Figure 4.59) whereas blends of CA changed both degradation pattern and mechanism of pure polymers, especially at first decomposition step of pure polymers (see figure 4.59). Moreover, it was also speculated that with increase in CA content, the degradation pattern of both polymers would reduce to single step degradation. An example can be seen from 20% CA loadings and its degradation pattern (see Figure 4.59). Thus, it was confirmed that plasticisers could improve or compromise thermal stability of composite and bring changes in decomposition temperatures of polymers.

Unlike CA, since PEG produced cooperative effects (both thermally and mechanically) with both polymers without its self destruction at elevated temperatures, its implications on degradation kinetics of pure polymers was interesting part of the investigation. Therefore, pure polymers and blends of PEG were further studied. Different kinetic factors [such as degree of degradation ( $\alpha$ ), order of reaction ( $n$ ), reaction rate constant ( $k_1$ ), activation energy ( $E_{a\_degradation}$ ) and pre-exponential factor ( $A$ )] were calculated. Isothermal degradation kinetics were investigated by two mathematical

approaches: (a) conventional kinetic equations, (b) MacCallum approach (MacCallum, 1989) as detailed below.

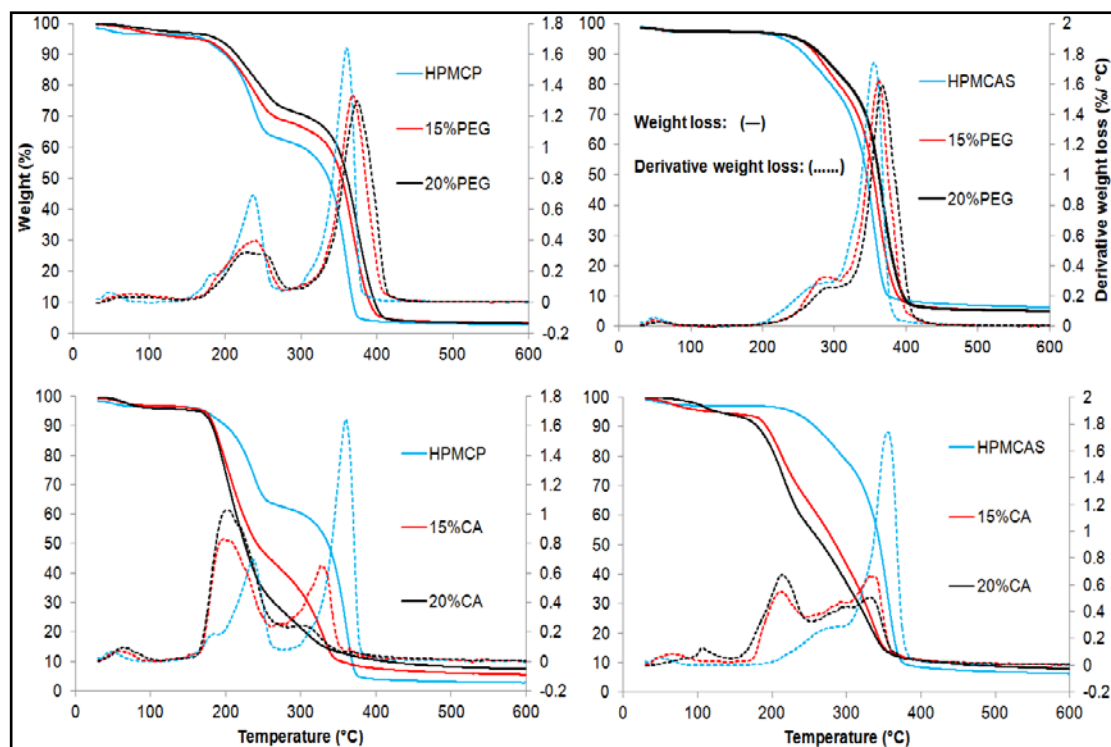


**Figure 4.59: TGA and DTGA of polymer blends.**

#### 4.4.2.2 Conventional equations of thermal degradation kinetics

Isothermal weight loss of independent samples of pure and blends of polymers was utilised to calculate degree of degradation ( $\alpha$ ) and plots of  $\alpha$  over the isothermal temperatures were investigated using equations 2.6 and 2.7. Since  $\alpha$  is the ratio of initial mass to final, it was speculated to be a decomposition ratio. According to Vega-Baudrit and co workers, the decomposition ratio of a sample increases with increase in the temperature of the system and the temperature at which the ratio drops from its earlier temperature indicates completion of decomposition (Vega-Baudrit et al., 2008). For example, decomposition ratios (i.e. values of  $\alpha$  as a function of time) of both polymers increased with temperature and beyond 190 and 240 °C the decomposition ratio of HPMCP and HPMCAS decreased respectively

(see Figure 4.60). However, with the PEG blends the decomposition ratio did not decrease at 190 and 240 °C indicating that decomposition was not complete.

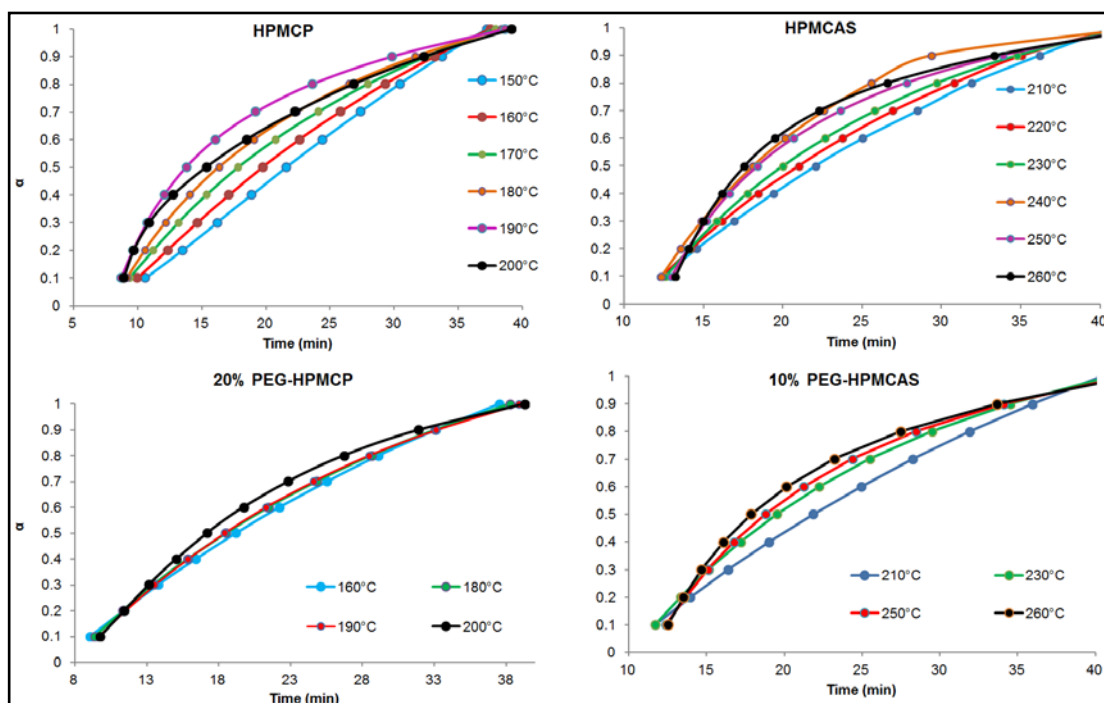


**Figure 4.60: Decomposition ratios of polymeric samples.**

Further, kinetic parameters such as ' $n$ ' and ' $k_1$ ' were investigated. A plot of  $\log(d\alpha/dt)$  against  $\log(1 - \alpha)$  was utilised and a straight line obtained from the chart yielded values of  $n$  (slope) and  $k_1$  (*intercept*). A representative figure showing a linearity between the plot of  $\log(d\alpha/dt)$  and  $\log(1 - \alpha)$  is shown in Figure 4.61b. The method was repeated at several temperatures and values of  $n$  as well as  $k_1$  were obtained for different polymeric samples and values are presented in Table 4.20 and Table 4.21. It should be noted that the variance and standard deviation given are presented based on a triplicate set of data calculated for each sample at every temperature.

The values of  $n$  for pure HPMCP and HPMCAS increased from 0.16 to 1.20 and 0.42 to 1.16 within the ranges 150-200 °C and 210-250 °C respectively (see table 4.20 and 4.21) while for the PEG blends  $n$  was

decreased remaining below unity. It was noted that, when PEG-HPMCP samples were compared against virgin polymer, values of  $n$  decreased and at higher temperatures, the values of  $n$  were observed to be similar. However, blends of PEG-HPMCAS produced a consistent drop in the values of  $n$  over the entire range of temperature with the drop being proportional to plasticiser content in the mixture.

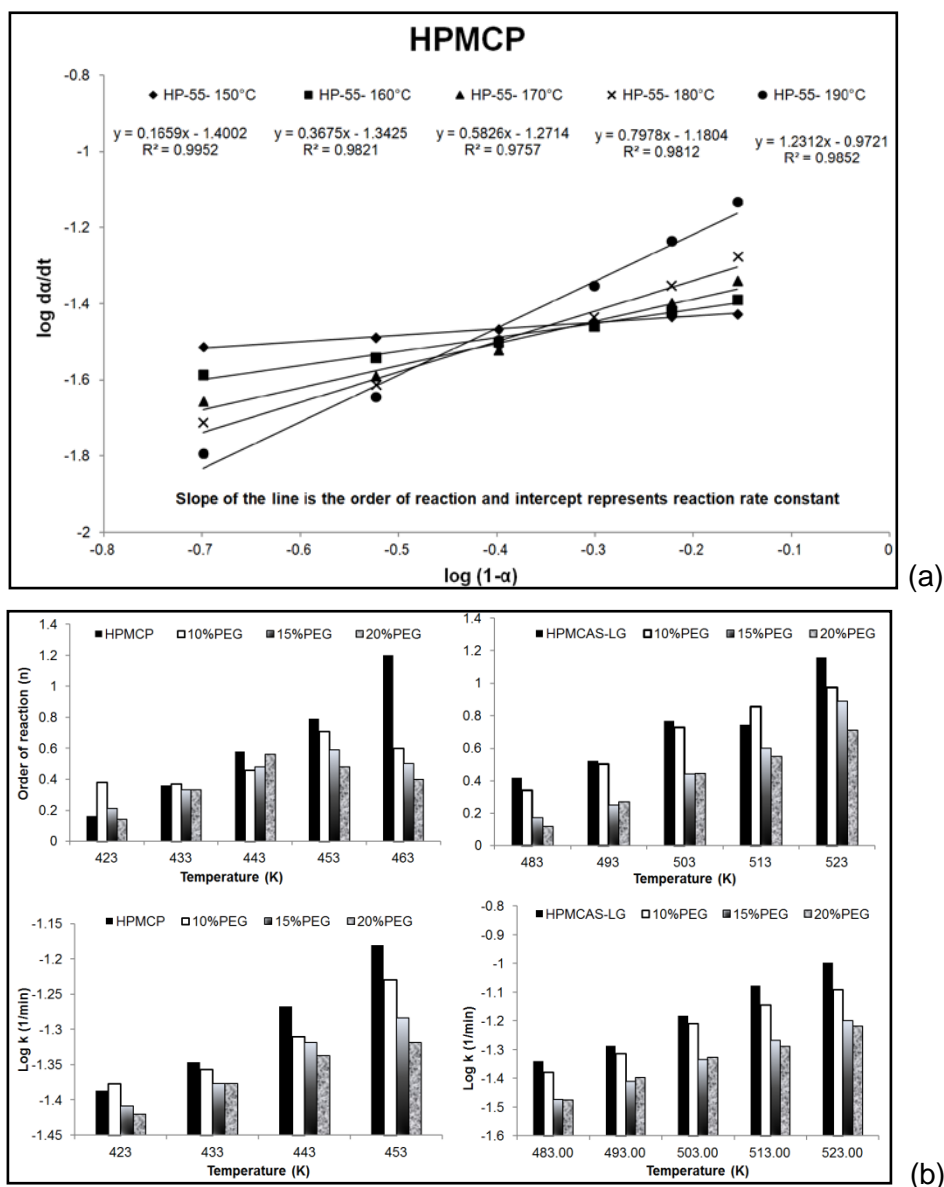


Figure 4.61: (a) Graph of  $\alpha$  versus T (b) Kinetic expressions of polymeric samples over range of temperatures and concentrations.

**Table 4.20: Calculated kinetic parameters for HPMCAS samples.**

$T_{iso}$ (K)		483	493	503	513	523	$E_a$ (KJ/mol)	A
HPMCAS	n	$0.42 \pm 0.0141$	$0.52 \pm 0.0325$	$0.77 \pm 0.0375$	$0.74 \pm 0.0167$	$1.16 \pm 0.0142$	$18.82 \pm 0.65$	2126.17
	k	$0.046 \pm 0.0014$	$0.052 \pm 0.0013$	$0.066 \pm 0.0014$	$0.084 \pm 0.0020$	$0.101 \pm 0.0006$		
	r <sup>2</sup>	0.9557	0.9716	0.9947	0.9924	0.9949		
10% PEG	n	$0.33 \pm 0.0173$	$0.49 \pm 0.0097$	$0.72 \pm 0.0266$	$0.85 \pm 0.0231$	$0.97 \pm 0.0044$	$15.67 \pm 0.50$	333.88
	k	$0.042 \pm 0.0002$	$0.049 \pm 0.0015$	$0.062 \pm 0.0002$	$0.072 \pm 0.0002$	$0.081 \pm 0.0015$		
	r <sup>2</sup>	0.9856	0.991	0.9922	0.9939	0.9931		
15% PEG	n	$0.17 \pm 0.0101$	$0.24 \pm 0.0123$	$0.43 \pm 0.0126$	$0.59 \pm 0.0240$	$0.88 \pm 0.0176$	$14.5 \pm 0.359$	136.3
	k	$0.034 \pm 0.0020$	$0.039 \pm 0.0021$	$0.046 \pm 0.0012$	$0.054 \pm 0.0016$	$0.063 \pm 0.0024$		
	r <sup>2</sup>	0.9838	0.9934	0.9905	0.9908	0.995		
20% PEG	n	$0.11 \pm 0.0063$	$0.26 \pm 0.0251$	$0.44 \pm 0.0162$	$0.54 \pm 0.0139$	$0.71 \pm 0.0164$	$13.12 \pm 0.194$	63.25
	k	$0.033 \pm 0.0021$	$0.040 \pm 0.0024$	$0.047 \pm 0.0016$	$0.051 \pm 0.0014$	$0.060 \pm 0.0011$		
	r <sup>2</sup>	0.9966	0.9942	0.9922	0.9886	0.9989		

**Table 4.21: Calculated kinetic parameters for HPMCP samples.**

$T_{iso}$ (K)		423	433	443	453	463	$E_a$ (KJ/mol)	A
HPMCP	n	$0.16 \pm 0.0144$	$0.36 \pm 0.0075$	$0.58 \pm 0.0211$	$0.79 \pm 0.0213$	$1.20 \pm 0.0708$	$11.61 \pm 0.7071$	77.97
	k	$0.04 \pm 0.0036$	$0.045 \pm 0.0024$	$0.054 \pm 0.00072$	$0.066 \pm 0.0071$	$0.045 \pm 0.0049$		
	$r^2$	0.9952	0.9821	0.9757	0.9812	0.9852		
10% PEG	n	$0.38 \pm 0.0144$	$0.37 \pm 0.0078$	$0.46 \pm 0.0282$	$0.71 \pm 0.0494$	$0.65 \pm 0.0425$	$6.97 \pm 0.1414$	3.72
	k	$0.044 \pm 0.0007$	$0.044 \pm 0.0022$	$0.049 \pm 0.0021$	$0.059 \pm 0.0028$	$0.044 \pm 0.0074$		
	$r^2$	0.9468	0.9721	0.9943	0.9636	0.9663		
15% PEG	n	$0.21 \pm 0.0353$	$0.33 \pm 0.0355$	$0.48 \pm 0.0495$	$0.59 \pm 0.0211$	$0.61 \pm 0.0422$	$6.8 \pm 0.1462$	3.58
	k	$0.039 \pm 0.0007$	$0.042 \pm 0.0007$	$0.048 \pm 0.0021$	$0.052 \pm 0.0028$	$0.039 \pm 0.0021$		
	$r^2$	0.9671	0.9716	0.994	0.9706	0.9736		
20% PEG	n	$0.14 \pm 0.0221$	$0.33 \pm 0.0215$	$0.46 \pm 0.0282$	$0.48 \pm 0.0491$	$0.56 \pm 0.0630$	$6.33 \pm 0.2121$	2.44
	k	$0.038 \pm 0.0014$	$0.042 \pm 0.0007$	$0.046 \pm 0.0014$	$0.048 \pm 0.0014$	$0.038 \pm 0.0070$		
	$r^2$	0.9822	0.9849	0.9713	0.9864	0.9934		

In terms of reaction rate for HPMCAS and its blends,  $k_1$  decreased with increasing PEG content. However, for HPMCP with PEG: at the lower temperatures and at different PEG loadings, the  $n$  and  $k_1$  values showed fluctuation without any clear trend. However, beyond 170 °C (443K) the values of  $n$  and  $k_1$  were reversed i.e. values were reduced in a specific order [see Figure 4.61(b) at 443 and 453 K]. To obtain degradation activation energy ( $E_{a\_degradation}$ ), the values of  $k_1$  obtained at various temperatures were utilised in equation 2.8 and plots of  $\log k_1$  against  $1/T_{iso}$  were produced (Figure 4.62). The slope of the line was utilised for calculation of  $E_{a\_degradation}$  and intercept yielded pre-exponential factor (A). From Table 4.20 and 4.21, three observations were noted where  $E_{a\_degradation}(\text{HPMCAS}) > E_{a\_degradation}(\text{HPMCP})$ ,  $E_{a\_degradation}(\text{pure polymer}) > E_{a\_degradation}(\text{blends})$  and marginal difference between values of  $E_{a\_degradation}$  of blends of HPMCP.

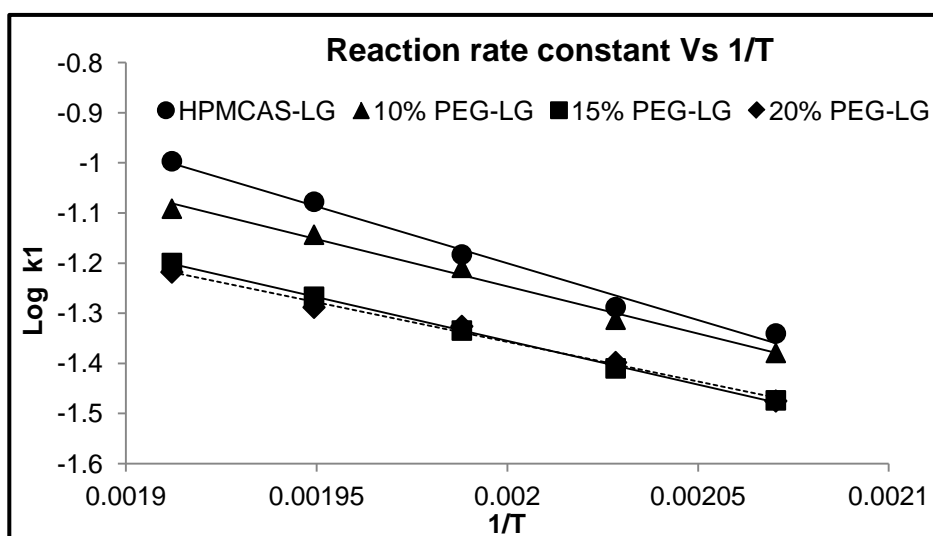


Figure 4.62: A graph of  $\log k_1$  over the range of temperature.

Another observation is that the  $E_{a\_degradation}$  values for the blends of HPMCP were observed to be approximately half that for the pure polymer whereas blends of HPMCAS reduced linearly by a factor of 1.1 to 1.3 with increase in plasticiser content. It was indicated that PEG is providing stability

to the polymer due to which polymer weight loss reduced and resulted to reduction in kinetic parameters. In other words, if the additive is providing stability to the polymer,  $E_{a\_degradation}$  of the blends should be higher than that of the parent polymer. However, this assumption was not seen in the current studies since  $E_{a\_degradation}$  (pure polymer) >  $E_{a\_degradation}$  (blends). Nonetheless, this observation lead to an important aspect which coincides with the observation reported by Vega-Baudrit and co-workers. According to the authors, the appearance of such a situation suggests that *"although polymer degrades at a higher rate with lower initial degradation and at a maximum rate within decomposition temperatures, it needs higher activation energy for degradation compared to polymeric blends"* (Vega-Baudrit et al., 2008).

For  $E_{a\_degradation}$  and constant A, a direct relationship was noted where increase and decrease in the values of  $E_{a\_degradation}$  was balanced by its pre-exponential factor value (Table 4.20 and 4.21). This behaviour is normally termed as a 'kinetic compensation effect' or 'compensation effect (CE)' (Zsako, 1976 , Garn, 1975). Kinetic compensation effect is generally observed in every family of reactions in order to maintain values of  $k_1$ , and it is a linear representation between Arrhenius parameters: A and  $E_a$ . Several theories have been put forward to explain this kind of behaviour during kinetic investigations, however two aspects such as thermodynamic entropy-enthalpy correlation and/or a common centre involving a number of reactions or isokinetic temperature behaviour (Gupta and Viswanath, 1996) have been discussed in the literature.

Earlier, for pure and blends of HPMCP polymers reversal of kinetic parameters beyond 170 °C (443 K) were noted and to correlate this effect, detailed studies were carried out where plots of  $\log k_1$  against  $1/T_{iso}$  for virgin and blends of both polymers were compared independently. An

important point was noticed during this comparison supporting the reversal of kinetic parameters of HPMCP. It was noted that the family of reactions intersected at a common point on the x-axis at 170 °C (443 K) and beyond this point, the rate of reactions was reversed. According to literature reports, such a point is referred to as the 'isokinetic temperature point' at which reaction rates of chain of reactions becomes identical (Barrie, 2012).

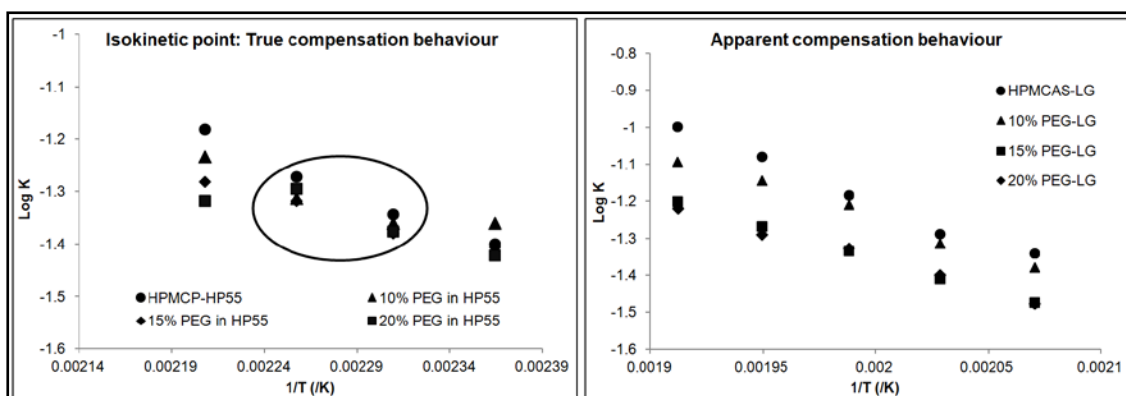


**Figure 4.63:  $E_a$  and A dependence for the polymer plasticiser blends.**

Investigations of this isokinetic point in the samples of HPMCP clearly differentiated the nature of compensatory behaviour of  $E_a$  and A. The compensatory behaviour for chains of reactions often indicate a maintenance of the reaction rate constant and the presence of isokinetic point during the family of reactions indicates true compensation behaviour. In contrast, when the chain of reactions shows this compensatory effect without any isokinetic point, the compensation is often regarded as 'apparent compensation behaviour' (Gupta and Viswanath, 1996 , Barrie, 2012 , Blanco *et al.*, 2011). Thus, based on these observations, it was speculated that pure and blends of HPMCP were following true compensation behaviour whereas HPMCAS was following apparent compensation behaviour. Thus, reversals in the kinetic parameters of blends of HPMCP were thought to be justified (Figure 4.63).

#### 4.4.2.3 Thermal degradation kinetics by MacCallum method

MacCallum contributed significantly in the research of degradation kinetics and his equations are widely investigated in degradation kinetic studies which can be observed from various research articles (Abate *et al.*, 2002 , Abate *et al.*, 2005 , Regnier and Guibe, 1997). MacCallum initially co-worked with Schoff and later developed his own degradation kinetic equations (MacCallum, 1989 , MacCallum and Schoff, 1971). According to the MacCallum and Schoff method, the conventional degradation equation was integrated considering,  $n \neq 1$ . However, this approach was later found highly limited since it was applicable to such systems where degree degradation or fractional conversion (M) was less than 0.3 (MacCallum and Schoff, 1971). Therefore to overcome these problems, MacCallum later developed different equations which are discussed below (MacCallum, 1989).

According to MacCallum, degree of degradation is defined as,

$$\alpha = \frac{W_{initial} - W_{final}}{W_{initial}} \quad \text{Equation 4.20}$$

Thus, the material degradation then modified to

$$\frac{d(1-\alpha)}{dt} = k_1 * f(1 - \alpha) \quad \text{Equation 4.21}$$

MacCallum later converted  $f(1 - \alpha)$  to its integrated form to put a new equation,

$$F(1 - \alpha) = kt \quad \text{Equation 4.22}$$

Where  $t$  is the time. Since function of  $\alpha$  should remain constant over the range of the temperature, MacCallum then compared the equations with the Arrhenius form and rewritten as,

$$\log t = \frac{E_a}{RT} + \log [ F(1 - \alpha) ] - \log A \quad \text{Equation 4.23}$$

Thus, when a graph of  $\log t$  against  $1/T$  at fixed values of degree of degradation is plotted, it should produce a straight line of which the slope represents  $\frac{E_a}{R}$  and intercept produces  $\log[F(1 - \alpha)] - \log A$ .

**Table 4.22: Investigation of kinetic parameters by MacCallum method.**

$\alpha$	$E_a$ (KJ/mol)				Regression ( $r^2$ )			
	HPMCP	10% PEG	15% PEG	20% PEG	HPMCP	10% PEG	15% PEG	20% PEG
1	5.70	2.59	2.04	3.88	0.76	0.85	0.65	0.55
2	9.75	0.59	5.16	7.60	0.86	0.89	0.69	0.53
3	12.65	0.69	7.38	10.21	0.89	0.91	0.76	0.60
4	14.96	7.20	9.05	12.22	0.90	0.96	0.79	0.63
5	16.92	8.56	10.32	13.83	0.91	0.95	0.80	0.66
6	18.60	9.64	11.26	15.16	0.92	0.93	0.80	0.67
8	18.16	8.67	7.18	6.29	0.92	0.81	0.63	0.51
10	17.99	8.91	7.55	7.44	0.91	0.75	0.65	0.56
Standard Deviation	$\pm 4.46$	$\pm 3.88$	$\pm 2.92$	$\pm 3.39$				

By applying these mathematical modifications of MacCallum, the weight loss data of virgin and blends of HPMCP were initially investigated and degree of degradation calculated according to equation 4.20. Similarly, further modifications were made to investigate degradation kinetics of polymeric materials. A fixed degree of degradations (1 to 10%) were considered since percentage degradations of different samples over the range of temperatures were variable. Considering these assumptions, graphs of  $\log t$  against  $1/T$  were plotted for all samples and the straight lines obtained from these values were utilised to calculate the activation energy of the virgin and blends of the polymer. Table 4.22 represents the calculated activation energy of

degradation reactions for HPMCAS and blends of HPMCP over the investigated fixed degrees of degradations.

It was observed that activation energy values of virgin polymer increased linearly until the value of  $\alpha$  reaches 5% and beyond this point the activation energy remained fairly constant to 18 kJ/Mol. Similar effects were observed with 10% PEG however, the activation energy dropped at the  $\alpha$  values of 2 and 3. The 15 and 20% PEG blends of HPMCP showed increase in  $E_a$  values up to 6% and both blends showed drop in activation energy at higher values of  $\alpha$ . On average, over fixed degrees of degradation (up to 10%), the observed  $E_a$  values required to degrade a mole of polymer was comparable with that of the conventional technique shown above. However, the variance or standard deviation observed in the case of MacCallum method was significantly higher than that of the conventional method. Furthermore, with the blends, the values of standard deviation was significantly higher where in some cases at the values of  $\alpha = 4, 5$ ; the standard deviation for  $E_a$  was  $\pm 5.01$ . Moreover, the regression values obtained during these calculations were non-satisfactory where very few samples showed regression values more than 0.90. Therefore the validity, reliability and/or model fitting of MacCallum equations for the virgin and blends of HPMCP and HPMCAS are thought doubtful.

To investigate these findings and the non-satisfactory responses obtained using the MacCallum method for this current work some observations were made from the work of others (Abate *et al.*, 2005, Blanco *et al.*, 2011). It was observed that MacCallum equations are only applicable to the materials which follow single step degradation. In other words, MacCallum calculations are valid only "when the degree of polymerisation of largest molecule that can evaporate from the sample" (Atkinson and Maccallum,

1972 , Atkinson and Maccallum, 1971). Although current investigations of degradation kinetics of HPMCAS and HPMCP were limited to its first degradation step, evaporation of acidic substitutions is relatively smaller molecules compared to the largest molecule, HPMC backbone. Moreover, the degradation of these polymers is a two step degradation mechanism. Further, deducing degradation kinetics by this method for dual or multiple degradation steps requires modifications of mathematical functions which is beyond the scope of this current work. One of the major advantages of the conventional degradation equation approach is it requires zero approximations and it can be applied for multistep degradation transitions. Thus the virgin and blends of HPMCAS were not investigated further using the MacCallum method.

#### *4.4.2.4 Melt rheology based degradation kinetics*

In the current section, degradation kinetics of cellulose ester derivatives based on their rheology data is presented. Thermal sensitivity and thermal degradation kinetics of pure polymer and polymeric blends is already discussed in the earlier section. However, it is important to note that HME involves the application of shear and influences of thermo-mechanical forces resulting into degradation of materials can cause radical drops in melt viscosity. Isothermal degradation kinetics of HPMCAS and HPMCP clearly indicate that both polymers are following first order degradation kinetics due to chain scission and, in order to investigate similar effects during thermo-mechanical events, a time sweep test was conducted.

Mechanical properties (including mechanical degradation) are strongly dependent upon shear and temperature for the given period of time and melt stability of the polymer can be anticipated at the preliminary stages of investigations by means of this test. Therefore, mechanical degradation and

degradation kinetics of cellulose ester derivatives with/without plasticisers was performed by dynamic time sweep test.

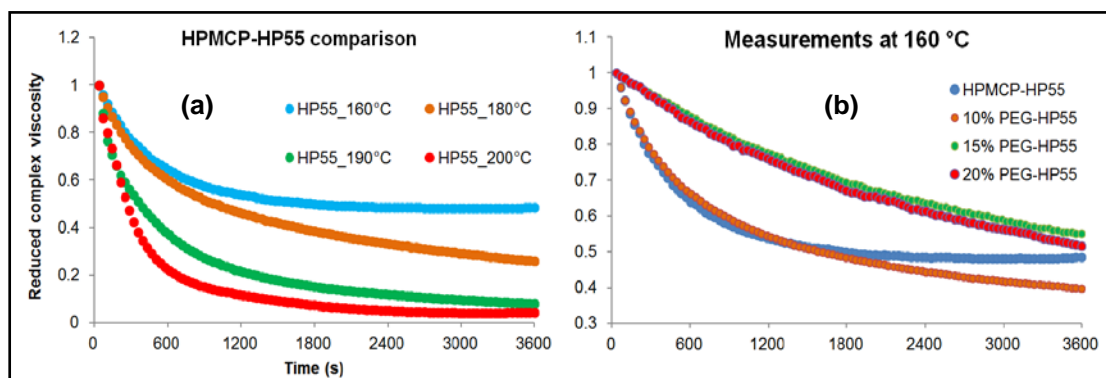


**Figure 4.64: Reduced complex viscosity against time for polymeric samples (a) HPMCP (b) with blends of PEG.**

Independent samples of virgin and blends of polymers were exposed to a range of temperatures (same as isothermal degradation kinetic studies) and tested at isothermal conditions at 0.01 % strain amplitude and 10 Hz frequency over 60 minutes and the melt viscosity of the polymers was measured. Further the values of complex viscosities were converted into reduced complex viscosity values ( $\eta_{\text{reduced}}$ ) and a graph of  $\eta_{\text{reduced}}$  versus time was studied. A representative chart of reduced complex viscosity as a function of time for samples of virgin polymers investigated and decaying ratio blends of polymers measured at 160 °C is presented in the Figure 4.64a and b. It can be seen that the values of  $\eta_{\text{reduced}}$  gradually reduced with increase in time and temperature; however, interestingly the decaying rates or slopes of these samples were increased noticeably with temperature. During the investigation, at 160 °C until 180 °C the reduced viscosity graph showed a gradual drop in the viscosity values however, when the temperature was raised above the 180°C an accelerated viscosity drop followed by a more gradual decay at times greater than 1800 seconds was observed. The viscosity of the material decreased to 50% at 180 °C and 80% at 200 °C

within the first ten minutes of the experiment suggesting consistent decay of the material following 'an order' with increase in the temperature (Figure 4.64a). Based on the thermal degradation kinetics results it was anticipated that PEG would improve the decaying slopes of HPMCP blends. The decaying curves of different concentrations of PEG investigated over the range of temperature supported this assumption - the PEG mixed samples of HPMCP not only improved the decaying slopes but these slopes were gradually improved over temperature showing their influence with percentage loadings at each temperature. From Figure 4.64b, it can be seen that decaying slope is in order of HPMCP > 10% > 15% > 20% PEG at 160 °C with similar behaviours over all temperatures. Similar results were obtained for HPMCAS samples when they were tested 200-250 °C.

The complex viscosity data was modelled for degradation kinetic studies by the mathematical model of Daly *and* co-workers group (Daly *et al.*, 2005). Degradation kinetics based on polymer melt rheology is generally performed by frequency sweep zero shear viscosity or WLF method however, the majority of work published on such criteria suggests the utilisation of time sweep tests since material under investigation experiences constant mechanical shear conditions.

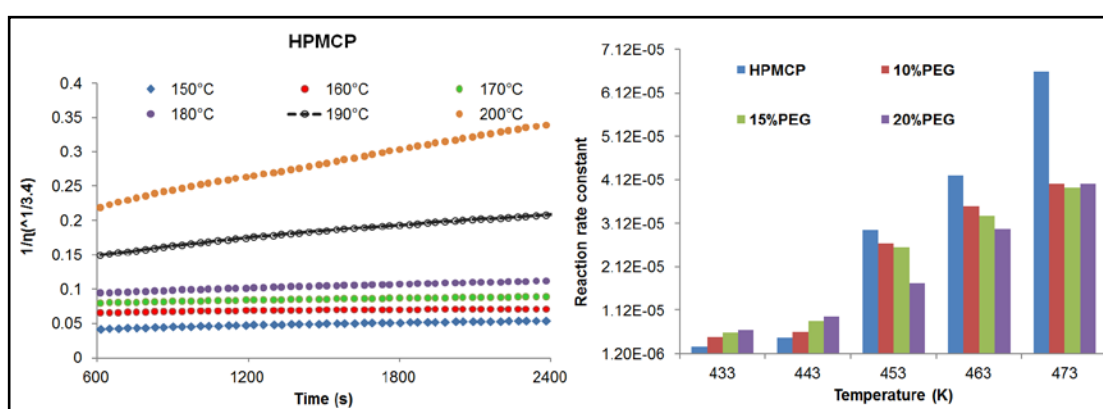


**Figure 4.65: (a) Rheology data for determination of degradation kinetics of HPMCP and (b) comparison of  $k_a$  values over temperatures.**

According to the equations of Daly *et al.*, 2005, the viscosity values of polymeric samples were converted to its  $[1/\eta^{(1/3.4)}]$ . A graph of  $1/\eta^{(1/3.4)}$  versus time was plotted and the rate of reaction,  $k_a$  was calculated based on the slopes of the lines over the range of temperatures (Virgin and PEG blends of HPMCP: 150 - 200 °C; virgin and PEG blends of HPMCAS: 200-260 °C). A linear trend was observed (Figure 4.65). The slopes of the lines especially from 150 to 170°C (423 - 443 K) were observed reduced compared with the rest of the temperatures however, with increase in temperature the slope of the lines increased. Similar results were obtained with HPMCAS polymer at the said temperatures. As a result, the value of  $k_a$  was also expected to increase with increase in temperature (see Figure 4.65b).

At the initial temperatures minor fluctuations in the values of  $k_a$  were observed with different PEG loadings however, when temperature passed beyond 170 °C (443 K), the rate of degradation was reduced (Figure 4.65b). Similar results were obtained while investigating the same blends in the thermal degradation kinetic models due to the presence of isokinetic temperature point. Further, with increase in temperature from 160 to 200 °C, the  $k_a$  values of HPMCP increased by factor 10 while in the case 10, 15 and 20% PEG these values were increased by 8, 6.5 and 6 factors over the range of temperatures. This reduction in degradation rate constant was noticeable where with maximum concentration of PEG, close to 50% reduction in the apparent degradation rate constant value were observed (Figure 4.65b).

Further, the values of  $k_a$  were considered for Arrhenius relationship and energy of activation values were established. The relationship between  $\log k_a$  versus  $1/T$  (Figure 4.66) yielded  $E_a$  values with the regression values greater than 0.90 (see Table 4.23). For example  $E_a$  values of HPMCAS, HPMCP and

their 20% PEG blends were found to be 17.45, 57.51, 7.49 (20%PEG-HPMCAS) and 36.23 (20%PEG-HPMCP) kJ/mol.

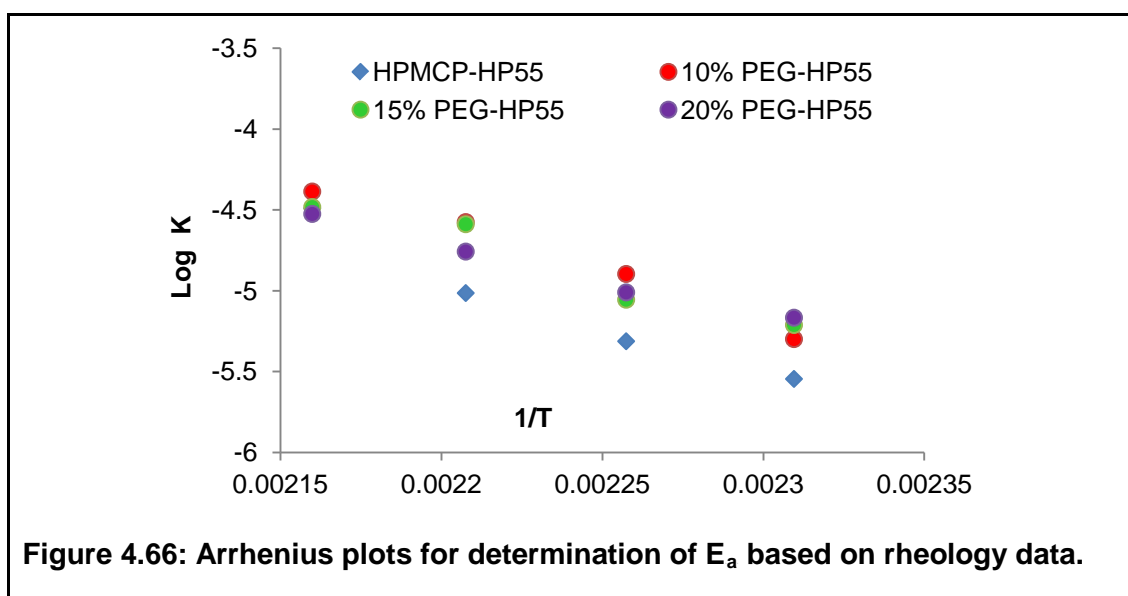


**Table 4.23: Degradation Kinetic parameters determined by Daly et al.**

	HPMCP	10% PEG	15% PEG	20% PEG	HPMCAS	10% PEG	15% PEG	20% PEG
Ea (kJ/Mol)	57.51 ± 0.24	51.13 ± 0.17	44.27 ± 0.52	36.23 ± 0.18	17.46 ± 0.36	11.69 ± 0.14	8.52 ± 0.16	7.49 ± 0.27

#### 4.4.3 Summary

Utilising a systematic approach, advanced analytical techniques as well as hyphenated techniques and based on degradation products of polymers, a step wise degradation mechanism was constructed. This mechanism was also designed by considering two important parameters: degradation in inert environment (highly sophisticated) and degradation of polymer in presence of oxygen (applicable to HME like processes) which can be useful while investigating polymeric applications in HME.

Degradation kinetics of HPMCP and HPMCAS clearly indicated that isothermal method of analysis is one of the better methods to investigate degradation kinetic modelling since it eliminates the errors of heating rates.

Moreover, applications of different mathematical models of degradation kinetics yielded varying parameters of reaction rate constants; however, the energy of activation values calculated by both techniques provided similar values. One of the important observations from this study was the compensatory effects of energy of activation and pre-exponential factor through presence and absence of isokinetic point suggesting true and apparent compensation effects. These results also provided valuable support for reversal of kinetic parameters. It was also summarised that different named equations requires consideration of material degradation stages and thus, kinetic studies involving standard isothermal degradation equations are still recommended.

Similar to thermal degradation kinetics, polymer degradation kinetics of polymers was investigated based on melt rheology data. Considering the first order of kinetics, equations of Daly *et al* were employed and it was observed that HPMCP shows higher degradation rates than HPMCAS and mechanical degradation of the polymer increases with shear rate. On the other hand, with the blends of PEG, the degradation rate increased with plasticisers' concentration at the lowest temperatures however, at higher temperatures the degradation rate reduced. These observations were in accordance with the thermal degradation kinetic studies where it was speculated that the degradation of HPMCP would be controlled and flow properties-processibility can be improved with PEG. The  $E_a$  values of HPMCAS and their blends calculated both by thermal and rheological methods were equivalent however variation was noted with HPMCP's activation energy values. The values of  $E_a$  under mechanical degradation were three times higher than thermal values for HPMCP. This indicates that higher mechanical energy will be required to break HPMCP molecule in the temperature range of 150 - 200 °C compared to thermal.

## Chapter 5. Conclusions

The work in the current dissertation is focused on a systematic study of methodologies to identify salient polymer properties for their suitability in HME. Conventional polymers including, HPMCAS and HPMCP, are constantly considered for HME applications due to their wide range of tailored physicochemical properties. However, the behaviour of these polymers under the demanding processing regimes in HME, and their interactions with APIs as well as plasticisers, are poorly studied in literature. Although the processing behaviour of these two polymers is well documented in the context of conventional processing, similar knowledge on these polymers in emerging technologies like HME is highly limited. There is sparse knowledge about their material properties and processibility at elevated pressures and temperature. Therefore, thermal, thermodynamic, rheological, thermochemical and degradation kinetic properties of HPMCAS and HPMCP along with model plasticisers and APIs are evaluated and their suitability in the context of HME is discussed.

Some key conclusions were drawn from this study to conclude each polymers' suitability for HME. Thermal properties of the polymers are addressed initially. Though HPMCAS and HPMCP are processed over similar processing temperatures (150 to 200 °C) required for HME, these values are misleading, especially for HPMCP. HPMCP is observed to produce significant weight loss between 150 to 200 °C while HPMCAS produced marginal loss when studied isothermally for 30 minutes. This showed that thermal properties of HPMCP are severely compromised where as HPMCAS has better thermal stability and suitable for processing below 200 °C. However, with the mixtures of PEG-HPMCP thermal stability of HPMCP can be improved and less degradation is obtained compared with the other two

plasticisers TEC and CA. However, suitability of the PEG-HPMCP blends for HME still remains highly questionable as it is entirely based on the added API as well as applications.

Solubility parameters calculated for both polymers provided an important insight about thermodynamic properties of polymers. Both polymers, being amorphous, viscous, of high  $T_g$ , strong supporter of H-bond interactions and having  $\delta$  in the range of 25 to 26  $\text{MPa}^{1/2}$  are observed suitable carriers for most of BCS class II APIs and plasticisers for the manufacture of amorphous solid dispersions (ASD). Attainment of homogeneous single phase ASD is a major challenge in HME based formulations although recrystallisation inhibitors such as HPMCAS and HPMCP are used. This clearly indicates that there is a distinct gap between theoretical and practical aspects of manufacturing ASD by HME. In the current dissertation, solid state miscibility, the  $T_g$  of mixture and glass forming ability (GFA) are carefully compared against Gibbs free energy based phase diagrams. These studies revealed an important insight about their inter-relation and utility for manufacturing ASD. For instance, the phase diagram predicted 15 and 20% compositions of PEG and CA with both polymers would eventually phase separate since these compositions were lying in the zone 6 of phase diagram (see Figure 4.35). However, when the times taken for phase separation are considered blends of CA separated within a month whereas PEG blends only displayed phase separation at the end of 2 years. This was attributed to GFA of PEG (strong glass former) and CA (poor glass former) which resulted in difference time dependent phase separation.

Low and high shear rheological properties of the pure materials provided a comprehensive overview of polymeric melt properties. HPMCAS displayed stable melt flow compared to HPMCP in many instances. Studies with three

plasticisers indicated that selection of plasticisers with these two polymers is vital for producing stable melt flow inside extruder. The blends with CA provided poor flow properties whereas PEG not only improved melt stability but also prevented polymer degradation during mechanical stress. Further, though TEC has been used widely with these polymers in solution state studies, the applicability of TEC (unstable > 150 °C) with HPMCAS and HPMCP as a plasticiser would be highly limited and subject to an upper processing temperature. Further, melt activation energy calculated for pure polymers suggested that HPMCAS ( $E_a = 10$  kJ/Mol) requires lower energy compared to HPMCP (30 kJ/Mol) and much lower than other extruding pharmaceutical polymers such as Eudragit (106kJ/Mol) to overcome viscosity barrier to flow inside melt extruder. This suggested that HPMCAS has relatively easy processability in HME over other polymers.

Thermo-chemical stability of pure and polymer blends brought precise information about polymers suitability over the range of HME conditions. HPMCP is observed to produce highly reactive degradation product phthalic anhydride (PAH) and phthalic acid (PA) in significant amounts during extrusion whereas marginal acid release was noted from HPMCAS. Considering the latest guidelines of EMA, utility of HPMCP in extrusion studies would be questionable since degradation products PA and PAH can be harmful for human reproductive systems. Another important observation was noted when these polymers were studied with APIs for thermo-chemical stability. It was concluded that APIs containing sulfonyl urea, free hydroxyl and amine groups should be carefully screened for esterification reactions with degradation products of polymers since these polymers are not suitable with such APIs.

One of the important methodologies applied in this study was thermal and rheology based degradation kinetic approaches. HPMCP underwent substantial degradation both thermally and mechanically below 200 °C, as determined by function of degree of degradation and order of kinetics whereas quantitative degradation kinetic estimations can be done for HPMCAS only when the temperature is > 200 °C. Further, an important insight was revealed related to implications of plasticisers on degradation kinetics of the parent polymer. PEG formed a stable composite whereas blends with CA compromised the thermal degradation kinetics and mechanisms of both polymers. This indicated that plasticisers do affect degradation kinetics of the parent polymers and this must be considered when used in HME.

To conclude, suitability of HPMCP is highly debated for HME and demands extreme care in use. HPMCAS is relatively much better than HPMCP in many instances but is one should be cautious and give proper consideration to selection of API and plasticiser for their applications in HME processing and product performance.

## Chapter 6. Future perspectives

Results obtained from the above studies provided a comprehensive background about polymeric material properties suitable for HME processing. However there is plenty of scope to take this study further. Therefore, the following future perspectives are made with respect to different grades of HPMCAS and HPMCP, more additive studies, thermodynamic approaches, investigations of co-processed excipients, exploration of chemical interactions with APIs-their analogues and finally mathematical modelling of polymer melt viscosities and/or computational modelling of melt flow simulations of HPMCAS and HPMCP at different screw configurations for HME

### A. Polymeric grades and additive studies

- In the current work, mainly the HPMCAS-LG and HPMCP-HP55 polymeric grades were utilised. Examination of other grades such as HPMCAS (MG and HF) and HPMCP (HP50 and HP55) should be studied extensively on the similar platform.
- Explore different physico-chemically stable solid state as well as liquid state plasticisers suitable for producing homogenous mixture during HME processing. Further implications of these plasticisers as well as PEG analogues on polymer melt viscosity in order to find optimum plasticiser concentrations suitable for thermodynamic and rheological properties.
- Investigations of HPMCAS-PEG and HPMCP-PEG as co-processed excipients for melt granulation approaches and utilisation of these blends with different APIs to improve functionality as well as processability in HME.
- To explore feasibility of a range of APIs and their analogues for their extrudability with these polymers

B. Approaches and experimentations

- By investigating stable polymer-plasticiser blends (a homogeneous amorphous blend) and its use with API for manufacturing ASD by thermodynamic equations.
- Experiments to find out effect of extrusion conditions on molecular weight of the polymer by advanced polymer chromatography (APC) by developing a new method for quick analysis.
- To perform die swelling and extensional melt viscosity experiments on capillary extruder

## REFERENCES

- Abate, L., *et al.* (2002) The isothermal degradation of some polyetherketones: a comparative kinetic study between long-term and short-term experiments. *Polymer Degradation and Stability*, **75** (3), 465-471.
- Abate, L., *et al.* (2005) Kinetics of the isothermal degradation of model polymers containing ether, ketone and sulfone groups. *Polymer Degradation and Stability*, **87** (2), 271-278.
- Advani, S. G. and Sozer, E. M. (2012) *Process Modeling in Composites Manufacturing, Second Edition*. CRC Press.
- Agusto, R. and Boehme, W. (1974) *Production of phthalimide*.
- Ahmed, J. and Ramaswamy, H. S. (2005) Effect of Temperature on Dynamic Rheology and Colour Degradation Kinetics of Date Paste. *Food and Bioproducts Processing*, **83** (3), 198-202.
- Al-Obaidi, H. and Buckton, G. (2009) Evaluation of griseofulvin binary and ternary solid dispersions with HPMCAS. *AAPS PharmSciTech*, **10** (4), 1172-7.
- Albertsson, A. C. (2001) *Degradable Aliphatic Polyesters*. Springer Science & Business Media, 2001.
- Alemaskin, K., *et al.* (2004) Index for Simultaneous Dispersive and Distributive Mixing Characterization in Processing Equipment. *International Polymer Processing*, **19** (4), 327-334.
- Ali, S. (2010) *Soluplus®- The solid solution. Opening New Doors in Solubilization*. BASF, [cited 15 May 2013]. Available from [http://www.pharma-ingredients.basf.com/Documents/ENP/Brochure/EN/RZ\\_BASF\\_Broschure\\_Soluplus.pdf](http://www.pharma-ingredients.basf.com/Documents/ENP/Brochure/EN/RZ_BASF_Broschure_Soluplus.pdf).
- Aljaberi, A., *et al.* (2009) Functional performance of silicified microcrystalline cellulose versus microcrystalline cellulose: a case study. *Drug Dev Ind Pharm*, **35** (9), 1066-71.
- Andres, G. O., *et al.* (2001) Kinetic study of the hydrolysis of phthalic anhydride and aryl hydrogen phthalates. *J Org Chem*, **66** (23), 7653-7.
- Andrews, G. P. (2007) Advances in solid dosage form manufacturing technology. *Philos Transact A Math Phys Eng Sci*, **365** (1861), 2935-49.
- Angell, C. A. (1991) Relaxation in liquids, polymers and plastic crystals- strong / fragile patterns and problems. *Journal of Non-Crystalline Solids*, **133**, Part 1 (0), 13-31.
- Ao, Z. M. and Jiang, Q. (2006) Size effects on miscibility and glass transition temperature of binary polymer blend films. *Langmuir*, **22** (3), 1241-6.
- Apichatwatana, N. (2011). *Hot melt extrusion for the production of controlled drug delivery systems*. Dissertation for the academic degree of Doctor of Science. The Free University of Berlin.
- Aquasolve-as, A. A. *Physcial and chemical properties handbook*. Ashland Inc, [cited 12th December 2014]. Available from [http://www.ashland.com/Ashland/Static/Documents/ASI/PC\\_12624\\_Aqua\\_Solve\\_AS\\_Handbook.pdf](http://www.ashland.com/Ashland/Static/Documents/ASI/PC_12624_Aqua_Solve_AS_Handbook.pdf).

- Askadskii, A. A., *et al.* (1977) The assessment of the cohesive energy density between low molecular weight liquids and polymers. *Polymer Science U.S.S.R.*, **19** (5), 1159-1169.
- Atkinson, J. and Maccallum, J. R. (1971) The Kinetics of Thermal Decomposition of Polymers. *Journal of Macromolecular Science: Part A - Chemistry*, **5** (5), 945-956.
- Atkinson, J. and Maccallum, J. R. (1972) Kinetics of thermal decomposition of polymers. II. *Journal of Polymer Science Part A-2: Polymer Physics*, **10** (5), 811-822.
- Aubin, M. and Prud'homme, R. E. (1988) Analysis of the glass transition temperature of miscible polymer blends. *Macromolecules*, **21** (10), 2945-2949.
- B. Janković, *et al.* (2008) Isothermal kinetics of dehydration of equilibrium swollen poly(acrylic acid) hydrogel. *Journal of Thermal Analysis and Calorimetry*, **92** (3), 821-827.
- Babcock Walter C, F. D. T., Lyon David Keith, Miller Warren Kenyon, Smithey Daniel Tod (2008) *Pharmaceutical Compositions With Enhanced Performance*. Accept.: 23rd October. US 2008/0262107 A1
- Bagley, E. B. (1957) End Corrections in the Capillary Flow of Polyethylene. *Journal of Applied Physics*, **28** (5), 624-627.
- Baird, J. A. and Taylor, L. S. (2012) Evaluation of amorphous solid dispersion properties using thermal analysis techniques. *Adv Drug Deliv Rev*, **64** (5), 396-421.
- Baldrick, P. (2000) Pharmaceutical excipient development: the need for preclinical guidance. *Regul Toxicol Pharmacol*, **32** (2), 210-8.
- Barra, J., *et al.* (1997) The expanded Hansen approach to solubility parameters. Paracetamol and citric acid in individual solvents. *J Pharm Pharmacol*, **49** (7), 644-51.
- Barrie, P. J. (2012) The mathematical origins of the kinetic compensation effect: 1. The effect of random experimental errors. *Phys Chem Chem Phys*, **14** (1), 318-26.
- Barton, A. F. M. (1991) Handbook of Solubility Parameters and Other Cohesion Parameters. In: second ed. Florida: CRC Press Inc.
- Bejugam, N. K., *et al.* (2009) Influence of Formulation Factors on Tablet Formulations with Liquid Permeation Enhancer Using Factorial Design. *AAPS PharmSciTech*, **10** (4), 1437-1443.
- Beyler, C. and Hirschler, M. (2002) Thermal decomposition of polymers. *SFPE handbook of fire protection engineering*, **2**.
- Bharate, S. S., *et al.* (2010) Incompatibilities of pharmaceutical excipients with active pharmaceutical ingredients: a comprehensive review. *Journal of Excipients and Food Chemicals*, **1** (3), 3-26.
- Bhardwaj, S. P., *et al.* (2014) Mechanism of amorphous itraconazole stabilization in polymer solid dispersions: role of molecular mobility. *Mol Pharm*, **11** (11), 4228-37.
- Blanco, I., *et al.* (2011) The regression of isothermal thermogravimetric data to evaluate degradation  $E_a$  values of polymers: A comparison with literature

- methods and an evaluation of lifetime prediction reliability. *Polymer Degradation and Stability*, **96** (11), 1947-1954.
- Borde, B., *et al.* (2002) Calorimetric analysis of the structural relaxation in partially hydrated amorphous polysaccharides. I. Glass transition and fragility. *Carbohydrate Polymers*, **48** (1), 83-96.
- Breitenbach, J. (2002) Melt extrusion: from process to drug delivery technology. *Eur J Pharm Biopharm*, **54** (2), 107-17.
- Bruck, S. D. (1965) Thermally stable polymeric materials. *Journal of Chemical Education*, **42** (1), 18.
- Bruno Paillard, *et al.* (2011) *A Comparison of Three Extrusion Systems*. PharmTech.com, [cited 25 November 2013]. Available from <http://www.pharmtech.com/comparison-three-extrusion-systems>.
- Casana, G. V., *et al.* (2010) Agrochemical formulations of microcapsules for compounds containing carboxamide groups. Google Patents.
- Charles, M. H. (2007) Solubility Parameters - An Introduction. In: *Hansen Solubility Parameters*. CRC Press, pp. 1-26.
- Chatterjee, P. K. and Conrad, C. M. (1968) Thermogravimetric analysis of cellulose. *Journal of Polymer Science Part A-1: Polymer Chemistry*, **6** (12), 3217-3233.
- Chemical-Forums (2011) *Mechanism of formation phthalimide*. [cited 04 March 2015]. Available from <http://www.chemicalforums.com/index.php?topic=49269.0>.
- Cherdron, H. (1978) *Polymere: Introduction to Polymer Science and Technology: An SPE Textbook*. Hrsg. von H. S. Kaufmann, J. J. Falcetta. John Wiley & Sons, New York, London 1977, X, 613 S., zahlr. Abb. und Tab., geb. £ 20.65. *Nachrichten aus Chemie, Technik und Laboratorium*, **26** (10), 660-661.
- Cogswell, F. N. (1997) *Polymer melt rheology, a guide for industrial practice*. Cambridge, England: Woodhead publishing limited.
- Cooksey, C. (2010) *Methanolysis of phthalic anhydride; Phthalic acid monomethyl ester*. [cited 8th August 2013]. Available from <http://cssp.chemspider.com/Article.aspx?id=428>.
- Cowie, J. M. G. (1968) Estimation of the cohesive energy density of a polymer from critical opalescence measurements. *Canadian Journal of Chemistry*, **46** (24), 3919-3921.
- Cox, W. P. and Merz, E. H. (1958) Correlation of dynamic and steady flow viscosities. *Journal of Polymer Science*, **28** (118), 619-622.
- Crawford, R. J. (1998) *Plastics Engineering*. Oxford: Elsevier Butterworth-Heinemann.
- Crowley, M. M., *et al.* (2007a) Process for the preparation of a hot-melt extruded laminate. United States of America, Auxilium Us Holdings, Llc.
- Crowley, M. M., *et al.* (2004) Physicochemical properties and mechanism of drug release from ethyl cellulose matrix tablets prepared by direct compression and hot-melt extrusion. *Int J Pharm*, **269** (2), 509-22.

- Crowley, M. M., *et al.* (2002) Stability of polyethylene oxide in matrix tablets prepared by hot-melt extrusion. *Biomaterials*, **23** (21), 4241-8.
- Crowley, M. M., *et al.* (2007b) Pharmaceutical applications of hot-melt extrusion: part I. *Drug Dev Ind Pharm*, **33** (9), 909-26.
- Dahiya, J. B., *et al.* (2008) Kinetics of isothermal and non-isothermal degradation of cellulose: model-based and model-free methods. *Polymer International*, **57** (5), 722-729.
- Daly, P. A., *et al.* (2005) Thermal degradation kinetics of poly(3-hydroxybutyrate-co-3-hydroxyhexanoate). *Journal of Applied Polymer Science*, **98** (1), 66-74.
- De Brabander, C., *et al.* (2002) Characterization of ibuprofen as a nontraditional plasticizer of ethyl cellulose. *J Pharm Sci*, **91** (7), 1678-85.
- Djuris, J., *et al.* (2013) Preparation of carbamazepine-Soluplus solid dispersions by hot-melt extrusion, and prediction of drug-polymer miscibility by thermodynamic model fitting. *Eur J Pharm Biopharm*, **84** (1), 228-37.
- Donnelly, C., *et al.* (2015) Probing the effects of experimental conditions on the character of drug-polymer phase diagrams constructed using Flory-Huggins theory. *Pharm Res*, **32** (1), 167-79.
- Drebushchak, V. A., *et al.* (2008) Transitions among five polymorphs of chlorpropamide near the melting point. *Journal of Thermal Analysis and Calorimetry*, **93** (2), 343-351.
- Edge, S., *et al.* (1999) The Location of Silicon Dioxide in Silicified Microcrystalline Cellulose. *Pharmacy and Pharmacology Communications*, **5** (6), 371-376.
- Elaine Kenny, D. D., Clement Higginbotham, Luke Geever (2013) Processing and Characterisation of Various Polymer Blends to Develop Implant for Tissue Engineering Applications. *Journal of Asian Scientific Research*, **3** (6), 654-669.
- Elkordy, A. A., *et al.* (2013) Spironolactone release from liquisolid formulations prepared with Capryol™ 90, Solutol® HS-15 and Kollicoat® SR 30 D as non-volatile liquid vehicles. *European Journal of Pharmaceutics and Biopharmaceutics*, **83** (2), 203-223.
- European-Medicines-Agency (2014) Guideline on the use of phthalates as excipients in human medicinal products. (EMA/CHMP/SWP/362974/2012), 11.
- Fang, L. Y., *et al.* (2011) Oral pharmaceutical compositions in a solid dispersion comprising preferably posaconazole and hpmcas. Google Patents.
- Fathy, M. (2006) Physicochemical characterization of ibuprofen/hypromellose acetate succinate solid dispersions. *Mansoura J. Pharm. Sci*, **22**, 224-237.
- Flory, P. J. (1942) Thermodynamics of High Polymer Solutions. *The Journal of Chemical Physics*, **10** (1), 51-61.
- Flory, P. J. (1953) *Principles of Polymer Chemistry*. Cornell University Press.
- Fokin, A. V., *et al.* (1988) Study of the products of the reaction of succinic anhydride derivatives with urea. *Bulletin of the Academy of Sciences of the USSR, Division of chemical science*, **37** (8), 1701-1703.

- Follonier, N., *et al.* (1995) Various ways of modulating the release of diltiazem hydrochloride from hot-melt extruded sustained release pellets prepared using polymeric materials. *Journal of Controlled Release*, **36** (3), 243-250.
- Follonier, N., Doelker, E., & Cole, E. T. (1994) Evaluation of hot-melt extrusion as a new technique for the production of polymer-based pellets for sustained release capsules containing high loadings of freely soluble drugs. *Drug Dev. Ind. Pharm*, **20** (8), 1323-1339.
- Fukui, E., *et al.* (2001) An in vitro investigation of the suitability of press-coated tablets with hydroxypropylmethylcellulose acetate succinate (HPMCAS) and hydrophobic additives in the outer shell for colon targeting. *J Control Release*, **70** (1-2), 97-107.
- Fule, R. and Amin, P. (2014) Hot Melt Extruded Amorphous Solid Dispersion of Posaconazole with Improved Bioavailability: Investigating Drug-Polymer Miscibility with Advanced Characterisation. *BioMed Research International*, **2014**, 16.
- Garn, P. (1975) An examination of the kinetic compensation effect. *Journal of thermal analysis*, **7** (2), 475-478.
- Ghebremeskel, A. N., *et al.* (2006) Use of surfactants as plasticizers in preparing solid dispersions of poorly soluble API: stability testing of selected solid dispersions. *Pharm Res*, **23** (8), 1928-36.
- Ghosh, I., *et al.* (2011) Comparison of HPMC based polymers performance as carriers for manufacture of solid dispersions using the melt extruder. *Int J Pharm*, **419** (1-2), 12-9.
- Gogos, C. G., *et al.* (2012) Laminar Dispersive and Distributive Mixing with Dissolution and Applications to Hot-Melt Extrusion. In: *Hot-Melt Extrusion: Pharmaceutical Applications*. John Wiley & Sons, Ltd, pp. 261-284.
- Gopferich, A. (1996) Mechanisms of polymer degradation and erosion. *Biomaterials*, **17** (2), 103-114.
- Gowda, V., *et al.* (2014) Influence of Prosolv and Prosolv:Mannitol 200 direct compression fillers on the physico-mechanical properties of atorvastatin oral dispersible tablets. *Pharm Dev Technol*.
- Grassie, N. and Scott, G. (1988) *Polymer Degradation and Stabilisation*. Cambridge University Press.
- Greenhalgh, D. J., *et al.* (1999) Solubility parameters as predictors of miscibility in solid dispersions. *Journal of Pharmaceutical Sciences*, **88** (11), 1182-1190.
- Gruber, P. and O'Brien, M. (2005) Polylactides "NatureWorks® PLA". In: *Biopolymers Online*. Wiley-VCH Verlag GmbH & Co. KGaA.
- Gupta, M. C. and Viswanath, S. G. (1996) Kinetic compensation effect in the thermal degradation of polymers. *Journal of thermal analysis*, **47** (4), 1081-1091.
- Guru, G., *et al.* (2012) Miscibility, thermal and mechanical studies of methylcellulose/poly (vinyl alcohol) blends. *International journal of research in pharmacy and chemistry*, **2** (4), 957-968.
- Gustavo V. Barbosa-Cánovas, A. J. F., Shelly J. Schmidt, Theodore P. Labuza (2008) *Water Activity in Foods: Fundamentals and Applications*. Wiley.

- Hampson, F. W. and Manley, T. R. (1976) A thermoanalytical comparison between ram and screw extruded polypropylene. *Polymer*, **17** (8), 723-726.
- Hancock, B. C., *et al.* (1999) Determination of the viscosity of an amorphous drug using thermomechanical analysis (TMA). *Pharm Res*, **16** (5), 672-5.
- Hansen, C. M. (2002) *Hansen Solubility Parameters: A User's Handbook*. CRC Press.
- Harjunen, P., *et al.* (2002) Lactose modifications enhance its drug performance in the novel multiple dose Taifun DPI. *Eur J Pharm Sci*, **16** (4-5), 313-21.
- Harrison, G. M. and Melik, D. H. (2006) Application of degradation kinetics to the rheology of poly(hydroxyalkanoates). *Journal of Applied Polymer Science*, **102** (2), 1794-1802.
- Heintz, R. (2014) *Evaluating Active Ingredients in Pharmaceutical Hot Melt Extrusion Products with Raman Imaging*. American Pharmaceutical Review, [cited 22 March 2015]. Available from <http://www.americanpharmaceuticalreview.com/Featured-Articles/170904-Evaluating-Active-Ingredients-in-Pharmaceutical-Hot-Melt-Extrusion-Products-with-Raman-Imaging/>.
- Heljo, V. P., *et al.* (2013) The effect of relative humidity on the physical properties of two melibiose monohydrate batches with differing particle size distributions and surface properties. *J Pharm Sci*, **102** (1), 195-203.
- Higgins, J. S., *et al.* (2010a) *A simple approach to polymer mixture miscibility*. Vol. 368.
- Higgins, J. S., *et al.* (2010b) *A simple approach to polymer mixture miscibility*. *Philosophical Transactions of the Royal Society of London A: Mathematical, Physical and Engineering Sciences*, **368** (1914), 1009-1025.
- Hoflyzer, D. W. V. K. A. P. J. (1976) Properties of polymers, their estimation and correlation with chemical structure, 1976, 620 pp. In: 2 ed. Amsterdam - Oxford - New York: Elsevier Scientific Publishing Company, p. 620.
- Horst, R. and Wolf, B. A. (1994) Calculation of shear influences on the phase separation of polymer blends exhibiting upper critical solution temperatures. *Rheologica Acta*, **33** (2), 99-1071.
- Huang, J., *et al.* (2008) Drug-polymer interaction and its significance on the physical stability of nifedipine amorphous dispersion in microparticles of an ammonio methacrylate copolymer and ethylcellulose binary blend. *J Pharm Sci*, **97** (1), 251-62.
- Huang, Y. and Dai, W.-G. (2014) Fundamental aspects of solid dispersion technology for poorly soluble drugs. *Acta Pharmaceutica Sinica B*, **4** (1), 18-25.
- Hughey, J., *et al.* (2010) Dissolution Enhancement of a Drug Exhibiting Thermal and Acidic Decomposition Characteristics by Fusion Processing: A Comparative Study of Hot Melt Extrusion and KinetiSol® Dispersing. *AAPS PharmSciTech*, **11** (2), 760-774.
- Hunter, N. E., *et al.* (2010) The use of dynamic vapour sorption methods for the characterisation of water uptake in amorphous trehalose. *Carbohydr Res*, **345** (13), 1938-44.

- Hurduc, N., *et al.* (2007) The Non-isothermal Degradation Process of some Polyethers and Azo-polyethers. *High Performance Polymers*.
- Ipec (2013) *Certificate of Analysis Guide for Pharmaceutical Excipients*. Available from <http://ipec-europe.org/uploads/coa-guide-2013.pdf>.
- Isaac Ghebre-Sellassie and Martin, C. (2003) *Pharmaceutical Extrusion Technology*. New York: Marcel Dekker Inc.
- Ivanisevic, I. (2010) Physical stability studies of miscible amorphous solid dispersions. *J Pharm Sci*, **99** (9), 4005-12.
- Iyer, R., *et al.* (2013) The Impact of Hot Melt Extrusion and Spray Drying on Mechanical Properties and Tableting Indices of Materials Used in Pharmaceutical Development. *Journal of Pharmaceutical Sciences*, **102** (10), 3604-3613.
- James, M. and Feng, Z. (2003) Melt-Extruded Controlled-Release Dosage Forms. In: *Pharmaceutical Extrusion Technology*. (Drugs and the Pharmaceutical Sciences) Informa Healthcare.
- Jan H. Los, W. J. P. V. E., and Elias Vlieg (2002) Metastable States in Multicomponent Liquid-Solid Systems II: Kinetic Phase Separation. *The Journal of Physical Chemistry B*, **106** (29), 7331-7339.
- Jan Pospíšil, Z. H., Zdeněk Kruliš, Stanislav Nešpůrek, Shin-Ichi Kuroda (1999) Degradation and aging of polymer blends I. Thermomechanical and thermal degradation. *Polymer Degradation and Stability*, **65** (3), 405-414.
- Jani, R., Patel, Dasharath (2015) Hot melt extrusion: An industrially feasible approach for casting orodispersible film. *Asian Journal of Pharmaceutical Sciences*, (0).
- Janssens, S. and Van Den Mooter, G. (2009) Review: physical chemistry of solid dispersions. *Journal of Pharmacy and Pharmacology*, **61** (12), 1571-1586.
- Jin, F. and Tatavarti, A. (2010) Tableability assessment of conventional formulations containing Vitamin E tocopheryl polyethylene glycol succinate. *International Journal of Pharmaceutics*, **389** (1-2), 58-65.
- Job, G. and Herrmann, F. (2006) Chemical potential- a quantity in search of recognition. *European journal of physics*, **27** (2), 353.
- Judd, M. D. and Norris, A. C. (1973) The determination of kinetic parameters for some solid state reactions. *Journal of thermal analysis*, **5** (2-3), 179-192.
- Kaerger, J. S., *et al.* (2004) Influence of particle size and shape on flowability and compactibility of binary mixtures of paracetamol and microcrystalline cellulose. *Eur J Pharm Sci*, **22** (2-3), 173-9.
- Kaialy, W., *et al.* (2012) Dry powder inhalers: mechanistic evaluation of lactose formulations containing salbutamol sulphate. *Int J Pharm*, **423** (2), 184-94.
- Kaistha, K. K. (1969) Selective assay procedure for chlorpropamide in the presence of its decomposition products. *J Pharm Sci*, **58** (2), 235-7.
- Karandikar, H., *et al.* (2015) Systematic identification of thermal degradation products of HPMCP during hot melt extrusion process. *International Journal of Pharmaceutics*, **486** (1-2), 252-258.

- Kelly, A. L. (1997). *On-Line Shear And Extensional Rheometry of Polymer Melts In The Extrusion Process*. The Degree Of Doctor Of Philosophy. University Of Bradford.
- Kemsley, J. (2014) *Eyes On Excipients*. American Chemical Society, [cited 13th November 2014]. Available from <http://cen.acs.org/articles/92/i5/Eyes-Excipients.html>.
- Kidokoro, M., *et al.* (2002) Application of fluidized hot-melt granulation (FHMg) for the preparation of granules for tableting; properties of granules and tablets prepared by FHMg. *Drug Dev Ind Pharm*, **28** (1), 67-76.
- Kittel, C. (2004) *Introduction to solid state physics*. Wiley India Pvt. Limited.
- Klaric, I., U. Roje, and T. Kovacic, J. (1993) Thermal degradation of poly(vinyl chloride)/poly( $\hat{1}\pm$ -methylstyrene-acrylonitrile) blends. *Polymer Degradation and Stability*, **40** (1), 91-96.
- Kokubo, S. O. A. H. (2008) Application of HPMC and HPMCAS to Aqueous Film Coating of Pharmaceutical Dosage Forms. In: JAMES W. MCGINITY, L. A. F. (Ed.) *Drugs and the pharmaceutical sciences; Aqueous polymeric coatings for pharmaceutical dosage forms* Vol. 176. New York: Informa Healthcare USA.
- Kothari, K., *et al.* (2015) The role of drug-polymer hydrogen bonding interactions on the molecular mobility and physical stability of nifedipine solid dispersions. *Mol Pharm*, **12** (1), 162-70.
- Kricheldorf, H. R., *et al.* (2004) *Handbook of Polymer Synthesis: Second Edition*. Taylor & Francis.
- Krongauz, V. V. (2010) Crosslink density dependence of polymer degradation kinetics: Photocrosslinked acrylates. *Thermochimica Acta*, **503-504** (0), 70-84.
- Kulicke, W. M. and Porter, R. S. (1980) Relation between steady shear flow and dynamic rheology. *Rheologica Acta*, **19** (5), 601-605.
- Kurtz, S. M., *et al.* (2006) Anisotropy and oxidative resistance of highly crosslinked UHMWPE after deformation processing by solid-state ram extrusion. *Biomaterials*, **27** (1), 24-34.
- Larkin, P. (2011) Chapter 6 - IR and Raman Spectra-Structure Correlations: Characteristic Group Frequencies. In: *Infrared and Raman Spectroscopy*. Oxford: Elsevier, pp. 73-115.
- Leuner, C. and Dressman, J. (2000) Improving drug solubility for oral delivery using solid dispersions. *Eur J Pharm Biopharm*, **50** (1), 47-60.
- Li, J. and Mei, X. (2006) Applications of Cellulose and Cellulose Derivatives in Immediate Release Solid Dosage. In: *Polysaccharides for Drug Delivery and Pharmaceutical Applications*. (ACS Symposium Series) Vol. 934. American Chemical Society, pp. 19-55.
- Li, X.-G., *et al.* (1999) Thermal decomposition of cellulose ethers. *Journal of Applied Polymer Science*, **73** (14), 2927-2936.
- Li, Y., *et al.* (2014) Interactions between drugs and polymers influencing hot melt extrusion. *Journal of Pharmacy and Pharmacology*, **66** (2), 148-166.

- Lin, D. and Huang, Y. (2010) A thermal analysis method to predict the complete phase diagram of drug-polymer solid dispersions. *Int J Pharm*, **399** (1-2), 109-15.
- Liu, J., *et al.* (2002) Dynamics of pharmaceutical amorphous solids: the study of enthalpy relaxation by isothermal microcalorimetry. *J Pharm Sci*, **91** (8), 1853-62.
- Liu, Z. and Yuan, Q. (2006) Synthesis of <sup>15</sup>N-labeled phthalimide. *Appl Radiat Isot*, **64** (7), 760-2.
- Lourdin, D., *et al.* (2002) Structural relaxation and physical ageing of starchy materials. *Carbohydrate Research*, **337** (9), 827-833.
- Lu, J., *et al.* (2014) Assessment of Processing Window of Hypromellose Acetate Succinate (HPMCAS) for HotMelt Extrusion. AAPS. San Diego, USA.
- Luukkonen, P., *et al.* (2001) Characterization of microcrystalline cellulose and silicified microcrystalline cellulose wet masses using a powder rheometer. *Eur J Pharm Sci*, **13** (2), 143-9.
- Lyons, J. G., *et al.* (2008) The significance of variation in extrusion speeds and temperatures on a PEO/PCL blend based matrix for oral drug delivery. *Int J Pharm*, **351** (1-2), 201-8.
- Maccallum, J. R. (1989) Comprehensive Polymer science: The synthesis, characterisation, reactions and applications of polymers In: BEVINGTON, G. A. A. J. C. (Ed.) Vol. I. Oxford: Pergamon Press, p. 903.
- Maccallum, J. R. and Schoff, C. K. (1971) A method for determining the order of a reaction. *Journal of Polymer Science Part B: Polymer Letters*, **9** (5), 395-398.
- Maciejewski, M. A. R., R. (1987) Correlation between isothermal and rising temperature experiments. Thermal decomposition of diammonium hydrophosphate. *Thermochimica Acta*, **113** (0), 305-320.
- Mahmah, O., *et al.* (2014) A comparative study of the effect of spray drying and hot-melt extrusion on the properties of amorphous solid dispersions containing felodipine. *Journal of Pharmacy and Pharmacology*, **66** (2), 275-284.
- Majidi, S., *et al.* (2011) Rheological evaluation of wet masses for the preparation of pharmaceutical pellets by capillary and rotational rheometers. *Pharm Dev Technol*.
- Mako, A., *et al.* (2009) Formulation of thermoresponsive and bioadhesive gel for treatment of oesophageal pain and inflammation. *Eur J Pharm Biopharm*, **72** (1), 260-5.
- Maniruzzaman, M., *et al.* (2012) A Review of Hot-Melt Extrusion: Process Technology to Pharmaceutical Products. *ISRN Pharmaceutics*, **2012**, 436763.
- Maniruzzaman, M., *et al.* (2013) Dissolution enhancement of poorly water-soluble APIs processed by hot-melt extrusion using hydrophilic polymers. *Drug Dev Ind Pharm*, **39** (2), 218-27.
- Mano, J. F., *et al.* (2003) Thermal properties of thermoplastic starch/synthetic polymer blends with potential biomedical applicability. *J Mater Sci Mater Med*, **14** (2), 127-35.

- Marsac, P. J., *et al.* (2007) *Formation and Stabilization of Amorphous Molecular Level Solid Dispersions*. Purdue University.
- Marsac, P. J., *et al.* (2010) Effect of temperature and moisture on the miscibility of amorphous dispersions of felodipine and poly(vinyl pyrrolidone). *J Pharm Sci*, **99** (1), 169-85.
- Marshall Steinberg, L. B., Alan Mercill (2001) *From Inactive Ingredients to Pharmaceutical Excipients*. [cited 18 November 2014]. Available from <http://www.pharmtech.com/pharmtech/data/articlestandard//pharmtech/512001/5533/article.pdf>.
- Mcginity, J. W., Zhang, F. (2002) *Hot-melt extrudable pharmaceutical formulation*.
- Mezger, T. G. (2006) *The Rheology Handbook*. Hannover, Vincentz network.
- Miller-Chou, B. A. and Koenig, J. L. (2003) A review of polymer dissolution. *Progress in Polymer Science*, **28** (8), 1223-1270.
- Moreton, C. (2010) *Functionality and Performance of Excipients in a Quality-by-Design World, Part IX: New Excipients*. Compare networks, [cited 26th August 2014]. Available from <http://www.americanpharmaceuticalreview.com/Featured-Articles/116638-Functionality-and-Performance-of-Excipients-in-a-Quality-by-Design-World-Part-IX-New-Excipients/>.
- Nachaegari, *et al.* (2004) Coprocessed Excipients for Solid Dosage Forms. *Pharmaceutical Technology*.
- Nakamichi K., *et al.* (2002) The role of the kneading paddle and the effects of screw revolution speed and water content on the preparation of solid dispersions using a twin-screw extruder. *Int J Pharm*, **241** (2), 203-11.
- Nakamichi K., *et al.* (1996) Preparation of Nifedipine-Hydroxypropylmethylcellulose phthalate solid dispersion by twin screw extruder and its evaluation. *J. Pharm. Sci. Technol. Jpn*, **56**, 15-22.
- Nishi, T. and Wang, T. T. (1975) Melting Point Depression and Kinetic Effects of Cooling on Crystallization in Poly(vinylidene fluoride)-Poly(methyl methacrylate) Mixtures. *Macromolecules*, **8** (6), 909-915.
- Nishida, H., *et al.* (2009) Selective Depolymerization and Effects of Homolysis of Poly(L-lactic acid) in a Blend with Polypropylene. *International Journal of Polymer Science*, **2009**.
- Nist (2011) *NIST Chemistry WebBook*. The National Institute of Standards and Technology (NIST), U.S. Secretary of Commerce on behalf of the United States of America, [cited 24 November 2014]. Available from <http://webbook.nist.gov/chemistry/>.
- Olmo, I. G. and Ghaly, E. S. (1999) Compressional characterization of two dextrose-based directly compressible excipients using an instrumented tablet press. *Pharm Dev Technol*, **4** (2), 221-31.
- Omidian H, K. P. K., Sinko P (2006) Pharmaceutical Polymers. In: *Martin's Physical Pharmacy and Pharmaceutical Sciences*. Lippincott Williams & Wilkins.
- Onda, Y., *et al.* (1980) Ether-ester derivatives of cellulose and their applications. (US 05/944,177), 10.

- Pajula, K., *et al.* (2010) Predicting the Formation and Stability of Amorphous Small Molecule Binary Mixtures from Computationally Determined Flory-Huggins Interaction Parameter and Phase Diagram. *Molecular Pharmaceutics*, **7** (3), 795-804.
- Palade, L.-I., *et al.* (2001) Melt Rheology of High I-Content Poly(lactic acid). *Macromolecules*, **34** (5), 1384-1390.
- Paradkar, A., *et al.* (2009) Shear and extensional rheology of hydroxypropyl cellulose melt using capillary rheometry. *J Pharm Biomed Anal*, **49** (2), 304-10.
- Parthasaradhi, R. B., *et al.* (2013) *Ritonavir compositions*. WO2013128467 A1.
- Pasztor, E., *et al.* (2011) New formulation of in situ gelling Metolose-based liquid suppository. *Drug Dev Ind Pharm*, **37** (1), 1-7.
- Patel, H. S., Viral; Upadhyay, Umesh (2011) New pharmaceutical excipients in solid dosage forms - A review. *International Journal of Pharmacy & Life Sciences*, **2** (8), 1006.
- Patterson, J. E., *et al.* (2007) Preparation of glass solutions of three poorly water soluble drugs by spray drying, melt extrusion and ball milling. *Int J Pharm*, **336** (1), 22-34.
- Paudel, A., *et al.* (2010) Theoretical and experimental investigation on the solid solubility and miscibility of naproxen in poly(vinylpyrrolidone). *Mol Pharm*, **7** (4), 1133-48.
- Pearce, E. M. (1977) Properties of polymers, their estimation and correlation with chemical structure – (2nd rev. ed.), D. W. Van Krevelen, Elsevier, Amsterdam – Oxford – New York, 1976, 620 pp. *Journal of Polymer Science: Polymer Letters Edition*, **15** (1), 56-56.
- Pharmacopeia, U. S. (USP29) *USP Monographs: Ibuprofen* [cited 15th November 2014]. Available from <http://www.pharmacopeia.cn/usp.asp>.
- Pharmacopeia, U. S. (USP29-NF24) *Good Manufacturing Practices for Bulk Pharmaceutical Excipients*. [cited 10th November 2014]. Available from <http://www.pharmacopeia.cn/usp.asp>.
- Pifferi, G. and Restani, P. (2003) The safety of pharmaceutical excipients. *// Farmaco*, **58** (8), 541-550.
- Pimbert, S., *et al.* (2005) Relations between Glass Transition Temperatures in Miscible Polymer Blends and Composition: From Volume to Mass Fractions. *Macromolecular Symposia*, **222** (1), 259-264.
- Popescu, M., *et al.* (2009) Crystalline-amorphous and amorphous-amorphous transitions in phase-change materials. *Journal of Non-Crystalline Solids*, **355** (37- 42), 1820-1823.
- Potuzak, M., *et al.* (2013) Are the dynamics of a glass embedded in its elastic properties? *The Journal of Chemical Physics*, **138** (12), 12A501-5.
- Prodduturi, S., *et al.* (2005) Solid-state stability and characterization of hot-melt extruded poly(ethylene oxide) films. *J Pharm Sci*, **94** (10), 2232-45.
- Qian, F., *et al.* (2010) Drug-polymer solubility and miscibility: Stability consideration and practical challenges in amorphous solid dispersion development. *J Pharm Sci*, **99** (7), 2941-7.

- Qian, R. and Yu, Y. (2009) Transition of polymers from rubbery elastic state to fluid state. *Frontiers of Chemistry in China*, **4** (1), 1-9.
- Qiu, Y., *et al.* (2009) *Developing Solid Oral Dosage Forms: Pharmaceutical Theory & Practice*. Academic Press; .
- Rao, A. (2010) *Rheology of Fluid and Semisolid Foods: Principles and Applications: Principles and Applications*. Springer.
- Raquez, J.-M., *et al.* (2008) Recent Advances in Reactive Extrusion Processing of Biodegradable Polymer-Based Compositions. *Macromolecular Materials and Engineering*, **293** (6), 447-470.
- Regnier, N. and Guibe, C. (1997) Methodology for multistage degradation of polyimide polymer. *Polymer Degradation and Stability*, **55** (2), 165-172.
- Remya, K. S., *et al.* (2010) Formulation Development, Evaluation and Comparative Study of Effects of Super Disintegrants in Cefixime Oral Disintegrating Tablets. *Journal of Young Pharmacists : JYP*, **2** (3), 234-239.
- Repka, M. A., *et al.* (2007) Pharmaceutical applications of hot-melt extrusion: Part II. *Drug Dev Ind Pharm*, **33** (10), 1043-57.
- Repka, M. A., *et al.* (2013) Properties and Applications of Hypromellose Acetate Succinate (HPMCAS) for Solubility Enhancement Using Melt Extrusion. In: *Melt Extrusion*. (AAPS Advances in the Pharmaceutical Sciences Series) Vol. 9. Springer New York, pp. 107-121.
- Rina Chokshi, H. Z. (2004) Hot-melt extrusion technique: a review. *Iranian Journal of Pharmaceutical Research*, **3** (1), 3-16.
- Rippie, E. G. and Johnson, J. R. (1969) Regulation of dissolution rate by pellet geometry. *Journal of Pharmaceutical Sciences*, **58** (4), 428-431.
- Roblegg, E., *et al.* (2011) Use of the direct compression aid Ludiflash((R)) for the preparation of pellets via wet extrusion/spheronization. *Drug Dev Ind Pharm*, **37** (10), 1231-43.
- Rothen-Weinhold, A., *et al.* (2000) Formation of peptide impurities in polyester matrices during implant manufacturing. *European Journal of Pharmaceutics and Biopharmaceutics*, **49** (3), 253-257.
- Rozycki, C. A. M. M. (1987) Method of the selection of the  $g(\hat{\pm})$  function based on the reduced-time plot. *Thermochimica Acta*, **122** (2), 339-354.
- Rubinstein, M. and Colby, R. H. (2003) *Polymer Physics*. OUP Oxford.
- Rudolf, B., *et al.* (1995) Pressure-volume-temperature behaviour of molten polymers. *Polymer Bulletin*, **34** (1), 109-116.
- Rüffler, *et al.* (2009) Chemical Potential from the Beginning. In: *Chemistry Education in the ICT Age*. Springer, pp. 41-55.
- Rumondor, A. C., *et al.* (2009a) Effects of polymer type and storage relative humidity on the kinetics of felodipine crystallization from amorphous solid dispersions. *Pharm Res*, **26** (12), 2599-606.
- Rumondor, A. C. F., *et al.* (2009b) Effects of Moisture on the Growth Rate of Felodipine Crystals in the Presence and Absence of Polymers. *Crystal Growth & Design*, **10** (2), 747-753.

- Rumondor, A. C. F., *et al.* (2009c) Phase Behavior of Poly(vinylpyrrolidone) Containing Amorphous Solid Dispersions in the Presence of Moisture. *Molecular Pharmaceutics*, **6** (5), 1492-1505.
- Rumondor, A. C. F. and Taylor, L. S. (2009) Effect of Polymer Hygroscopicity on the Phase Behavior of Amorphous Solid Dispersions in the Presence of Moisture. *Molecular Pharmaceutics*, **7** (2), 477-490.
- Sakai, T. and Thommes, M. (2014) Investigation into mixing capability and solid dispersion preparation using the DSM Xplore Pharma Micro Extruder. *J Pharm Pharmacol*, **66** (2), 218-31.
- Sakellariou, P., *et al.* (1986) The solubility parameters of some cellulose derivatives and polyethylene glycols used in tablet film coating. *International Journal of Pharmaceutics*, **31** (1-2), 175-177.
- Salamone, J. C. (1996) *Polymeric Materials Encyclopedia, Twelve Volume Set*. Taylor & Francis.
- Sarode, A. (2010). *Amorphous solid solutions using hot melt extrusion*. University of Rhode Island.
- Sarode, A. L., *et al.* (2014) Stability assessment of hypromellose acetate succinate (HPMCAS) NF for application in hot melt extrusion (HME). *Carbohydrate Polymers*, **101** (0), 146-153.
- Sarode, A. L., *et al.* (2013a) Hot melt extrusion (HME) for amorphous solid dispersions: Predictive tools for processing and impact of drug-polymer interactions on supersaturation. *Eur J Pharm Sci*, **48** (3), 371-384.
- Sarode, A. L., *et al.* (2013b) Supersaturation, nucleation, and crystal growth during single- and biphasic dissolution of amorphous solid dispersions: Polymer effects and implications for oral bioavailability enhancement of poorly water soluble drugs. *European Journal of Pharmaceutics and Biopharmaceutics*, (0).
- Schneider, H. A. (1988) The Gordon-Taylor equation. Additivity and interaction in compatible polymer blends. *Die Makromolekulare Chemie*, **189** (8), 1941-1955.
- Scholler-Gyure, M., *et al.* (2013) Steady-state pharmacokinetics of etravirine and lopinavir/ritonavir melt extrusion formulation, alone and in combination, in healthy HIV-negative volunteers. *J Clin Pharmacol*, **53** (2), 202-10.
- Science.Gov (2015) *HPMCAS and HPMCP*. [cited 1 January 2015]. Available from <http://www.science.gov/index.html>.
- Shao, Z. J., *et al.* (2002) Drug release from Kollicoat SR 30D-coated nonpareil beads: evaluation of coating level, plasticizer type, and curing condition. *AAPS PharmSciTech*, **3** (2), E15.
- Shau-Tarng Lee and Ramesh, N. S. (2004) *Polymeric Foams: Mechanisms and Materials*. CRC Press.
- Shin-Etsu (2009) NF Hypromellose Acetate Succinate and Hypromellose Phthalate NF. *Shin Etsu*. Shin Etsu.
- Siepmann, F., *et al.* (2006a) Drugs acting as plasticizers in polymeric systems: a quantitative treatment. *J Control Release*, **115** (3), 298-306.
- Siepmann, F., *et al.* (2006b) Aqueous HPMCAS coatings: Effects of formulation and processing parameters on drug release and mass transport

- mechanisms. *European Journal of Pharmaceutics and Biopharmaceutics*, **63** (3), 262-269.
- Siepmann, F., *et al.* (2008) Polymer blends for controlled release coatings. *J Control Release*, **125** (1), 1-15.
- Sigma-Aldrich (2014) *Chlorpropamide impurity B, European Pharmacopoeia (EP) Reference Standard*. Sigma-Aldrich, [cited 30 November 2014]. Available from <http://www.sigmaaldrich.com/catalog/product/fluka/c1905020?lang=en&region=GB>.
- Silva, R., *et al.* (2010) Miscibility influence in the thermal stability and kinetic parameters of poly (3-hydroxybutyrate)/poly (ethylene terephthalate) sulphonated blends. *Polymer*, **20**, 153-158.
- Singhal, S., *et al.* (2011) Hot melt extrusion technique. *WebmedCentral, PHARMACEUTICAL SCIENCES* **2**(1).
- Sinha, S., *et al.* (2010) Solid dispersion as an approach for bioavailability enhancement of poorly water-soluble drug ritonavir. *AAPS PharmSciTech*, **11** (2), 518-27.
- Six, K., *et al.* (2003a) Characterization of solid dispersions of itraconazole and hydroxypropylmethylcellulose prepared by melt extrusion, Part II. *Pharm Res*, **20** (7), 1047-54.
- Six, K., *et al.* (2003b) Identification of phase separation in solid dispersions of itraconazole and Eudragit E100 using microthermal analysis. *Pharm Res*, **20** (1), 135-8.
- Staniforth, J. (2003) Pharmaceutical superdisintegrant. Google Patents.
- Stuart, B. H. (2005a) Organic Molecules. In: *Infrared Spectroscopy: Fundamentals and Applications*. John Wiley & Sons, Ltd, pp. 71-93.
- Stuart, B. H. (2005b) Spectral Analysis. In: *Infrared Spectroscopy: Fundamentals and Applications*. John Wiley & Sons, Ltd, pp. 45-70.
- Sun, H., *et al.* (2014) Rheology of Entangled Polymers Not Far above Glass Transition Temperature: Transient Elasticity and Intersegmental Viscous Stress. *Macromolecules*, **47** (16), 5839-5850.
- Swarbrick, J. and Boylan, J. C. (1990) *Encyclopedia of pharmaceutical technology* (Comparative Biochemistry and Physiology Part A: Physiology) Vol. 12. Marcel Dekker, New York.
- Tanno, F., *et al.* (2004) Evaluation of hypromellose acetate succinate (HPMCAS) as a carrier in solid dispersions. *Drug Dev Ind Pharm*, **30** (1), 9-17.
- Tant, R., *et al.* (1997) *Ionomers: Synthesis, Structure, Properties and Applications*. Springer.
- Thoma, K. and Bechtold, K. (1999) Influence of aqueous coatings on the stability of enteric coated pellets and tablets. *Eur J Pharm Biopharm*, **47** (1), 39-50.
- Thomas Rades, K. G., Kirsten Greaser (2013) Molecular structure, properties and states of matter. In: FELTON, L. A. (Ed.) *Remington - Essentials of Pharmaceutics*. Pharmaceutical Press.

- Tian, Y., *et al.* (2013) Construction of drug-polymer thermodynamic phase diagrams using Flory-Huggins interaction theory: identifying the relevance of temperature and drug weight fraction to phase separation within solid dispersions. *Mol Pharm*, **10** (1), 236-48.
- Tobyn, M. J., *et al.* (1998) Physicochemical comparison between microcrystalline cellulose and silicified microcrystalline cellulose. *International Journal of Pharmaceutics*, **169** (2), 183-194.
- Valducci, R., *et al.* (2010) Pharmaceutical formulations for the oral administration of ppi. Google Patents.
- Vasu Dev, R., *et al.* (2009) Identification of degradation products in stressed tablets of Rabeprazole sodium by HPLC-hyphenated techniques. *Magn Reson Chem*, **47** (5), 443-8.
- Vega-Baudrit, J., *et al.* (2008) Kinetics of isothermal degradation studies in adhesives by thermogravimetric data: effect of hydrophilic nanosilica fillers on the thermal properties of thermoplastic polyurethane-silica nanocomposites. *Recent Pat Nanotechnol*, **2** (3), 220-6.
- Vlachopoulos, J. and Strutt, D. (2003) The Role of Rheology in Polymer Extrusion. *New Technology for Extrusion Conference*.
- Wang, L., *et al.* (2007) Synthesis and characterization of hydroxypropyl methylcellulose and ethyl acrylate graft copolymers. *Carbohydrate Polymers*, **68** (4), 626-636.
- Who. 2009 *Stability Testing of Active Pharmaceutical Ingredients and Finished Pharmaceutical Products*. (953).
- Wilson, A. S. (1996) *Plasticisers: Selection, Applications and Implications*. Rapra Technology Limited.
- Winter, M. E. D. R. A. H. H. (1994) The effect of entanglements on the rheological behaviour of polybutadiene critical gels. *Rheologica Acta*, **33**, 220-237.
- Wool, R. P. (1993) Polymer entanglements. *Macromolecules*, **26** (7), 1564-1569.
- Work, W. J., *et al.* (2004) Definition of terms related to polymer blends, composites, and multiphase polymeric materials (IUPAC Recommendations 2004). *Pure and Applied Chemistry*.
- Wu, Y., *et al.* (2011a) Reactive Impurities in Excipients: Profiling, Identification and Mitigation of Drug-Excipient Incompatibility. *AAPS PharmSciTech*, **12** (4), 1248-1263.
- Wu, Y., *et al.* (2011b) Reactive impurities in excipients: profiling, identification and mitigation of drug-excipient incompatibility. *AAPS PharmSciTech*, **12** (4), 1248-63.
- Wytttenbach, N., *et al.* (2005) Drug-excipient compatibility testing using a high-throughput approach and statistical design. *Pharm Dev Technol*, **10** (4), 499-505.
- Yadav, A. V., *et al.* (2009) Co-Crystals: A Novel Approach to Modify Physicochemical Properties of Active Pharmaceutical Ingredients. *Indian Journal of Pharmaceutical Sciences*, **71** (4), 359-370.

- Yang, D., *et al.* (2007) Effect of the melt granulation technique on the dissolution characteristics of griseofulvin. *International Journal of Pharmaceutics*, **329** (1-2), 72-80.
- Yaws, C. L. (2015) *The Yaws Handbook of Physical Properties for Hydrocarbons and Chemicals: Physical Properties for More Than 54,000 Organic and Inorganic Chemical Compounds, Coverage for C1 to C100 Organics and Ac to Zr Inorganics.* Elsevier Science.
- Yoshinari, T., *et al.* (2002) Moisture induced polymorphic transition of mannitol and its morphological transformation. *Int J Pharm*, **247** (1-2), 69-77.
- Zedong Dong and Choi, D. S. (2008) Hydroxypropyl Methylcellulose Acetate Succinate: Potential Drug–Excipient Incompatibility. *AAPS PharmSciTech*, **9** (3), 991-997.
- Zhao, Y., *et al.* (2011) Prediction of the thermal phase diagram of amorphous solid dispersions by flory–huggins theory. *Journal of Pharmaceutical Sciences*, **100** (8), 3196-3207.
- Zsako, J. (1976) The kinetic compensation effect. *Journal of thermal analysis*, **9** (1), 101-108.

# Appendix I

## 1. Thermodynamic phase diagram of Chlorpropamide:

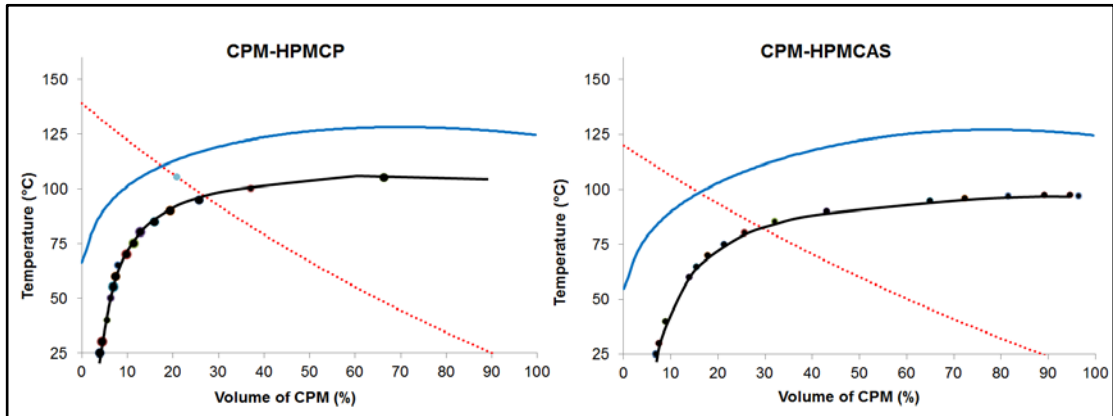


Figure 6.1: Phase diagrams of CPM mixtures with HPMCAS and HPMCP

It can be seen from the above figure that miscibility of CPM with both polymers was limited was less than 10% of drug loadings and its maximum loading with HPMCP and HPMCAS was noted to be 4% and 7% respectively.

## 2. Cox-Merz rule:

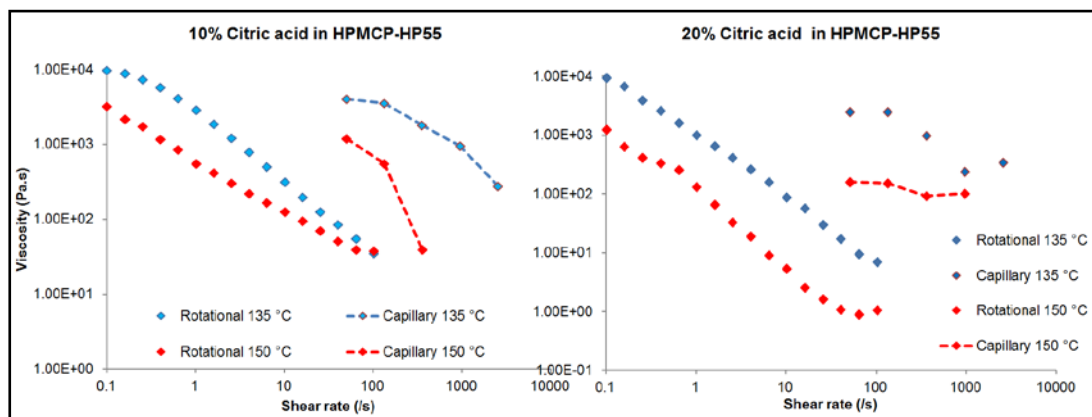


Figure 6.2: Cox Merz applications for the blends of CA-HPMCP.

From the figure 6.1 it can be seen that the blends of CA-HPMCP did not align with the observed rotational and capillary viscosity measurements and these results were similar to that of data of both HPMCAS and HPMCP

whereas deviating from the data produced by that of TEC and PEG mixed polymeric blends.

### 3. Motor load studies with the blends of TEC:

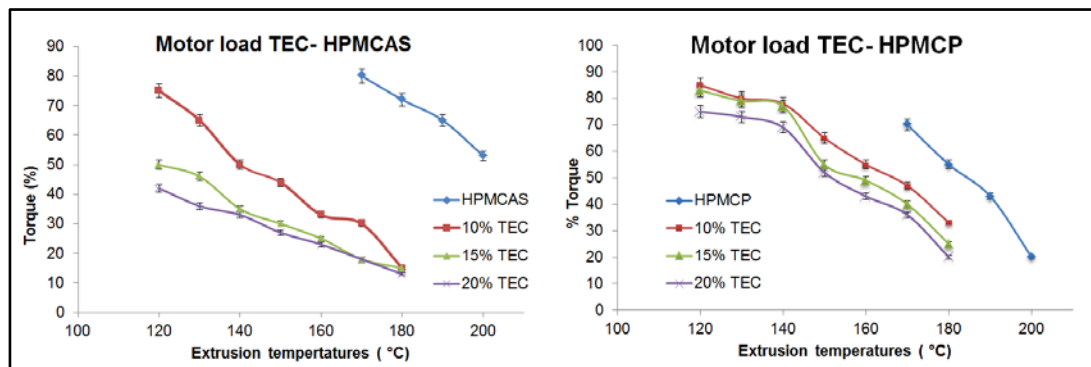


Figure 6.3: Percentage torque versus extrusion temperatures for TEC-HPMCP and TEC-HPMCAS

### 4. Degradation mechanism of HPMCAS:

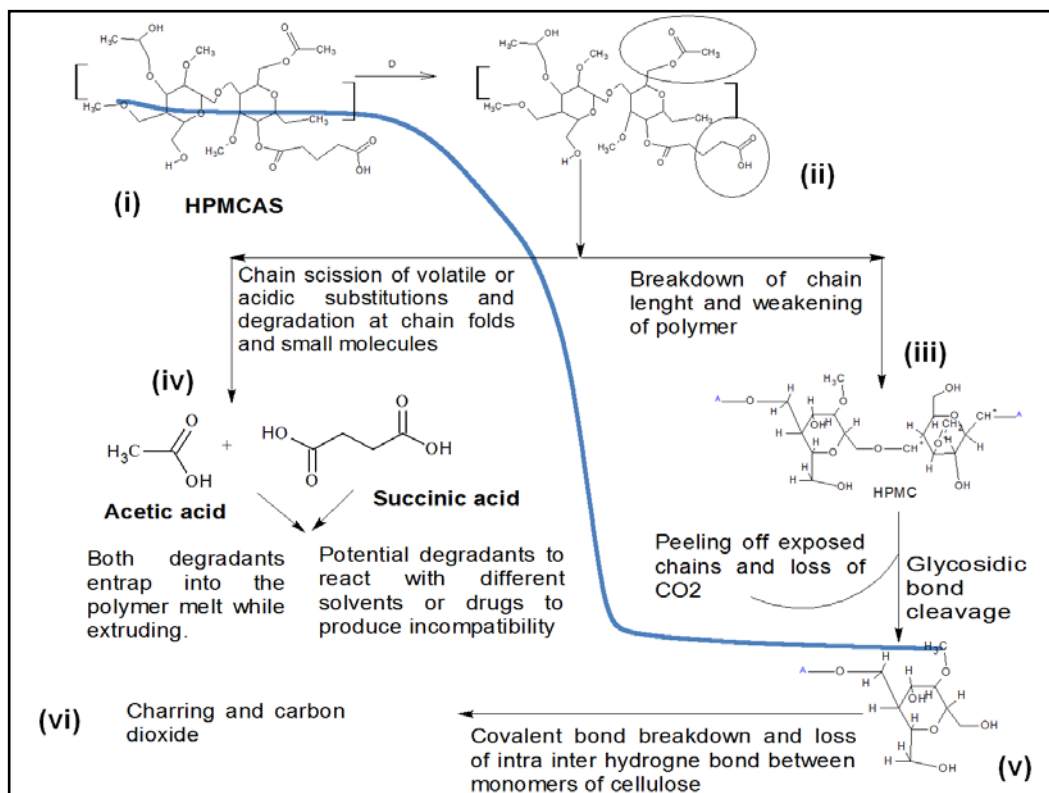


Figure 6.4: Schematic representation of degradation mechanism of HPMCAS

## Appendix II

### Original Publication

- Karandikar Hrushikesh, Ambardekar Rohan, Kelly Adrian, Gough Tim and Paradkar Anant (2015). Systematic identification of thermal degradation products of HPMCP during hot melt extrusion process. *International Journal of Pharmaceutics*, 486 (1-2), 252-258.

### Manuscripts under preparation

- Karandikar Hrushikesh, Kelly Adrian, Gough Tim and Paradkar Anant. Influence of plasticisers on degradation kinetics of HPMCAS and HPMCP polymers. *Phys. Chem. Chem. Phys., The Royal Society of Chemistry.*
- Karandikar Hrushikesh, Kelly Adrian, Gough Tim and Paradkar Anant. Conflicts and chemical interactions of cellulose ester derivatives during hot melt extrusion. *International Journal of Pharmaceutics. Elsevier.*

### List of Conferences

- Karandikar Hrushikesh, Kelly Adrian, Gough Tim and Paradkar Anant. Importance of shear and extensional rheology of HPMCAS for its applications in hot melt extrusion using capillary rheometry (Poster and oral presentation), UK Pharm Sci- 2013.
- Karandikar Hrushikesh, Kelly Adrian, Gough Tim and Paradkar Anant. Estimation of thermal degradation of cellulose esters during thermal processing (Poster and oral presentation). UK Pharm Sci- 2012.